UNIVERSITÀ DELLA CALABRIA

UNIVERSITA' DELLA CALABRIA

Dipartimento di di Farmacia e Scienze della Salute e della

Nutrizione

Dottorato di Ricerca in
Medicina Traslazionale

CICLO
XXIX

Stimulatory actions of IGF-I are mediated by IGF-IR cross-talk with GPER and DDR1 in mesothelioma and lung cancer cells

Settore Scientifico Disciplinare: MED/04

Coordinatore: Ch.mo Prof. Sebastiano Andò

Firma _____

Supervisore/Tutor: Ch.mo Prof. Marcello Maggiolini

Firma _Marcello Maggiolini_

Dottoranda: Dott.ssa Silvia Avino

Firma _Silvia Av___

UNIVERSITÀ DELLA CALABRIA

UNIVERSITÀ DELLA CALABRIA

Dipartimento di Farmacia e Scienze della Salute e della Nutrizione

Dottorato di Ricerca in
Medicina Traslazionale

CICLO
XXIX

Stimulatory actions of IGF-I are mediated by IGF-IR cross-talk with GPER and DDR1 in mesothelioma and lung cancer cells

Settore Scientifico Disciplinare: MED/04

Coordinatore: Ch.mo Prof. Sebastiano Andò

Supervisore/Tutor: Ch.mo Prof. Marcello Maggiolini

Dottoranda: Dott.ssa Silvia Avino

Index

Chapter III
Results

Chapter IV

Abstract

Insulin-like growth factor-I (IGF-I)/IGF-I receptor (IGF-IR) system has been largely involved in the pathogenesis and development of various tumors. We have previously demonstrated that IGF-IR cooperates with the G-protein estrogen receptor (GPER) and the collagen receptor discoidin domain 1 (DDR1) that are implicated in cancer progression. Here, we provide novel evidence regarding the molecular mechanisms through which IGF-I/IGF-IR signaling triggers a functional cross-talk with GPER and DDR1 in both mesothelioma and lung cancer cells. In particular, we show that IGF-I activates the transduction network mediated by IGF-IR leading to the up-regulation of GPER and its main target genes CTGF and EGR1 as well as the induction of DDR1 target genes like MATN-2, FBN-1, NOTCH 1 and HES-1. Of note, certain DDR1-mediated effects upon IGF-I stimulation required both IGF-IR and GPER as determined knocking-down the expression of these receptors. The aforementioned findings were nicely recapitulated in important biological outcomes like IGF-I promoted chemotaxis and migration of both mesothelioma and lung cancer cells. Overall, our data suggest that IGF-I/IGF-IR system triggers stimulatory actions through both GPER and DDR1 in aggressive tumors as mesothelioma and lung tumors. Hence, this novel signaling pathway may represent a further target in setting innovative anticancer strategies.

Chapter I

Introduction

1.1   Lung cancer and Mesothelioma

1.1.1 Lung cancer

Lung cancer is the leading cause of cancer-associated death worldwide and has one of the poorest prognoses among all cancer types (Ford et al. 2007). It is estimated that lung cancer is diagnosed in about 1.8 million patients and causes more than 1.5 million deaths each year (Fitzmaurice et al. 2015; Chen et al. 2008). Partly due to the increasing number of risk factors, as smoking and environmental pollution, the incidence of lung cancer was significantly increased in the past decades in many developing countries (Chen et al. 2008; Guo et al. 2012; Guo et al. 2015).

Studies of pulmonary carcinogenicity and respiratory inflammation have shown high risk for respiratory diseases and lung carcinogenesis in humans from exposures to various inhalable dusts, mineral fibers, airborne particulate matter (PM) and ozone. Ambient air pollution, containing PM smaller than aerodynamic diameter of 2.5 μm ($PM_{2.5}$), has gained particular attention in recent years as a main factor in the increased incidence of respiratory diseases, including lung cancer (Valavanidis et al. 2013; Aust et al. 2002; Nagai et al. 2010; Chuang et al. 2012; Strak et al. 2012). Tobacco smoke also plays an important role in augmenting the risk of epithelial inflammation and lung cancer due to its high carcinogenic potential and the synergistic effects with other respirable particulates leading to oxidative stress and increased production of mediators of pulmonary inflammation (Gardi et al. 2012; Sangani et al. 2011; Møller et al. 2008). Both oxidative damage and inflammation have been related to high risk of

diverse tumors. In particular, the mechanisms by which inflammation can contribute to carcinogenesis include genomic instability, alterations in epigenetic events and gene transcription, enhanced cell proliferation and invasion, resistance to apoptosis, tumor neovascularization and metastasis (Azad et al. 2008).

Lung cancer is highly heterogeneous as it can arise in many different sites in the bronchial tree, therefore presenting variable symptoms and signs depending on its anatomic location. 70% of patients diagnosed with lung cancer present with advanced stage disease (Lemjabbar-Alaoui et al 2015). Lung cancer has been classified in different ways in order to minimize the number of unclassifiable lesions and to provide the basis for improved tumor diagnosis and therapy (Brambilla et al. 2001). The classification based on the type and the anatomic location of the tumor accounts (Table 1):

1) The Non-small-cell lung carcinoma (NSCLC) represents about 80% to 85% of lung cancers and its overall 5-year survival rate is 15%. Early stage tumors are treated primarily by complete surgical resection, yet 30 − 55% of patients will develop recurrence or die for the disease. NSCLC can be classified in:

- Squamous cell lung cancers (SQCLC), which represent about 25%–30% of all lung tumors and tend to arise in the main bronchi and advance to the carina.

- Adenocarcinomas (AdenoCA) that account for approximately 40% of all lung cancers and consist of tumors arising in peripheral bronchi. Adenocarcinoma is the most common histologic subtype of lung cancer in most countries, accounting for almost half of all lung tumors. It is the most frequent in younger males (<50 yrs old) and in women of all ages, in never smokers and in former smokers. Difficulties in adenocarcinoma sub-classification arise from its histologically heterogeneity. Mixed pattern adenocarcinomas are more common than tumors showing a single pattern (e.g. acinar, papillary, bronchioloalveolar, and solid adenocarcinoma with mucin formation) (Curado et al. 2007; Brambilla et al. 2001).

- Bronchioloalveolar cancers (BAC), now reclassified into adenocarcinoma in situ (AIS) and minimally invasive adenocarcinoma (MIA), arise in alveoli and spread through the interalveolar connections. AIS and MIA patients present a good disease-free survival after complete resection (5-year rate nears 100%) (Travis et al. 2013; Rubin et al 2012).

- Large cell anaplastic carcinomas (LCAC), also termed NSCLC not otherwise specified (NOS), are more proximal in location and locally tend to invade the mediastinum and its structures early. NSCLC-NOS comprises about 10% of all NSCLC and behaves similarly to small cell cancers with a rapid fatal spread.

2) Small cell lung cancers (SCLCs) derived from the hormonal cells of the lung, are the most differentiated tumors and tend to be central mediastinal malignancies. SCLCs comprise 10%–15% of all lung cancers, and are extremely aggressive disseminating rapidly into submucosal lymphatic vessels and regional lymph nodes, and almost always present without a bronchial invasion.

Table 1. Classification of lung tumors including their location.

Tumor type	Tumor subtype	Location
NSCLC	Squamous cell carcinoma	Develop from cells that line the airways Found in the left/ right bronchus at the center of the lung
	Adenocarcinoma	Develop from airway mucus-producing cells Found in the lung outer edge
	Large cell carcinoma	Found in any lung area
	Sarcomatid carcinoma	Tumors with sarcoma-like elements Found in the central and peripheral lung
	Adenosquamous carcinoma	Develop in glandular, squamous, and large-cell differentiation areas
	Carcinoid tumor	Develop from cells of the diffuse neuroendocrine system Found along large airway walls
	Salivary gland tumor	Develop as a glandular tumor in the trachea or large bronchi
SCLC		Develop in the larger airways and in the major bronchus wall
Mesothelioma	Epithelioid Sarcomatoid Desmoplastic Biphasic	Develop along mesothelial surfaces of pleural and peritoneal cavities

Table 1

Chapter I

The international TNM classification of the lung is based on the staging system, which describes the anatomical extent of the disease (Fig. 1.1). The T category describes the size and extent of the primary tumor. The N category describes the extent of involvement of regional lymph nodes. The M category describes the presence or absence of distant metastatic spread. The addition of numbers to these categories describes the extent of the cancer. All possible combinations of the T, N, and M categories are then used to create TNM subset.
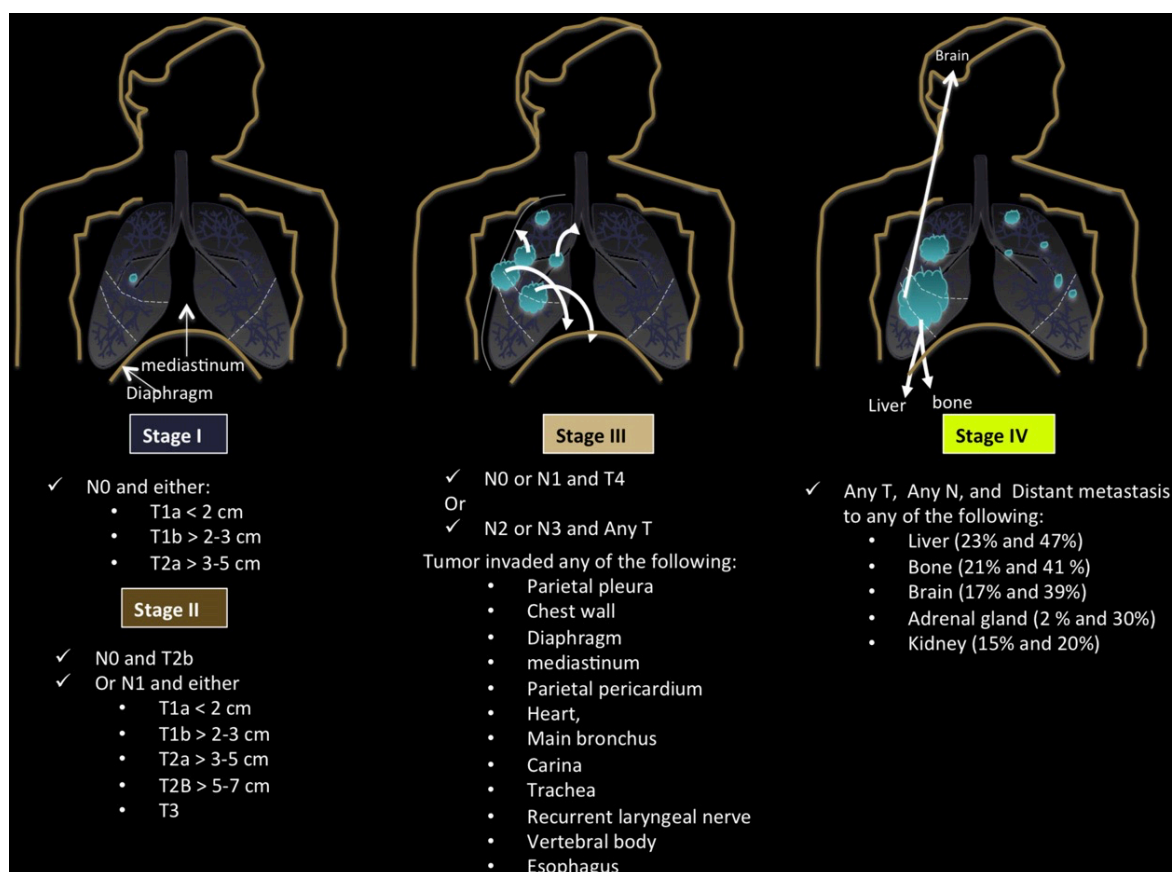
Figure 1.1

1.1.2 Mesothelioma

Smoking has been considered the main etiologic factor for lung cancer, however, several environmental contaminants like asbestos, arsenic, cadmium, nickel and silica, play an important role toward the development of lung tumor (Silvestri et al. 2013). Among the aforementioned environmental pollutants, asbestos has been particularly acknowledged as prompting factor in malignant mesothelioma (MM), which is an aggressive cancer that arises

from mesothelial cells lining lung, pleura or peritoneum (Rajer et al. 2014; Carbone et al. 2012). The pleural cavity is the most common site of origin of this tumor (Davidson 2015). The malignant pleural mesothelioma (MPM) is one of the most clinically aggressive malignancies, with the majority of patients succumbing to their disease within 2 years of diagnosis. The combination of surgery with chemotherapy has in recent years led to improvement in the survival and life quality of MPM patients, whereas targeted therapy has to date failed to have major clinical impact in this disease (Campbell et al. 2011). Asbestos refers to a family of silicate minerals divided into two major groups: the serpentine form of asbestos-chrysotile and the amphibole forms (crocidolite, anthophyllite, actinolite amosite and tremolite) (Carbone et al., 2002). Chronic inflammatory processes, which are caused by the deposition of asbestos fibers and the subsequent release of cytokines and growth factors by macrophages and mesothelial cells, have been shown to play an active role toward the development of pleural MM (Rascoe et al. 2012; Valavanidis et al. 2013). The duration, quality and intensity of the exposure are important variables in any mineral fiber related disease (Carbone et al. 2012). In particular, it has been recently demonstrated that asbestos induces necrotic cell death with resultant release of HMGB-1 in the extra-cellular space. HMGB-1 causes a chronic inflammatory response, macrophage accumulation and the secretion of TNF-alpha which, activating NF-kB, leads to HM survival (Yang et al., 2010) (Figure 1.2).
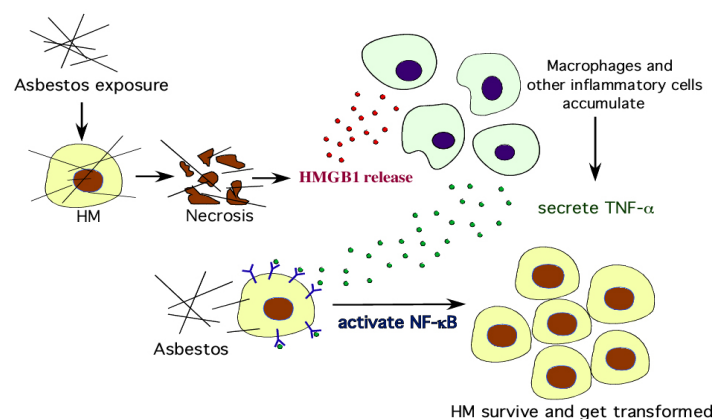
Figure 1.2

Chapter I

At the early stage of pleural mesothelioma, small nodules are found in the parietal pleura (not in the visceral pleura) that eventually extend along the pleural surface. Parietal and visceral pleurae show adhesion, and the tumor encloses the entire lung parenchyma. Few cases of peritoneal mesothelioma have been reported at the early stage and, consequently, little is known in terms of pathology and disease progression during the early stage (Inai 2008; Nonaka et al. 2005). Most of peritoneal mesothelioma is found as a diffuse tumor involving intestinal serosa or as a tumor located at the omentum or mesentery.

Histological classification of mesothelioma includes (Travis et al. 2013):

- epithelioid type 60%

- sarcomatoid type 20%

- biphasic type 20%

- desmoplastic (1–2%), and special variants only appear sporadically (several percentages).

Moreover, the last effect of the persistent inflammation caused by asbestos fibers accumulation is the pulmonary fibrosis, which in turn may create a favorable environment for the development of lung and pleura malignancies (Carbone et al. 2012; Mossman et al. 2011).

1.2   G-protein coupled receptors (GPCRs)

G-protein coupled receptors (GPCRs) are the largest family of cell-surface molecules involved in signal transmission and constitute the most prominent pharmacological targets in biomedicine (Dorsam and Gutkind 2007; Lappano and Maggiolini 2011; Pierce et al 2002). These proteins are characterized by a seven-transmembrane domain structure with an extracellular amino-terminus and an intracellular carboxyl-terminus (O'Hayre et al 2013). Over the last years, a number of studies has provided evidence on the crucial role elicited by

these receptors in various physiological processes including cardiac function, immune responses, neurotransmission and sensory functions (such as vision, taste and olfaction). However, their aberrant activity or expression also contributes to some of the most prevalent human diseases (O'Hayre et al 2013; Pierce et al 2002; Lappano and Maggiolini 2011). GPCRs owe their name to their interaction with heterotrimeric G proteins (composed of an α, β and γ subunit), which bind to the guanine nucleotide GDP in its basal state (Lappano and Maggiolini 2012; Pierce et al. 2002). A wide variety of ligands, including peptide and non-peptide neurotransmitters, hormones, amino acids, ions, lipids, odorant molecules and light, activate various GPCRs that regulate multiple biological responses including growth, migration, invasion and angiogenesis in normal and cancer cells (Lappano and Maggiolini 2012; Marinissen and Gutkind 2001). Upon activation by ligand binding, GDP is released and replaced by GTP, which leads to subunit dissociation into a βγ dimer and the GTP-bound α monomer (Lappano and Maggiolini 2012; Neves et al. 2002) (Figure 1.3). Consequently, the Gα and Gβγ complexes stimulate diverse effector molecules, which include adenylyl and guanylyl cyclases, phosphodiesterases, phospholipase A2 (PLA2), phospholipase C (PLC) and phosphoinositide 3-kinases (PI3Ks), thereby activating or inhibiting the production of a variety of second messengers such as cAMP, cGMP, diacylglycerol, inositol (1,4,5)-trisphosphate [Ins(1,4,5)P3], phosphatidyl inositol (3,4,5)- trisphosphate [PtdIns(3,4,5)P3], arachidonic acid and phosphatidic acid, in addition to promoting increases in the intracellular concentration of Ca^{2+} and the opening or closing of a variety of ion channels (Gutkind 2001).
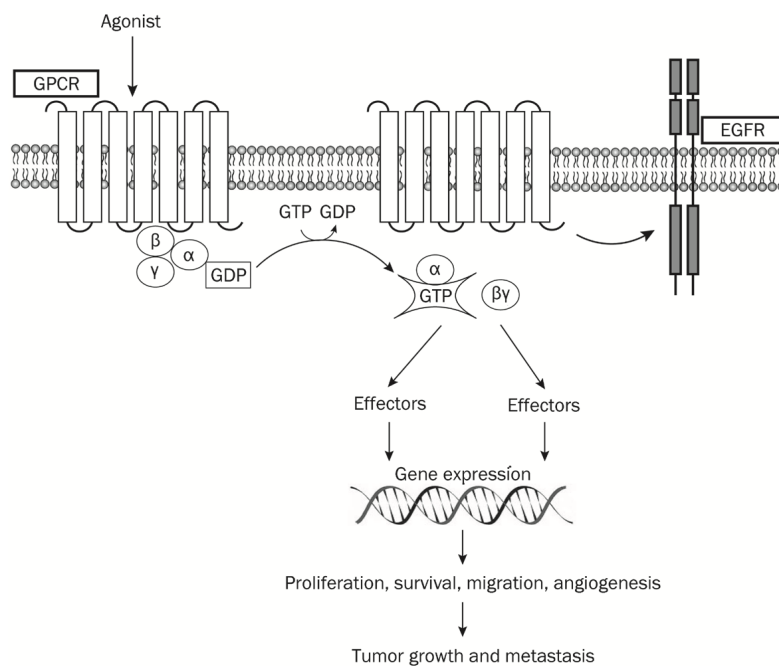
Figure 1.3

Given the number, diversity and complexity of GPCRs, it is not surprising that their effectors extensively cooperate with other transduction pathways playing a critical role in signal transmission and integration (Lappano and Maggiolini 2011). For instance, activated GPCRs interact with cell-surface molecules including growth factor receptors which belong to the receptor tyrosine kinases (RTKs) family (Lappano and Maggiolini 2012; Daub 1996). In particular, multilayered cross-talk between GPCRs and growth factor receptors has an instrumental role in orchestrating downstream signaling molecules that are implicated in cancer development, angiogenesis and metastasis (Lappano and Maggiolini 2011). For instance, agonist-stimulated GPCRs have been shown to transactivate the epidermal growth factor receptor (EGFR) through the matrix metalloproteinases (MMP)-mediated release of EGF-like ligands and the subsequent generation of transduction signals that contribute to cancer progression (Blobel et al. 2005; Daub et al 1997; Filardo et al. 2000; Pierce et al. 2001). In a variety of tumors, like colon, lung, breast, head and neck, prostate and ovarian cancers, it has been demonstrated that a cross-talk between GPCRs and EGFR leads to tumor

development and metastasis (Filardo et al. 2000; Pierce et al. 2001; Hart et al. 2005). Likewise, a connection between the insulin-like growth factor-I receptor (IGF-IR) transduction pathway and GPCR-mediated signaling has been involved in many physiological functions and a variety of malignancies (Kisfalvi et al. 2009; Rozengurt 2010; Young et al. 2010). In addition, a strict dependence of the IGF-I signaling on GPCRs was reported in many physiological functions as well as in the development of diverse tumors (Young et al. 2010; Kisfalvi et al. 2009). On the basis of these findings, various GPCRs and their targets have been considered as promising therapeutic targets in drug discovery toward innovative anti-cancer strategies.

1.2.1 G-protein estrogen receptor (GPER)

In the last years, numerous studies have suggested that the G-protein estrogen receptor (GPER, formerly called GPR30) mediates estrogen signals in a wide number of normal and cancer cells (Maggiolini and Picard 2010). GPER was first identified as an orphan member of the 7-transmembrane receptor family by multiple groups in the late 1990s (Carmeci et al. 1997; Takada et al. 1997). GPER belongs to the rhodopsin-like receptor superfamily and its gene is mapped to chromosome 7p22.3 (Carmeci et al. 1997). Several studies have reported the presence of GPER at the plasma membrane, in the endoplasmic reticulum, in the Golgi apparatus as well as in the nuclear compartment (Filardo et al. 2007; Madeo and Maggiolini 2010; Pupo et al. 2014). GPER mediated signaling triggers the transactivation of EGFR, the rapid phosphorylation of the mitogen-activated protein kinases (MAPKs) ERK1/2 (Filardo et al. 2000), the activation of the PI3-kinase (PI3K) transduction pathway (Revankar et al. 2005), the increase in cAMP concentrations (Filardo et al. 2002; Thomas et al. 2005) and the mobilization of intracellular calcium (Revankar et al. 2005). Through these rapid actions, GPER induces a specific gene signature that in turn induces relevant biological responses as

cell proliferation, migration and angiogenesis (Maggiolini et al. 2004; Albanito et al. 2007; Pandey et al. 2009; Vivacqua et al. 2012; De Francesco et al 2014) (Fig.1.4).
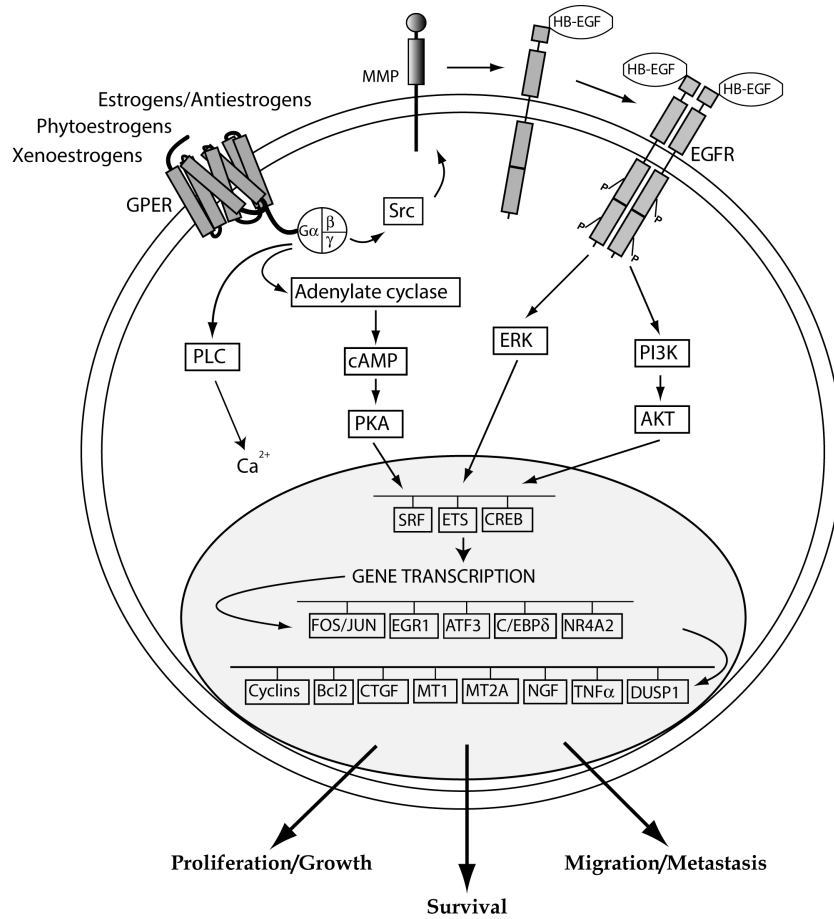
Figure 1.4

GPER was also demonstrated to mediate the stimulatory action of estrogens in cancer-associated fibroblasts (CAFs), indicating its potential to contribute to cancer progression also through these important players of the tumor microenvironment (Madeo and Maggiolini 2010; De Francesco et al 2013).

GPER is expressed in diverse malignancies, including breast, endometrial, ovarian, thyroid, lung and prostate cancer cells, pancreatic epithelial neoplasms, choriocarcinoma and testicular germ cells (Maggiolini and Picard 2010; Bouskine 2009; Siegfried 2009; Liu et al 2015; Chan

2010; Glass 2011; Chevalier 2012). Moreover, our previous studies have shown that ligand-activated growth factor receptors up-regulate GPER expression in diverse types of cancer cells (Albanito et al. 2008; Vivacqua et al. 2009; De Marco et al. 2012). In particular, EGF and IGF-I were shown to induce GPER expression at both mRNA and protein levels (Albanito et al. 2008; Vivacqua et al. 2009; De Marco et al. 2012), hence highlighting the functional cross-talk which may occur between GPER, EGFR and IGF-IR signaling in estrogen-sensitive tumors (Lappano et al. 2013) (Fig.1.5).
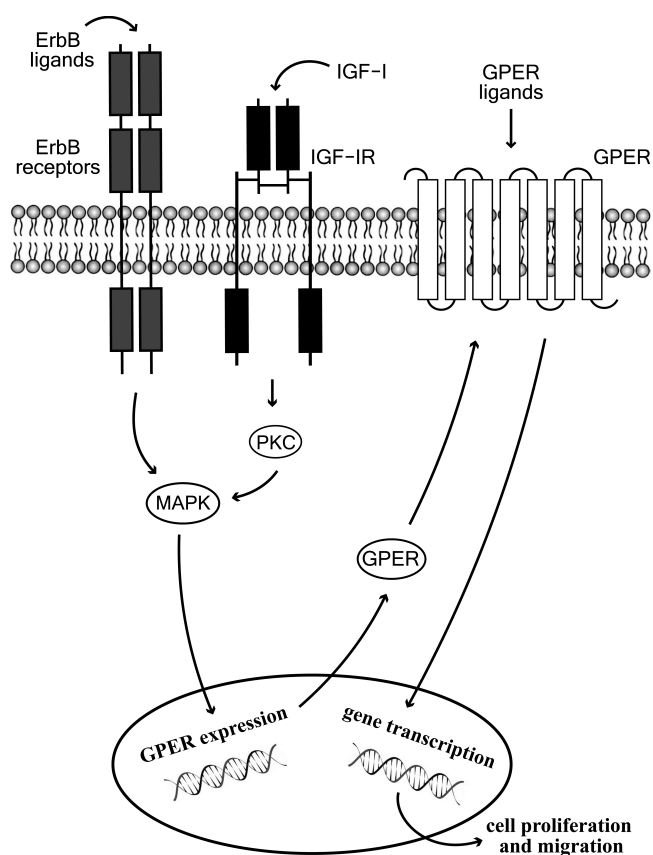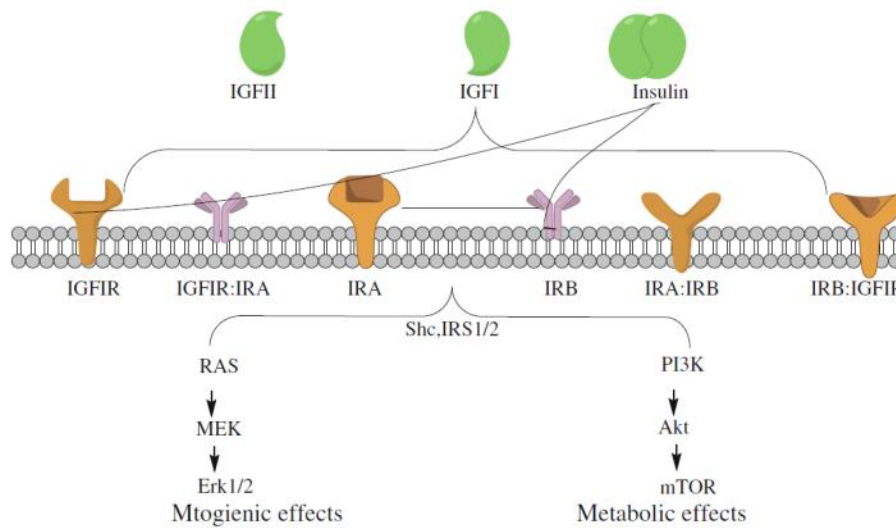

Figure 1.5

1.3   Insulin-like growth factor-I

The IGF system includes in mammals at least three ligands, insulin and the insulin-like growth factors I and II (IGF-I and IGF-II), six high affinity binding proteins (IGFBP-1 to 6)

and four cell surface receptors (i.e. the IGF-I receptor (IGF-IR), the insulin receptor (IR), the insulin receptor-related receptor (IRR) and the Mannose-6-phosphate/IGF-II receptor (M6P/IGF-IIR) (Bartella et al. 2012; Morgan, J.C.et al.1987) (Figure 1.6). The insulin and IGF-I are phylogenetically related peptides that play a major role as regulators of energy metabolism as well as development, growth and reproduction in response to nutrient availability (Bartke 2005).

Figure 1.6

IGFs are small, single-chain polypeptide ligands (7–8 kD) with an intact C-domain derived from prepropeptides in a manner similar to insulin (Beauchamp et al. 2010). The mature IGF-I and IGF-II peptides consist of α and β domains that are homologous to β and α chains of insulin. Furthermore, in the cellular microenvironment, six IGF-binding proteins (IGFBP1–6) are present, which are not only crucial in regulating the bioavailability of IGFs by competing with IGFR and IGFBP proteases but also modulate the balance between IGFs and IGFBPs (Singh et al. 2014). IGFBPs and IGFs comprise a major superfamily of protein hormones that regulate mitogenesis, differentiation, survival, and other IGF-stimulated events in both normal and cancerous cells (Renehan et al. 2004). IGF-s are largely secreted from the liver, but also by extrahepatic tissues. IGF-I is mainly under the control of the pituitary growth hormone

(GH), while the regulation of IGF-II is less well understood (Casa et al. 2007; Reiss et al. 2001). The expression of IGFs is also influenced by several hormones including estrogens, thyrotropin, adrenocorticotropic hormone, as well as other growth factors such as EGF (Epidermal Growth Factor), FGF (Fibroblast Growth Factor), PDGF (Platelet-Derived Growth Factor). In physiological conditions, insulin and IGF-I are regulated by the endocrine system and act as hormones, and specifically bind to their cognate receptor (IR and IGF-IR respectively). However, in cancer tissues both IGF-I and IGF-II are often locally produced in a deregulated manner and act through autocrine and paracrine mechanisms (Samani et al. 2007).

1.3.1 IGF-I/IGF-IR signaling in cancer

IGF-IR is a protein tyrosine kinase (RTK) that belongs to the IGF system and regulates many crucial aspects of cellular physiology (Belfiore and Malaguarnera 2011). IGF-IR activation is initiated when ligands bind to the extracellular α-subunit, which undergoes to a conformational change that activates the tyrosine kinase activity and trans-phosphorylation of the β-subunits. Intra-chain phosphorylation allows the recruitment and activation of numerous docking proteins, including the IRS family members (IRS-1, IRS-2) and adaptors molecules as Shc and Grb2 (Pessin and Saltiel 2001). These substrates, in turn, are involved in the activation of transduction pathways that transmit the receptor signals to intracellular signaling cascades like MAPK, PI3K and the Janus kinase/signal transducer and activator of transcription pathway (JAK/STAT), which mediate important biological responses as glucose metabolism regulation, cell proliferation, inhibition of apoptosis, cell size, cell survival (Samani et al 2007; Belfiore 2007). In this regard, IGF-IR, which is often overexpressed in diverse cancer cell types, affects tumor development, progression and resistance to therapies (Carboni et al. 2005; Franks et al. 2016; Scagliotti et al. 2008; Sachdev et al. 2007). In

particular, the IGF system and related receptors as well as IGF-binding proteins have been established as important regulators of tumor initiation and progression in several malignancies, including pleural MM and lung cancer (Belfiore et al. 2009; Kai et al. 2009; Matà et al. 2016; Scagliotti et al. 2012). Moreover, a dysregulated IGF system has been shown to be implicated in various chronic diseases, such as pulmonary fibrosis (Lee et al. 2014; Hung et al. 2013).

Recently, GPER was shown to interact with IGF-IR in estrogen receptor (ER)-negative breast cancer cells (Pisano et al. 2016) as well as it has been demonstrated the capability of IGF-I to regulate GPER expression and function in ER-positive breast and endometrial cancer cells (De Marco et al. 2013). In particular, the increase of GPER levels induced by IGF-I occurred through the IGF-IR/PKCδ/ERK/ transduction pathway and involved also ER (De Marco et al. 2013).

In addition, an increasing body of data has demonstrated that important biological responses in cancer involve functional interactions of IGF-IR with the collagen receptor discoidin domain receptor 1 (DDR1), an other members of RTK family, that has been found overexpressed in diverse malignancies, including lung carcinomas, and implicated in cancer progression (Valiathan et al. 2012; Lappano and Maggiolini 2011; Liu et al. 2014; Song et al. 2004). Interestingly, this cross-talk occurs also independently of the collagen binding actions of DDR1 and, in human breast cancer cells, amplifies the stimulatory biological effects of IGF-I toward proliferation, migration and colony formation. Moreover, through a signaling pathway involving Akt/miR-199a-5p, IGF-I is able to upregulate DDR1 (Matà et al. 2016; Malaguarnera et al. 2015).

1.4   DDR1 and cancer

The extracellular matrix (ECM) is an essential, dynamic and versatile part of the milieu of a

cell that directly or indirectly regulates almost all cellular behavior and the major developmental processes (Wiseman et al. 2003; Stickens et al. 2004; Rebustini et al. 2009; Lu et al. 2011). The ECM not only confers structural properties to tissues but it is also able to regulate cell proliferation, survival, migration and invasion (Lu et al. 2012). A diverse array of specialized cell surface receptors binds extrinsic factors such as mitogens, differentiation factors, cell membrane-bound molecules or extracellular matrix (ECM) proteins, and then transmit signals through the plasma membrane (Vogel et al. 2006). The Type I collagen, one of the most abundant ECM constituents, exhibits high density and altered architecture in cancer and is causally linked to tumor formation and metastasis (Provenzano et al. 2006, 2008). Many of the cell surface receptors belong to the family of RTKs characterized by an extracellular ligand binding domain, a single transmembrane domain and a catalytic tyrosine kinase domain. One subfamily of RTKs are the Discoidin Domain Receptors (DDRs) defined by the discoidin homology region in their extracellular domain and represented by two members: the discoidin domain receptor 1 and 2 (DDR1 and DDR2) (Fig.1.7).
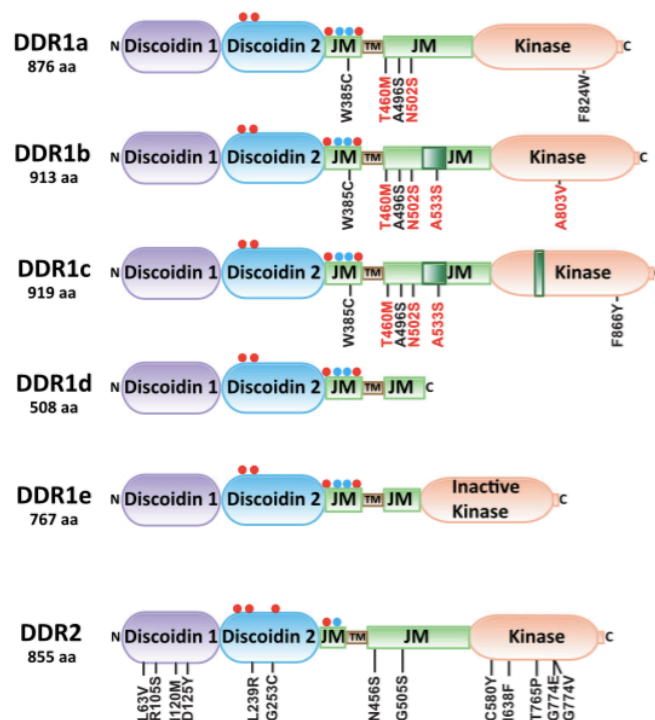
Figure 1.7

Chapter I

DDR1 was first identified in the *Dictyostelium discoideum* and was shown to mediate cell aggregation (Rammal et al. 2016; Vogel et al., 1997). DDR2 shares highly conserved sequences with DDR1 (Carafoli et al., 2009). Both receptors are activated upon binding to collagen. In particular, DDR1 is activated by various types of collagen including type I, IV, V, VI, and VIII, whereas DDR2 is only activated by fibrillar collagens as type I, III, and type X (Shrivastava et al., 1997; Vogel et al., 1997; Leitinger and Kwan, 2006). In contrast with other RTKs as EGFR and fibroblast growth factor receptor (FGFR), which display a rapid and transient activation (Dengjel et al., 2007), DDR1 and DDR2 are unique in that they exhibit a delayed and sustained phosphorylation upon binding to collagen (Vogel et al., 1997). Furthermore, many RTKs undergo negative regulation such as receptor/ligand internalization and subsequent degradation or dephosphorylation by phosphatases (Avraham and Yarden, 2011). In the case of DDRs, phosphorylation levels may persist up to 18 h (Vogel et al., 1997).

Notably, numerous studies have linked the expression, activation and dysregulation of DDRs to the progression of diverse tumors (Rammal et al. 2016; Valiathan et al., 2012; Ford et al., 2007). In this context, recently it has been discovered that, in breast cancer cells and in transfected fibroblasts, the collagen receptor DDR1 associates with the IGF-IR in an IGF-I dependent manner, suggesting that the growth factor contributes to a functional cross-talk between IGF-IR and DDR1 in cancer (Malaguarnera et al. 2015). Of note, this interaction amplifies the stimulatory actions of IGF-I toward breast cancer cell proliferation, migration and colony formation (Matà et al. 2016; Malaguarnera et al. 2015).

1.5 Aim of the study

The aim of the present study was to provide novel insights into the molecular mechanisms by which IGF-I/IGF-IR system may trigger stimulatory responses, as gene expression changes, chemotactic motility and migration, in IST-MES1 mesothelioma and A549 lung cancer cells.

Chapter II

Materials and Methods

2.1 Reagents

IGF-I, SB202190 (SB) and collagen I from rat tail were obtained from Sigma-Aldrich Inc. (Milan, Italy). PD98059 (PD) and 3-bromo-5-t-butyl-4-hydroxybenzylidenemalonitrile (AG1024) were purchased from Calbiochem (DBA, Milan, Italy). All compounds were solubilized in dimethylsulfoxide, except PD and IGF-I, which were dissolved in ethanol and in water, respectively. DDR1-IN-1 dihydrochloride (DDR-1 in) was purchased from Tocris Bioscience (Space, Milan, Italy).

2.2 Cell cultures

IST-MES1 malignant mesothelioma cells were kindly provided by Dr. Orengo (Istituto Nazionale per la Ricerca sul Cancro, Genova, Italy). Cells were previously characterized (Orengo et al. 1999) and were grown in Nutrient Mixture F-10 Ham (Ham's F-10) medium supplemented with 10% fetal bovine serum (FBS) and 100 μg/ml penicillin/streptomycin. A549 lung cancer cells were obtained by ATCC, used <6 months after resuscitation and maintained in DMEM/F12 (Dulbecco's modified Eagle's medium) supplemented with phenol red 10% FBS and 100 μg/ml penicillin/streptomycin. All cell lines were cultured at 37°C in 5% CO_2 and switched to medium without serum the day before immunoblots and reverse transcription-PCR experiments.

2.3 Plasmids and luciferase assays

The GPER luciferase expression vector (promGPER) was previously described (Recchia et al. 2011). The CTGF luciferase reporter plasmid (promCTGF) (-1999/+ 36)-luc was a gift from Dr. Chaqour. EGR1-luc plasmid, containing the -600 to +12 5'-flanking sequence from the human EGR1 gene, was kindly provided by Dr. Safe (Texas A&M University). The plasmid DN/cfos, which encodes a c-fos mutant that heterodimerizes with c-fos dimerization partners but does not allow DNA biding (Gerdes et al. 2006), was a kind gift from Dr C Vinson (NIH, Bethesda, MD, USA). The Renilla luciferase expression vector pRL-TK (Promega, Milan, Italy) was used as internal transfection control. Cells ($1x10^5$) were plated into 24-well dishes with 500 μl/well culture medium containing 10% FBS. Transfection were performed using X-treme GENE 9 DNA transfection reagent as recommended by the manufacturer (Roche Diagnostics, Milan, Italy), with a mixture containing 0.5 μg of reporter plasmid and 10 ng of pRL-TK. After 24 h, treatments were added and cells were incubated for 18 h. Luciferase activity was measured using the Dual Luciferase Kit (Promega, Milan, Italy) according to the manufacturer's recommendations. Firefly luciferase activity was normalized to the internal transfection control provided by the Renilla luciferase activity. Normalized relative light unit values obtained from cells treated with vehicle were set as 1-fold induction upon which the activity induced by treatments was calculated.

2.4 Gene silencing experiments

Cells were plated onto 10-cm dishes and transfected by X-treme GENE 9 DNA Transfection Reagent for 24 h before treatments with a control vector, a specific shRNA sequence for each target gene. The shIGF-IR and the respective control plasmids (shRNA) were purchased from SA Bioscience Corp. (Frederick, MD, USA) and used according to the manufacturer's recommendations. The short hairpin (sh)RNA constructs to knock down the expression of

Chapter II

GPER and the unrelated shRNA control construct have been described previously (Albanito et al. 2008).

2.5 Gene expression studies

Total RNA was extracted and cDNA was synthesized by reverse transcription as previously described (Rigiracciolo et al 2015, 2016). The expression of selected genes was quantified by real-time PCR using Step One sequence detection system (Applied Biosystems, Milan, Italy). Gene-specific primers were designed using Primer Express version 2.0 software (Applied Biosystems Inc. Milan, Italy) and are as follows: GPER Fwd 5′-ACACACCTGGGTGGACACAA-3′ and Rev 5′-GGAGCCAGAAGCCACATCTG-3'; HES-1 Fwd 5′-TCAACACGACACCGGATAAA-3′ and Rev 5′-CCGCGAGCTATCTTTCTTCA-3′; NOTCH 1 Fwd 5′-AATGGCGGGAAGTGTGAAGC-3′ and Rev 5′-GCATAGTCTGCCACGCCTCT-3′; MTN-2 Fwd 5′-CTCCGAGTGGGCCAGTAAAG-3′ and Rev 5′- CTGGCTCAGATTCTGTTGGCT-3′; FBN-1 Fwd 5′-GCCGCATATCTCCTGACCTC-3′ and Rev 5′-GTCGATACACGCGGAGATGT-3′; 18S Fwd 5′- GGCGTCCCCCAACTTCTTA-3′ and Rev 5′-GGGCATCACAGACCTGTTATT-3′. Assays were performed in triplicate and the results were normalized for 18S expression and then calculated as fold induction of RNA expression.

2.6 Western blot analysis

Cells were processed according to a previously described protocol (Santolla et al. 2015) to obtain protein lysate that was electrophoresed through a reducing SDS/10% (w/v) polyacrylamide gel, electroblotted onto a nitrocellulose membrane and probed with primary antibodies against antiphosphotyrosine antibody (4G10) (Merck Millipore, Milan, Italy), IGF-IR (7G11), GPER (N-15), CTGF (L-20), phosphorylated ERK1/2 (E-4), ERK2 (C-14), NOTCH 1 (C-20), EGR1 (588), phosphorylated p-38 (D-8), p-38 (A-12), β-actin (C2), (Santa

21

Cruz Biotechnology, DBA, Milan, Italy). Proteins were detected by horseradish peroxidase-linked secondary antibodies (DBA, Milan, Italy) and revealed using the ECL System (GE Healthcare).

2.7 Co-immunoprecipitation

Cells were lysed using 200 µl RIPA buffer with a mixture of protease inhibitors containing 1.7mg/ml aprotinin, 1mg/ml leupeptin, 200mmol/L phenylmethylsulfonyl fluoride, 200mmol/L sodium orthovanadate, and 100mmol/L sodium fluoride. A total of 100 µg proteins were incubated for 2 h with 2 µg of the appropriate antibody (GPER, N-15; IGF-1R, 7G11) and 20 µl of protein A/G agarose immunopreciptation reagent (Santa Cruz Biotechnology, DBA, Milan, Italy). Samples were centrifuged at 13,000 rpm for 5 min at 4°C to pellet beads. After four washes in PBS, samples were resuspended in RIPA buffer with protease inhibitors and SDS sample buffer. Western Blot analysis was performed as described above.

2.8 Migration assay

Migration assays were performed using Boyden chambers (Costar Transwell, 8 mm polycarbonate membrane, Sigma Aldrich, Milan, Italy). Cells were transfected in regular growth medium. After 8 h, cells were trypsinized and seeded in the upper chambers. Treatments were added to the medium without serum in the bottom wells where applicable, cells on the bottom side of the membrane were fixed and counted 8 hours after seeding.

2.9 Time-lapse microscopy

Cells (1×10^5) were seeded in 6-well plates and maintained in regular growth medium for 24 h. For knockdown experiments, cells were transfected for 24 h with shRNA constructs directed against IGF-IR or GPER and with an unrelated shRNA construct. Thereafter, cells were treated and transferred into a time-lapse microscopy platform, equipped with a heated stage chamber (Cytation™3 Cell Imaging Multi-Mode Reader, Biotek, Winooski, VT). Cells were maintained at routine incubation settings (37 °C, 5% CO_2) using temperature and gas controllers. To evaluate chemotaxis the images were recorded using Cytation 3 Cell Imaging Multimode Reader and the software Gen5 (BioTek, Winooski, VT) in 10 min intervals for 8 hours. Then, the images were processed as a movie using the software Adobe Creative Cloud Premier Pro CC. Frames collected every 10 minutes are displayed at a rate of 10 frames s^{-1}.

2.10 Statistical analysis

Statistical analysis was performed using ANOVA followed by Newman-Keuls' testing to determine differences in means. $P < 0.05$ was considered as statistically significant.

Chapter III

Results

3.1 IGF-I stimulates GPER expression through IGF-IR/ERK/p-38 transduction signaling

On the basis of previous studies showing that IGF-I triggers stimulatory effects in malignant mesothelioma as well as in lung cancer cells (Kim et al. 2014; Liu et al. 2004), we began our study evaluating the transduction signaling activated by IGF-I in IST-MES1 mesothelioma and A549 lung cancer cells, which were used as model system.
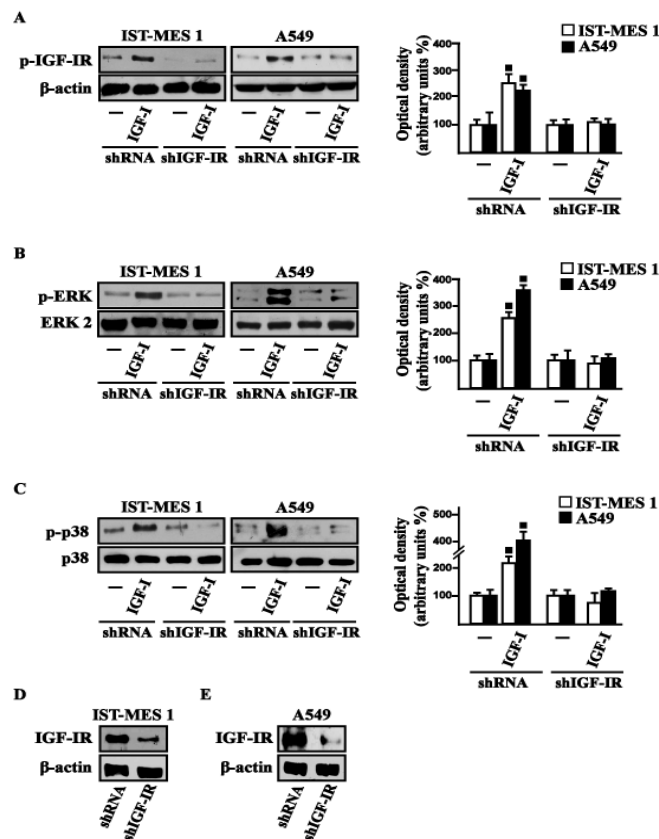

Figure 3.1 IGF-IR (A), ERK (B) and p-38 (C) phosphorylation in cells transfected for 24 h with shRNA or shIGF-IR treated or not with vehicle (-) or 100 ng/ml IGF-I for 15 min. (D-E) Efficacy of IGF-IR silencing. Data shown are the mean ± SD of three independent experiments. (■) $p<0.05$ for cells receiving vehicle (-) versus treatments.

First, we determined that in both cell types IGF-I induces the phosphorylation of IGF-IR and both ERK and p-38. As expected, these responses were no longer observed after IGF-IR silencing (Fig. 3.1).

The activation of ERK triggered by IGF-I was abolished in the presence of the IGF-IR inhibitor AG and the MEK inhibitor PD, but it still persisted using the p-38 inhibitor SB. The phosphorylation of p-38 was prevented by AG and SB, but not in the presence of PD (Fig. 3.2).
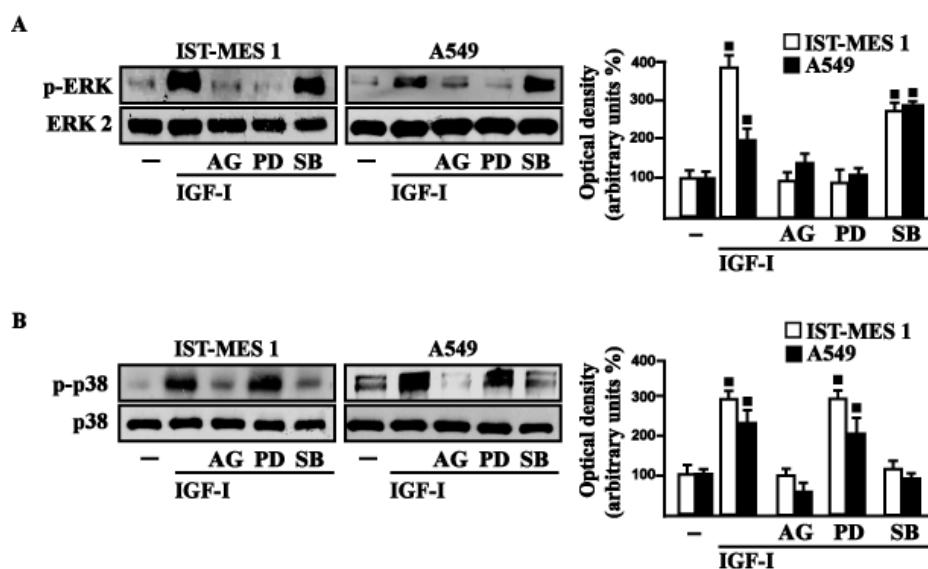
Figure 3.2 ERK (A) and p-38 (B) activation in cells treated for 15 min with vehicle (-) or 100 ng/ml IGF-I alone and in combination with either 1 μM IGF-IR inhibitor tyrphostin AG1024 (AG), or 1 μM MEK inhibitor PD98059 (PD) or 1 μM p38 inhibitor SB202190 (SB). Side panels show densitometric analysis of the blots normalized to β-actin, ERK2 and p38 that served as loading controls respectively for pIGF-IR, pERK and p-p38. Data shown are the mean ± SD of three independent experiments. (■) $p < 0.05$ for cells receiving vehicle (-) versus treatments.

On the basis of our previous data showing that IGF-I signaling cooperates with several GPCR family members, including GPER, toward cancer progression (Lappano and Maggiolini 2011; De Marco et al. 2013), we evaluated whether IGF-I regulates GPER expression in IST-MES1 and A549 cells. In this regard, time-course experiments demonstrated that IGF-I up-regulates GPER at both mRNA (Fig. 3.3A) and protein levels (Fig. 3.3B). Moreover, we ascertained

that these responses to IGF-I occurred through IGF-IR, as the induction of GPER mRNA (data not shown) and protein levels (Fig. 3.3C-E) was abolished by knocking-down IGF-IR expression. Recapitulating the aforementioned findings, the transactivation of the GPER promoter by IGF-I was prevented by IGF-IR silencing (Fig. 3.3F), and the IGF-I induced GPER protein up-regulation was abrogated in the presence of AG, PD and SB (Fig. 3.3G). Taken together, these results indicate that the IGF-I/IGF-IR transduction pathway stimulates GPER expression through ERK and p-38 signaling. In order to further investigate this functional cross-talk between IGF-IR and GPER, we performed co-immunoprecipitation studies determining that IGF-I triggers also a direct interaction between these receptors in both IST-MES1 and A549 cells upon either 1 h (data not shown) or 8 h treatment with IGF-I (Fig. 3.3H-I), thus suggesting that the interaction between IGF-IR and GPER may occur without a newly protein expression of GPER.
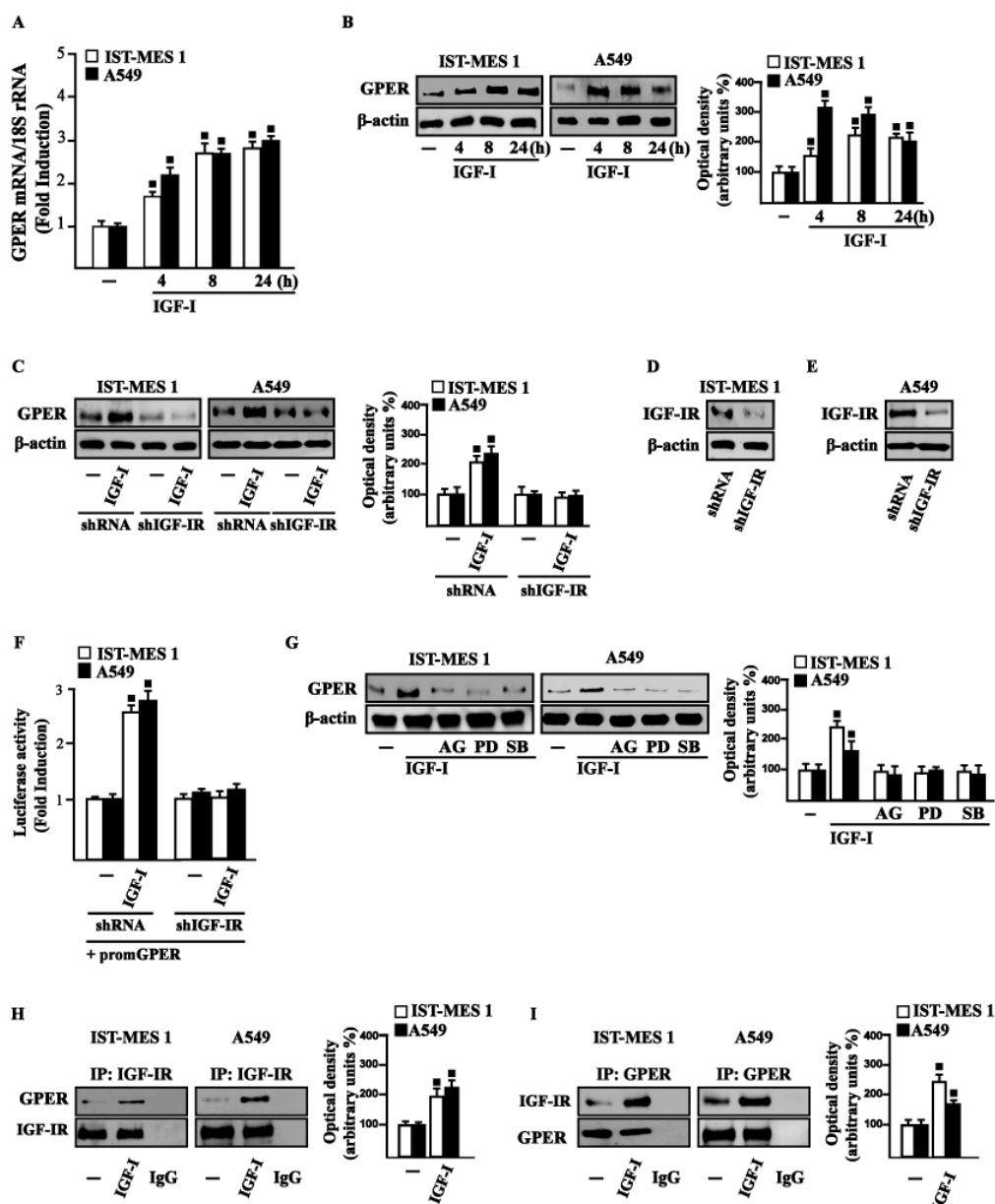
Figure 3.3 (A) mRNA expression of GPER in cells treated with either vehicle (-) or 100 ng/ml IGF-I, as evaluated by real-time PCR. Results obtained from experiments performed in triplicate were normalized for 18S expression and shown as fold change of RNA expression compared to cells treated with vehicle. (B) GPER protein levels were evaluated by immunoblotting in cells treated with either vehicle (-) or 100 ng/ml IGF-I, as indicated. (C) GPER protein expression in cells transfected for 24 h with either shRNA or shIGF-IR and then treated for 8 h with vehicle (-) or 100 ng/ml IGF-I. (D-E) Efficacy of IGF-IR silencing. (F) Cells were transfected for 24 h with shRNA or shIGF-IR together with the GPER promoter construct. Then, cells were treated for 18 h with vehicle (-) or 100 ng/ml IGF-I. The luciferase activities were normalized to the internal transfection control, and values of cells receiving vehicle (-) were set as one fold induction upon which the activity induced by treatments was calculated. (G) GPER protein levels in cells treated for 8 h with vehicle (-) or 100 ng/ml IGF-I alone or in combination with 1 μM IGF-IR inhibitor tyrphostin AG1024 (AG), 1 μM MEK inhibitor PD98059 (PD) and 1 μM p38 inhibitor SB202190 (SB). Side panels show densitometric analysis of the blots normalized to β-actin. (H-I) Co-immunoprecipitation studies performed in cells treated for 8 h with vehicle (-) or 100 ng/ml IGF-I, as indicated. In control samples, non-specific IgG was used instead of the primary antibody. (H) Side panel show densitometric analysis of the blot normalized to IGF-IR. (I) Side panel show densitometric analysis of the blot normalized to GPER. Data shown are the mean ± SD of three independent experiments. (■) $p < 0.05$ for cells receiving vehicle (-) versus treatments.

3.2 IGF-I triggers the expression of GPER target genes

Considering that in our previous study (Pandey et al. 2009) we demonstrated that GPER mediates a specific gene signature, here we evaluated whether, in IST-MES1 and A549 cells, IGF-I was able to affect the expression of certain GPER target genes like CTGF and EGR1, which have been involved in fibrotic responses in mesothelioma and lung cancer cells (Fujii et al. 2012; Wang et al. 2014; Shan et al. 2015). Indeed, in time-course experiments we found that IGF-I increases the mRNA and protein levels of both CTGF and EGR1 (Fig. 3.4).
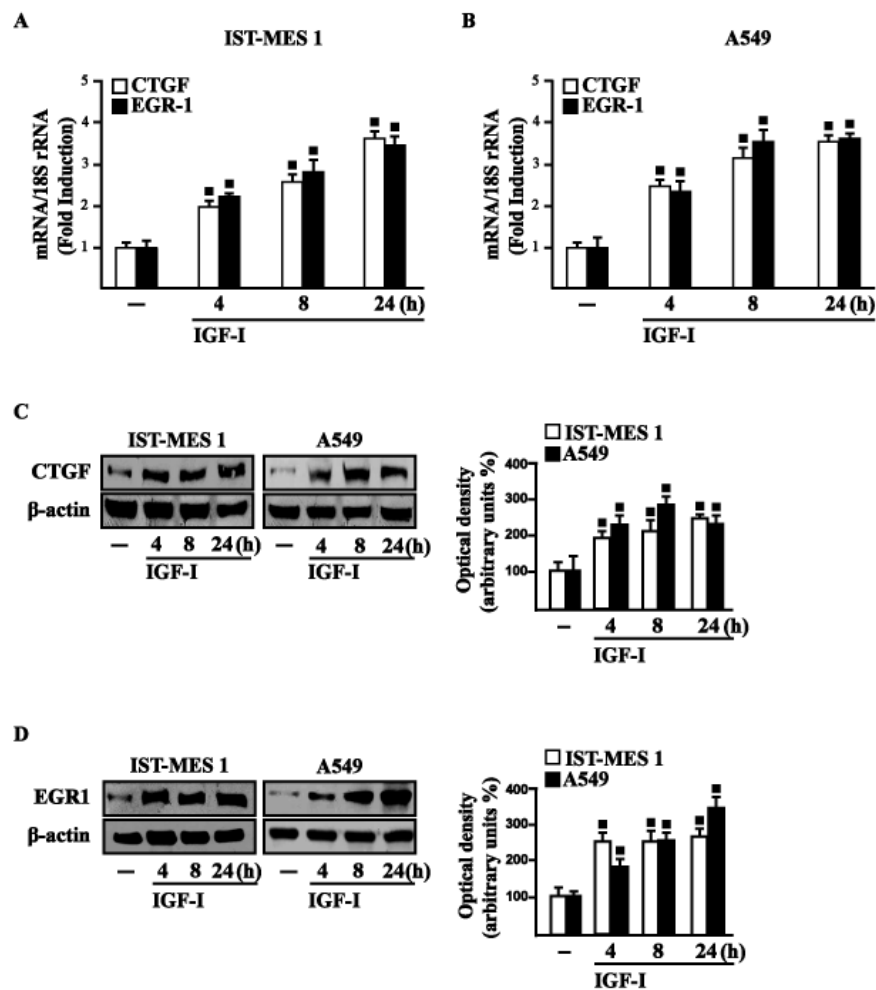
Figure 3.4 (A-B) mRNA expression of CTGF and EGR1 in cells treated with either vehicle (-) or 100 ng/ml IGF-I, as evaluated by real-time PCR. Results obtained from experiments performed in triplicate were normalized for 18S expression and shown as fold change of RNA expression compared to cells treated with vehicle. CTGF (C) and EGR1 (D) protein levels were evaluated by immunoblotting in cells treated with vehicle (-) or 100 ng/ml IGF-I, as indicated. Side panels show densitometric analysis of the blots normalized to β-actin and each data point represents the mean ± SD of three independent experiments. (■) p<0.05 for cells receiving vehicle (-) versus treatments.
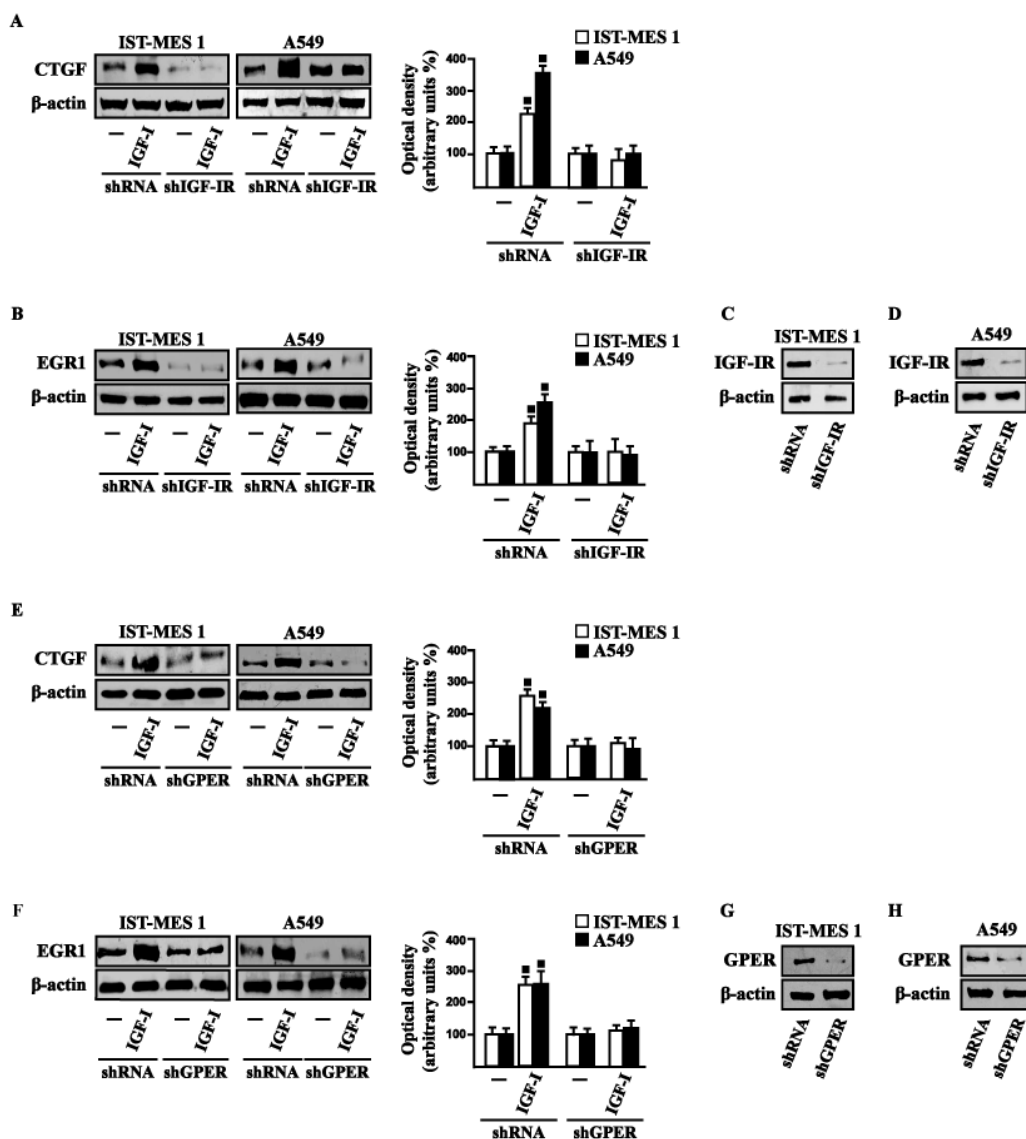
Figure 3.5 (A-F) CTGF and EGR1 protein levels in cells transfected for 24 h with shRNA, shIGF-IR or shGPER and then treated for 8 h with either vehicle (-) or 100 ng/ml IGF-I. Efficacy of IGF-IR (C-D) and GPER (G-H) silencing. Side panels show densitometric analysis of the blots normalized to β-actin. Data shown are the mean ± SD of three independent experiments. (■) p<0.05 for cells receiving vehicle (-) versus treatments.

Next, we determined that this action of IGF-I involves not only the IGF-IR but also GPER, as the silencing of each of these receptors prevented gene changes (Fig. 3.5).

In accordance with these observations, the IGF-I transactivation of CTGF (Fig. 3.6A) and EGR1 (Fig. 3.6B) promoters required both IGF-IR and GPER, as demonstrated by knocking down the expression of these receptors.

Chapter III

As c-fos plays a main role in the up-regulation of GPER target genes (Pandey et al. 2009; Maggiolini and Picard 2010), we next determined that the promoter transactivation of both CTGF and EGR1 is abrogated by co-transfecting a dominant-negative form of c-fos (DN/c-fos) in IST-MES1 and A549 cells (Fig. 3.6C). Collectively, these findings provide novel mechanisms through which IGF-I/IGF-IR transduction signaling regulates GPER target genes like CTGF and EGR1 in mesothelioma and lung cancer cells.
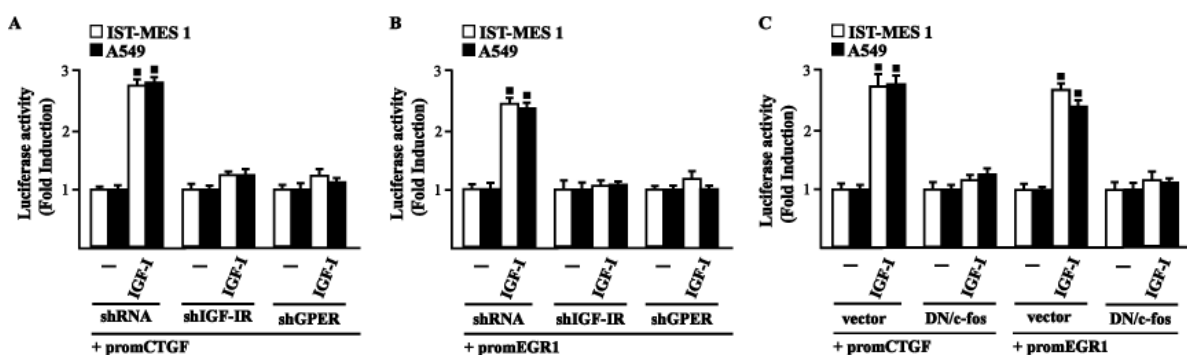
Figure 3.6 (A-B) Cells were transfected for 24 h with shRNA, shIGF-IR or shGPER together with the CTGF or EGR1 promoter construct. Then, cells were treated for 18 h with vehicle (-) or 100 ng/ml IGF-I. (C) Cells were transfected for 24 h with a dominant negative form of c-fos (DN/c-fos) together with the CTGF or EGR1 promoter construct. Then, cells were treated for 18 h with vehicle (-) or 100 ng/ml IGF-I. The luciferase activities were normalized to the internal transfection control, and values of cells receiving vehicle (-) were set as one fold induction upon which the activity induced by treatments was calculated. Data shown are the mean ± SD of three independent experiments. (■) $p < 0.05$ for cells receiving vehicle (-) versus treatments.

3.3 IGF-IR and GPER are both involved in IGF-I regulation of DDR1 target genes

Considering that in diverse model systems IGF-I stimulates the synthesis of collagen (Blackstock et al. 2014; Sukhanov et al. 2011; Sukhanov et al. 2007), we next established that

Chapter III

IGF-I regulates in both IST-MES1 and A549 cells the mRNA expression of COL1A1 (Fig. 3.7A) that encodes the major component of type I collagen (Inamori et al. 2007). We previously reported that IGF-IR functionally interacts with DDR1, which is activated by various collagen types including type I collagen. Therefore, we first ascertained that, in both IST-MES1 and A549 cells, several DDR1 target genes such as matrilin-2 (MATN-2), fibrillin-1 (FBN-1), NOTCH 1 and HES-1, are induced by the DDR1 agonist COL1 (Fig. 3.7B-C) and abrogated by the DDR1 inhibitor (DDR1 IN) (Fig. 3.7D-E).
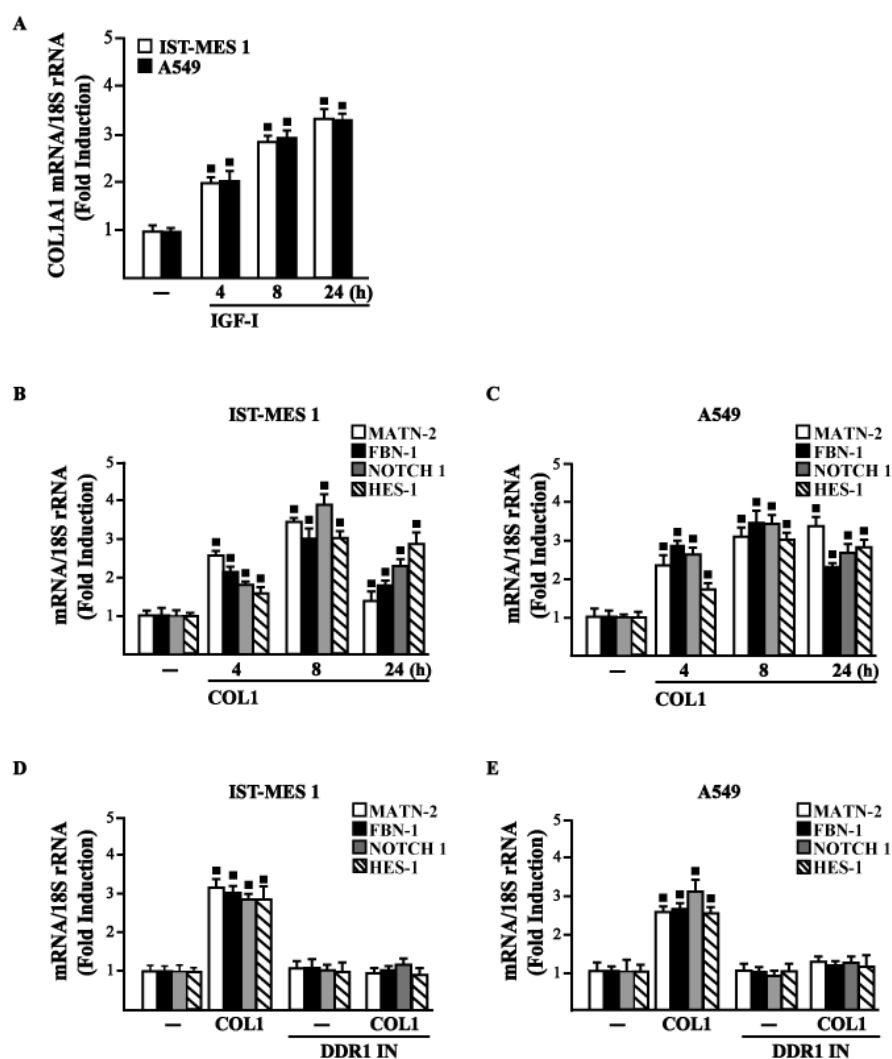
Figure 3.7 (A) mRNA expression of COL1A1 in IST-MES 1 and A549 cells treated with vehicle (-) or 100 ng/ml IGF-I, as evaluated by real-time PCR. mRNA expression of MATN-2, FBN-1, NOTCH 1 and HES-1 in IST-MES 1 (B, D) and A549 (C, E) cells treated with vehicle (-) or 10 μg/ml COL1 alone or in combination with 1 μM DDR1 inhibitor (DDR1 IN), as indicated. Results obtained from experiments performed in triplicate were normalized for 18S expression and shown as fold change of RNA expression compared to cells treated with vehicle. (■) $p < 0.05$ for cells receiving vehicle (-) versus treatments.

Chapter III

Then, we assessed that these DDR1 target genes are also stimulated by IGF-I (Fig. 3.8A-B) and that this response was inhibited by DDR1 IN (Fig. 3.8C-D) as well as by silencing IGF-IR (Fig. 3.8E-F) or GPER (Fig. 3.8G-H).
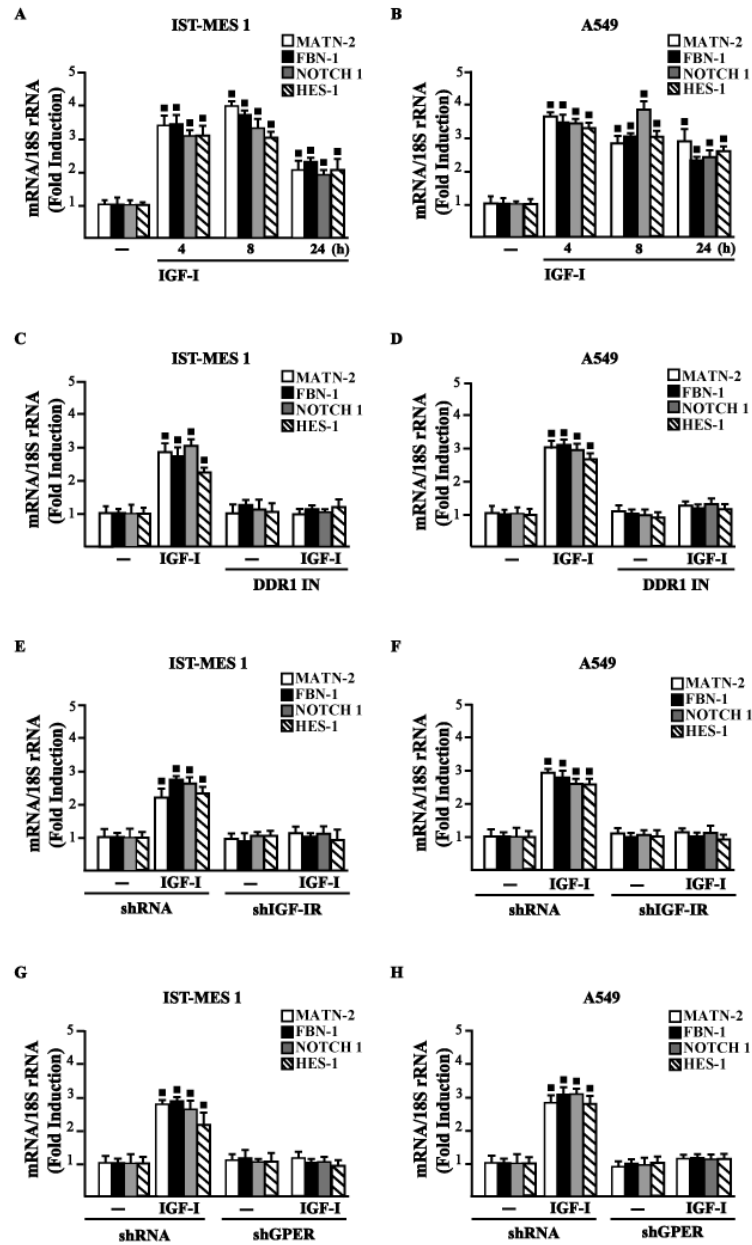
Figure 3.8 (A-D) mRNA expression of MATN-2, FBN-1, NOTCH 1 and HES-1 in cells treated with vehicle (-) or 100 ng/ml IGF-I alone or in combination with 1 μM DDR1 inhibitor (DDR1 IN), as indicated. (E-H) mRNA expression of MATN-2, FBN-1, NOTCH 1 and HES-1 in cells transfected for 24 h with shRNA, shIGF-IR or shGPER and then treated for 8 h with vehicle (-) or 100 ng/ml IGF-I. Results obtained from experiments performed in triplicate were normalized for 18S expression and shown as fold change of RNA expression compared to cells treated with vehicle. (■) $p < 0.05$ for cells receiving vehicle (-) versus treatments.
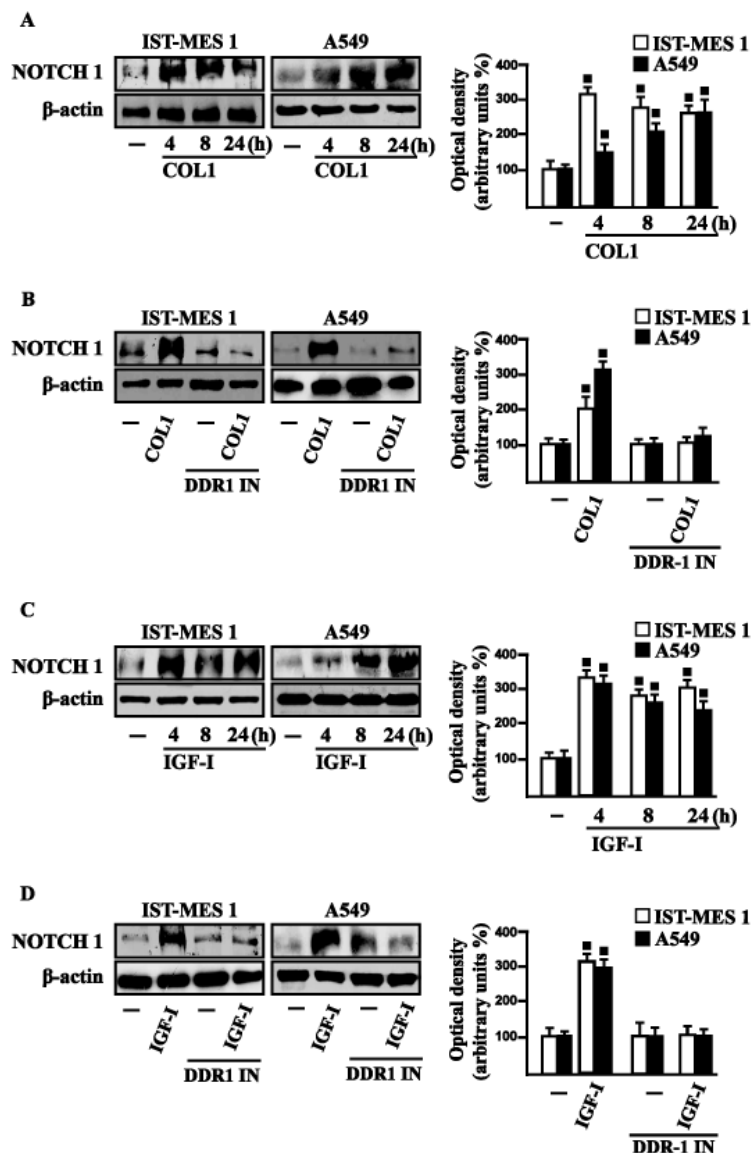
Chapter III

In accordance with these findings, we determined that the NOTCH 1 protein induction by COL1 and IGF-I is prevented in the presence of the DDR1 IN in IST-MES1 and A549 cells (Fig. 3.9).

Figure 3.9 (A) NOTCH 1 protein levels in cells treated with vehicle (-) or 10 μg/ml COL1, as indicated. (B) NOTCH 1 protein levels in cells treated for 8 h with vehicle (-) or 10 μg/ml COL1 alone and in combination with 1 μM DDR1 inhibitor (DDR1 IN). (C) NOTCH 1 protein levels in cells treated with vehicle (-) or 100 ng/ml IGF-I, as indicated. (D) NOTCH 1 protein levels in cells treated for 8 h with vehicle (-) or 100 ng/ml IGF-I alone and in combination with 1 μM DDR1 inhibitor (DDR1 IN). Side panels show densitometric analysis of the blots normalized to β-actin and each data point represents the mean ± SD of three independent experiments. (■) $p<0.05$ for cells receiving vehicle (-) versus treatments.

Accordingly, IGF-I was not able to trigger NOTCH 1 protein expression when IGF-IR (Fig. 3.10A-C) or GPER (Fig. 3.10D-F) was silenced. Altogether, these results indicate that, in

Chapter III

both mesothelioma and lung cancer cells, IGF-I may up-regulate DDR1 target genes, and that

this action involves not only IGF-IR but also a cross-talk with GPER.
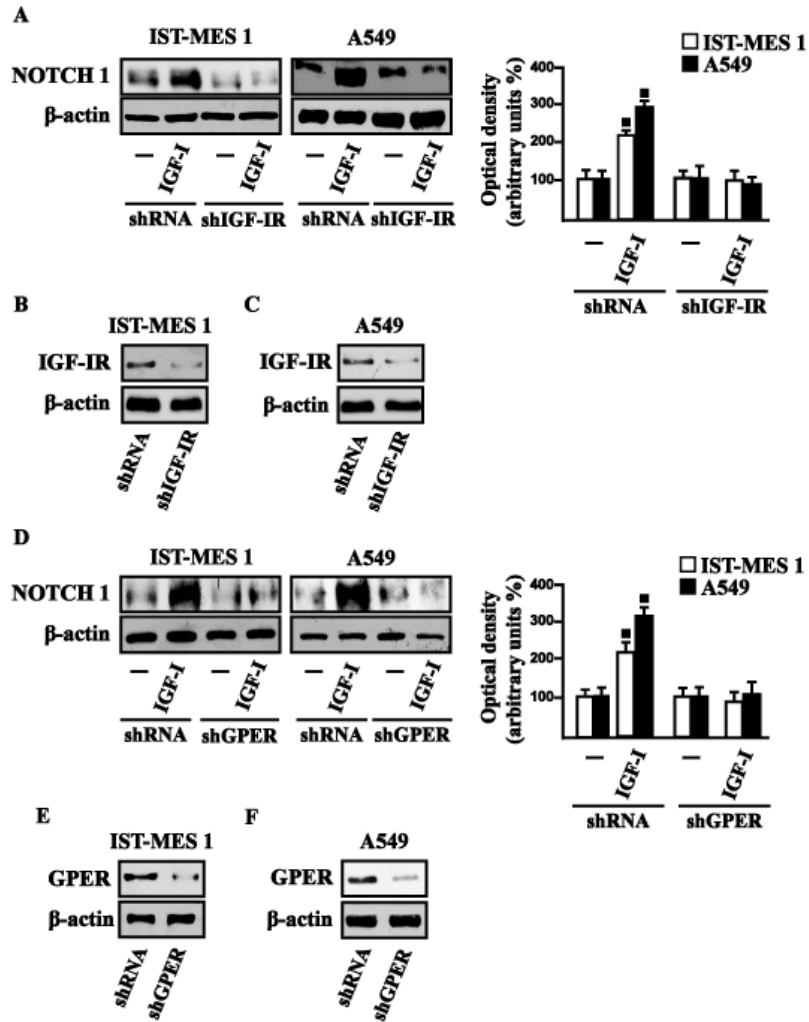
Figure 3.10 NOTCH 1 protein levels in cells transfected for 24 h with shIGF-IR (A) or shGPER (D) and then treated for 8 h with vehicle (-) or 100 ng/ml IGF-I. Efficacy of IGF-IR (B-C) and GPER (E-F) silencing. Side panels show densitometric analysis of the blots normalized to β-actin. (■) $p<0.05$ for cells receiving vehicle (-) versus treatments.

3.4 DDR1, IGF-IR and GPER contribute to the chemotaxis and migration of mesothelioma and lung cancer cells

Previous studies have reported that IGF-I stimulates chemotactic and chemokinetic motility in mesothelioma cells (Liu and Klominek 2004). Moreover, DDR1 also plays an important role in promoting cell-cell interactions and cell migration in various cell contexts (Wang et al. 2009; Yeh et al. 2011; Eswaramoorthy et al. 2010; Hidalgo-Carcedo et al. 2011). Further extending these data, in IST-MES1 cells, we found that IGF-I induces chemotactic motility through DDR1, as this response was abolished by DDR1 IN (Fig. 3.11A). Moreover, we ascertained that the chemotactic motility induced by IGF-I requires also IGF-IR and GPER as the aforementioned effect was prevented silencing the expression of these receptors (Fig. 3.11B).

B

Figure 3.11. (A) Chemotactic motility in cells treated for 8 h with vehicle (-) or 100 ng/ml IGF-I, alone or in presence of 1 μM DDR1 inhibitor (DDR1 IN). (B) Chemotactic motility in cells transfected for 24 h with shGPER or shIGF-IR, as indicated, and then treated for 8 h with vehicle (-) or 100 ng/ml IGF-I. Images shown were captured from time lapse microscopy experiments and are representative of three random fields from three independent experiments.

Similar findings occurred in A549 cells (data not shown). Likewise, we determined that IST-MES1 and A549 cell migration induced by both IGF-I and COL1 is abolished using DDR1 IN (Fig. 3.12A), whereas the silencing of IGF-IR or GPER abolished cell migration triggered by IGF-I, as determined by Boyden chamber assay (Fig. 3.12B). Collectively, our data indicate novel cross-talk and biological functions exerted by IGF-I toward tumor progression.
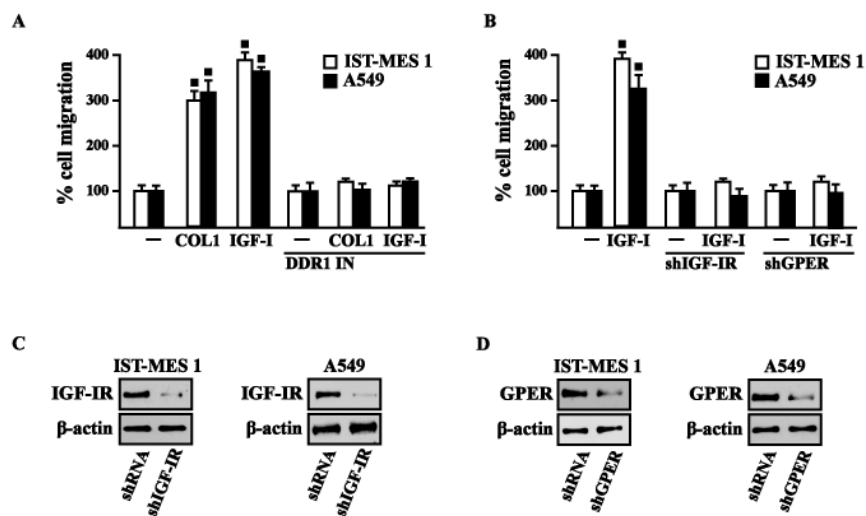
Figure 3.12. *COL1 and IGF-I stimulate IST-MES 1 and A549 cell migration through DDR1, IGF-IR and GPER.* (A) The migration of IST-MES 1 and A549 cells upon 8 h treatment with vehicle (-), 10 µg/ml COL1 or 100 ng/ml IGF-I alone and in combination with 1 µM DDR1 inhibitor (DDR1 IN), as evaluated by Boyden Chamber assay. (B) The migration of IST-MES 1 and A549 cells induced by 8 h treatment with 100 ng/ml IGF-I was prevented knocking down IGF-IR and GPER expression, as evaluated by Boyden Chamber assay. Efficacy of IGF-IR (C-D) and GPER (E-F) silencing. Values represent the mean ± SD of three independent experiments. (●) indicates $p < 0.05$ for cells treated with vehicle (–) versus treatments.

Chapter IV

Discussion

In the present study we provide novel evidence regarding the molecular mechanisms by which IGF-I triggers biological responses in mesothelioma and lung cancer cells. In particular, we show a complex functional cooperation involving IGF-IR, GPER and DDR1 through which IGF-I up-regulates first the expression of COL1A1 and certain DDR1 target genes, thereafter stimulating cancer cell motility and chemotactic response (Fig. 3.13).
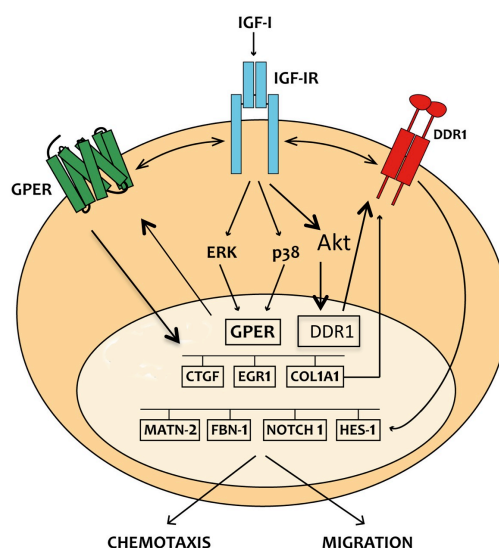
Figure 3.13. Schematic representation of the signaling network between IGF-IR, GPER and DDR1 activated by IGF-I. IGF-I stimulates the expression of GPER and its target genes, then IGF-IR and GPER trigger the IGF-I regulation of DDR1 target genes. The functional cross-talk of IGF-IR, GPER and DDR1 contributes to the chemotaxis and migration observed in cancer cells.

Lung cancer is a high heterogeneous tumor that can arise in different sites of the bronchial tree and one of the most common types of human malignancies (Travis et al. 2011; Guo et al. 2015). The incidence of lung cancer depends on toxic effects of inhaled substances such as tobacco, asbestos, arsenic, cadmium, nickel and silica (Ahuja et al. 2015). The environmental pollutant asbestos is also considered the main cause of the insurgence of malignant

mesothelioma (MM), which is a rare and aggressive tumor that springs from mesothelial cells lining lung, pleura or peritoneum (Rajer et al. 2014; Carbone et al. 2012; Rascoe et al. 2012; Lenters et al. 2011; Straif et al. 2009). The deposition of asbestos fibers has been also related to chronic inflammatory processes as well as to pulmonary fibrosis, which in turn may create a favorable environment for the development of lung and pleura malignancies (Rascoe et al. 2012; Mossman et al. 2011). As it concerns the multifaceted mechanisms and factors involved in pulmonary fibrosis and neoplasia, an increased expression and activation of DDR1 have been reported (Avivi-Green et al. 2006; Lemeer et al. 2012; Matsuyama et al. 2005; Heinzelmann-Schwarz et al. 2004). To date, DDR1 has been shown to play an important role in cancer progression by regulating the interactions of tumor cells with the surrounding collagen matrix, therefore leading to pro-migratory and pro-invasive responses (Valiathan et al. 2012). Furthermore, collagen activated DDR1 triggers diverse pro-survival pathways toward anti-apoptotic, proliferative and aggressive features in cancer cells (Valiathan et al. 2012). In this regard, it should be noted that several types of collagen are able to bind to and activate DDR1, which then regulates cell and tissue homeostasis acting as a collagen sensor (Valiathan et al. 2012; Vogel et al. 2006). Of note, an abnormal expression and deposition of collagen has been associated with cancer development (Tavazoie et al. 2008; Ramaswamy et al. 2003). As it concerns the synthesis and extracellular accumulation of diverse types of collagen, cytokines and growth factors like IGF-I, the epidermal growth factor (EGF) and the transforming growth factor-βl have been reported to promote these effects (Blackstock et al. 2014; Sukhanov et al. 2011; Sukhanov et al. 2007; Grande et al. 1997). Notably, we previously showed that, in breast cancer cells, IGF-I may upregulate DDR1 expression through a signaling pathway involving the DDR1 regulatory miR-199a-5p (Matà et al. 2016). Moreover, the activation of one of the main IGF-I transduction signaling, the IGF-IR/PI3K/Akt cascade, inhibits miR-199a-5p expression, thus relieving its inhibition upon DDR1 gene and allowing DDR1 upregulation. In turn, DDR1 increases IGF-IR expression

through post-transcriptional mechanisms and amplifies IGF-I downstream signaling and biological effects, such as proliferation, migration and colony formation (Matà et al. 2016). Indeed, previous studies showed that DDR1 directly interacts with IGF-IR, and that this interaction is enhanced by IGF-I stimulation, which promotes rapid DDR1 tyrosine-phosphorylation and co-internalization of the DDR1 - IGF-IR complex (Malaguarnera et al. 2015). This interaction was shown to occur in a panel of human breast cancer cells as well as in mouse fibroblasts (R- cells) co-transfected with the human IGF-IR and DDR1, indicating that it is not cell-specific. Notably, the formation of this DDR1 − IGF-IR complex did not require the presence of collagen, the canonical DDR1 ligand. In addition, the critical role of IGF-IR in DDR1 activation and biological actions is supported by the finding that collagen-dependent DDR1 phosphorylation was impaired in the absence of IGF-IR (Malaguarnera et al. 2015). Extending these previous studies, in the present study we show that IGF-I through the cognate receptor IGF-IR is able to induce COL1A1 expression (Vogel et al. 2006). Moreover, a panel of DDR1 target genes could be also induced by IGF-I through the previously described functional cross-talk involving IGF-IR and DDR1. Taken together, these findings show that DDR1, besides enhancing the activation of typical IGF-IR downstream cascades, the PI3K/Akt and the ERK1/2 cascades, following cell exposure to IGF-I, modifies significantly these IGF-I effects by allowing the induction of typical DDR1 target genes. These effects confirm the relevance of DDR1 in the amplification and diversification of IGF-I signaling pathways in cancer. We have previously demonstrated that IGF-IR may also functionally interact with the non-canonical estrogen receptor GPER. Indeed, through the IGF-IR/PKCδ/ERK/c-fos/AP1 transduction pathway, IGF-I up-regulates GPER, which plays an important role in sustaining proliferation and migration in response to IGF-I in breast and endometrial human cancer cells (De Marco et al. 2013). In close accordance with these findings, we now show that the functional cooperation between IGF-IR and DDR1 also requires GPER, and that both DDR1 and GPER are critical to the chemotactic motility

stimulated by IGF-I in mesothelioma and lung cancer cells. Notably, we now show that GPER and IGF-IR co-immunoprecipitate in lung and mesothelioma cells (Fig. 3.3), indicating that GPER and IGF-IR also interact. Taken together all these data strongly suggest the possible formation of a ternary functional complex involving IGF-IR – DDR1 – GPER. However, further studies are needed to fully elucidate this aspect. These data may be of a particular interest as GPER expression has been associated with negative clinical features and poor survival rates in diverse types of malignancies (Filardo et al. 2006; Smith et al. 2007; Smith et al. 2009; Marjon et al. 2014). In the last years, extensive studies were therefore performed in order to better characterize the role of GPER in cancer development, including the mechanisms and factors involved in its expression. For instance, we determined that EGF and IGF-I, insulin and further tumorigenic factors like hypoxia and endothelin-1 up-regulate GPER expression in diverse cancer cell contexts (De Marco et al. 2013; De Marco et al. 2014; Albanito et al. 2008; Recchia et al. 2011; De Francesco et al. 2013; De Francesco et al. 2014; Bartella et al. 2016). Our present findings provide significant new insights on the well-established role played by the IGF axis in cancer (Belfiore et al. 2009; Belfiore et al. 2011; Kai et al. 2009; Carboni et al. 2005; Franks et al. 2016; Hoang et al. 2004; Liu et al. 2014; Rozengurt et al. 2010; Baserga et al. 2003; Yakar et al. 2005; Novosyadlyy et al. 2010) that involves also the interaction of IGF-IR with other RTKs and GPCRs in diverse tumor histotypes (Lappano and Maggiolini 2011 Rozengurt et al. 2010; Kisfalvi et al. 2009; Akekawatchai et al. 2005). In particular, our findings might be relevant in devising new therapeutical strategies in cancers with a dysregulated IGF system. In the last decade, much effort has been made in targeting the IGF-IR in these malignancies (Gombos et al. 2010). In particular, both small-molecule IGF-IR tyrosine kinase inhibitors, and humanized monoclonal antibodies with blocking activity to the IGF-IR, have been investigated in Phase III trials of advanced non-small cell lung cancers (Scagliotti and Novello 2012). Unfortunately, in spite of very promising preclinical studies, clinical trials have clearly indicated that only a small

minority of malignancies do respond to target therapies when IGF-IR is the sole target (Fidler et al. 2012), because the frequent occurrence of resistance mechanisms arising by the complex signaling network involving the IGF-IR (Scotlandi and Belfiore 2012).

Overall, on the basis of our data the multifaceted signaling network between IGF-IR, GPER and DDR1 could be taken into account in setting innovative combined strategies targeting these pathways in mesothelioma and lung cancers.

References

Ahuja J., Kanne J.P., Meyer C.A. Occupational lung disease. Semin Roentgenol. 2015; 50: 40-51

Akekawatchai C., Holland J.D., Kochetkova M., Wallace J.C., McColl S.R. Transactivation of CXCR4 by the insulin-like growth factor-1 receptor (IGF-1R) in human MDA-MB-231 breast cancer epithelial cells. J Biol Chem. 2005; 280: 39701-8.

Albanito L., Madeo A., Lappano R., Vivacqua A., Rago V., Carpino A., Oprea T.I., Prossnitz E.R., Musti A.M., Andò S., Maggiolini M. G protein-coupled receptor 30 (GPR30) mediates gene expression changes and growth response to 17β- estradiol and selective GPR30 ligand G1 in ovarian cancer cells. Cancer Res. 2007; 67(4):1859-66.

Albanito L., Sisci D., Aquila S., Brunelli E., Vivacqua A., Madeo A., Lappano R., Pandey D.P., Picard D., Mauro L., Andò S., Maggiolini M. Epidermal growth factor induces G protein-coupled receptor 30 expression in estrogen receptor- negative breast cancer cells. Endocrinology, 2008; 149(8):3799–3808.

Arpino G., Weiss H., Lee A.V., Schiff R., De Placido S., Osborne C.K., Elledge R.M. Estrogen receptor-positive, progesterone receptor-negative breast cancer: association with growth factor receptor expression and tamoxifen resistance. J Natl Cancer Inst. 2005; 97(17):1254-61.

Aust A.E., Balla J.C., Hu A.A. Lighty, J.S.; Smith, K.R.; Straccia, A.M.; Veranth, J.M.; Young, W.C. Particle characteristics responsible for effects on human lung epithelial cells. Res. Rep. Health Effects Inst. 2002; 110:1-65;

Avivi-Green C., Singal M., Vogel W.F. Discoidin domain receptor 1-deficient mice are resistant to bleomycin-induced lung fibrosis. Am J Respir Crit Care Med. 2006; 174: 420-7.
Avraham R., Yarden Y. Feedback regulation of EGFR signalling: decision making by early and delayed loops. Nat. Rev. Mol. Cell Biol. 2011; 12(2):104–117.

Azad N., Rojanasakul Y., Vallyathan V. Inflammation and lung cancer: Roles of reactive oxygen/nitrogen species. J. Toxicol. Environ. Health B Crit. Rev. 2008; 11:1–15.

Bartella V., De Francesco E.M., Perri M.G., Curcio R., Dolce V., Maggiolini M., Vivacqua A. The G protein estrogen receptor (GPER) is regulated by endothelin-1 mediated signaling in cancer cells. Cell Signal. 2016; 28: 61-71.

Bartella V., De Marco P., Malaguarnera R., Belfiore A., Maggiolini M. New advances on the functional cross-talk between insulin-like growth factor-I and estrogen signaling in cancer. Cellular Signalling, 2012; 24(8):1515–1521.

Bartke A. Minireview: role of the growth hormone/insulin-like growth factor system in mammalian aging. Endocrinology. 2005; 146(9):3718-23.

References

Barton M. Position paper: the membrane estrogen receptor GPER – clues and questions. Steroids, 2012; 77:935–942.

Baserga R., Peruzzi F., Reiss K. The IGF-1 receptor in cancer biology. Int J Cancer. 2003; 107: 873-7.

Beauchamp M-C., Yasmeen A., Knafo A., Gotlieb W.H. Targeting insulin and insulin-like growth factor pathways in epithelial ovarian cancer. J Oncol. 2010, 2010:257058.

Belfiore A. The role of insulin receptor isoforms and hybrid insulin/IGF-I receptors in human cancer. Curr Pharm Des. 2007; 13(7):671-86.

Belfiore A., Frasca F., Pandini G., Sciacca L., Vigneri R. Insulin receptor isoforms and insulin receptor/insulin-like growth factor receptor hybrids in physiology and disease. Endocr Rev. 2009; 30: 586-623.

Belfiore A., Malaguarnera R. Insulin receptor and cancer. Endocr Relat Cancer, 2011; 18(4):R125-47.

Blackstock C.D., Higashi Y., Sukhanov S., Shai S.Y., Stefanovic B., Tabony A.M., Yoshida T., Delafontaine P. Insulin-like growth factor-1 increases synthesis of collagen type I via induction of the mRNA-binding protein LARP6 expression and binding to the 5' stem-loop of COL1a1 and COL1a2 mRNA. J Biol Chem 2014; 289: 7264-74

Blobel C.P. ADAMs: key components in EGFR signalling and development. Nature Reviews Molecular Cell Biology, 2005; 6(1):32-43.

Bouskine A., Nebout M., Brücker-Davis M., Benahmed M., Fenichel P. Low doses of bisphenol A promote human seminoma cell proliferation by activating PKA and PKG via a membrane G-protein-coupled estrogen receptor. Environmental Health Perspectives, 2009; 17(7):1053-8.

Brambilla E., Travis W.D., Colby T.V., Corrinz B., Shimosato Y. The new World Health Organization classification of lung tumours, 2001; 18: 1059-68.

Campbell N.P., Kindler H.L. Update on malignant pleural mesothelioma. Semin Respir Crit Care Med. 2011; 32:102-10.

Carafoli F., Bihan D., Stathopoulos S., Konitsiotis A.D., Kvansakul M., Farndale R.W., Leitinger B., Hohenester E. Crystallographic insight into collagen recognition by discoidin domain receptor 2. Structure. 2009; 17(12):1573-81.

Carbone M, Kratzke RA, Testa JR. The pathogenesis of mesothelioma. Semin Oncol. 2002; 29: 2– 17.

Carbone M., Ly B.H., Dodson R.F., Pagano I., Morris P.T., Dogan U.A., Gazdar A.F., Pass H.I., Yang H. Malignant mesothelioma: facts, myths, and hypotheses. J Cell Physiol. 2012; 227: 44-58.

References

Carbone M., Ly B.H., Dodson R.F., Pagano I., Morris P.T., Dogan U.A., Gazdar A.F., Pass H.I., Yang H. Malignant mesothelioma: facts, myths, and hypotheses. J Cell Physiol. 2012; 227: 44-58.

Carboni J.M., Lee A.V., Hadsell D.L., Rowley B.R., Lee F.Y., Bol D.K., Camuso A.E., Gottardis M., Greer A.F., Ho C.P., Hurlburt W., Li A., Saulnier M., Velaparthi U., Wang C., Wen M.L., Westhouse R.A., Wittman M., Zimmermann K., Rupnow B.A., Wong T.W. Tumor development by transgenic expression of a constitutively active insulin-like growth factor I receptor. Cancer Res. 2005; 65(9):3781-7.

Carmeci C., Thompson D.A., Ring H.Z., Francke U., Weigel R.J. Identification of a gene (GPR30) with homology to the G-protein-coupled receptor superfamily associated with estrogen receptor expression in breast cancer. Genomics, 1997; 45(3):607-17.

Casa A.J. Dearth R.K., Litzenburger B.C., Lee A.V., Cui X., Frontiers in Bioscience 13, 2008; 3273–3287.

Casa A.J., Dearth R.K., Litzenburger B.C., Lee A.V., Cui X. The type I insulin-like growth factor receptor pathway: a key player in cancer therapeutic resistance. Front Biosci. 2008; 13:3273-87.

Chan Q.K., Lam H.M., Ng C.F., Lee A.Y., Chan E.S., Ng H.K., Ho S.M., Lau K.M. Activation of GPR30 inhibits the growth of prostate cancer cells through sustained activation of Erk1/2, c-jun/c-fos-dependent upregulation of p21, and induction of G(2) cell-cycle arrest. Cell Death and Differentiation, 2010; 17(9):1511-23.

Chen W., Zheng R., Zeng H., Zhang S. Epidemiology of lung cancer in China. Thorac Cancer. 2015; 6(2):209-15

Chevalier N., Vega A., Bouskine A., Siddeek B., Michiels J.F., Chevallier D., Fénichel P. GPR30, the non-classical membrane G protein related estrogen receptor, is overexpressed in human seminoma and promotes seminoma cell proliferation. PLoS ONE, 2012; 7(4):e34672

Chiang S.H., Baumann C.A., Kanzaki M., Thurmond D.C., Watson R.T., Neudauer C.L., Macara I.G., Pessin J.E., Saltiel A.R. Insulin-stimulated GLUT4 translocation requires the CAP-dependent activation of TC10. Nature, 2001; 410(6831):944-8.

Chuang H.C., Fan C.W., Chen K.Y., Chang-Chien G.P., Chan C.C., Vasoactive alteration and inflammation induced by polycyclic aromatic hydrocarbons and trace metals of vehicle exhaust particles. Toxicol. Lett. 2012; 214(2):131–136.

Curado M.P., Edwards H.R, Shin H., Storm J., Ferlay M.H., Boyle P. Cancer Incidence in Five Continents, Vol. IX. Lyon: IARC Scientific Publications, 2007.

Daub H., Wallasch C., Lankenau A., Herrlich A., Ullrich A. Signal characteristics of G protein-transactivated EGF receptor. EMBO Journal, 1997; 16(23):7032-44.

Daub H., Weiss F.U., Wallasch C., Ullrich A. Role of transactivation of the EGF receptor in signalling by G-protein-coupled receptors, Nature, 1996; 379(6565):557-60.

References

Davidson B. Prognostic factors in malignant pleural mesothelioma. Hum Pathol. 2015; 46(6):789-804

De Francesco E.M., Lappano R., Santolla M.F., Marsico S., Caruso A., Maggiolini M. HIF-1α/GPER signaling mediates the expression of VEGF induced by hypoxia in breast cancer associated fibroblasts (CAFs). Breast Cancer Res. 2013; 15: R64.

De Francesco E.M., Pellegrino M., Santolla M.F., Lappano R., Ricchio E., Abonante S., Maggiolini M. GPER mediates activation of HIF1α/VEGF signaling by estrogens. Cancer Res. 2014; 74: 4053-64.

De Francesco EM, Lappano R, Santolla MF, Marsico S, Caruso A, Maggiolini M. HIF-1α/GPER signaling mediates the expression of VEGF induced by hypoxia in breast cancer associated fibroblasts (CAFs). Breast Cancer Res. 2013; 15(4):R64.

De Francesco EM, Pellegrino M, Santolla MF, Lappano R, Ricchio E, Abonante S, Maggiolini M. GPER mediates activation of HIF1α/VEGF signaling by estrogens. Cancer Res. 2014; 74(15):4053-64

De Marco P., Bartella V., Vivacqua A., Lappano R., Santolla M.F., Morcavallo A., Pezzi V., Belfiore A., Maggiolini M. Insulin-like growth factor-I regulates GPER expression and function in cancer cells. Oncogene, 2012; 32: 678-88.

De Marco P., Bartella V., Vivacqua A., Lappano R., Santolla M.F., Morcavallo A., Pezzi V., Belfiore A., Maggiolini M. Insulin-like growth factor-I regulates GPER expression and function in cancer cells. Oncogene. 2013; 32: 678-88

De Marco P., Romeo E., Vivacqua A., Malaguarnera R., Abonante S., Romeo F., Pezzi V., Belfiore A., Maggiolini M. GPER1 is regulated by insulin in cancer cells and cancer-associated fibroblasts. Endocr Relat Cancer. 2014; 21:739-53.

Dengjel J., Akimov V., Olsen J. V., Bunkenborg J., Mann M., Blagoev B., Andersen J.S. Quantitative proteomic assessment of very early cellular signaling events. Nat. Biotechnol. 2007; 25(5):566–568.

Dorsam R.T., Gutkind J.S. G-protein-coupled receptors and cancer. Nature Rev Cancer 2007; 7: 79–94;

E.R. Prossnitz, M. Barton, The G-protein-coupled estrogen receptor GPER in health and disease. Nature Reviews Endocrinology, 2011; 7(12):715-26

Eswaramoorthy R., Wang C.K., Chen W.C., Tang M.J., Ho M.L., Hwang C.C., Wang H.M., Wang C.Z. DDR1 regulates the stabilization of cell surface E-cadherin and E-cadherin-mediated cell aggregation. J Cell Physiol. 2010; 224: 387-97.

Fidler M.J., Shersher D.D., Borgia J.A., Bonomi P. Targeting the insulin-like growth factor receptor pathway in lung cancer: problems and pitfalls. Ther Adv Med Oncol. 2012; 4: 51-60.

References

Filardo E.J, Quinn J., Pang Y., Graeber C., Shaw S., Dong J., Thomas P. Activation of the novel estrogen receptor G Protein-Coupled Receptor 30 (GPR30) at the plasma membrane. Endocrinology, 2007; 48(7): 3236–3245.

Filardo E.J, Quinn J.A., Bland K.I. and Frackelton A.R. Jr. Estrogen-induced activation of Erk-1and Erk-2 requires the G protein-coupled receptor homolog, GPR30, and occurs via transactivation of the epidermal growth factor receptor through release of HB-EGF. Molecular Endocrinology, 2000; 14(10):1649-60.

Filardo E.J., Graeber C.T., Quinn J.A., Resnick M.B., Giri D., De Lellis R.A., Steinhoff M.M., Sabo E. Distribution of GPR30, a seven membrane-spanning estrogen receptor, in primary breast cancer and its association with clinicopathologic determinants of tumor progression. Clin Cancer Res. 2006; 12:6359-66.

Filardo E.J., Graeber C.T., Quinn J.A., Resnick M.B., Giri D., DeLellis R.A., Steinhoff M.M., Sabo E. Distribution of GPR30, a seven membrane-spanning estrogen receptor, in primary breast cancer and its association with clinicopathologic determinants of tumor progression. Clin Cancer Res. 2006; 12: 6359-66

Filardo E.J., Quinn J.A., Frackelton A.R. Jr., Bland K.I. Estrogen action via the G protein-coupled receptor, GPR30: stimulation of adenylyl cyclase and cAMP-mediated attenuation of the epidermal growth factor receptor-to-MAPK signaling axis. Molecular Endocrinology, 2002; 16(1):70-84.

Fitzmaurice C., Dicker D., Pain A., Hamavid H., Moradi-Lakeh M., MacIntyre M.F., Allen C., Hansen G., Woodbrook R., Wolfe C., Hamadeh R.R., Moore A.,et al. The global burden of cancer 2013. JAMA Oncology, 2015; 1(4):505-27

Ford C. E., Lau S. K., Zhu C. Q., Andersson T., Tsao M. S. Vogel, W. F. Expression and mutation analysis of the discoidin domain receptors 1 and 2 in non-small cell lung carcinoma. Br. J. Cancer, 2007; 96(5):808–814.

Franks S.E., Briah R., Jones R.A., Moorehead R.A. Unique roles of Akt1 and Akt2 in IGF-IR mediated lung tumorigenesis. Oncotarget. 2016; 7: 3297-316.

Fujii M., Nakanishi H., Toyoda T., Tanaka I., Kondo Y., Osada H., Sekido Y. Convergent signaling in the regulation of connective tissue growth factor in malignant mesothelioma: TGFβ signaling and defects in the Hippo signaling cascade. Cell Cycle, 2012; 11: 3373-9

Gardi C. Valacchi G. Cigarette smoke and ozone effect on murine inflammatory responses. Ann. N.Y. Acad. Sci. 2012; 1259:104–111.

Gerdes M.J., Myakishev M., Frost N.A., Rishi V., Moitra J., Acharya A., Levy M.R., Park S.W., Glick A., Yuspa S.H., Vinson C. Activator protein-1 activity regulates epithelial tumor cell identity. Cancer Res 2006; 66(15):7578-88.

Glass J.P., Parasher G., Arias-Pulido H., Donohue R., Prossnitz E.R., Cerilli L.A. Mesothelin and GPR30 staining among a spectrum of pancreatic epithelial neoplasms. International Journal of Surgical Pathology, 2011; 19(5):588-96

References

Gombos A., Metzger-Filho O., Dal Lago L., Awada-Hussein A. Clinical development of insulin-like growth factor receptor--1 (IGF-1R) inhibitors: at the crossroad? Invest New Drugs. 2012; 30: 2433-42.
GPER, IGF-IR, and EGFR transduction signaling are involved in stimulatory effects of zinc in breast cancer cells and cancer-associated fibroblasts. Mol Carcinog. 2016, doi: 10.1002/mc.22518. [Epub ahead of print]

Grande J.P., Melder D.C., Zinsmeister A.R. Modulation of collagen gene expression by cytokines: stimulatory effect of transforming growth factor-beta1, with divergent effects of epidermal growth factor and tumor necrosis factor-alpha on collagen type I and collagen type IV. J Lab Clin Med. 1997; 130: 476-86

Guo L., Zhang T., Xiong Y., Yang Y. Roles of NOTCH1 as a Therapeutic Target and a Biomarker for Lung Cancer: Controversies and Perspectives. Dis Markers. 2015; 2015:520590

Guo P., Huang Z.L., Yu P., Li K. Trends in cancer mortality in China: an update," Annals of Oncology, 2012; 23(10)2755–2762.

Hart S., Fischer O.M., Prenzel N., Zwick-Wallasch E., Schneider M., Hennighausen L., Ullrich A. GPCR-induced migration of breast carcinoma cells depends on both EGFR signal transactivation and EGFR-independent pathways. Biological Chemistry, 2005; 386(9):845-55.

Heinzelmann-Schwarz V.A., Gardiner-Garden M., Henshall S.M., Scurry J., Scolyer R.A., Davies M.J., Heinzelmann M., Kalish L.H., Bali A., Kench J.G, Edwards L.S., Vanden Bergh P.M., Hacker N.F., Sutherland R.L., O'Brien P.M. Overexpression of the cell adhesion molecules DDR1, Claudin 3, and Ep-CAM in metaplastic ovarian epithelium and ovarian cancer. Clin Cancer Res 2004; 10: 4427-4436
Hidalgo-Carcedo C., Hooper S., Chaudhry S.I., Williamson P., Harrington K., Leitinger B., Sahai E. Collective cell migration requires suppression of actomyosin at cell-cell contacts mediated by DDR1 and the cell polarity regulators Par3 and Par6. Nat Cell Biol. 2011; 13:49-58.
Hoang C.D., Zhang X., Scott P.D., Guillaume T.J., Maddaus M.A., Yee D., Kratzke R.A. Selective activation of insulin receptor substrate-1 and -2 in pleural mesothelioma cells: association with distinct malignant phenotypes. Cancer Res. 2004; 64: 7479–85.

Hung C.F., Rohani M.G., Lee S.S., Chen P., Schnapp L.M. Role of IGF-1 pathway in lung fibroblast activation. Respir Res. 2013; 14: 102.

Inai K. Pathology of mesothelioma. Environ Health Prev Med. 2008; 13: 60-4.

Inamori Y., Ota M., Inoko H., Okada E., Nishizaki R., Shiota T., Mok J., Oka A., Ohno S., Mizuki N. The COL1A1 gene and high myopia susceptibility in Japanese. Hum Genet. 2007; 122: 151-7

Jala V.R., Radde B.N., Haribabu B., Klinge C.M. Enhanced expression of G-protein coupled estrogen receptor (GPER/GPR30) in lung cancer. BMC Cancer 2012; 12: 624.

References

Kai K., D'Costa S., Sills R.C., Kim Y. Inhibition of the insulin-like growth factor 1 receptor pathway enhances the antitumor effect of cisplatin in human malignant mesothelioma cell lines. Cancer Lett. 2009; 278: 49-55

Kim I.Y., Kim B.C., Seong D.H., Lee D.K., Seo J.M., Hong Y.J., Kim H.T., Morton R.A., Kim S.J. Raloxifene, a mixed estrogen agonist/antagonist, induces apoptosis in androgen-independent human prostate cancer cell lines. Cancer Res. 2002; 62(18):5365-9.

Kim J.S., Kim E.S., Liu D., Lee J.J., Solis L., Behrens C., Lippman S.M., Hong W.K., Wistuba I.I., Lee H.Y. Prognostic implications of tumoral expression of insulin like growth factors 1 and 2 in patients with non-small-cell lung cancer. Clinical Lung Cancer, 2014; 15 :213-221.

Kisfalvi K., Eibl G., Sinnett-Smith J., Rozengurt E. Metformin disrupts crosstalk between G protein-coupled receptor and insulin receptor signaling systems and inhibits pancreatic cancer growth. Cancer Research, 2009; 69(16):6539-45.

Lai J.S., Brown L.G., True L.D., Hawley S.J., Etzioni R.B., Higano C.S., Ho S.M., Vessella R.L., Corey E. Urology 64 2004; (4) 814–820.

Lappano R, De Marco P, De Francesco EM, Chimento A, Pezzi V, Maggiolini M. Cross-talk between GPER and growth factor signaling. J Steroid Biochem Mol Biol. 2013; 137:50-6.

Lappano R., Maggiolini M. G protein-coupled receptors: novel targets for drug discovery in cancer. Nat Rev Drug Discov. 2011; 10: 47-60.

Lappano R., Maggiolini M. GPCRs and cancer, Acta Pharmacologica Sinica, 2012; 33(3):351-62.

Lau K.M., La Spina M., Long J., Ho S.M. Cancer Research 60 2000; (12) 3175–3182.

Lee H., Kim S.R., Oh Y., Cho S.H., Schleimer R.P., Lee Y.C. Targeting insulin-like growth factor-I and insulin-like growth factor-binding protein-3 signaling pathways. A novel therapeutic approach for asthma. Am J Respir Cell Mol Biol. 2014; 50: 667-77.

Leitinger B., Kwan A.P. The discoidin domain receptor DDR2 is a receptor for type X collagen. Matrix Biol. 2006; 25, 355–364

Lemeer S., Bluwstein A., Wu Z., Leberfinger J., Müller K., Kramer K., Kuster B. Phosphotyrosine mediated protein interactions of the discoidin domain receptor 1. J Proteomics. 2012; 75: 3465-77.

Lenters V., Vermeulen R., Dogger S., Stayner L., Portengen L., Burdorf A., Heederik D. A meta-analysis of asbestos and lung cancer: is better quality exposure assessment associated with steeper slopes of the exposure-response relationships? Environ Health Perspect. 2011; 119: 1547-55.

Liu C., Liao Y., Fan S., Tang H., Jiang Z., Zhou B., Xiong J., Zhou S., Zou M., Wang J. G protein-coupled estrogen receptor (GPER) mediates NSCLC progression induced by 17β-estradiol (E2) and selective agonist G1. Med Oncol. 2015; 32: 104.

References

Liu Z., Klominek J. Chemotaxis and chemokinesis of malignant mesothelioma cells to multiple growth factors. Anticancer Res. 2004; 24: 1625-30

Lu P., Takai K., Weaver V.M., Werb Z. Extracellular matrix degradation and remodeling in development and disease. Cold Spring Harb Perspect Biol. 2011; 3(12).

Lu P., Weaver V. M., and Werb Z. The extracellular matrix: a dynamic niche in cancer progression. J. Cell Biol. 196, 2012; 395–406.

Madeo A. and Maggiolini M. Nuclear alternate estrogen receptor GPR30 mediates 17β-Estradiol-induced gene expression and migration in breast cancer associated fibroblasts. Cancer Res. 2010, 70(14):6036-46

Maggiolini M., Picard D. The unfolding stories of GPR30, a new membrane-bound estrogen receptor. J Endocrinol. 2010; 204(2):105-14.

Maggiolini M., Vivacqua A., Fasanella G., Recchia A.G., Sisci D., Pezzi V., Montanaro D., Musti A.M., Picard D., Andò S. The G protein-coupled receptor GPR30 mediates c-fos up-regulation by 17beta-estradiol and phytoestrogens in breast cancer cells. Journal of Biological Chemistry, 2004; 279(26):27008-16

Malaguarnera R., Nicolosi M.L., Sacco A., Morcavallo A., Vella V., Voci C., Spatuzza M., Xu S.Q., Iozzo R.V., Vigneri R., Morrione A., Belfiore A. Novel cross talk between IGF-IR and DDR1 regulates IGF-IR trafficking, signaling and biological responses. Oncotarget 2015; 6:16084-105

Marinissen M.J., Gutkind J.S. G-protein-coupled receptors and signaling networks: emerging paradigms. Trends Pharmacol Sci. 2001; 22(7):368-76.

Marjon N.A., Hu C., Hathaway H.J., Prossnitz E.R. G protein-coupled estrogen receptor regulates mammary tumorigenesis and metastasis. Mol Cancer Res. 2014; 12: 1644-54.

Matà R., Palladino C., Nicolosi M.L., Lo Presti A.R., Malaguarnera R., Ragusa M., Sciortino D., Morrione A., Maggiolini M., Vella V., Belfiore A. IGF-I induces upregulation of DDR1 collagen receptor in breast cancer cells by suppressing MIR-199a-5p through the PI3K/AKT pathway. Oncotarget 2016; 7(7):7683-700.

Matsuyama W., Watanabe M., Shirahama Y., Oonakahara K., Higashimoto I., Yoshimura T, Osame M., Arimura K. Activation of discoidin domain receptor 1 on CD14-positive bronchoalveolar lavage fluid cells induces chemokine production in idiopathic pulmonary fibrosis. J Immunol 2005; 174: 6490-8

Matthews J., Gustafsson J.A. Estrogen signaling: a subtle balance between ER alpha and ER beta. Mol Interv. 2003; 3(5):281-92.

Meyer M.R., Barton M. ERalpha, ERbeta, and gpER: novel aspects of oestrogen receptor signalling in atherosclerosis. Cardiovasc Res. 2009; 83(4):605-10.

References

Migliaccio A., Castoria G., Di Domenico M., de Falco A., Bilancio A., Lombardi M., Barone M.V., Ametrano D., Zannini M.S., Abbondanza C., Auricchio F. EMBO Journal 19 2000; (20) 5406–5417.

Møller P., Folkmann J.K., Forchhammer L., Bräuner E.V., Danielsen P.H., Risom L., Loft S. Air pollution, oxidative damage to DNA, and carcinogenesis. Cancer Lett. 2008; 266: 84–97. Morgan D.O., Edman J.C., Standring D.N., Fried V.A, Smith M.C., Roth R.A., Rutter W.J., Nature (1987); 329 (6137):301–307.

Mossman B.T., Lippmann M., Hesterberg T.W., Kelsey K.T., Barchowsky A., Bonner J.C. Pulmonary endpoints (lung carcinomas and asbestosis) following inhalation exposure to asbestos. J Toxicol Environ Health B Crit Rev. 2011; 14: 76-121.

Nagai H., Toyokuni S. Biopersistent fiber-induced inflammation and carcinogenesis: Lessons learned from asbestos toward safety of fibrous nanomaterials. Arch. Biochem. Biophys. 2010; 502(1): 1–7.

Neves S.R., Ram P.T., Iyengar R. G protein pathways. Science, 2002; 296: 1636–9
Nonaka D., Kusamura S., Baratti D. Diffuse malignant mesothelioma of the peritoneum: a clinicopathological study of 35 patients treated locoregionally at a single institution. Cancer, 2005; 104: 2181–8.

Novosyadlyy R., Lann D.E., Vijayakumar A., Rowzee A., Lazzarino D.A., Fierz Y., Carboni J.M., Gottardis M.M., Pennisi P.A., Molinolo A.A., Kurshan N., Mejia W., Santopietro S., Yakar S, Wood TL, LeRoith D. Insulin-mediated acceleration of breast cancer development and progression in a nonobese model of type 2 diabetes. Cancer Res. 2010; 70: 741-751.

O'Hayre M., Vázquez-Prado J., Kufareva I., Stawiski E.W., Handel T.M., Seshagiri S. and Gutkind J.S. The emerging mutational landscape of G proteins and G-protein-coupled receptors in cancer. 2013; 13(6):412-24

Orengo A.M., Spoletini L., Procopio A., Favoni R.E., De Cupis A., Ardizzoni A., Castagneto B., Ribotta M., Betta P.G., Ferrini S., Mutti L. Establishment of four new mesothelioma cell lines: characterization by ultrastructural and immunophenotypic analysis. Eur Respir J. 1999; 13(3):527-34.

Pandey D.P, Lappano R., Albanito L., Madeo A., Maggiolini M., Picard D. Estrogenic GPR30 signalling induces proliferation and migration of breast cancer cells through CTGF. EMBO J. 2009; 28(5):523-32

Parkin D.M., Bray F., Ferlay J., Pisani P. Global cancer statistics, 2002. CA Cancer J Clin. 2005; 55: 74 –108.

Pettersson K., Gustafsson J.A. Role of estrogen receptor beta in estrogen action. Annu Rev Physiol. 2001; 63:165-92.

Pierce K.L., Luttrell L.M., Efkowitz R.J.L. New mechanisms in heptahelical receptor signaling to mitogen activated protein kinase cascades. Oncogene, 2001; 20(13):1532-9.

References

Pierce K.L., Premont R.T., Lefkowitz R.J. Seven-transmembrane receptors. Nat Rev Mol Cell Biol 2002; 3: 639–50.

Pillai K., Pourgholami M.H., Chua T.C., Morris D.L. Oestrogen receptors are prognostic factors in malignant peritoneal mesothelioma. J Cancer Res Clin Oncol. 2013; 139(6):987-94.

Pinton G., Brunelli E., Murer B., Puntoni R., Puntoni M., Fennell D.A., Gaudino G., Mutti L., Moro L. Estrogen receptor-beta affects the prognosis of human malignant mesothelioma. Cancer Res. 2009; 69: 4598-604.

Pisano A, Santolla MF, De Francesco EM, De Marco P, Rigiracciolo DC, Perri MG, Vivacqua A, Abonante S, Cappello AR, Dolce V, Belfiore A, Maggiolini M, Lappano R. Prossnitz, E. R. & Maggiolini, M. Mechanisms of estrogen signaling and gene expression via GPR30. Mol. Cell Endocrinol. 2009; 308(1-2):32-8.

Provenzano P.P., Eliceiri K.W., Campbell J.M., Inman D.R., White J.G., Keely, P.J. Collagen reorganization at the tumor-stromal interface facilitates local invasion. BMC Med. 2006; 4:38.

Provenzano P.P., Inman D.R., Eliceiri K.W., Knittel J.G., Yan L., Rueden C.T., White J.G., Keely P.J. Collagen density promotes mammary tumor initiation and progression. BMC Med. 2008; 6:11.

Pupo M., Pisano A., Abonante S., Maggiolini M., Musti A.M. GPER activates Notch signaling in breast cancer cellsand cancer-associated fibroblasts (CAFs). The International Journal of Biochemistry & Cell Biology. 2014; 46:56– 67.

Rajer M., Zwitter M., Rajer B. Pollution in the working place and social status: co-factors in lung cancer carcinogenesis. Lung Cancer, 2014; 85: 346-50.

Ramaswamy S., Ross K.N., Lander E.S., Golub T.R. A molecular signature of metastasis in primary solid tumors. Nat Genet. 2003; 33: 49-54.

Rascoe P.A., Jupiter D., Cao X., Littlejohn J.E., Smythe W.R. Molecular pathogenesis of malignant mesothelioma. Expert Rev Mol Med. 2012; 14: e12.

Rebustini I.T., Myers C., Lassiter K.S., Surmak A., Szabova L., Holmbeck K., Pedchenko V., Hudson B.G., Hoffman M.P. MT2-MMP- dependent release of collagen IV NC1 domains regulates submandibular gland branching morphogenesis. Dev. Cell. 2009; 17:482–493.

Recchia A.G., De Francesco E.M., Vivacqua A., Sisci D., Panno M.L., Andò S., Maggiolini M. The G protein-coupled receptor 30 is up-regulated by hypoxia-inducible factor-1alpha (HIF-1alpha) in breast cancer cells and cardiomyocytes. J Biol Chem. 2011; 286: 10773-82.

Reiss K., Wang J.Y., Romano G., Tu X., Peruzzi F., Baserga R. Mechanisms of regulation of cell adhesion and motility by insulin receptor substrate-1 in prostate cancer cells. Oncogene, 2001; 20(4):490-500.

References

Renehan A.G., Zwahlen M., Minder C., O'Dwyer S.T., Shalet S.M., Egger M. Insulin-like growth factor (IGF)-I, IGF binding protein- and cancer risk: systematic review and meta-regression analysis. Lancet. 2004, 363:1346–53.

Revankar C.M., Cimino D.F., Sklar L.A., Arterburn J.B., Prossnitz E.R. A trans-membrane intracellular estrogen receptor mediates rapid cell signaling. Science, 2005; 307(5715):1625-30

Rigiracciolo D.C., Scarpelli A., Lappano R., Pisano A., Santolla M.F., De Marco P., Cirillo F., Cappello A.R., Dolce V., Belfiore A., Maggiolini M., De Francesco E.M. Copper activates HIF-1α/GPER/VEGF signalling in cancer cells. Oncotarget, 2015; 6(33): 34158-77

Rigiracciolo D.C., Scarpelli A., Lappano R., Pisano A., Santolla M.F., Avino S., De Marco P., Bussolati B., Maggiolini M., De Francesco E.M. GPER is involved in the stimulatory effects of aldosterone in breast cancer cells and breast tumor-derived endothelial cells. Oncotarget, 2016; 7(1): 94-111

Rozengurt E., Sinnett-Smith J., Kisfalvi K. Crosstalk between insulin/insulin- like growth factor-1 receptors and G protein-coupled receptor signaling systems: a novel target for the antidiabetic drug metformin in pancreatic cancer. Clinical Cancer Research, 2010; 16(9):2505-11.

Rubin P., Hansen J.T. TNM Staging Atlas With Oncoanatomy. Lippincott Williams and Wilkins, 2012.

Sachdev D., Yee D. Disrupting insulin-like growth factor signaling as a potential cancer therapy. Mol Cancer Ther. 2007; 6:1–12.

Sanchez T., Hla T. Structural and functional characteristics of S1P receptors. J Cell Biochem, 2004; 92(5):913-22.

Sangani R.G., Ghio A.J. Lung injury after cigarette smoking is particle related. Int. J. Chron. Obstruct. Pulmon. Dis. 2011; 6:191–198.

Santolla M.F., Avino S., Pellegrino M., De Francesco E.M., De Marco P., Lappano R., Vivacqua A., Cirillo F., Rigiracciolo D.C., Scarpelli A., Abonante S., Maggiolini M. SIRT1 is involved in oncogenic signaling mediated by GPER in breast cancer. Cell Death and Disease, 2015; 6:e1834.

Scagliotti G.V. and Novello S. The role of the insulin-like growth factor signaling pathway in non-small cell lung cancer and other solid tumors. Cancer Treat Rev. 2012; 38: 292-302.

Scotlandi K. and Belfiore A. Targeting the Insulin-Like Growth Factor (IGF) System Is Not as Simple as Just Targeting the Type 1 IGF Receptor. Am Soc Clin Oncol Educ Book. 2012: 599-604.

Shan L.N., Song Y.G., Su D., Liu Y.L., Shi X.B., Lu S.J. Early Growth Response Protein-1 Involves in Transforming Growth factor-β1 Induced Epithelial-Mesenchymal Transition and Inhibits Migration of Non-Small-Cell Lung Cancer Cells. Asian Pac J Cancer Prev. 2015; 16: 4137-42

References

Shia J, Qin J, Erlandson RA, King R, Illei P, Nobrega J, Yao D, Klimstra DS. Malignant mesothelioma with a pronounced myxoid stroma: a clinical and pathological evaluation of 19 cases. Virchows Arch. 2005; 447(5):828-34.

Shrivastava A., Radziejewski C., Campbell E., Kovac L., Mcglynn M., Ryan, T. E., Davis S., Goldfarb M.P., Glass D.J., Lemke G., Yancopoulos G.D. An orphan receptor tyrosine kinase family whose members serve as nonintegrin collagen receptors. Mol. Cell. 1997; 1(1):25–34. Siegfried J.M., Hershberger P.A., Stabile L.P. Estrogen receptor signaling in lung cancer. Semin Oncol. 2009; 36: 524-31.

Silvestri G.A., Gonzalez A.V., Jantz M.A., Margolis M.L., Gould M.K., Tanoue L.T., Harris L.J., Detterbeck F.C. Methods for staging non-small cell lung cancer: Diagnosis and management of lung cancer, 3rd ed: American College of Chest Physicians evidence-based clinical practice guidelines. Chest. 2013; 143: e211S-50S

Singh P., Alex J.M., Bast F. Insulin receptor (IR) and insulin-like growth factor receptor 1 (IGF-1R) signaling systems: novel treatment strategies for cancer. Med Oncol. 2014, 31:805.

Smith H.O., Arias-Pulido H., Kuo D.Y., Howard T., Qualls C.R., Lee S.J., Verschraegen C.F., Hathaway H.J., Joste N.E., Prossnitz E.R. GPR30 predicts poor survival for ovarian cancer. Gynecol Oncol. 2009; 114(3):465-71

Smith H.O., Leslie K.K., Singh M., Qualls C.R., Revankar C.M., Joste N.E., Prossnitz E.R. GPR30: a novel indicator of poor survival for endometrial carcinoma. Am J Obstet Gynecol. 2007; 196: 386.e1-9

Song R.X., Barnes C.J., Zhang Z., Bao Y., Kumar R., Santen R.J. Proceedings of the National Academy of Sciences of the United States of America 101 2004; (7) 2076–2081.

Stickens D., Behonick D.J., Ortega N., Heyer B., Hartenstein B., Yu Y., Fosang A.J., Schorpp-Kistner M., Angel P., Werb Z. Altered endochondral bone development in matrix metalloproteinase 13-deficient mice. Development, 2004. 131:5883–5895.

Straif K., Benbrahim-Tallaa L., Baan R., Grosse Y., Secretan B., El Ghissassi F., Bouvard V., Guha N., Freeman C., Galichet L., Cogliano V. WHO International Agency for Research on Cancer Monograph Working Group. A review of human carcinogens--Part C: metals, arsenic, dusts, and fibres. Lancet Oncol. 2009; 10:453-4.

Strak M., Janssen N.A., Godri K.J., Gosens I., Mudway I.S., Cassee F.R., Lebret E., Kelly F.J., Harrison R.M., Brunekreef B., Steenhof M, Hoek G. Respiratory health effects of airborne particulate matter: The role of particle size, composition, and oxidative potential-the RAPTES project. Environ. Health Perspect. 2012; 120(8):1183–1189.

Sukhanov S., Higashi Y., Shai S.Y., Blackstock C., Galvez S., Vaughn C., Titterington J., Delafontaine P. Differential requirement for nitric oxide in IGF-1-induced anti-apoptotic, anti-oxidant and anti-atherosclerotic effects. FEBS Lett. 2011; 585: 3065-72

Sukhanov S., Higashi Y., Shai S.Y., Vaughn C., Mohler J., Li Y., Song Y.H., Titterington J., Delafontaine P. IGF-1 reduces inflammatory responses, suppresses oxidative stress, and

References

decreases atherosclerosis progression in ApoE-deficient mice. Arterioscler Thromb Vasc Biol. 2007; 2684-90.

Takada Y., Kato C., Kondo S., Korenaga R., Ando J. Cloning of cDNAs encoding G protein-coupled receptor expressed in human endothelial cells exposed to fluid shear stress. Biochem Biophys Res Commun. 1997; 240(3):737-41.

Tavazoie S.F., Alarcón C., Oskarsson T., Padua D., Wang Q., Bos P.D., Gerald W.L., Massagué J. Endogenous human microRNAs that suppress breast cancer metastasis. Nature, 2008; 451: 147-52.

Thomas P., Pang Y., Filardo E.J., Dong J. Identity of an estrogen membrane receptor coupled to a G protein in human breast cancer cells. Endocrinology, 2005; 146(2):624-32.

Travis W.D, Brambilla E., Riely G.J. New pathologic classification of lung cancer: relevance for clinical practice and clinical trials, J. Clin. Oncol. 2013; 31: 992–1001.

Travis W.D., Brambilla E., Noguchi M., Nicholson A.G., Geisinger K., Yatabe Y., Powell C.A., Beer D., Riely G., Garg K., Austin J.H., Rusch V.W., Hirsch F.R. Scagliotti G., Mitsudomi T., Huber R.M., Ishikawa Y., Jett J., Sanchez-Cespedes M., Sculier J.P., Takahashi T., Tsuboi M., Vansteenkiste J., Wistuba I., Yang P.C., Aberle D., Brambilla C., Flieder D., Franklin W., Gazdar A., Gould M., Hasleton P., Henderson D., Johnson B., Johnson D., Kerr K., Kuriyama K., Lee J.S., Miller V.A., Petersen I., Roggli V., Rosell R., Saijo N., Thunnissen E., Tsao M., Yankelewitz D. International Association for the Study of Lung Cancer/American Thoracic Society/European Respiratory Society: international multidisciplinary classification of lung adenocarcinoma: executive summary. J Thorac Oncol. 2011; 6:244-85.

Valavanidis A., Vlachogianni T., Fiotakis K., Loridas S. Pulmonary oxidative stress, inflammation and cancer: respirable particulate matter, fibrous dusts and ozone as major causes of lung carcinogenesis through reactive oxygen species mechanisms. Int J Environ Res Public Health, 2013; 10(9): 3886-907.

Valiathan R.R., Marco M., Leitinger B., Kleer C.G., Fridman R. Discoidin domain receptor tyrosine kinases: new players in cancer progression. Cancer Metastasis Rev. 2012; 31(1-2): 295-321.

Vivacqua A., Lappano R., De Marco P., Sisci D., Aquila S., De Amicis F., Fuqua S.A., Andò S., Maggiolini M. G protein-coupled receptor 30 expression is up-regulated by EGF and TGF alpha in estrogen receptor alpha-positive cancer cells. Molecular Endocrinology, 2009; 23(11):1815–1826.

Vivacqua A., Romeo E., De Marco P., De Francesco E.M., Abonante S., Maggiolini M. GPER mediates the Egr-1 expression induced by 17 β-estradiol and 4-hydroxitamoxifen in breast and endometrial cancer cells. Breast Cancer Research and Treatment, 2012; 133(3):1025-35.

Vogel W., Gish G.D., Alves F., Pawson T. The discoidin domain receptor tyrosine kinases are activated by collagen. Mol Cell. 1997; 1(1):13-23.

References

Vogel W.F., Abdulhussein R., Ford C.E. Sensing extracellular matrix: an update on discoidin domain receptor function. Cell Signal. 2006; 18: 1108-16.

Wang C.Z., Yeh Y.C., Tang M.J. DDR1/E-cadherin complex regulates the activation of DDR1 and cell spreading. Am J Physiol Cell Physiol. 2009; 297: C419-29.

Wang L., Chen Z., Wang Y., Chang D., Su L., Guo Y., Liu C. TR1 promotes cell proliferation and inhibits apoptosis through cyclin A and CTGF regulation in non-small cell lung cancer. Tumour Biol. 2014; 35: 463-8

Wiseman B.S., Sternlicht M.D., Lund L.R., Alexander C.M., Mott J., Bissell M.J., Soloway P., Itohara S., Werb Z. Site-specific inductive and inhibitory activities of MMP-2 and MMP-3 orchestrate mammary gland branching morphogenesis. J. Cell Biol. 2003; 162:1123–1133.

Yakar S., Leroith D., Brodt P. The role of the growth hor- mone/insulin-like growth factor axis in tumor growth and progression: Lessons from animal models. Cytokine Growth Factor Rev. 2005; 16: 407-420.

Yang H., Rivera Z., Jube S., Nasu M., Bertino P., Goparaju C., Franzoso G., Lotze M.T., Krausz T., Pass H.I., Bianchi M.E., Carbone M. Programmed necrosis induced by asbestos in human mesothelial cells causes high-mobility group box 1 protein release and resultant inflammation. Proc Natl Acad Sci U S A. 2010; 107: 12611–12616.

Yeh Y.C., Wu C.C., Wang Y.K., Tang M.J. DDR1 triggers epithelial cell differentiation by promoting cell adhesion through stabilization of E-cadherin. Mol Biol Cell. 2011; 22: 940-53.

Young S.H., Rozengurt E. Crosstalk between insulin receptor and G protein-coupled receptor signaling systems leads to Ca2+ oscillations in pancreatic cancer PANC-1 cells. Biochemical and Biophysical Research Communications, 2010; 401(1):154-8.

Publications

1. Stimulatory actions of IGF-I are mediated by IGF-IR cross-talk with GPER and DDR1 in mesothelioma and lung cancer cells. **Avino S**, De Marco P, Cirillo F, Santolla MF, De Francesco EM, Perri MG, Rigiracciolo D, Dolce V, Belfiore A, Maggiolini M, Lappano R, Vivacqua A. Oncotarget. 2016 Jun 30;7:52710-52728

2. Protective role of GPER agonist G-1 on cardiotoxicity induced by doxorubicin. De Francesco EM, Rocca C, Scavello F, Amelio D, Rigiracciolo D, Pasqua T, Scarpelli A, **Avino S**, Cirillo F, Amodio N, Cerra MC, Maggiolini M, Angelone T. Journal of Cellular Physiology. 2016 Sep 8. [Epub ahead of print]

3. GPER signalling in both cancer-associated fibroblasts and breast cancer cells mediates a feedforward IL1β/IL1R1 response. De Marco P, Lappano R, De Francesco EM, Cirillo F, Pupo M, **Avino S**, Vivacqua A, Abonante S, Picard D, Maggiolini M. Sci Rep. 2016 Apr 13;6:24354.

4. Recent Advances on the Role of G Protein-Coupled Receptors in Hypoxia-Mediated Signaling. Lappano R, Rigiracciolo D, De Marco P, **Avino S**, Cappello AR, Rosano C, Maggiolini M, De Francesco EM. AAPS J. 2016 Mar;18:305-10.

5. GPER is involved in the stimulatory effects of aldosterone in breast cancer cells and breast tumor-derived endothelial cells. Rigiracciolo DC, Scarpelli A, Lappano R, Pisano A, Santolla MF, **Avino S**, De Marco P, Bussolati B, Maggiolini M, De Francesco EM. Oncotarget. 2016 Jan 5;7:94-111.

6. Inactivating mutations in GNA13 and RHOA in Burkitt's lymphoma and diffuse large B-cell lymphoma: a tumor suppressor function for the Gα13/RhoA axis in B cells. O'Hayre M, Inoue A, Kufareva I, Wang Z, Mikelis CM, Drummond RA, **Avino S**, Finkel K, Kalim KW, Di Pasquale G, Guo F, Aoki J, Zheng Y, Lionakis MS, Molinolo AA, Gutkind JS. Oncogene. 2015 Nov 30;35:3771-8.

7. SIRT1 is involved in oncogenic signaling mediated by GPER in breast cancer. Santolla MF, **Avino S**, Pellegrino M, De Francesco EM, De Marco P, Lappano R, Vivacqua A, Cirillo F, Rigiracciolo DC, Scarpelli A, Abonante S, Maggiolini M. Cell Death Dis. 2015 Jul 30;6:e1834.

8. Identification of two benzopyrroloxazines acting as selective GPER antagonists in breast cancer cell and cancer-associated fibroblasts. Maggiolini M, Santolla MF, **Avino S**, Aiello F, Rosano C, Garofalo A, Grande F. Future Med Chem. 2015;7:437-48.

- **Titolo Tesi: Stimulatory actions of IGF-I are mediated by IGF-IR cross-talk with GPER and DDR1 in mesothelioma and lung cancer cells (SSD: MED/04)**

- **Tutor Accademico: Prof. Marcello Maggiolini, Dipartimento di Farmacia e Scienze della Salute e della Nutrizione.**

- **Relazione Scientifica**

Scopo principale della ricerca è stato quello di valutare i meccanismi molecolari coinvolti nello sviluppo e nella progressione del mesotelioma, tumore aggressivo che coinvolge la superficie mesoteliale della pleura, delle cavità peritoneali e più raramente del pericardio e della cavità vaginale dei testicoli (1). Le cellule del mesotelio svolgono un ruolo chiave nel mantenimento dell'omeostasi degli organi interni e nell'endocitosi di sostanze estranee ed è proprio questa caratteristica alla base della loro predisposizione alla trasformazione neoplastica (2). Il mesotelioma colpisce nel 90% dei casi il sesso maschile ed il principale fattore di rischio è rappresentato dall'esposizione occupazionale all'asbesto.

Il mesotelioma maligno della pleura (MPM) è la forma più comune di mesotelioma ed è causato dalla trasformazione neoplastica delle cellule mesoteliali in seguito all'esposizione alle fibre aerodisperse di asbesto (3). L'esordio clinico avviene dopo un lunghissimo periodo di latenza compreso fra i 15 e i 60 anni, successivo all'inalazione delle fibre del minerale. Inoltre, le cellule tumorali, a causa della presenza di alti livelli di espressione di metalloproteasi della matrice, capaci di degradare sia la membrana plasmatica che i componenti della matrice extracellulare stromale, possiedono elevate capacità di invasione dei tessuti circostanti (4). Il decorso della malattia è molto rapido da 6 mesi ad 1 anno e raramente giunge alla metastatizzazione.

La patogenesi del mesotelioma coinvolge diversi pathways trasduzionali, in particolare quelli attivati da fattori di crescita come l'Epidermal Growth Factor (EGF) e Insulin-like Growth Factor 1 (IGF-I), oltre a composti ad attività estrogenica (5-6). A tal riguardo, numerosi studi hanno riportato che, il complesso sistema IGF, comprendente i fattori di crescita Insulino-simili (IGFs), i corrispettivi recettori e le proteine leganti IGF, risulta essere un importante regolatore della carcinogenesi e della progressione di numerosi tumori, tra cui il mesotelioma maligno della pleura e il tumore polmonare (7-11). In particolare, l'elevata espressione del recettore di IGF-I (IGF-IR) in diverse linee cellulari tumorali, è stata associata alla genesi e progressione tumorale oltre che alla resistenza farmacologica (9, 12-14). Diversi studi hanno, inoltre dimostrato, che le risposte biologiche mediate da IGF-I coinvolgono l'interazione tra IGF-IR e altre classi di recettori come ad

1

esempio quelli accoppiati a proteine G (GPCRs) e quelli tirosin-chinasici (RTK), tra cui discoidin domain receptor tyrosine kinase 1 (DDR1) che è over-espresso in diversi tipi di tumori, tra cui il tumore polmonare (15-17). Inoltre, recenti studi hanno indicato l'esistenza di un cross-talk funzionale tra IGF-IR e il recettore estrogenico accoppiato a proteine G, noto come GPR30/GPER, la cui espressione e funzione è regolata da IGF-I attraverso la via trasduzionale IGF-IR/PKC/MAPK in diverse linee cellulari (18-19). Sulla base di tali osservazioni, scopo principale dell'attività di ricerca svolta durante il corso del Dottorato di Ricerca, è stato quello di valutare nuovi meccanismi molecolari attraverso i quali IGF-I può indurre importanti risposte biologiche in cellule di mesotelioma IST-MES1 e di tumore polmonare A549. In particolare, i nostri studi hanno dimostrato che IGF-I è in grado di indurre l'up-regolazione dei livelli proteici di GPER e dei suoi geni target CTGF ed EGR1 attraverso il coinvolgimento del pathway trasduzionale IGF-IR/ERK/p-38. Inoltre, è stato osservato che il trattamento con IGF-I induce nelle cellule IST-MES1 e A549 l'up-regolazione di Collagen Type I Alpha 1 (COL1A1) e di alcuni geni target di DDR1 quali MATN-2, FBN-1, NOTCH 1 e HES-1. Al fine di valutare il coinvolgimento di GPER ed IGF-IR nell'attivazione dei geni target di DDR1 in seguito al trattamento con IGF-I, abbiamo silenziato l'espressione di entrambi i recettori con uno specifico short hairpin (shGPER e shIGF-IR). In entrambe le linee cellulari, abbiamo osservato che l'up-regolazione dei geni è stata completamente abrogata nelle suddette condizioni sperimentali. Tali risultati suggeriscono che l'aumento dell'espressione dei geni target di DDR1, indotta da IGF-I coinvolge IGF-IR, nonché la sua interazione funzionale con GPER. E' stata infine valutata la capacità di IGF-I di indurre risposte biologiche complesse coinvolte nella progressione tumorale. In particolar modo, abbiamo osservato che il silenziamento dell'espressione di GPER e di IGF-IR in cellule IST-MES1 e A549, ha inibito la capacità di IGF-I di stimolare la chemiotassi e la migrazione indotte in entrambe le linee cellulari. I dati ottenuti hanno dimostrato che l'attività stimolatoria svolta da IGF-I in tumori aggressivi come il mesotelioma e il tumore polmonare può coinvolgere un cross-talk funzionale tra IGF-IR, GPER e DDR1, che rappresenta dunque un nuovo target molecolare da utilizzare in strategie terapeutiche innovative nei suddetti tipi di tumore.

Bibliografia:

1. Tischoff I, Neid M, Neumann V, Tannapfel A. Pathohistological diagnosis and differential diagnosis. Recent Results Cancer Research 2011; 189: 57-78.

2. Mutsaers SE. The mesothelial cell. The International Journal of Biochemistry & Cell Biology 2004; 36: 9-16.

3. Liu W, Ernst JD, Broaddus VC. Phagocytosis of crocidolite asbestos induces oxidative stress, DNA damage, and apoptosis in mesothelial cells. American Journal of Respiratory Cell and Molecular Biology 2000; 23: 371-8.

4. Vogelzang NJ, Porta C, Mutti L. New agents in the management of advanced mesothelioma. Seminars in Oncology 2005; 32: 336-50.

5. Whitson BA, Kratzke RA. Molecular pathway in malignant pleural mesothelioma. Cancer Letters 2006; 239: 183-9.

6. Pinton G, Brunelli E, Murer B, Puntoni R, Puntoni M, Fennell DA, Gaudino G, Mutti L, Moro L. Estrogen receptor-beta affects the prognosis of human malignant mesothelioma. Cancer Research 2009; 69: 4598-604.

7. Belfiore A, Frasca F, Pandini G, Sciacca L, Vigneri R. Insulin receptor isoforms and insulin receptor/insulin-like growth factor receptor hybrids in physiology and disease. Endocr Rev. 2009; 30: 586-623.

8. Belfiore A, Malaguarnera R. Insulin receptor and cancer. Endocr Relat Cancer. 2011; 18: R125-47.

9. Kai K, D'Costa S, Sills RC, Kim Y. Inhibition of the insulin-like growth factor 1 receptor pathway enhances the antitumor effect of cisplatin in human malignant mesothelioma cell lines. Cancer Lett. 2009; 278: 49-55.

10. Matà R, Palladino C, Nicolosi ML, Lo Presti AR, Malaguarnera R, Ragusa M, Sciortino D, Morrione A, Maggiolini M, Vella V, Belfiore A. IGF-I induces upregulation of DDR1 collagen receptor in breast cancer cells by suppressing MIR-199a-5p through the PI3K/AKT pathway. Oncotarget. 2016; 7: 7683-700.

11. Scagliotti GV and Novello S. The role of the insulin-like growth factor signaling pathway in non-small cell lung cancer and other solid tumors. Cancer Treat Rev. 2012; 38: 292-302.

12. Carboni JM, Lee AV, Hadsell DL, Rowley BR, Lee FY, Bol DK, Camuso AE, Gottardis M, Greer AF, Ho CP, Hurlburt W, Li A, Saulnier M, et al. Tumor development by transgenic expression of a constitutively active insulin-like growth factor I receptor. Cancer Res. 2005; 65: 3781-7.

13. Franks SE, Briah R, Jones RA, Moorehead RA. Unique roles of Akt1 and Akt2 in IGF-IR mediated lung tumorigenesis. Oncotarget. 2016; 7: 3297-316.

14. Hoang CD, Zhang X, Scott PD, Guillaume TJ, Maddaus MA, Yee D, Kratzke RA. Selective activation of insulin receptor substrate-1 and -2 in pleural mesothelioma cells: association with distinct malignant phenotypes. Cancer Res. 2004; 64: 7479–85.

15. Lappano R and Maggiolini M. G protein-coupled receptors: novel targets for drug discovery in cancer. Nat Rev Drug Discov. 2011; 10: 47-60.

16. Liu C, Zhang Z, Tang H, Jiang Z, You L, Liao Y. Crosstalk between IGF-1R and other tumor promoting pathways. Curr Pharm Des. 2014; 20: 2912-21.

17. Valiathan RR, Marco M, Leitinger B, Kleer CG, Fridman R. Discoidin domain receptor tyrosine kinases: new players in cancer progression. Cancer Metastasis Rev. 2012; 31: 295-321

18. De Marco P, Bartella V, Vivacqua A, Lappano R, Santolla MF, Morcavallo A, Pezzi V, Belfiore A, Maggiolini M. Insulin-like growth factor-I regulates GPER expression and function in cancer cells. Oncogene. 2013; 32: 678-88.

19. De Marco P, Cirillo F, Vivacqua A, Malaguarnera R, Belfiore A, Maggiolini M. Novel Aspects Concerning the Functional Cross-Talk between the Insulin/IGF-I System and Estrogen Signaling in Cancer Cells. Front Endocrinol (Lausanne). 2015; 6: 30.

- **Pubblicazioni della Dott.ssa Silvia Avino durante il corso di dottorato**:

1. **Avino S**, De Marco P, Cirillo F, Santolla MF, De Francesco EM, Perri MG, Rigiracciolo D, Dolce V, Belfiore A, Maggiolini M, Lappano R, Vivacqua A. Stimulatory actions of IGF-I are mediated by IGF-IR cross-talk with GPER and DDR1 in mesothelioma and lung cancer cells. Oncotarget; 7:52710-52728. 2016.

2. De Francesco EM, Rocca C, Scavello F, Amelio D, Rigiracciolo D, Pasqua T, Scarpelli A, **Avino S**, Cirillo F, Amodio N, Cerra MC, Maggiolini M, Angelone T. Protective role of GPER agonist G-1 on cardiotoxicity induced by doxorubicin. Journal of Cellular Physiology. 2016. [Epub ahead of print]

3. De Marco P, Lappano R, De Francesco EM, Cirillo F, Pupo M, **Avino S**, Vivacqua A, Abonante S, Picard D, Maggiolini M. GPER signalling in both cancer-associated fibroblasts and breast cancer cells mediates a feedforward IL1β/IL1R1 response. Sci Rep.; 6:24354. 2016.

4. Lappano R, Rigiracciolo D, De Marco P, **Avino S**, Cappello AR, Rosano C, Maggiolini M, De Francesco EM. Recent Advances on the Role of G Protein-Coupled Receptors in Hypoxia-Mediated Signaling. AAPS J.; 18:305-10. 2016.

5. Rigiracciolo DC, Scarpelli A, Lappano R, Pisano A, Santolla MF, **Avino S**, De Marco P, Bussolati B, Maggiolini M, De Francesco EM. GPER is involved in the stimulatory effects of aldosterone in breast cancer cells and breast tumor-derived endothelial cells. Oncotarget; 7:94-111. 2016.

6. O'Hayre M, Inoue A, Kufareva I, Wang Z, Mikelis CM, Drummond RA, **Avino S**, Finkel K, Kalim KW, Di Pasquale G, Guo F, Aoki J, Zheng Y, Lionakis MS, Molinolo AA, Gutkind JS. Inactivating mutations in GNA13 and RHOA in Burkitt's lymphoma and diffuse large B-cell lymphoma: a tumor suppressor function for the Gα13/RhoA axis in B cells. Oncogene; 35:3771-8. 2015.

7. Santolla MF, **Avino S**, Pellegrino M, De Francesco EM, De Marco P, Lappano R, Vivacqua A, Cirillo F, Rigiracciolo DC, Scarpelli A, Abonante S, Maggiolini M. SIRT1

is involved in oncogenic signaling mediated by GPER in breast cancer. Cell Death Dis.; 6:e1834. 2015.

8. Maggiolini M, Santolla MF, **Avino S**, Aiello F, Rosano C, Garofalo A, Grande F. Identification of two benzopyrroloxazines acting as selective GPER antagonists in breast cancer cell and cancer-associated fibroblasts. Future Med Chem.; 7:437-48. 2015.

- **Congressi:**
  - 10-13 Settembre 2016. **The 7th EMBO Meeting 2**, **Mannheim (Germany).** Presentazione Poster: IGF-I triggers stimulatory effects in mesothelioma and lung cancer cells through a functional interaction of IGF-IR with GPER and DDR1.
  - 4-6 Ottobre 2016. **2° Congresso Nazionale SIPMeL - 33° Congresso Nazionale SIPMeT - 3° Congresso dell'Area di Patologia e Medicina di Laboratorio**, **Montesilvano (PE).** Presentatione Poster: IGF-I/IGF-IR transduction system involves GPER and DDR1 in the stimulation of Mesothelioma and Lung Cancer cells.

- **Stage:**
  - Stage di un anno (Luglio 2014-Luglio 2015) svolto presso il Laboratorio di Ricerca diretto dal Prof. J. Silvio Gutkind – National Institute of Dental and Craniofacial Research - National Institutes of Health, Bethesda, Maryland, USA.

- **Corsi:**
  - Ottobre-Novembre 2015. Corso di Informatica. Docente del corso l'Ing. Andrea Tagarelli. 2 CFU;
  - 24 Novembre al 3 Dicembre 2015. NMR for organic and biological chemistry: Old experiments for new applications. Theoretical and practical overview. Docente del corso: Ignacio Delso Hernàndez. Sala Terenzi. 2 CFU

- **Seminari:**
  - 7 Marzo 2014. Titolo del seminario: *"Biomonitoraggio umano del mercurio"*. Relatore: Dott. Alessandro Alimonti. Aula Circolare, Edificio Polifunzionale-Unical.
  - 28 Marzo 2014. Titolo del seminario: "Le promesse della Medicina Genomica". Relatore: Dott. Emiliano Giardina. Aula Seminari Centro Sanitario- Unical.
  - 8 e 9 Maggio 2014. Titolo del Seminario: "Salute e Donazione". Aula Circolare dell'Ateneo.
  - 23 Giugno 2014. Titolo del seminario: Characterization of tryptophan metabolism in the central nervous system. Relatrice: Dott.ssa Judit Heredi. Aula Seminari (ex Dipartimento Farmacobiologico).
  - 8 Ottobre 2015. Titolo del seminario: "Salute dell'ambiente e salute umana: il caso del destino ambientale delle diossine in Campania". Relatore: Dott. Nic Pacini. Aula Seminari (ex farmaco biologico) del Dipartimento di Farmacia e Scienze della Salute e della Nutrizione.
  - 23 ottobre 2015. Titolo del seminario: "FAO WORLD FOOD DAY". Relatrice: Dott.ssa Gabriella Lo Feudo. Aula Magna – Unical.
  - 10 dicembre 2015. Titolo del Seminario: "An Atomistic View of Human Diseases". Relatrice: Dott.ssa Alessandra Magistrato. Dipartimento di Chimica e Tecnologie Chimiche (aula Terenzi).
  - 9 Marzo 2016. Titolo del Seminario: "Photochemical modelling of [FeFe]-hydrogenases: from photophysical properties to H2 photo-production". Relatore: Dr. Luca Bertini presso il Dipartimento di Chimica e Tecnologie Chimiche (aula Seminari).
  - 21 Aprile 2016. Titolo del seminario: "DoniAMO". Aula Circolare del Dipartimento di Farmacia e Scienze della Salute e della Nutrizione.
  - 10 Giugno 2016. Titolo del seminario: Imaging, Genomica e nuove possibile Terapie. Relatore: Sebastiano Andò; Gianfranco Filippelli. Ariha Hotel (Via Guglielmo Marconi, 58-Rende - CS).
  - 15 Giugno 2016. Titolo del seminario: How to prevent dyslipidaemia without causing hepatic steatosis or ketosis. Prof Victor Zammit. Sala Stampa del Centro Congressi presso l'Università della Calabria.

Stimulatory actions of IGF-I are mediated by IGF-IR cross-talk with GPER and DDR1 in mesothelioma and lung cancer cells

Silvia Avino[1,*], Paola De Marco[1,*], Francesca Cirillo[1], Maria Francesca Santolla[1], Ernestina Marianna De Francesco[1], Maria Grazia Perri[1], Damiano Rigiracciolo[1], Vincenza Dolce[1], Antonino Belfiore[2], Marcello Maggiolini[1], Rosamaria Lappano[1,] and Adele Vivacqua[1,**]**

[1] Department of Pharmacy, Health and Nutritional Sciences, University of Calabria, Rende, Italy

[2] Endocrinology, Department of Health Sciences, University Magna Graecia of Catanzaro, Catanzaro, Italy

[*] These authors have contributed equally to this work

[**] Joint senior Authors

Correspondence to: *Marcello Maggiolini*, **email**: *marcellomaggiolini@yahoo.it*

ABSTRACT

Insulin-like growth factor-I (IGF-I)/IGF-I receptor (IGF-IR) system has been largely involved in the pathogenesis and development of various tumors. We have previously demonstrated that IGF-IR cooperates with the G-protein estrogen receptor (GPER) and the collagen receptor discoidin domain 1 (DDR1) that are implicated in cancer progression. Here, we provide novel evidence regarding the molecular mechanisms through which IGF-I/IGF-IR signaling triggers a functional cross-talk with GPER and DDR1 in both mesothelioma and lung cancer cells. In particular, we show that IGF-I activates the transduction network mediated by IGF-IR leading to the up-regulation of GPER and its main target genes CTGF and EGR1 as well as the induction of DDR1 target genes like MATN-2, FBN-1, NOTCH 1 and HES-1. Of note, certain DDR1-mediated effects upon IGF-I stimulation required both IGF-IR and GPER as determined knocking-down the expression of these receptors. The aforementioned findings were nicely recapitulated in important biological outcomes like IGF-I promoted chemotaxis and migration of both mesothelioma and lung cancer cells. Overall, our data suggest that IGF-I/IGF-IR system triggers stimulatory actions through both GPER and DDR1 in aggressive tumors as mesothelioma and lung tumors. Hence, this novel signaling pathway may represent a further target in setting innovative anticancer strategies.

INTRODUCTION

Lung cancer is the most frequent cause of cancer incidence and mortality worldwide at least in part due to the increasing number of risk factors in diverse developing countries [1-2]. To date, smoking has been considered the main etiologic factor for lung cancer [3-4], however, several environmental contaminants like asbestos, arsenic, cadmium, nickel and silica, play an important role toward the development of this neoplasia [5]. Among the aforementioned environmental pollutants, asbestos has been particularly acknowledged as prompting factor in malignant mesothelioma (MM), which is an aggressive cancer that arises from mesothelial cells lining lung, pleura or peritoneum [6-7]. Chronic inflammatory processes caused by the deposition of asbestos fibers and the subsequent release of cytokines and growth factors by macrophages and mesothelial cells have been shown to play an active role toward the development of both pleural MM and lung cancer [7-8].

In this vein, the IGF system, the complex system involving the insulin-like growth factors (IGFs) and related receptors as well as IGF-binding proteins, has been established as an important regulator of tumor initiation

and progression in several malignancies, including pleural MM and lung cancer [9-13]. In particular, the IGF-I receptor (IGF-IR), which is often overexpressed in diverse cancer cell types, affects tumor development, progression and resistance to therapies [11, 14-16]. Moreover, a dysregulated IGF system has been shown to be implicated in various chronic diseases, such as pulmonary fibrosis [17-18].

An increasing body of data has demonstrated that the biological responses mediated by IGF-I involve functional interactions of IGF-IR with diverse signal molecules belonging to other members of the receptor tyrosine kinase (RTK) family [19-20]. In this context, we recently discovered a novel functional cross-talk between IGF-IR and the collagen receptor discoidin domain receptor 1 (DDR1), a molecule also overexpressed in diverse malignancies, including lung carcinomas, and implicated in cancer progression [21]. Interestingly, this cross-talk occurs also independently of the collagen binding actions of DDR1 and, in human breast cancer cells, amplifies the stimulatory biological effects of IGF-I toward proliferation, migration and colony formation. Moreover, through a signaling pathway involving Akt/ miR-199a-5p, IGF-I is able to upregulate DDR1 [12, 22].

In addition to RTKs, IGF-IR interacts with other important signaling molecules like G protein-coupled receptors (GPCRs) [19, 23]. These functional interactions have also important implications in the development and progression of diverse types of tumors [23-24]. In particular, we found that IGF-IR activation engages the G protein estrogen receptor (GPER/GPR30)-mediated signaling toward the stimulation of proliferation and migration of different cancer cell types [25-26]. Interestingly, high expression levels of GPER were detected in lung cancer cells and involved in growth stimulatory effects [24, 27-28]. To date, other signaling molecules have been implicated in the development of MM including the estrogen receptor (ER)β that may act as a tumor suppressor [29-30]. Therefore, the multifaceted mechanisms and the transduction network of factors involved in the progression of the aforementioned malignancies remain to be fully understood.

In this study, we found that mesothelioma and lung cancer cells show a new complex functional cross-talk involving IGF-IR, GPER and DDR1, which affects gene expression and biological effects in response to IGF-I. Our data, therefore, further extend the molecular mechanisms by which IGF-I may affect tumor progression in mesothelioma and lung cancer, hence providing novel targets in the aforementioned aggressive malignancies.
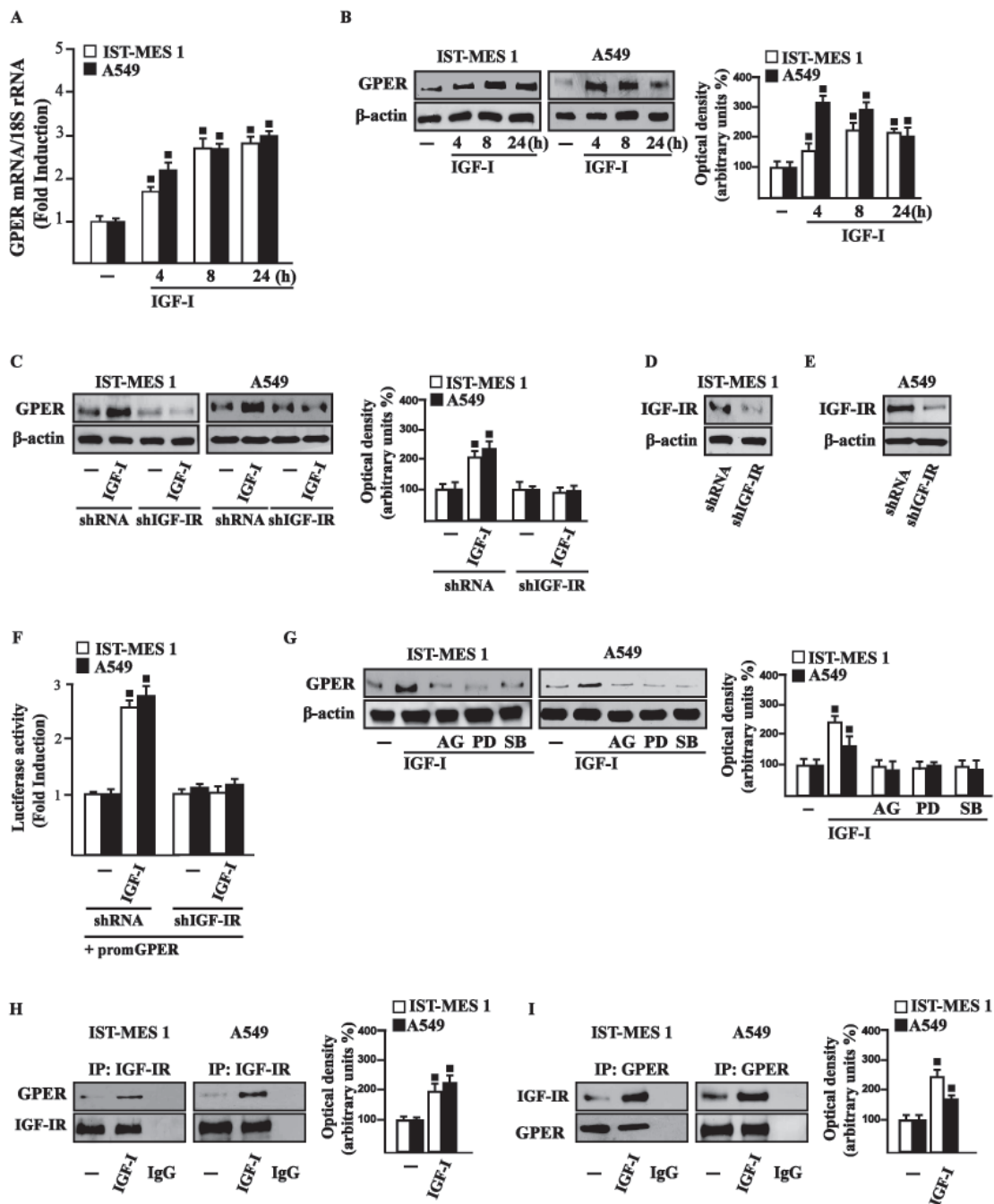
RESULTS

IGF-I stimulates GPER expression through IGF-IR/ERK/p-38 transduction signaling

On the basis of previous studies showing that IGF-I triggers stimulatory effects in malignant mesothelioma as well as in lung cancer cells [31-32], we began our study evaluating the transduction signaling activated by IGF-I in IST-MES1 mesothelioma and A549 lung cancer cells, which were used as model system. First, we determined that in both cell types IGF-I induces the phosphorylation of IGF-IR (Figure 1A) and both ERK (Figure 1B) and p-38 (Figure 1C). As expected, these responses were no longer observed after IGF-IR silencing (Figure 1 A-1E). The activation of ERK triggered by IGF-I was abolished in the presence of the IGF-IR inhibitor AG and the MEK inhibitor PD, but it still persisted using the p-38 inhibitor SB (Figure 1F). The phosphorylation of p-38 was prevented by AG and SB, but not in the presence of PD (Figure 1G). In addition, we assessed that the phosphorylation of IGF-IR induced by IGF-I is inhibited exclusively by AG, but not in the presence of PD and SB (data not shown), then suggesting that the activation of both ERK and p-38 relies directly on IGF-IR phosphorylation upon IGF-I exposure. On the basis of our previous data showing that IGF-I signaling cooperates with several GPCR family members, including GPER, toward cancer progression [19, 25], we evaluated whether IGF-I regulates GPER expression in IST-MES1 and A549 cells. In this regard, time-course experiments demonstrated that IGF-I up-regulates GPER at both mRNA (Figure 2A) and protein levels (Figure 2B). Moreover, we ascertained that these responses to IGF-I occurred through IGF-IR, as the induction of GPER mRNA (data not shown) and protein levels (Figure 2C-2E) was abolished by knocking-down IGF-IR expression. Recapitulating the aforementioned findings, the transactivation of the GPER promoter by IGF-I was prevented by IGF-IR silencing (Figure 2F), and the IGF-I induced GPER protein up-regulation was abrogated in the presence of AG, PD and SB (Figure 2G). Taken together, these results indicate that the IGF-I/IGF-IR transduction pathway stimulates GPER expression through ERK and p-38 signaling. In order to further investigate this functional cross-talk between IGF-IR and GPER, we performed co-immunoprecipitation studies determining that IGF-I triggers also a direct interaction between these receptors in both IST-MES1 and A549 cells upon either 1 h (data not shown) or 8 h treatment with IGF-I (Figure 2H-2I), thus suggesting that the interaction between IGF-IR and GPER may occur without a newly protein expression of GPER.
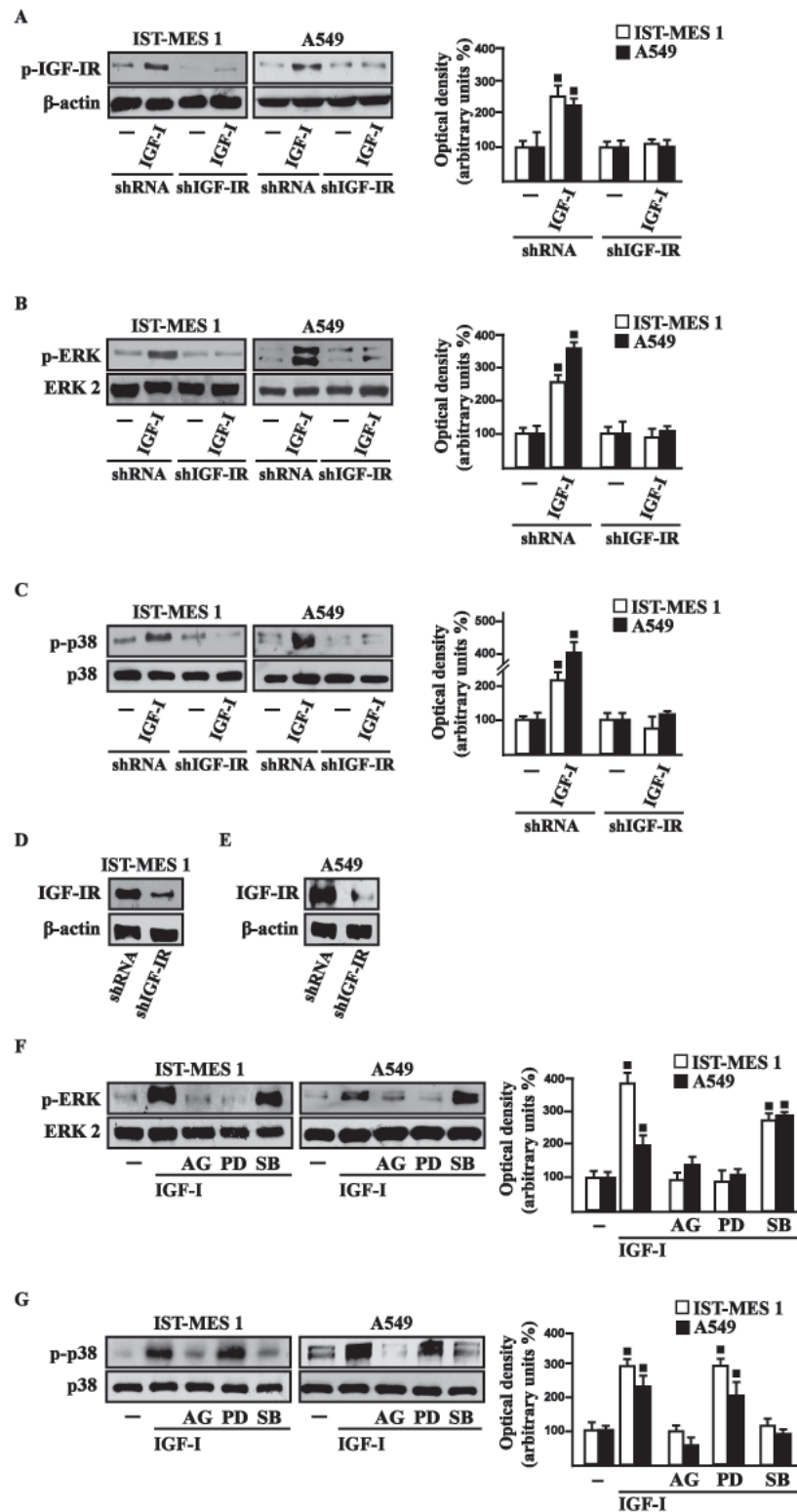
Figure 1: Rapid activation of transduction signaling by IGF-I in IST-MES 1 and A549 cells. IGF-IR **A.**, ERK **B.** and p-38 **C.** phosphorylation in cells transfected for 24 h with shRNA or shIGF-IR treated with vehicle (-) or 100 ng/ml IGF-I for 15 min. **D.-E.** Efficacy of IGF-IR silencing. ERK **F.** and p-38 **G.** activation in cells treated for 15 min with vehicle (-) or 100 ng/ml IGF-I alone and in combination with either 1 μM IGF-IR inhibitor tyrphostin AG1024 (AG), or 1 μM MEK inhibitor PD98059 (PD) or 1 μM p38 inhibitor SB202190 (SB). Side panels show densitometric analysis of the blots normalized to β-actin, ERK2 and p38 that served as loading controls respectively for pIGF-IR, pERK and p-p38. Data shown are the mean ± SD of three independent experiments. (■) $p < 0.05$ for cells receiving vehicle (-) *versus* treatments.

Figure 2: IGF-I up-regulates GPER expression in IST-MES 1 and A549 cells. A. mRNA expression of GPER in cells treated with either vehicle (-) or 100 ng/ml IGF-I, as evaluated by real-time PCR. Results obtained from experiments performed in triplicate were normalized for 18S expression and shown as fold change of RNA expression compared to cells treated with vehicle. **B.** GPER protein levels were evaluated by immunoblotting in cells treated with either vehicle (-) or 100 ng/ml IGF-I, as indicated. **C.** GPER protein expression in cells transfected for 24 h with either shRNA or shIGF-IR and then treated for 8 h with vehicle (-) or 100 ng/ml IGF-I. **D.-E.** Efficacy of IGF-IR silencing. **F.** Cells were transfected for 24 h with shRNA or shIGF-IR together with the GPER promoter construct. Then, cells were treated for 18 h with vehicle (-) or 100 ng/ml IGF-I. The luciferase activities were normalized to the internal transfection control, and values of cells receiving vehicle (-) were set as one fold induction upon which the activity induced by treatments was calculated. **G.** GPER protein levels in cells treated for 8 h with vehicle (-) or 100 ng/ml IGF-I alone or in combination with 1 μM IGF-IR inhibitor tyrphostin AG1024 (AG), 1 μM MEK inhibitor PD98059 (PD) and 1 μM p38 inhibitor SB202190 (SB). Side panels show densitometric analysis of the blots normalized to β-actin. **H.-I.** Co-immunoprecipitation studies performed in cells treated for 8 h with vehicle (-) or 100 ng/ml IGF-I, as indicated. In control samples, non-specific IgG was used instead of the primary antibody. **H.** Side panel show densitometric analysis of the blot normalized to IGF-IR. **I.** Side panel show densitometric analysis of the blot normalized to GPER. Data shown are the mean ± SD of three independent experiments. (■) $p < 0.05$ for cells receiving vehicle (-) *versus* treatments.

IGF-I triggers the expression of GPER target genes

In our previous study [33] we established that GPER mediates a specific gene signature, therefore, we evaluated whether, in IST-MES1 and A549 cells, IGF-I is able to affect the expression of certain GPER target genes like CTGF and EGR1, which have been involved in fibrotic responses in mesothelioma and lung cancer cells [34-36]. Indeed, in time-course experiments we found that
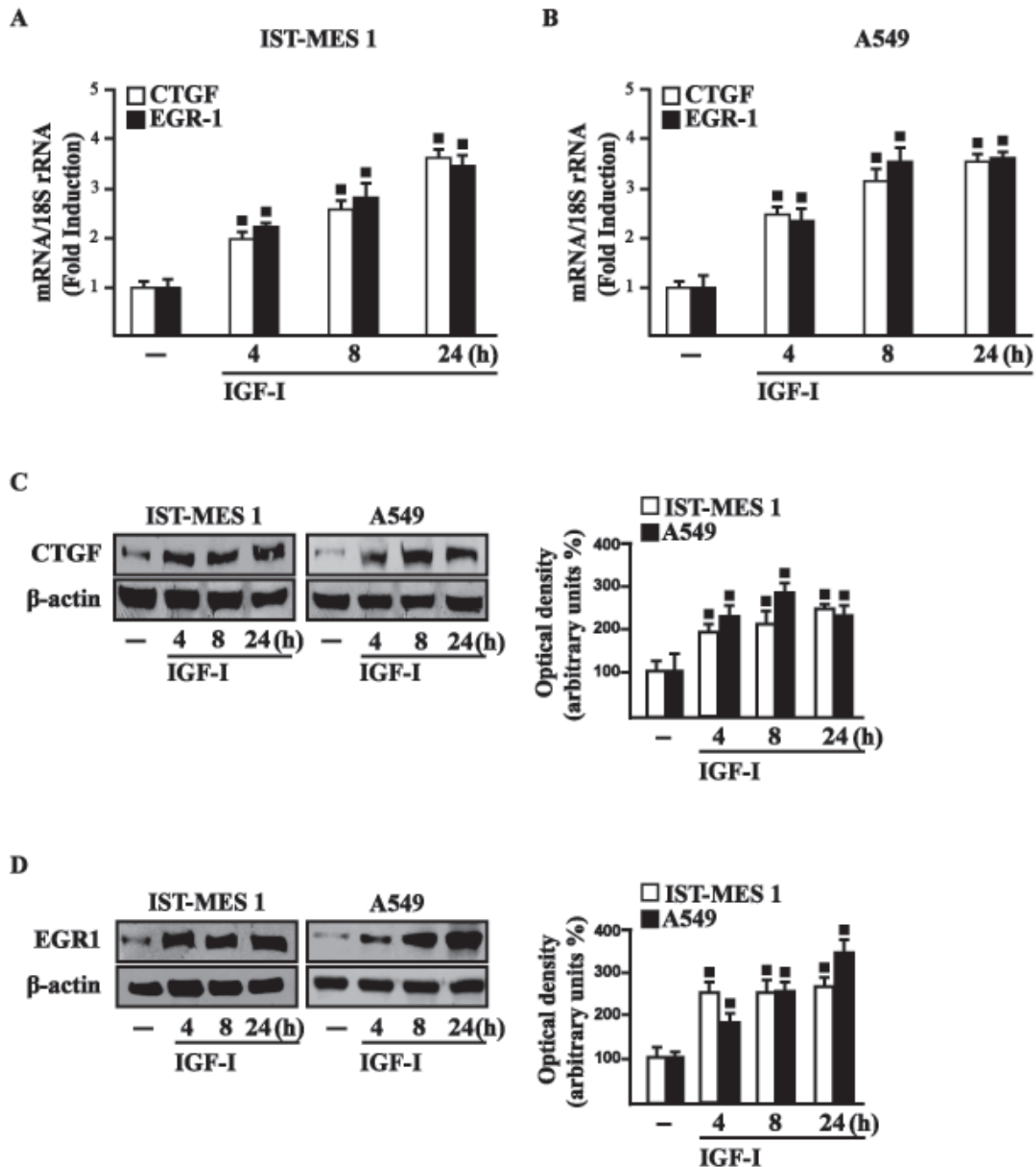
Figure 3: IGF-I up-regulates CTGF and EGR1 expression in IST-MES 1 and A549 cells. (A-B) mRNA expression of CTGF and EGR1 in cells treated with either vehicle (-) or 100 ng/ml IGF-I, as evaluated by real-time PCR. Results obtained from experiments performed in triplicate were normalized for 18S expression and shown as fold change of RNA expression compared to cells treated with vehicle. CTGF **C.** and EGR1 **D.** protein levels were evaluated by immunoblotting in cells treated with vehicle (-) or 100 ng/ml IGF-I, as indicated. Side panels show densitometric analysis of the blots normalized to β-actin and each data point represents the mean ± SD of three independent experiments. (■) *p* < 0.05 for cells receiving vehicle (-) *versus* treatments.

IGF-I increases the mRNA (Figure 3A-3B) and protein levels (Figure 3C-3D) of both CTGF and EGR1. Next, we determined that this action of IGF-I involves not only the IGF-IR but also GPER, as the silencing of each of these receptors prevented gene changes (Figure 4A-4H). In accordance with these observations, the IGF-I transactivation of CTGF (Figure 4I) and EGR1 (Figure 4J) promoters required both IGF-IR and GPER, as demonstrated by knocking down the expression of these receptors. As c-fos plays a main role in the up-regulation of GPER target genes [33, 37], we next determined that the promoter transactivation of both CTGF and EGR1 is abrogated by co-transfecting a dominant-negative form of c-fos (DN/c-fos) in IST-MES1 and A549 cells (Figure 4K). Collectively, these findings provide novel mechanisms through which IGF-I/IGF-IR transduction signaling regulates GPER target genes like CTGF and EGR1 in mesothelioma and lung cancer cells.

IGF-IR and GPER are both involved in IGF-I regulation of DDR1 target genes

Considering that in diverse model systems IGF-I stimulates the synthesis of collagen [38-40], we next established that IGF-I regulates in both IST-MES1 and A549 cells the mRNA expression of COL1A1 (Figure 5A) that encodes the major component of type I collagen [41]. We previously reported that IGF-IR functionally interacts with DDR1, which is activated by various collagen types including type I collagen. Therefore, we first ascertained that, in both IST-MES1 and A549 cells, several DDR1 target genes such as matrilin-2 (MATN-2), fibrillin-1 (FBN-1), NOTCH 1 and HES-1, are induced by the DDR1 agonist COL1 (Figure 5B-5C) and abrogated by the DDR1 inhibitor (DDR1 IN) (Figure 5D-5E). Then, we assessed that these DDR1 target genes are also stimulated by IGF-I (Figure 6A-6B) and that this response was inhibited by DDR1 IN (Figure 6C-6D) as well as by silencing IGF-IR (Figure 6E-6F) or GPER (Figure 6G-6H). In accordance with these findings, we determined that the NOTCH 1 protein induction by COL1 and IGF-I is prevented in the presence of the DDR1 IN in IST-MES1 and A549 cells (Figure 7). Accordingly, IGF-I was not able to trigger NOTCH 1 protein expression when IGF-IR (Figure 8A-8C) or GPER (Figure 8D-8F) were silenced. Altogether, these results indicate that, in both mesothelioma and lung cancer cells, IGF-I may up-regulate DDR1 target genes, and this action involves not only IGF-IR but also a cross-talk with GPER.

DDR1, IGF-IR and GPER contribute to the chemotaxis and migration of mesothelioma and lung cancer cells

Previous studies have reported that IGF-I stimulates chemotactic and chemokinetic motility in mesothelioma cells [32]. Moreover, DDR1 also plays an important role in promoting cell-cell interactions and cell migration in various cell contexts [42-45]. Further extending these data, in IST-MES1 cells, we found that both IGF-I and COL1 induce chemotactic motility, which requires DDR1, as these responses were abolished by DDR1 IN (Videos 1-6). Moreover, we ascertained that the chemotactic motility induced by IGF-I requires also IGF-IR and GPER as the aforementioned effect was prevented silencing the expression of these receptors (Videos 7-12). Similar findings occurred in A549 cells (data not shown). Likewise, we determined that IST-MES1 and A549 cell migration induced by both IGF-I and COL1 is abolished using DDR1 IN (Figure 9A), whereas the silencing of IGF-IR or GPER abolished cell migration triggered by IGF-I, as determined by Boyden chamber assay (Figure 9B). Collectively, our data indicate novel cross-talk and biological functions exerted by IGF-I toward tumor progression.

DISCUSSION

In the present study we provide novel evidence regarding the molecular mechanisms by which IGF-I triggers biological responses in mesothelioma and lung cancer cells. In particular, we show a complex functional cooperation involving IGF-IR, GPER and DDR1 through which IGF-I up-regulates first the expression of COL1A1 and certain DDR1 target genes, thereafter stimulating cancer cell motility and chemotactic response (Figure 10).

Lung cancer is a highly heterogeneous tumor that can arise in different sites of the bronchial tree [1-2]. The incidence of lung cancer depends on toxic effects of inhaled substances such as tobacco, asbestos, arsenic, cadmium, nickel and silica [46]. The environmental pollutant asbestos is also considered the main cause of the insurgence of malignant mesothelioma (MM), which is a rare and aggressive tumor that springs from mesothelial cells lining lung, pleura or peritoneum [5-7, 47-48]. The deposition of asbestos fibers has been also related to chronic inflammatory processes as well as to pulmonary fibrosis, which in turn may create a favorable environment for the development of lung and pleura malignancies [6, 49]. As it concerns the multifaceted mechanisms and factors involved in pulmonary fibrosis and neoplasia, an increased expression and activation of DDR1 have been reported [50-53]. To date, DDR1 has been shown to play an important role in cancer progression by regulating the interactions of tumor cells with the surrounding
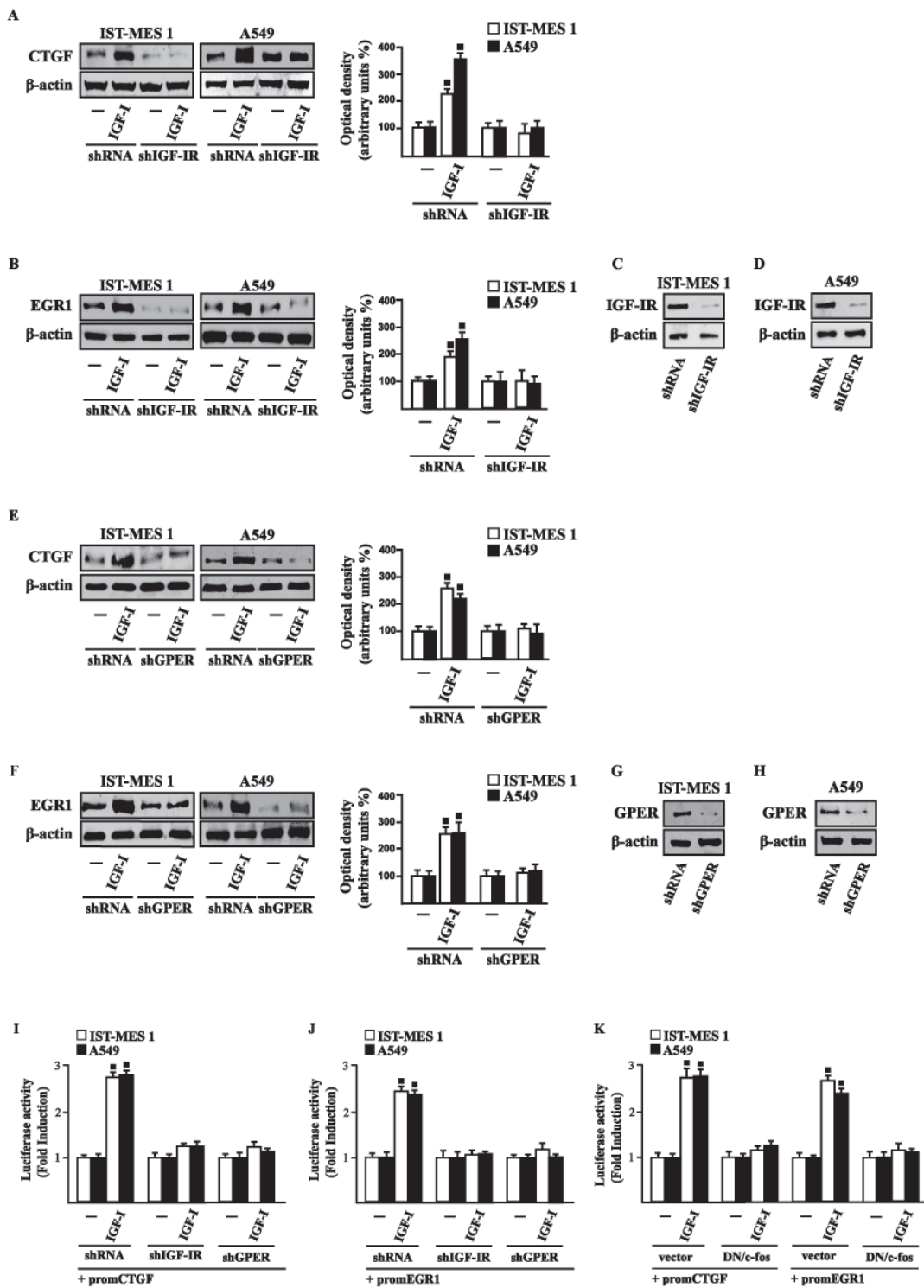
Figure 4: IGF-IR and GPER mediate CTGF and EGR1 stimulation by IGF-I in IST-MES 1 and A549 cells. A.-F. CTGF and EGR1 protein levels in cells transfected for 24 h with shRNA, shIGF-IR or shGPER and then treated for 8 h with either vehicle (-) or 100 ng/ml IGF-I. Efficacy of IGF-IR **C.-D.** and GPER **G.-H.** silencing. Side panels show densitometric analysis of the blots normalized to β-actin. **I.-J.** Cells were transfected for 24 h with shRNA, shIGF-IR or shGPER together with the CTGF or EGR1 promoter construct. Then, cells were treated for 18 h with vehicle (-) or 100 ng/ml IGF-I. **K.** Cells were transfected for 24 h with a dominant negative form of c-fos (DN/c-fos) together with the CTGF or EGR1 promoter construct. Then, cells were treated for 18 h with vehicle (-) or 100 ng/ml IGF-I. The luciferase activities were normalized to the internal transfection control, and values of cells receiving vehicle (-) were set as one fold induction upon which the activity induced by treatments was calculated. Data shown are the mean ± SD of three independent experiments. (■) $p < 0.05$ for cells receiving vehicle (-) *versus* treatments.
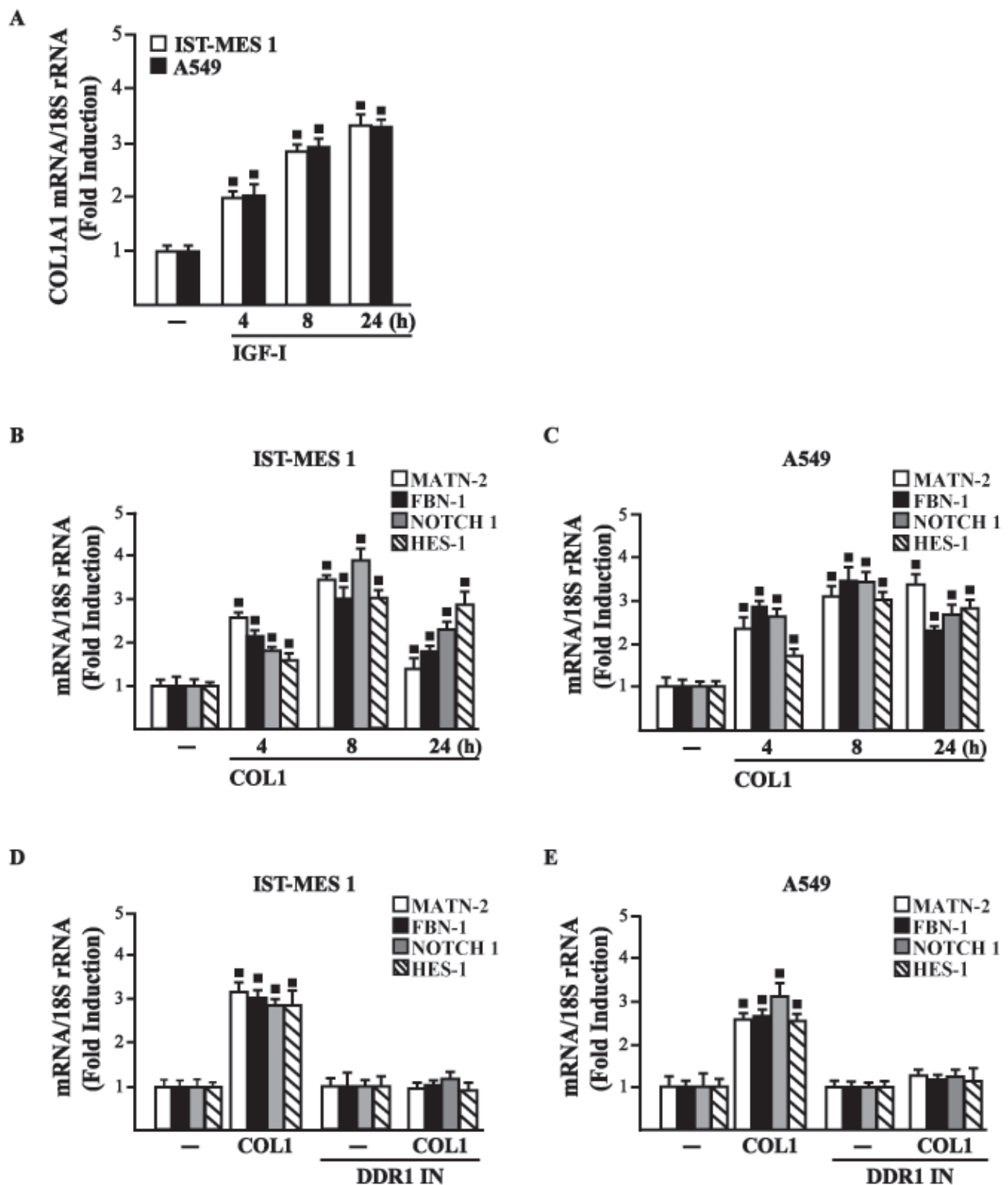
Figure 5: A. mRNA expression of COL1A1 in IST-MES 1 and A549 cells treated with vehicle (-) or 100 ng/ml IGF-I, as evaluated by real-time PCR. mRNA expression of MATN-2, FBN-1, NOTCH 1 and HES-1 in IST-MES 1 **B.**, **D.** and A549 **C.**, **E.** cells treated with vehicle (-) or 10 μg/ml COL1 alone or in combination with 1 μM DDR1 inhibitor (DDR1 IN), as indicated. Results obtained from experiments performed in triplicate were normalized for 18S expression and shown as fold change of RNA expression compared to cells treated with vehicle. (■) $p < 0.05$ for cells receiving vehicle (-) *versus* treatments.
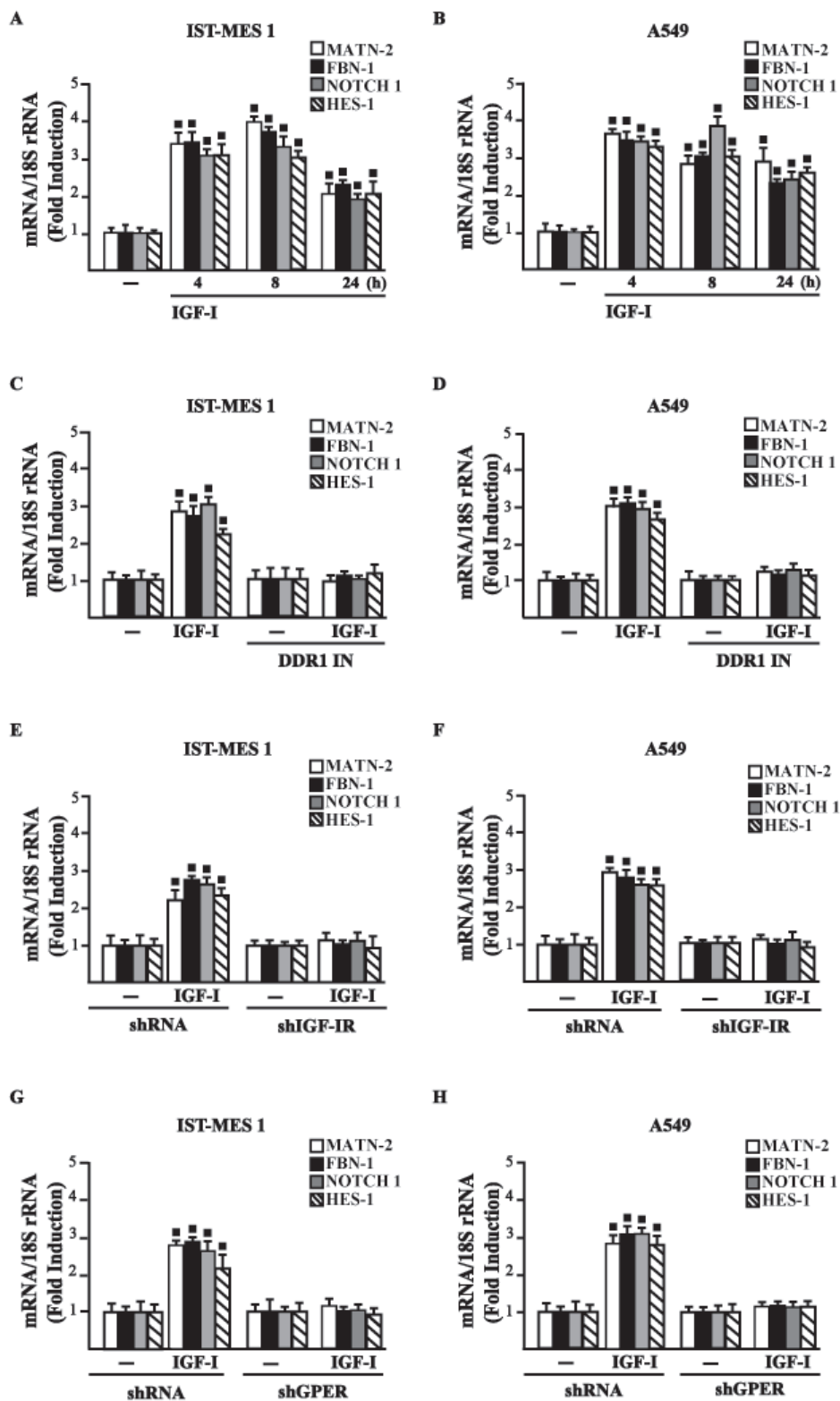
Figure 6: IGF-IR and GPER mediate the IGF-I induced up-regulation of COL1A1/DDR1 target genes in IST-MES 1 and A549 cells. A.-D. mRNA expression of MATN-2, FBN-1, NOTCH 1 and HES-1 in cells treated with vehicle (-) or 100 ng/ml IGF-I alone or in combination with 1 μM DDR1 inhibitor (DDR1 IN), as indicated. **E.-H.** mRNA expression of MATN-2, FBN-1, NOTCH 1 and HES-1 in cells transfected for 24 h with shRNA, shIGF-IR or shGPER and then treated for 8 h with vehicle (-) or 100 ng/ml IGF-I. Results obtained from experiments performed in triplicate were normalized for 18S expression and shown as fold change of RNA expression compared to cells treated with vehicle. (■) $p < 0.05$ for cells receiving vehicle (-) *versus* treatments.

collagen matrix, therefore leading to pro-migratory and pro-invasive responses [21]. Furthermore, collagen activated DDR1 triggers diverse pro-survival pathways toward anti-apoptotic, proliferative and aggressive features in cancer cells [21]. In this regard, it should be noted that several types of collagen are able to bind to and activate DDR1, which then regulates cell and tissue homeostasis acting as a collagen sensor [21, 54]. Of note, an abnormal expression and deposition of collagen has been associated with cancer development [55-56]. As it concerns the synthesis and extracellular accumulation of diverse types of collagen, cytokines and growth factors like IGF-I, the epidermal growth factor (EGF) and the transforming growth factor-βl have been reported to promote these effects [38-40, 57]. Notably, we previously showed that, in breast cancer cells, IGF-I may upregulate DDR1 expression through a signaling pathway involving the DDR1 regulatory miR-199a-5p [12]. Moreover, the activation of one of the main IGF-I transduction signaling, the IGF-IR/PI3K/Akt cascade, inhibits miR-199a-5p expression, thus relieving its inhibition upon DDR1 gene and allowing DDR1 upregulation. In turn, DDR1 increases IGF-IR expression through post-transcriptional mechanisms and amplifies IGF-I downstream signaling and biological effects, such as proliferation, migration and colony formation [12]. Indeed, we previously showed that DDR1 directly interacts with IGF-IR, and that this interaction is enhanced by IGF-I stimulation, which promotes rapid DDR1 tyrosine-phosphorylation and co-internalization of the DDR1 - IGF-IR complex [22]. This interaction was shown to occur in a panel of human breast cancer cells as well as in mouse fibroblasts (R- cells) co-transfected with the human IGF-IR and DDR1, indicating that it is not cell-specific. Notably, the formation of this DDR1 - IGF-IR complex did not require the presence of collagen, the canonical DDR1 ligand. In addition, the critical role of IGF-IR in DDR1 activation and biological actions is supported by the finding that collagen-dependent DDR1 phosphorylation was impaired in the absence of IGF-IR [22].

Extending these previous studies, we now show that IGF-I through the cognate receptor IGF-IR is able to induce COL1A1 expression [54]. Moreover, a panel of DDR1 target genes could be also induced by IGF-I through the previously described functional cross-talk involving IGF-IR and DDR1. Taken together, these findings show that DDR1, besides enhancing the activation of typical IGF-IR downstream cascades, the PI3K/Akt and the ERK1/2 cascades, following cell exposure to IGF-I, modifies significantly these IGF-I effects by allowing the induction of typical DDR1 target genes. These effects confirm the relevance of DDR1 in the amplification and diversification of IGF-I signaling pathways in cancer. We have previously demonstrated that IGF-IR may also functionally interact with the non-canonical estrogen receptor GPER. Indeed, through the
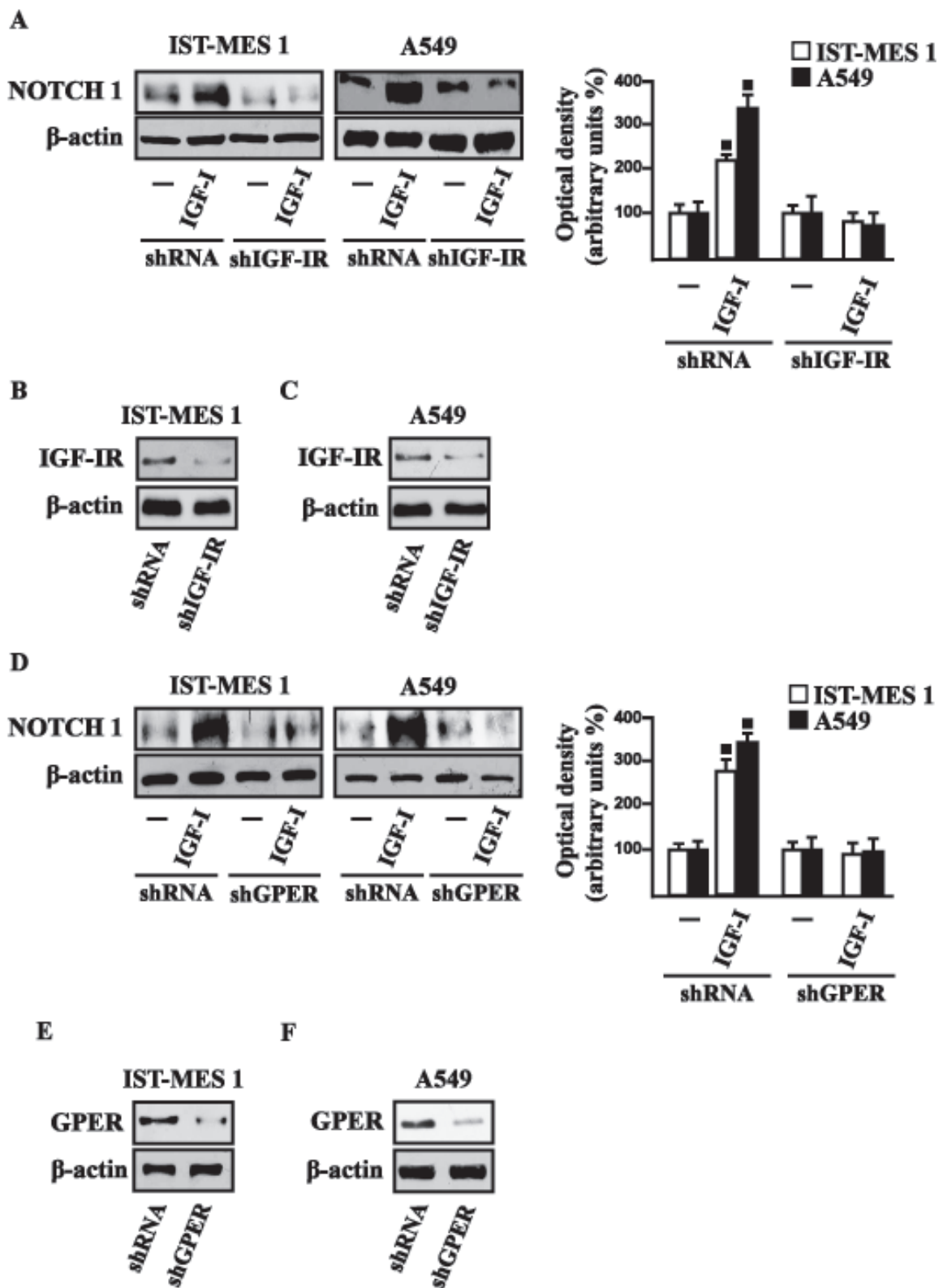
IGF-IR/PKCδ/ERK/c-fos/AP1 transduction pathway, IGF-I up-regulates GPER, which plays an important role in sustaining proliferation and migration in response to IGF-I in breast and endometrial human cancer cells [25]. In close accordance with these findings, we now show that the functional cooperation between IGF-IR and DDR1 also requires GPER, and that both DDR1 and GPER are critical to the chemotactic motility stimulated by IGF-I in mesothelioma and lung cancer cells. Notably, we now show that GPER and IGF-IR co-immunoprecipitate in lung and mesothelioma cells (Figure 2), indicating that GPER and IGF-IR also interact. Taken together all these data strongly suggest the possible formation of a ternary functional complex involving IGF-IR - DDR1 - GPER. However, further studies are needed to fully elucidate this aspect. These data may be of a particular interest as GPER expression has been associated with negative clinical features and poor survival rates in diverse types of malignancies [58-61]. In the last years, extensive studies were therefore performed in order to better characterize the role of GPER in cancer development, including the mechanisms and factors involved in its expression. For instance, we determined that EGF and IGF-I, insulin and further tumorigenic factors like hypoxia and endothelin-1 up-regulate GPER expression in diverse cancer cell contexts [25, 62-68].

Our present findings provide significant new insights on the well-established role played by the IGF axis in cancer [9-11, 14-16, 20, 23, 69-71] that involves also the interaction of IGF-IR with other RTKs and GPCRs in diverse tumor histotypes [19, 23, 72-73]. In particular, our findings might be relevant in devising new therapeutical strategies in cancers with a dysregulated IGF system. In the last decade, much effort has been made in targeting the IGF-IR in these malignancies [74]. In particular, both small-molecule IGF-IR tyrosine kinase inhibitors, and humanized monoclonal antibodies with blocking activity to the IGF-IR, have been investigated in Phase III trials of advanced non-small cell lung cancers [13]. Unfortunately, in spite of very promising preclinical studies, clinical trials have clearly indicated that only a small minority of malignancies do respond to target therapies when IGF-IR is the sole target [75], because the frequent occurrence of resistance mechanisms arising by the complex signaling network involving the IGF-IR [76].

Overall, on the basis of our data the multifaceted signaling network between IGF-IR, GPER and DDR1 could be taken into account in setting innovative combined strategies targeting these pathways in mesothelioma and lung cancers.
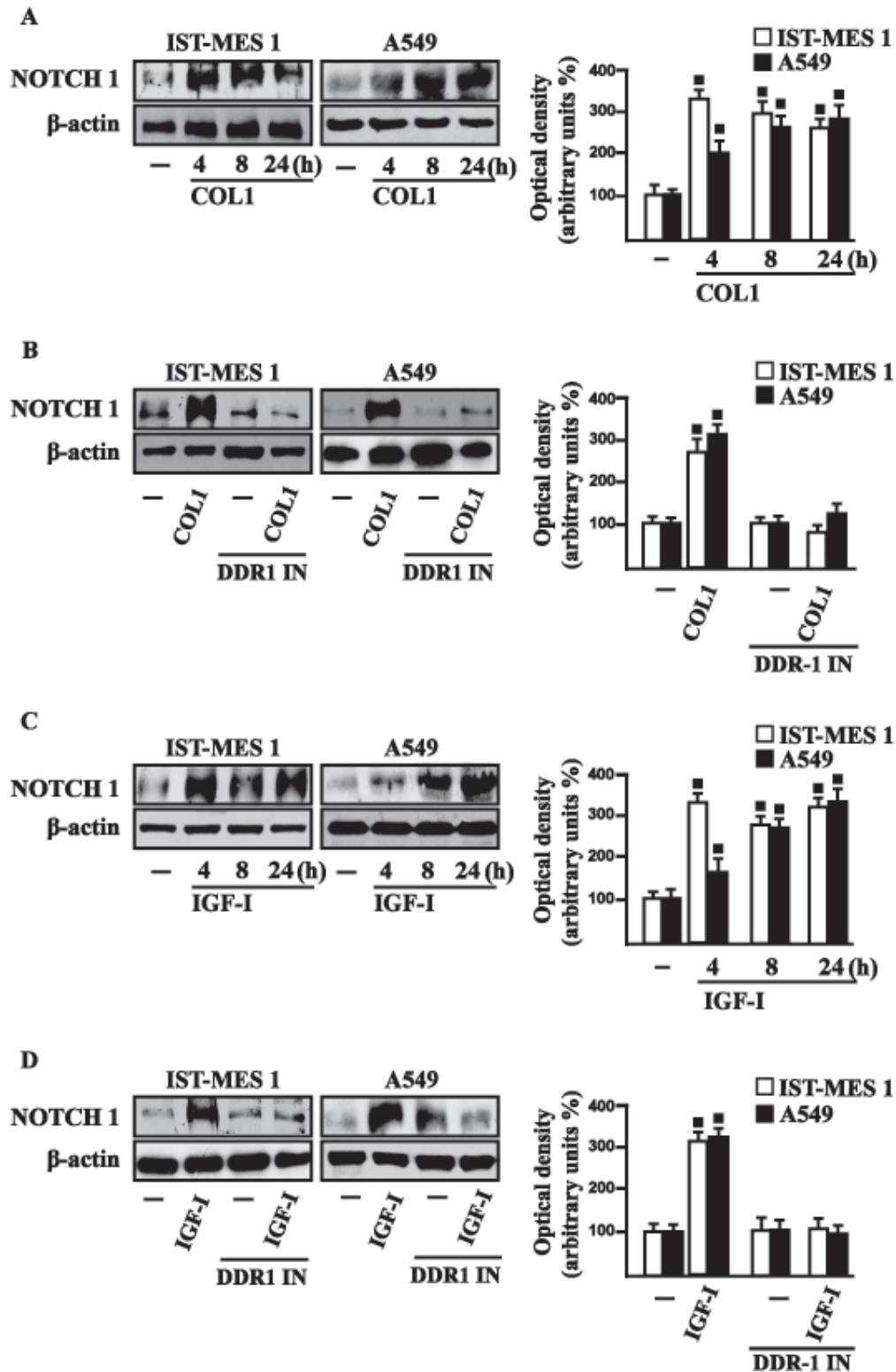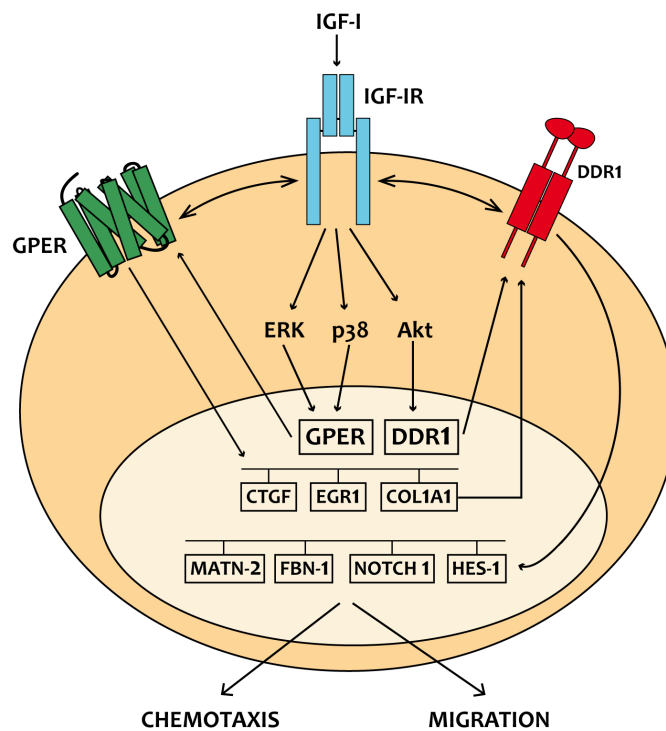
Figure 7: COL1 and IGF-I stimulate NOTCH 1 expression through DDR1 in IST-MES 1 and A549 cells. A. NOTCH 1 protein levels in cells treated with vehicle (-) or 10 µg/ml COL1, as indicated. **B.** NOTCH 1 protein levels in cells treated for 8 h with vehicle (-) or 10 µg/ml COL1 alone and in combination with 1 µM DDR1 inhibitor (DDR1 IN). **C.** NOTCH 1 protein levels in cells treated with vehicle (-) or 100 ng/ml IGF-I, as indicated. **D.** NOTCH 1 protein levels in cells treated for 8 h with vehicle (-) or 100 ng/ml IGF-I alone and in combination with 1 µM DDR1 inhibitor (DDR1 IN). Side panels show densitometric analysis of the blots normalized to β-actin and each data point represents the mean ± SD of three independent experiments. (■) $p < 0.05$ for cells receiving vehicle (-) *versus* treatments.

Figure 8: IGF-IR and GPER mediate the IGF-I induced up-regulation of NOTCH 1 in IST-MES 1 and A549 cells.
NOTCH 1 protein levels in cells transfected for 24 h with shIGF-IR **A.** or shGPER **D.** and then treated for 8 h with vehicle (-) or 100 ng/ml IGF-I. Efficacy of IGF-IR **B.-C.** and GPER **E.-F.** silencing. Side panels show densitometric analysis of the blots normalized to β-actin. (■) $p < 0.05$ for cells receiving vehicle (-) *versus* treatments.
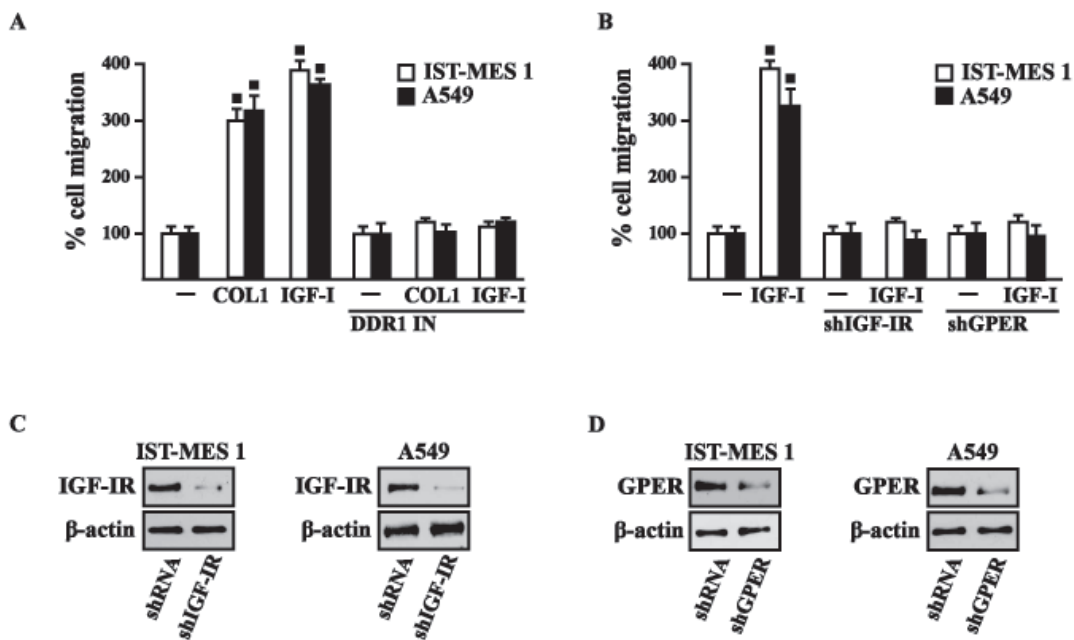
Figure 9: COL1 and IGF-I stimulate IST-MES 1 and A549 cell migration through DDR1, IGF-IR and GPER. **A.** The migration of IST-MES 1 and A549 cells upon 8 h treatment with vehicle (-), 10 µg/ml COL1 or 100 ng/ml IGF-I alone and in combination with 1 µM DDR1 inhibitor (DDR1 IN), as evaluated by Boyden Chamber assay. **B.** The migration of IST-MES 1 and A549 cells induced by 8 h treatment with 100 ng/ml IGF-I was prevented knocking down IGF-IR and GPER expression, as evaluated by Boyden Chamber assay. Efficacy of IGF-IR **C.-D.** and GPER **E.-F.** silencing. Values represent the mean ± SD of three independent experiments. (●) indicates $p < 0.05$ for cells treated with vehicle (-) *versus* treatments.

Figure 10: Schematic representation of the signaling network between IGF-IR, GPER and DDR1 activated by IGF-I. IGF-I stimulates the expression of GPER and its target genes, then IGF-IR and GPER trigger the IGF-I regulation of DDR1 target genes. The functional cross-talk of IGF-IR, GPER and DDR1 contributes to the chemotaxis and migration observed in cancer cells.

MATERIALS AND METHODS

Reagents

IGF-I, SB202190 (SB) and collagen I from rat tail were obtained from Sigma-Aldrich Inc. (Milan, Italy). PD98059 (PD) and 3-bromo-5-t-butyl-4-hydroxybenzylidenemalonitrile (AG1024) were purchased from Calbiochem (DBA, Milan, Italy). All compounds were solubilized in dimethylsulfoxide, except PD and IGF-I, which were dissolved in ethanol and in water, respectively. DDR1IN1 dihydrochloride (DDR-1 in) was purchased from Tocris Bioscience (Space, Milan, Italy).

Cell cultures

IST-MES1 malignant mesothelioma cells were kindly provided by Dr. Orengo (Istituto Nazionale per la Ricerca sul Cancro, Genova, Italy). Cells were previously characterized [77] and were grown in Nutrient Mixture F-10 Ham (Ham's F-10) medium supplemented with 10% fetal bovine serum (FBS) and 100 μg/ml penicillin/streptomycin. A549 lung cancer cells were obtained by ATCC, used < 6 months after resuscitation and maintained in DMEM/F12 (Dulbecco's modified Eagle's medium) supplemented with phenol red 10% FBS and 100 μg/ml penicillin/streptomycin. All cell lines were cultured at 37°C in 5% CO_2 and switched to medium without serum the day before immunoblots and reverse transcription-PCR experiments.

Plasmids and luciferase assays

The GPER luciferase expression vector (promGPER) was previously described [65]. The CTGF luciferase reporter plasmid (promCTGF) (-1999/+ 36)-luc was a gift from Dr. Chaqour. EGR1-luc plasmid, containing the -600 to +12 5'-flanking sequence from the human EGR1 gene, was kindly provided by Dr. Safe (Texas A&M University). The plasmid DN/cfos, which encodes a c-fos mutant that heterodimerizes with c-fos dimerization partners but does not allow DNA biding [78], was a kind gift from Dr C Vinson (NIH, Bethesda, MD, USA). The Renilla luciferase expression vector pRL-TK (Promega, Milan, Italy) was used as internal transfection control. Cells ($1x10^5$) were plated into 24-well dishes with 500 μl/well culture medium containing 10% FBS. Transfection were performed using X-treme GENE 9 DNA transfection reagent as recommended by the manufacturer (Roche Diagnostics, Milan, Italy), with a mixture containing 0.5 μg of reporter plasmid and 10 ng of pRL-TK. After 24 h, treatments were added and cells were incubated for 18 h. Luciferase activity was measured using the Dual Luciferase Kit (Promega, Milan, Italy) according to the manufacturer's recommendations. Firefly luciferase activity was normalized to the internal transfection control provided by the Renilla luciferase activity. Normalized relative light unit values obtained from cells treated with vehicle were set as 1-fold induction upon which the activity induced by treatments was calculated.

Gene silencing experiments

Cells were plated onto 10-cm dishes and transfected by X-treme GENE 9 DNA Transfection Reagent for 24 h before treatments with a control vector, a specific shRNA sequence for each target gene. The shIGF-IR and the respective control plasmids (shRNA) were purchased from SA Bioscience Corp. (Frederick, MD, USA) and used according to the manufacturer's recommendations. The short hairpin (sh)RNA constructs to knock down the expression of GPER and the unrelated shRNA control construct have been described previously [64].

Gene expression studies

Total RNA was extracted and cDNA was synthesized by reverse transcription as previously described [79-80]. The expression of selected genes was quantified by real-time PCR using Step One sequence detection system (Applied Biosystems, Milan, Italy). Gene-specific primers were designed using Primer Express version 2.0 software (Applied Biosystems Inc. Milan, Italy) and are as follows: GPER Fwd 5′- ACACACCTGGGTGGACACAA-3′ and Rev 5′-GGAGCCAGAAGCCACATCTG-3'; HES-1 Fwd 5′-TCAACACGACACCGGATAAA-3′ and Rev 5′-CCGCGAGCTATCTTTCTTCA-3′; NOTCH 1 Fwd 5′-AATGGCGGGAAGTGTGAAGC-3′ and Rev 5′-GCATAGTCTGCCACGCCTCT-3′; MTN-2 Fwd 5′-CTCCGAGTGGGCCAGTAAAG-3′ and Rev 5′- CTGGCTCAGATTCTGTTGGCT-3′; FBN-1 Fwd 5′-GCCGCATATCTCCTGACCTC-3′ and Rev 5′-GTCGATACACGCGGAGATGT-3′; 18S Fwd 5′- GGCGTCCCCCAACTTCTTA-3′ and Rev 5′-GGGCATCACAGACCTGTTATT-3′. Assays were performed in triplicate and the results were normalized for 18S expression and then calculated as fold induction of RNA expression.

Western blot analysis

Cells were processed according to a previously described protocol [81] to obtain protein lysate that was electrophoresed through a reducing SDS/10% (w/v) polyacrylamide gel, electroblotted onto a nitrocellulose membrane and probed with primary antibodies against antiphosphotyrosine antibody (4G10) (Merck Millipore,

Milan, Italy), IGF-IR (7G11), GPER (N-15), CTGF (L-20), phosphorylated ERK1/2 (E-4), ERK2 (C-14), NOTCH 1 (C-20), EGR1 (588), phosphorylated p-38 (D-8), p-38 (A-12), β-actin (C2), (Santa Cruz Biotechnology, DBA, Milan, Italy). Proteins were detected by horseradish peroxidase-linked secondary antibodies (DBA, Milan, Italy) and revealed using the ECL System (GE Healthcare).

Co-immunoprecipitation

Cells were lysed using 200 μl RIPA buffer with a mixture of protease inhibitors containing 1.7mg/ml aprotinin, 1mg/ml leupeptin, 200mmol/L phenylmethylsulfonyl fluoride, 200mmol/L sodium orthovanadate, and 100mmol/L sodium fluoride. A total of 100 μg proteins were incubated for 2 h with 2 μg of the appropriate antibody (GPER, N-15; IGF-1R, 7G11) and 20 μl of protein A/G agarose immunopreciptation reagent (Santa Cruz Biotechnology, DBA, Milan, Italy). Samples were centrifuged at 13,000 rpm for 5 min at 4°C to pellet beads. After four washes in PBS, samples were resuspended in RIPA buffer with protease inhibitors and SDS sample buffer. Western Blot analysis was performed as described above.

Migration assay

Migration assays were performed using Boyden chambers (Costar Transwell, 8 mm polycarbonate membrane, Sigma Aldrich, Milan, Italy). Cells were transfected in regular growth medium. After 8 h, cells were trypsinized and seeded in the upper chambers. Treatments were added to the medium without serum in the bottom wells where applicable, cells on the bottom side of the membrane were fixed and counted 8 hours after seeding.

Time-lapse microscopy

Cells (1×10^5) were seeded in 6-well plates and maintained in regular growth medium for 24 h. For knockdown experiments, cells were transfected for 24 h with shRNA constructs directed against IGF-IR or GPER and with an unrelated shRNA construct. Thereafter, cells were treated and transferred into a time-lapse microscopy platform, equipped with a heated stage chamber (Cytation™3 Cell Imaging Multi-Mode Reader, Biotek, Winooski, VT). Cells were maintained at routine incubation settings (37 °C, 5% CO_2) using temperature and gas controllers. To evaluate chemotaxis the images were recorded using Cytation 3 Cell Imaging Multimode Reader and the software Gen5 (BioTek, Winooski, VT) in 10 min intervals for 8 hours. Then, the images were processed as a movie using the software Adobe Creative Cloud Premier Pro CC. Frames collected every 10 minutes

are displayed at a rate of 10 frames s[-1].

Statistical analysis

Statistical analysis was performed using ANOVA followed by Newman-Keuls' testing to determine differences in means. $P < 0.05$ was considered as statistically significant.

GRANT SUPPORT

CONFLICTS OF INTEREST

The authors declare no conflict of interest.

REFERENCES

1. Travis WD, Brambilla E, Noguchi M, Nicholson AG, Geisinger K, Yatabe Y, Powell CA, Beer D, Riely G, Garg K, Austin JH, Rusch VW, Hirsch FR et al. International Association for the Study of Lung Cancer/ American Thoracic Society/European Respiratory Society: international multidisciplinary classification of lung adenocarcinoma: executive summary. Proc Am Thorac Soc. 2011; 8: 381-5.

2. Guo L, Zhang T, Xiong Y, Yang Y. Roles of NOTCH1 as a Therapeutic Target and a Biomarker for Lung Cancer: Controversies and Perspectives. Dis Markers. 2015; 2015: 520590.

3. Abdel-Rahman O. Targeting the MEK signaling pathway in non-small cell lung cancer (NSCLC) patients with RAS aberrations. Ther Adv Respir Dis. 2016.

4. Silvestri GA, Gonzalez AV, Jantz MA, Margolis ML, Gould MK, Tanoue LT, Harris LJ, Detterbeck FC. Methods for staging non-small cell lung cancer: Diagnosis and management of lung cancer, 3rd ed: American College of Chest Physicians evidence-based clinical practice guidelines. Chest. 2013; 143: e211S-50S.

5. Rajer M, Zwitter M, Rajer B. Pollution in the working place and social status: co-factors in lung cancer carcinogenesis. Lung Cancer. 2014; 85: 346-50.

6. Carbone M, Ly BH, Dodson RF, Pagano I, Morris PT, Dogan UA, Gazdar AF, Pass HI, Yang H. Malignant mesothelioma: facts, myths, and hypotheses. J Cell Physiol. 2012; 227: 44-58.

7. Rascoe PA, Jupiter D, Cao X, Littlejohn JE, Smythe WR. Molecular pathogenesis of malignant mesothelioma. Expert Rev Mol Med. 2012; 14: e12.

8. Valavanidis A, Vlachogianni T, Fiotakis K, Loridas S. Pulmonary oxidative stress, inflammation and cancer: respirable particulate matter, fibrous dusts and ozone as major causes of lung carcinogenesis through reactive oxygen species mechanisms. Int J Environ Res Public Health. 2013; 10: 3886-907.

9. Belfiore A, Frasca F, Pandini G, Sciacca L, Vigneri R. Insulin receptor isoforms and insulin receptor/insulin-like growth factor receptor hybrids in physiology and disease. Endocr Rev. 2009; 30: 586-623.

10. Belfiore A, Malaguarnera R. Insulin receptor and cancer. Endocr Relat Cancer. 2011; 18: R125-47.

11. Kai K, D'Costa S, Sills RC, Kim Y. Inhibition of the insulin-like growth factor 1 receptor pathway enhances the antitumor effect of cisplatin in human malignant mesothelioma cell lines. Cancer Lett. 2009; 278: 49-55.

12. Matà R, Palladino C, Nicolosi ML, Lo Presti AR, Malaguarnera R, Ragusa M, Sciortino D, Morrione A, Maggiolini M, Vella V, Belfiore A. IGF-I induces upregulation of DDR1 collagen receptor in breast cancer cells by suppressing MIR-199a-5p through the PI3K/AKT pathway. Oncotarget. 2016; 7: 7683-700. doi: 10.18632/oncotarget.6524.

13. Scagliotti GV and Novello S. The role of the insulin-like growth factor signaling pathway in non-small cell lung cancer and other solid tumors. Cancer Treat Rev. 2012; 38: 292-302.

14. Carboni JM, Lee AV, Hadsell DL, Rowley BR, Lee FY, Bol DK, Camuso AE, Gottardis M, Greer AF, Ho CP, Hurlburt W, Li A, Saulnier M, et al. Tumor development by transgenic expression of a constitutively active insulin-like growth factor I receptor. Cancer Res. 2005; 65: 3781-7.

15. Franks SE, Briah R, Jones RA, Moorehead RA. Unique roles of Akt1 and Akt2 in IGF-IR mediated lung tumorigenesis. Oncotarget. 2016; 7: 3297-316. doi: 10.18632/oncotarget.6489.

16. Hoang CD, Zhang X, Scott PD, Guillaume TJ, Maddaus MA, Yee D, Kratzke RA. Selective activation of insulin receptor substrate-1 and -2 in pleural mesothelioma cells: association with distinct malignant phenotypes. Cancer Res. 2004; 64: 7479-85.

17. Lee H, Kim SR, Oh Y, Cho SH, Schleimer RP, Lee YC. Targeting insulin-like growth factor-I and insulin-like growth factor-binding protein-3 signaling pathways. A novel therapeutic approach for asthma. Am J Respir Cell Mol Biol. 2014; 50: 667-77.

18. Hung CF, Rohani MG, Lee SS, Chen P, Schnapp LM. Role of IGF-1 pathway in lung fibroblast activation. Respir Res. 2013; 14: 102.

19. Lappano R and Maggiolini M. G protein-coupled receptors: novel targets for drug discovery in cancer. Nat Rev Drug Discov. 2011; 10: 47-60.

20. Liu C, Zhang Z, Tang H, Jiang Z, You L, Liao Y1.Crosstalk between IGF-1R and other tumor promoting pathways. Curr Pharm Des. 2014; 20: 2912-21.

21. Valiathan RR, Marco M, Leitinger B, Kleer CG, Fridman R. Discoidin domain receptor tyrosine kinases: new players in cancer progression. Cancer Metastasis Rev. 2012; 31: 295-321.

22. Malaguarnera R, Nicolosi ML, Sacco A, Morcavallo A, Vella V, Voci C, Spatuzza M, Xu SQ, Iozzo RV, Vigneri R, Morrione A, Belfiore A. Novel cross talk between IGF-IR and DDR1 regulates IGF-IR trafficking, signaling and biological responses. Oncotarget. 2015; 6: 16084-105. doi: 10.18632/oncotarget.3177.

23. Rozengurt E, Sinnett-Smith J, Kisfalvi K. Crosstalk between insulin/insulin-like growth factor-1 receptors and G protein-coupled receptor signaling systems: a novel target for the antidiabetic drug metformin in pancreatic cancer. Clin Cancer Res. 2010; 16: 2505-11.

24. Liu C, Liao Y, Fan S, Tang H, Jiang Z, Zhou B, Xiong J, Zhou S, Zou M, Wang J. G protein-coupled estrogen receptor (GPER) mediates NSCLC progression induced by 17β-estradiol (E2) and selective agonist G1. Med Oncol. 2015; 32: 104.

25. De Marco P, Bartella V, Vivacqua A, Lappano R, Santolla MF, Morcavallo A, Pezzi V, Belfiore A, Maggiolini M. Insulin-like growth factor-I regulates GPER expression and function in cancer cells. Oncogene. 2013; 32: 678-88.

26. De Marco P, Cirillo F, Vivacqua A, Malaguarnera R, Belfiore A, Maggiolini M. Novel Aspects Concerning the Functional Cross-Talk between the Insulin/IGF-I System and Estrogen Signaling in Cancer Cells. Front Endocrinol (Lausanne). 2015; 6: 30.

27. Jala VR, Radde BN, Haribabu B, Klinge CM. Enhanced expression of G-protein coupled estrogen receptor (GPER/GPR30) in lung cancer. BMC Cancer. 2012; 12: 624.

28. Siegfried JM, Hershberger PA, Stabile LP. Estrogen receptor signaling in lung cancer. Semin Oncol. 2009; 36: 524-31.

29. Pinton G, Brunelli E, Murer B, Puntoni R, Puntoni M, Fennell DA, Gaudino G, Mutti L, Moro L. Estrogen receptor-beta affects the prognosis of human malignant mesothelioma. Cancer Res. 2009; 69: 4598-604.

30. Pillai K, Pourgholami MH, Chua TC, Morris DL. Oestrogen receptors are prognostic factors in malignant peritoneal mesothelioma. J Cancer Res Clin Oncol. 2013; 139: 987-94.

31. Kim, JS, Kim, ES, Liu, D, Lee, JJ, Solis, L, Behrens, C, Lippman, SM, Hong, WK, Wistuba, II, Lee, HY. Prognostic implications of tumoral expression of insulin like growth factors 1 and 2 in patients with non-small-cell lung cancer. Clinical Lung Cancer. 2014; 15: 213-221.

32. Liu Z and Klominek J. Chemotaxis and chemokinesis of

malignant mesothelioma cells to multiple growth factors. Anticancer Res. 2004; 24: 1625-30.

33. Pandey DP, Lappano R, Albanito L, Madeo A, Maggiolini M, Picard D. Estrogenic GPR30 signalling induces proliferation and migration of breast cancer cells through CTGF. EMBO J. 2009; 28: 523-32.

34. Fujii M, Nakanishi H, Toyoda T, Tanaka I, Kondo Y, Osada H, Sekido Y. Convergent signaling in the regulation of connective tissue growth factor in malignant mesothelioma: TGFβ signaling and defects in the Hippo signaling cascade. Cell Cycle. 2012; 11: 3373-9.

35. Wang L, Chen Z, Wang Y, Chang D, Su L, Guo Y, Liu C. TR1 promotes cell proliferation and inhibits apoptosis through cyclin A and CTGF regulation in non-small cell lung cancer. Tumour Biol. 2014; 35: 463-8.

36. Shan LN, Song YG, Su D, Liu YL, Shi XB, Lu SJ. Early Growth Response Protein-1 Involves in Transforming Growth factor-β1 Induced Epithelial-Mesenchymal Transition and Inhibits Migration of Non-Small-Cell Lung Cancer Cells. Asian Pac J Cancer Prev. 2015; 16: 4137-42.

37. Maggiolini M, Picard D. The unfolding stories of GPR30, a new membrane-bound estrogen receptor. J Endocrinol. 2010; 204: 105-14.

38. Blackstock CD, Higashi Y, Sukhanov S, Shai SY, Stefanovic B, Tabony AM, Yoshida T, Delafontaine P. Insulin-like growth factor-1 increases synthesis of collagen type I *via* induction of the mRNA-binding protein LARP6 expression and binding to the 5' stem-loop of COL1a1 and COL1a2 mRNA. J Biol Chem 2014; 289: 7264-74.

39. Sukhanov S, Higashi Y, Shai SY, Blackstock C, Galvez S, Vaughn C, Titterington J, Delafontaine P. Differential requirement for nitric oxide in IGF-1-induced anti-apoptotic, anti-oxidant and anti-atherosclerotic effects. FEBS Lett. 2011; 585: 3065-72.

40. Sukhanov S, Higashi Y, Shai SY, Vaughn C, Mohler J, Li Y, Song YH, Titterington J, Delafontaine P. IGF-1 reduces inflammatory responses, suppresses oxidative stress, and decreases atherosclerosis progression in ApoE-deficient mice. Arterioscler Thromb Vasc Biol. 2007 Dec; 27: 2684-90.

41. Inamori Y, Ota M, Inoko H, Okada E, Nishizaki R, Shiota T, Mok J, Oka A, Ohno S, Mizuki N. The COL1A1 gene and high myopia susceptibility in Japanese. Hum Genet. 2007; 122: 151-7.

42. Wang CZ, Yeh YC, Tang MJ. DDR1/E-cadherin complex regulates the activation of DDR1 and cell spreading. Am J Physiol Cell Physiol. 2009; 297: C419-29.

43. Yeh YC, Wu CC, Wang YK, Tang MJ. DDR1 triggers epithelial cell differentiation by promoting cell adhesion through stabilization of E-cadherin. Mol Biol Cell. 2011; 22: 940-53.

44. Eswaramoorthy R, Wang CK, Chen WC, Tang MJ, Ho ML, Hwang CC, Wang HM, Wang CZ. DDR1 regulates the stabilization of cell surface E-cadherin and E-cadherin-mediated cell aggregation. J Cell Physiol. 2010; 224: 387-97.

45. Hidalgo-Carcedo C, Hooper S, Chaudhry SI, Williamson P, Harrington K, Leitinger B, Sahai E. Collective cell migration requires suppression of actomyosin at cell-cell contacts mediated by DDR1 and the cell polarity regulators Par3 and Par6. Nat Cell Biol. 2011; 13:49-58.

46. Ahuja J, Kanne JP, Meyer CA. Occupational lung disease. Semin Roentgenol. 2015; 50: 40-51.

47. Lenters V, Vermeulen R, Dogger S, Stayner L, Portengen L, Burdorf A, Heederik D. A meta-analysis of asbestos and lung cancer: is better quality exposure assessment associated with steeper slopes of the exposure-response relationships? Environ Health Perspect. 2011; 119: 1547-55.

48. Straif K, Benbrahim-Tallaa L, Baan R, Grosse Y, Secretan B, El Ghissassi F, Bouvard V, Guha N, Freeman C, Galichet L, Cogliano V; WHO International Agency for Research on Cancer Monograph Working Group. A review of human carcinogens—Part C: metals, arsenic, dusts, and fibres. Lancet Oncol. 2009; 10:453-4.

49. Mossman BT, Lippmann M, Hesterberg TW, Kelsey KT, Barchowsky A, Bonner JC. Pulmonary endpoints (lung carcinomas and asbestosis) following inhalation exposure to asbestos. J Toxicol Environ Health B Crit Rev. 2011; 14: 76-121.

50. Avivi-Green C, Singal M, Vogel WF. Discoidin domain receptor 1-deficient mice are resistant to bleomycin-induced lung fibrosis. Am J Respir Crit Care Med. 2006; 174: 420-7.

51. Lemeer S, Bluwstein A, Wu Z, Leberfinger J, Müller K, Kramer K, Kuster B. Phosphotyrosine mediated protein interactions of the discoidin domain receptor 1. J Proteomics. 2012; 75: 3465-77.

52. Matsuyama W, Watanabe M, Shirahama Y, Oonakahara K, Higashimoto I, Yoshimura T, et al. Activation of discoidin domain receptor 1 on CD14-positive bronchoalveolar lavage fluid cells induces chemokine production in idiopathic pulmonary fibrosis. J Immunol 2005; 174: 6490-8.

53. Heinzelmann-Schwarz VA, Gardiner-Garden M, Henshall SM, Scurry J, Scolyer RA, Davies MJ, Heinzelmann M, Kalish LH, Bali A, Kench JG, et al. Overexpression of the cell adhesion molecules DDR1, Claudin 3, and Ep-CAM in metaplastic ovarian epithelium and ovarian cancer. Clin Cancer Res 2004; 10: 4427-4436.

54. Vogel WF, Abdulhussein R, Ford CE. Sensing extracellular matrix: an update on discoidin domain receptor function. Cell Signal. 2006; 18: 1108-16.

55. Tavazoie SF, Alarcón C, Oskarsson T, Padua D, Wang Q, Bos PD, Gerald WL, Massagué J. Endogenous human microRNAs that suppress breast cancer metastasis. Nature. 2008; 451: 147-52.

56. Ramaswamy S, Ross KN, Lander ES, Golub TR. A molecular signature of metastasis in primary solid tumors. Nat Genet. 2003; 33: 49-54.

57. Grande JP, Melder DC, Zinsmeister AR. Modulation of collagen gene expression by cytokines: stimulatory effect of transforming growth factor-beta1, with divergent effects of epidermal growth factor and tumor necrosis factor-alpha on collagen type I and collagen type IV. J Lab Clin Med. 1997; 130: 476-86.

58. Filardo EJ, Graeber CT, Quinn JA, Resnick MB, Giri D, DeLellis RA, Steinhoff MM, Sabo E. Distribution of GPR30, a seven membrane-spanning estrogen receptor, in primary breast cancer and its association with clinicopathologic determinants of tumor progression. Clin Cancer Res. 2006; 12: 6359-66.

59. Smith HO, Arias-Pulido H, Kuo DY, Howard T, Qualls CR, Lee SJ, Verschraegen CF, Hathaway HJ, Joste NE, Prossnitz ER. GPR30 predicts poor survival for ovarian cancer. Gynecol Oncol. 2009; 114: 465-71.

60. Smith HO, Leslie KK, Singh M, Qualls CR, Revankar CM, Joste NE, Prossnitz ER. GPR30: a novel indicator of poor survival for endometrial carcinoma. Am J Obstet Gynecol. 2007; 196: 386.e1-11.

61. Marjon NA, Hu C, Hathaway HJ, Prossnitz ER. G protein-coupled estrogen receptor regulates mammary tumorigenesis and metastasis. Mol Cancer Res. 2014; 12: 1644-54.

62. De Marco P, Romeo E, Vivacqua A, Malaguarnera R, Abonante S, Romeo F, Pezzi V, Belfiore A, Maggiolini M. GPER1 is regulated by insulin in cancer cells and cancer-associated fibroblasts. Endocr Relat Cancer. 2014; 21:739-53.

63. Vivacqua A, Lappano R, De Marco P, Sisci D, Aquila S, De Amicis F, Fuqua SA, Andò S, Maggiolini M. G protein-coupled receptor 30 expression is up-regulated by EGF and TGF alpha in estrogen receptor alpha-positive cancer cells. Mol Endocrinol. 2009; 23: 1815-26.

64. Albanito L, Sisci D, Aquila S, Brunelli E, Vivacqua A, Madeo A, Lappano R, Pandey DP, Picard D, Mauro L, Andò S, Maggiolini M. Epidermal growth factor induces G protein-coupled receptor 30 expression in estrogen receptor-negative breast cancer cells. Endocrinology. 2008; 149: 3799-808.

65. Recchia AG, De Francesco EM, Vivacqua A, Sisci D, Panno ML, Andò S, Maggiolini M. The G protein-coupled receptor 30 is up-regulated by hypoxia-inducible factor-1alpha (HIF-1alpha) in breast cancer cells and cardiomyocytes. J Biol Chem. 2011; 286: 10773-82.

66. De Francesco EM, Lappano R, Santolla MF, Marsico S, Caruso A, Maggiolini M. HIF-1α/GPER signaling mediates the expression of VEGF induced by hypoxia in breast cancer associated fibroblasts (CAFs). Breast Cancer Res. 2013; 15: R64.

67. De Francesco EM, Pellegrino M, Santolla MF, Lappano R, Ricchio E, Abonante S, Maggiolini M. GPER mediates activation of HIF1α/VEGF signaling by estrogens. Cancer Res. 2014; 74: 4053-64.

68. Bartella V, De Francesco EM, Perri MG, Curcio R, Dolce V, Maggiolini M, Vivacqua A. The G protein estrogen receptor (GPER) is regulated by endothelin-1 mediated signaling in cancer cells. Cell Signal. 2016; 28: 61-71.

69. Baserga R, Peruzzi F, Reiss K. The IGF-1 receptor in cancer biology. Int J Cancer. 2003; 107: 873-7.

70. Yakar S, Leroith D, Brodt P. The role of the growth hormone/insulin-like growth factor axis in tumor growth and progression: Lessons from animal models. Cytokine Growth Factor Rev. 2005; 16: 407-420.

71. Novosyadlyy R, Lann DE, Vijayakumar A, Rowzee A, Lazzarino DA, Fierz Y, et al. Insulin-mediated acceleration of breast cancer development and progression in a nonobese model of type 2 diabetes. Cancer Res. 2010; 70: 741-751.

72. Kisfalvi K, Eibl G, Sinnett-Smith J, Rozengurt E. Metformin disrupts crosstalk between G protein-coupled receptor and insulin receptor signaling systems and inhibits pancreatic cancer growth. Cancer Res. 2009; 69: 6539-45.

73. Akekawatchai C, Holland JD, Kochetkova M, Wallace JC, McColl SR. Transactivation of CXCR4 by the insulin-like growth factor-1 receptor (IGF-1R) in human MDA-MB-231 breast cancer epithelial cells. J Biol Chem. 2005; 280: 39701-8.

74. Gombos A, Metzger-Filho O, Dal Lago L, Awada-Hussein A. Clinical development of insulin-like growth factor receptor—1 (IGF-1R) inhibitors: at the crossroad? Invest New Drugs. 2012; 30: 2433-42.

75. Fidler MJ, Shersher DD, Borgia JA, Bonomi P. Targeting the insulin-like growth factor receptor pathway in lung cancer: problems and pitfalls. Ther Adv Med Oncol. 2012; 4: 51-60.

76. Scotlandi K and Belfiore A. Targeting the Insulin-Like Growth Factor (IGF) System Is Not as Simple as Just Targeting the Type 1 IGF Receptor. Am Soc Clin Oncol Educ Book. 2012: 599-604.

77. Orengo AM, Spoletini L, Procopio A, Favoni RE, De Cupis A, Ardizzoni A, Castagneto B, Ribotta M, Betta PG, Ferrini S, Mutti L. Establishment of four new mesothelioma cell lines: characterization by ultrastructural and immunophenotypic analysis. Eur Respir J. 1999; 13: 527-34.

78. Gerdes MJ, Myakishev M, Frost NA, Rishi V, Moitra J, Acharya A, Levy MR, Park SW, Glick A, Yuspa SH, Vinson C. Activator protein-1 activity regulates epithelial tumor cell identity. Cancer Res 2006; 66: 7578-7588.

79. Rigiracciolo DC, Scarpelli A, Lappano R, Pisano A, Santolla MF, De Marco P, Cirillo F, Cappello AR, Dolce V, Belfiore A, Maggiolini M, De Francesco EM. Copper activates HIF-1α/GPER/VEGF signalling in cancer

cells. Oncotarget. 2015; 6: 34158-77. doi: 10.18632/oncotarget.5779.

80. Rigiracciolo DC, Scarpelli A, Lappano R, Pisano A, Santolla MF, Avino S, De Marco P, Bussolati B, Maggiolini M, De Francesco EM. GPER is involved in the stimulatory effects of aldosterone in breast cancer cells and breast tumor-derived endothelial cells. Oncotarget. 2016; 7: 94-111. doi: 10.18632/oncotarget.6475.

81. De Marco P, Lappano R, De Francesco EM, Cirillo F, Pupo M, Avino S, Vivacqua A, Abonante S, Picard D, Maggiolini M. GPER signalling in both cancer-associated fibroblasts and breast cancer cells mediates a feedforward IL1β/IL1R1 response. Scientific Reports 2016, in press.

Review Article

PROTECTIVE ROLE OF GPER AGONIST G-1 ON CARDIOTOXICITY INDUCED BY DOXORUBICIN[†]

Short title: GPER protects from cardiotoxicity

Ernestina M. De Francesco[1], Carmine Rocca[2], Francesco Scavello[2], Daniela Amelio[2], Teresa Pasqua[2], Damiano C. Rigiracciolo[1], Andrea Scarpelli[1], Silvia Avino[1], Francesca Cirillo[1], Nicola Amodio[4], Maria C. Cerra[2,3], Marcello Maggiolini[1] and Tommaso Angelone[2,3]

[1]Department of Pharmacy, Health and Nutritional Sciences, University of Calabria, Rende (CS);
[2]Department of Biology, Ecology and E.S., University of Calabria, Rende (CS);
[3]National Institute of Cardiovascular Research, Bologna.
[4]Dept. of Experimental and Clinical Medicine, University of Catanzaro Magna Græcia, Catanzaro.

Corresponding authors:

Prof. Marcello Maggiolini
Tel: + 39-0984 493076
Fax: +39-0984 493458
e-mail: marcellomaggiolini@yahoo.it
        marcello.maggiolini@unical.it
&

Prof.ssa Maria Carmela Cerra

Tel.: +39-0984 492907
Fax: +39-0984 492906
e-mail: maria_carmela.cerra@unical.it

ABSTRACT

The use of Doxorubicin (Dox), a frontline drug for many cancers, is often complicated by dose-limiting cardiotoxicity in approximately 20% of patients. The G-protein estrogen receptor GPER/GPR30 mediates estrogen action as the cardioprotection under certain stressful conditions. For instance, GPER activation by the selective agonist G-1 reduced myocardial inflammation, improved immunosuppression, triggered pro-survival signaling cascades, improved myocardial mechanical performance and reduced infarct size after ischemia/reperfusion (I/R) injury. Hence, we evaluated whether ligand-activated GPER may exert cardioprotection in male rats chronically treated with Dox. 1 week of G-1 (50 µg/kg/day) intraperitoneal administration mitigated Dox (3 mg/kg/day) adverse effects, as revealed by reduced TNF-α, IL-1β, LDH and ROS levels. Western blotting analysis of cardiac homogenates indicated that G-1 prevents the increase in p-c-jun, BAX, CTGF, iNOS and COX2 expression induced by Dox. Moreover, the activation of GPER rescued the inhibitory action elicited by Dox on the expression of BCL2, pERK and pAKT. TUNEL assay indicated that GPER activation may also attenuate the cardiomyocyte apoptosis upon Dox exposure. Using ex vivo Langendorff perfused heart technique, we also found an increased systolic recovery and a reduction of both infarct size and LDH levels in rats treated with G-1 in combination with Dox respect to animals treated with Dox alone. Accordingly, the beneficial effects induced by G-1 were abrogated in the presence of the GPER selective antagonist G15. These data suggest that GPER activation mitigates Dox-induced cardiotoxicity, thus proposing GPER as a novel pharmacological target to limit the detrimental cardiac effects of Dox treatment. This article is protected by copyright. All rights reserved

INTRODUCTION

Doxorubicin (Dox)-based treatments represent a highly effective therapeutic strategy in a large number of malignant diseases, including leukemias, lymphomas, sarcomas and breast cancer (Young et al., 1981). However, Dox generates reactive oxygen species (ROS) that may trigger cardiotoxicity leading to cardiomyopathy and heart failure (Carvalho et al., 2014). This response to Dox has limited its clinical use, therefore great attention has been addressed to the identification of novel pharmacological strategies able to mitigate the negative cardiovascular effects exerted by Dox.

The G-protein estrogen receptor GPER, also known as GPR30, has been largely implicated in the biological action of estrogens in diverse tissues, including the cardiovascular system (Maggiolini and Picard, 2010; Lindsey and Chappell, 2011; De Francesco et al., 2013a, 2014; Meyer et al., 2014, Zimmerman et al., 2016). In this regard, our and other previous studies have demonstrated that GPER is expressed in the rat and human heart and mediates a variety of beneficial cardiovascular effects (Filice et al., 2009; Patel et al., 2010). In addition, previous investigations have shown the cardioprotective actions mediated by GPER, particularly under stressful conditions characterized by increased ROS levels (De Francesco et al., 2013a, 2014; Meyer et al., 2014; Filice et al., 2009; Patel et al., 2010; Recchia et al., 2011). For instance, in a hypertensive rat heart model, the administration of the selective GPER ligand G-1 triggered beneficial negative inotropic and lusitropic effects, which were prevented in the presence of the selective GPER antagonist G15 (De Francesco et al., 2013a). These observations suggest that GPER may be considered as a valuable target in cardiovascular diseases characterized by increased oxidative stress. In this context, GPER activation by G-1 was shown to reduce infarct size and contractile dysfunctions after ischemia/reperfusion (I/R) injury through the involvement of PI3K kinase/AKT signalling pathway (Deschamps and Murphy, 2009). In addition, G-1 induced anti-inflammatory and pro-survival effects after I/R by reducing the production of TNF-alpha, interleukin (IL)-1beta and IL-6 as well as inhibiting mitochondria permeability transition pore opening (Weil et al., 2010; Bopassa et al., 2010). Consequently, GPER has emerged as a mediator of cardioprotection and a novel therapeutic target in cardiac diseases characterized by impaired oxidative balance.

In the present study we demonstrate that GPER activation by G-1 inhibits the adverse effects of Dox, as revealed by reduced TNF-α, IL-1β, ROS, LDH plasma and tissue levels. In rat heart homogenates, we found that G-1 also prevents the increase in p-c-jun, BAX, CTGF,

iNOS and COX2 expression upon Dox treatment. In addition, the activation of GPER prevented the inhibitory action elicited by Dox on BCL2, pERK, pAKT expression and attenuated the apoptotic actions exerted by Dox exposure. Likewise, GPER activation mitigated the adverse effects of Dox after I/R as evidenced by the increased systolic recovery and both reduced infarct size and LDH levels. Accordingly, the beneficial effects induced by G-1 were prevented in the presence of the GPER antagonist G15. These data suggest that GPER activation may mitigate Dox-induced cardiotoxicity, thus proposing GPER as a novel therapeutic target in cancer patients treated with Dox.

METHODS

Animals. Male Wistar rats (~300 g body weight) (Harlan Laboratories, Udine, Italy), identically housed under controlled lighting and temperature conditions, fed a standard diet and water ad libitum. All protocols were conducted in accordance with the Declaration of Helsinki, the Italian law (D.L. 26/2014), the Guide for the Care and Use of Laboratory Animals published by the US National Institutes of Health (2011) and the Directive 2010/63/EU of the European Parliament on the protection of animals used for scientific. The project was approved by the Italian Ministry of Health, Rome and by the ethics review board.

Drugs. Doxorubicin (Dox) was from Sigma Aldrich (Milan, Italy). 1-[4-(-6-Bromobenzol[1,3]diodo-5-yl)-3a,4,5,9-btetrahydro-3H-cyclopenta[c-]quinolin8yl]ethanone (G-1) and (3aS,4R,9bR)-4-(6-bromo-1,3-benzodioxol-5-yl)-3a,4,5,9b-3H-cyclopenta[c]quinolone (G15) were from Tocris Bioscience, distributed by Space (Milan, Italy). G-1 and G15 were dissolved in DMSO. Preliminary experiments showed that the presence of equivalent amounts of DMSO in KHs solution do not modify basal cardiac performance.

Experimental protocols

In vivo **treatment:** to evaluate whether G-1 counteracts Doxorubicin (Dox)-induced cardiotoxicity, animals were divided in five groups:

Group I (control): normal saline was i.p. administered each day throughout 1 week at a dose of 3 mL/kg/day.

Group II (Doxorubicin: Dox): Dox was i.p. administered each day throughout 1 week at a dose of 3 mg/kg/day, resulting in a cumulative dose of 21 mg/kg (Saad et al., 2004).

Group III (G-1: G-1): G-1 was i.p. administered each day at a dose of 50 μg/kg/day (De Francesco et al., 2013b; Filice E et al., 2009).

Group IV (Doxorubicin + G-1: Dox + G-1): Dox (3 mg/kg/day) in combination with G-1 (50 μg/kg/day) was i.p administered throughout 1 week.

Group V (Doxorubicin + G-1 + G15: Dox + G-1 + G15): Dox (3 mg/kg/day) in combination with G-1 (50 μg/kg/day) and G15 (160 μg/kg/day) was i.p. administered throughout 1 week (De Francesco et al., 2013b; Filice E et al., 2009).

Animals were sacrificed after 7 days in order to allow heart performance evaluation by Langendorff perfusion technique, plasma collection, as well as protein expression analysis on tissue homogenates. G-1 and G15 doses were chosen on the basis of preliminary dose-response curves (data not shown) and literature data (De Francesco et al., 2013a; Filice E et al., 2009). Dox dose was chosen on the basis of literature data (Saad et al., 2004).

Plasma collection. Blood samples were collected from the abdominal aorta with heparinized syringe. Plasma was then separated by centrifugation at 3000 g (15 minutes, 4°C) and stored at -80°C until assays. Blood samples were used to measure plasma levels of ROS, TNF-α, IL-1β and LDH, as described below.

Enzyme-Linked Immunosorbent Assay (ELISA). TNF-α and IL-1β determinations were performed by using ELISA system according to manufacturer's instructions (Thermo Scientific, Rockford, USA). To determine tissue levels of TNF-α and IL-1β, left ventricle of hearts of each group was homogenized using Ultra-Turrax®. Plasma samples and cardiac tissue homogenates were incubated with antibodies against TNF-α or IL-1β that were pre-coated to wells of microplates. After discarding samples, biotinylated antibodies were added and the incubation was continued. Biotinylated antibody solution was discarded and further incubation with streptavidin-HRP was continued. Finally, TMB (3,3′,5,5′-tetramethylbenzidine) solution was added and the absorbance was measured at 450 nm immediately after stopping the reaction by adding 2 M H_2SO_4.

Lactate Dehydrogenase (LDH) determinations. LDH was measured on both blood samples and samples of coronary effluent from isolated Langendorff heart perfusion. Samples of coronary effluent, during reperfusion, were withdrawn with a catheter inserted into the right ventricle via the pulmonary artery. Data (IU/L) were expressed as cumulative values for the entire reperfusion period. LDH released was determined by spectrophotometric analysis at 340 nM, using a classic procedure (Penna et al., 2006).

ROS production. ROS production was evaluated using the ELISA system, according to the manufacturer (Sunred Biological Technology, Shanghai, China). Briefly, blood samples from rats belonging to all experimental groups were collected from the abdominal aorta with heparinized syringe and centrifuged at 3000 g for 15 minutes (4°C) to obtain plasma. 40 μL of

plasma samples were then incubated in the presence of ROS-antibody labeled with Biotin and Streptavidin-HRP for 60 minutes at 37 °C. After chromogen addition, absorbance at 450 nm was immediately measured.

Gene expression studies. After chronic treatments, rat hearts (n= 6) were dissected, homogenized and processed for mRNA extraction, to evaluate the expression of GPER by real-time PCR using the Step OneTM sequence detection system (Applied Biosystems Inc., Milan, Italy), as previously described (De Francesco et al., 2013b). Gene-specific primers were designed using Primer Express version 2.0 software (Applied Biosystems Inc., Milan, Italy) and are as follows: GPER Fwd: 5'-TCTACCTACCCTCCCGTGTGG-3' and Rev:5'-AGGCAGGAGAGGAAGAGAGC-3'; 18S Fwd: 5'-TTTGTTGGTTTTCGGAACTGA -3' and Rev: 5'-CGTTTATGGTCGGAACTACGA -3'. 18S expression was used as a control.

Immunoblotting analysis. After chronic treatments, rat hearts (n = 6) were dissected, homogenized and processed for protein extraction, to evaluate protein expression by immunoblotting, as previously described (De Francesco et al., 2013b). After loading and transfer, membranes were blocked and incubated with primary polyclonal IgG antibody for GPER (N-15) phosphorylated ERK1/2 (E-4), phosphorylated AKT1/2/3 Ser 473-R, phosphorylated-c-Jun Ser 73, ERK2 (C-14), AKT/1/2/3 (H-136), c-Jun (N), iNOS (C11), COX2 (N-20), CTGF (L-20), BAX (6D150), BCL2 (C2), β-tubulin (H-235-2) and appropriate secondary HRP-conjugated antibodies, all purchased from Santa Cruz Biotechnology (DBA, Milan, Italy). Proteins and phosphoproteins levels were detected with horseradish peroxidase-linked secondary antibodies and revealed by using the Enhanced Chemiluminescence system (GE Healthcare, Milan, Italy).

Histological analysis. After chronic treatments and sacrifice, ventricular sections (3 hearts for each group), placed onto Superfrost Plus slides (Menzel-Glaser, Braunschwerg-Germany), were deparaffined, rehydrated and TUNEL staining (in situ Cell Death Detection Kit, POD from Roche Diagnostics-Germany) was performed, as previously described (Amelio et al., 2013). Briefly, sections incubated with proteinase K (20μg/mL; 37°C; 20-min) were washed, rinsed and incubated with TUNEL (37°C, 60-min); reaction was blocked by 3% BSA in PBS at room temperature. Horseradish peroxidase-conjugated antibodies were added and incubated at 37°C. Terminal deoxynucleotidyl transferase (TdT) enzyme was omitted for negative control. Nuclei were counterstained with hematoxylin. Apoptotic Index (AI) was calculated as $100 \times$ (number of myocytes TUNEL-positive cell nuclei per field/total number of cell nuclei per field). For each condition, four randomly selected fields were evaluated and averaged.

Ex vivo studies.

Perfusion method. In order to evaluate the cardiac parameters, at the end of the treatments rats were anesthetized with ethyl carbamate (2 g/kg body weight, i.p) and sacrificed. Then, hearts were rapidly excised, immediately placed in ice-cold perfusion buffer, cannulated via the aorta and perfused in the Langendorff apparatus at a constant flow-rate of 12 ml/min (37°C), as previously described (De Francesco et al., 2013a). To evaluate inotropism, the developed left ventricular pressure (dLVP; mmHg, index of contractile activity calculated from LVP-LVEDP) and the left ventricular end diastolic pressure (LVEDP; mmHg, index of contracture) were measured during the experiment by using PowerLab data acquisition system. Parameters were analyzed by using Chart software (ADInstruments, Oxford-UK), as previously reported (De Francesco et al., 2013a). Hearts were perfused with Krebs-Henseleit solution (KHs) (pH 7.4; gassed with 95 % O_2 and 5 % CO_2) containing (in mmol/l): 113.0 mM NaCl; 4.7 mM KCl; 1.2 mM $MgSO_4$; 25.0 mM $NaHCO_3$; 1.2 mM KH_2PO_4; 1.8 mM $CaCl_2$; 11,0 mM glucose; 1.1 mM mannitol; 5mM Na-pyruvate (Cerra et al., 2006).

Ischemia/Reperfusion (I/R) protocols. After chronic treatment, rats from each group were subjected to I/R protocol. Baseline parameters were recorded during the first 40 min of stabilization, then hearts were subjected to 30-min of global, no-flow ischemia followed by 120-min of reperfusion (I/R). The protocol of treatments for each group was:

Group I (Saline): rats were treated each day throughout 1 week with saline solution; n=6 hearts were stabilized and subjected to I/R protocol.

Group II (Dox): rats were treated each day throughout 1 week with a single dose i.p. of Dox, n=6 hearts were stabilized and subjected to I/R protocol.

Group III (G-1): rats were treated once a day (a single i.p. dose) for 1 week with G-1, n=6 hearts were stabilized and subjected to I/R protocol.

Group VI (Dox + G-1): rats were treated each day throughout 1 week with a single dose i.p. of G-1 in combination with Dox, n=6 hearts were stabilized and subjected to I/R protocol.

Group V (Dox + G-1+ G15): rats were treated each day throughout 1 week with a single dose i.p. of G-1 in combination with Dox and G15, n=6 hearts were stabilized and subjected to I/R protocol.

At the end of treatments, cardiac parameters were analysed by Langendorff technique. Administration of G15 alone, at the concentration used, did not influence I/R damages (data not shown). Cardiac performance before and after ischemia was evaluated by analyzing LVP recovery, as an index of contractile activity, and LVEDP as an index of contracture, defined as an increase in LVEDP of 4 mmHg above the baseline level (Penna et al., 2006;Cerra et al., 2006).

Infarct size (IS). Hearts were rapidly removed from the perfusion apparatus at the end of reperfusion. The left ventricle was dissected into 2- to 3-mm circumferential slices. After 20-min of incubation at 37°C in 0.1% solution of nitro blue tetrazolium in phosphate buffer, unstained necrotic tissue was carefully separated from stained viable tissue by an independent observer who was not aware of the nature of the intervention. The weights of the necrotic and non-necrotic tissues were then determined, and the necrotic mass was expressed as a percentage of total left ventricular mass, including septum (Penna et al., 2012).

A comprehensive diagram showing the experimental protocol for both *in-vivo* and *ex-vivo* studies is detailed below:
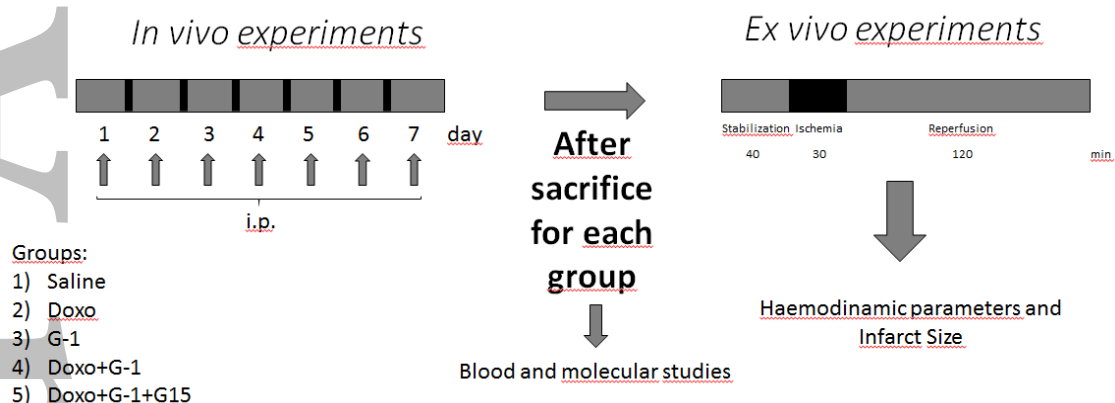
Statistics. All data were expressed as means±SEM. One-way ANOVA, non-parametric Mann Whitney-U test and Newman-Keuls Multiple Comparation Test (for post-ANOVA comparisons) were used when appropriate (Graphpad Prism5). A *p* value <0.05 was considered statistically significant.

RESULTS

GPER activation attenuates the increase of inflammatory and oxidative stress markers induced by Dox. We started our study by evaluating whether GPER mediates the reduction in inflammatory and oxidative stress markers in rats treated with Dox alone and in combination with the GPER selective agonist G-1 as well as the GPER selective antagonist G15. Following the experimental protocol described in Material and Methods section, at the end of all treatments, heart (n=6 for each group) weights were: saline group: 1.49±0.03g; Dox group: 2.09±0.14g*; G-1 group: 1.43±0.07g; Dox in combination with G-1: 1.52±0.05g; Dox in combination with G-1 and G15: 1.96±0.1g* (*p<0.05 vs saline).

IL-1β, TNF-α and LDH plasma levels were significantly increased in Dox-treated animals with respect to animals treated with saline (**Fig. 1A,B** and **Fig. 2A**). G-1 alone did not induce significant changes in IL-1β, TNF-α and LDH plasma levels with respect to the saline group (**Fig. 1A,B** and **Fig. 2A**). However, G-1 lowered the IL-1β, TNF-α and LDH plasma values observed upon Dox exposure, an effect no longer evident in the presence of the GPER antagonist G15 (**Fig. 1A,B** and **Fig. 2A**). In addition, G-1 counteracted the Dox-induced plasma levels of ROS, while G15 prevented the response triggered by G-1 (**Fig. 2B**). The levels of IL-1β were increased in the heart of rats treated with Dox alone and Dox in combination with G-1 and G15 with respect to animals treated with saline, G-1 and G-1 in combination with Dox (**Fig. 1C**). Similarly, TNF-α values were detected higher in animal groups treated with Dox alone and Dox in combination with G-1 and G15 respect to values detected in animals treated with saline, G-1 and G-1 in combination with Dox (**Fig. 1D**).

Ligand-activated GPER reverses certain biological responses triggered by doxorubicin. On the basis of the above findings suggesting that GPER activation mitigates the detrimental cardiac effects of Dox, we analysed whether GPER may reverse certain Dox-induced responses in cardiomyocytes. First, we assessed that in cardiac homogenates of all animal groups the chronic exposure to treatments do not determine any variation in GPER expression, as evaluated by real-time PCR and western blotting (**Fig. 3A-C**). Then, we evaluated main transduction signalling involved in cardiomyocytes survival as ERK1/2 and AKT (De Jonge et al., 2006). G-1 prevented the inhibition of ERK1/2 and AKT phosphorylation induced by Dox (**Fig. 3D,E**), while this effect was no longer evident in the presence of the GPER antagonist G15 (**Fig. 3D,E**). In addition, the phosphorylation of c-jun triggered by Dox was prevented by G-1 and rescued in the presence of G15 (**Fig. 3D,E**). Noteworthy, G-1 inhibited the up-regulation of BAX observed upon Dox treatment, however this effect of G-1 was abolished in the presence of G15 (**Fig. 3F,G**). Conversely, the down-regulation of the antiapoptotic factor BCL2 observed upon Dox treatment was prevented using G-1, while this action of G-1 was rescued using G15 (**Fig. 3F,G**). In addition, the up-regulation of iNOS, COX2 and CTGF triggered by Dox was abrogated in the presence of G-1 and rescued in the presence of G15 (**Fig. 3H,I**). Next, we evaluated whether G-1 may inhibit cardiomyocyte apoptosis upon Dox exposure. As shown in Figure 4, vehicle-treated hearts exhibited limited TUNEL-positive nuclei, while Dox treatment substantially increased the positivity (**Fig. 4B**). Furthermore, G-1 used in combination with Dox significantly reduced the number of apoptotic myocytes (**Fig. 4C,D**), however the action of G-1 was abolished using G15 (data not shown). Taken together, these data suggest that the activation of GPER may counteract

certain biological responses involved in the cardiotoxicity induced by Dox (Vejpongsa and Yeh, 2014; Tocchetti et al., 2014; Octavia et al., 2012; Mantawy et al., 2014).

GPER activation improves post-ischemic cardiac function. The possibility that G-1 treatment elicits cardioprotection was investigated in hearts from each group exposed to I/R manoeuvres by analysing both systolic and diastolic function. For *ex-vivo* experiments, the following basal cardiac parameters were obtained after 40 min equilibration: LVP = 74.13 ± 2.13, LVEDP = 5-8 mmHg**.** The endurance and stability of the preparations, analysed by measuring the performance variables every 10 min, showed that each heart was stable up to 180 min. Systolic function was represented by the level of developed left ventricular pressure (i.e., dLVP recovery). Results showed that the post ischemic performance of the heart from the saline group was characterized by a limited LVP recovery. In particular, at the end of reperfusion, dLVP was 39.9 ± 8.2 mmHg (about 50% of the basal value). The post ischemic performance was lower (dLVP: about 38%) in hearts from the group treated with Dox alone, while it resulted similar to the basal value when Dox was administered in combination with G-1 that lost its protective action using the selective GPER antagonist G15 (**Fig. 5**). Diastolic function is expressed by contracture development (i.e., LVEDP 4 mmHg or more above baseline level) (Pagliaro et al., 2003). In the saline group, I/R markedly increased LVEDP which resulted 38 ± 10 mmHg at the end of reperfusion with respect to 6.8 ± 0.8 mmHg in the baseline. In the Dox group, LVEDP was higher (33 ± 7 mmHg) respect to the baseline value (8.3 ± 1.4 mmHg) (**Fig. 5**). In heart of rats exposed to Dox in combination with G-1 and in those exposed to G-1 alone, at the end of the reperfusion, LVEDP was not significantly modified, being 5.6 ± 0.3 and 6.7±1 mmHg, respectively **(Fig. 5).** During reperfusion, G15 abolished the G-1 associated protection on contracture, as LVEDP at the end of reperfusion was 29.9 ± 3.8 mmHg (**Fig. 5**). Total infarct size (IS) was expressed as a percentage of left ventricular (LV) mass (**Fig. 6**). IS was 68.6 ± 3.4% in saline group, 78.2 ± 4.8% in Dox group, 76.3 ± 5% in the animal group treated with G-1 in combination with Dox and G15. The simultaneous administration of G-1 and Dox determined an IS of 44.5 ± 2%, which was similar to that observed in hearts exposed to G-1 alone (52.6 ± 2.6%) (**Fig. 6**), evidencing that G-1 is able to reduce the IS area induced by Dox. Next, a slight decrease in IS and a small increase in dLVP functional recovery were observed in animals treated with Dox and G-1 respect to the group treated with G-1 alone (**Fig. 5 and 6**). Interestingly, in Dox group the cumulative LDH release during reperfusion was significantly increased with respect to the saline group, while in the group of animals treated with G-1 in combination with Dox the

release of LDH was significantly reduced. As expected, the levels of LDH increased in the group of animals treated with Dox in combination with G-1 and G15 (data not shown).

DISCUSSION

Cardiotoxicity is one of the most important undesired complications of Dox treatment, which triggers the development of several dysfunctions and congestive heart failure (Carvalho et al., 2014; Octavia et al., 2012). Therefore, many approaches are currently investigated in order to minimize the severe side effects of Dox and improve its clinical effectiveness (Vejpongsa et al., 2014). In the present study, we demonstrated that ligand-activated GPER prevents the increase of TNF-α, IL-1β, ROS and LDH plasma and tissue levels induced by Dox. Moreover, we showed that in rat heart homogenates GPER activation abolishes the increase in p-c-jun, BAX, CTGF, iNOS and COX2 expression triggered by Dox treatment. We also determined that the activation of GPER rescues the inhibitory action elicited by Dox on BCL2, pERK, pAKT expression and attenuates apoptosis induced by Dox. Next, GPER activation mitigated the adverse effects of Dox after I/R insult, as evidenced by the ability of G-1 to increase systolic recovery, to reduce diastolic dysfunction and to decrease infarct size and plasma LDH levels. Further supporting the aforementioned data, the beneficial effects of G-1 on Dox-induced cardiotoxicity were prevented in the presence of the GPER antagonist G15, which has been largely acknowledged as specific inhibitor of GPER-mediated responses in diverse experimental models (Dennis et al., 2009). It should be noted that the experimental design was performed using male WKY rats that represent a unique model due to their minimal exposure to estrogens, which have been largely involved in GPER-mediated actions. Nonetheless, further studies are needed toward a better understanding of the potential of GPER to prevent the detrimental effects induced by Dox in the presence of different hormone exposures.

GPER mediates estrogenic signalling in diverse tissues like the cardiovascular system (Maggiolini and Picard 2010; Rigiracciolo et al., 2015a,b; Lappano et al., 2016; Tropea et al., 2015; De Francesco et al., 2013a; Prossnitz and Barton 2011; Meyer et al., 2011). In this regard, it has been demonstrated that GPER knockout mice exhibit both systolic and diastolic dysfunctions together with myocyte hypertrophy (Delbeck et al., 2011), suggesting that GPER may contribute to maintain cardiac mechanical performance. In addition, we have previously ascertained that GPER mediates a decreased contractility in Langendorff-perfused rat heart together with an increased phosphorylation of both ERK1/2 and eNOS (Filice et al., 2009), thus corroborating the cardiac beneficial effects mediated by GPER. Likewise, GPER has been involved in cell adaptation to stressful conditions like hypoxia and hypertension (De

Francesco et al., 2013a; Recchia et al., 2011). Accordingly, GPER activation contributed to the negative inotropic and lusitropic effects in male spontaneously hypertensive rat hearts (De Francesco et al., 2013a). Further extending the ability of GPER in mediating beneficial cardiac effects in a stressful environment, it has been shown that in isolated mice and rat hearts exposed to I/R, G-1 pre-treatment reduces IS and preserves the cardiac function through AKT and ERK1/2 activation and the reduction of inflammation (Deschamps and Murphy 2009; Weil et al., 2010). These data are in line with our findings showing that GPER activation may improve cardiac function and decrease IS, hence attenuating the negative effects of Dox on cardiac performance, myocytes viability and inflammation after I/R injury. Compelling evidence has involved in cardiomyocytes integrity after ischemic damage the AKT and ERK transduction signalling, also referred to as Reperfusion Injury Salvage Kinase (RISK) pathways, (de Jonge et al., 2006). In this regard, the downregulation of AKT and ERK transduction cascades has been shown to contribute to cardiomyocytes damage and apoptosis induced by Dox both in vitro and in vivo (Lou et al., 2005; Su et al., 2006). In accordance with these observations, our results suggest that GPER activation may trigger AKT and ERK1/2 transduction signalling as downstream mediators toward cell survival during I/R.

It has been shown that the response of innate immunity and acute inflammation mediated by iNOS are activated after cardiac injury (Abe et al., 2001). Notably, in the present study Dox-increased iNOS expression was prevented by G-1 treatment. In addition, G-1 reduced myocardial inflammation as evidenced by its ability to abolish the increase of COX2 and LDH cardiac levels upon Dox exposure. Moreover, G-1 administration counteracted the ability of Dox to increase the plasma and tissue levels of several inflammatory and damage markers like TNF-α, IL-1β and LDH, hence suggesting that GPER activation may attenuate these detrimental effects elicited by Dox. According to these data, genetic ablation of GPER in mice was associated with a pro-inflammatory state while the treatment with G-1 was effective in reducing inflammation (Meyer et al., 2014; Barton and Prossnitz, 2015). Our data indicated also that GPER activation may prevent the fibrotic response to Dox treatment, thus corroborating the acknowledged role of GPER as anti-fibrotic mediator in rat heart (De Francesco et al., 2013a). As it concerns the pro-survival and anti-apoptotic actions induced by G-1 treatment in combination with Dox, we provided evidence that GPER activation prevents the harmful action of Dox on pro-survival signalling cascades like ERK1/2 and AKT. Indeed, the ability of G-1 to reduce the apoptotic response triggered by Dox nicely fits with previous investigations showing that GPER may mediate pro-survival effects in several model systems including keratinocytes, breast cancer cells, myocardial cells and heart after

ischemia/reperfusion damage (Weil et al., 2010; Delbeck et al., 2011; Barton and Prossnitz, 2015; Kanda and Watanabe, 2003; Kabir et al., 2015).

Our findings pave the way for future investigations on the multifaceted mechanisms and mediators involved in GPER cardioprotection upon Dox exposure. In this regard, it has been demonstrated that Dox contributes to cardiac damage by inhibiting angiogenesis on human cardiac microvascular endothelial cells by reducing myocardial capillary density. This microvascular deficiency, described in cardiomyopathies such as diabetic and idiopathic dilated cardiomyopathies, promotes the progression of cardiac disease (Sun et al., 2016). On the contrary, GPER activation has been shown to contribute to the formation of new blood vessels particularly under stressful conditions (De Francesco et al., 2013b, Rigiracciolo et al., 2015). Additionally, Doxorubicin-dependent cardiomyopathy is associated with impaired Ca^{2+} handling in the sarcoplasmic reticulum, which resulted markedly decreased in Dox-treated hearts, leading to a reduced cardiac function (Arai et al., Circ Res, 86 (2000), pp. 8–14). At the same time, Kooptiwut et al., (2014) demonstrated in INS-1 cells that estrogen increases SERCA-2 expression. This suggests that the protective effect of G1 against Dox-dependent cardiotoxicity can be mediated by the increase of SERCA-2 expression.

Collectively, our results contribute to extend the current knowledge on the potential of GPER to exert beneficial cardiac effects in stressful conditions. As GPER activation may mitigate the cardiotoxicity exerted by Dox, our data suggest that combination therapies targeting GPER can represent a novel strategy in order to strengthen the usefulness of this anti-cancer drug.

CONFLICTS OF INTEREST: NONE DECLARED.

REFERENCES

Abe K, Tokumura M, Ito T, Murai T, Takashima A and Ibii N. 2001. Involvement of iNOS in postischemic heart dysfunction of stroke-prone spontaneously hypertensive rats. Am J Physiol Heart Circ Physiol 280:H668-H673.

Amelio D, Garofalo F, Wong WP, Chew SF, Ip YK, Cerra MC, Tota B. 2013. Nitric oxide synthase-dependent "on/off" switch and apoptosis in freshwater and aestivating lungfish, Protopterus annectens: skeletal muscle versus cardiac muscle. Nitric Oxide 32:1-12.

Arai M, Yoguchi A, Takizawa T, Yokoyama T, Kanda T, Kurabayashi M, Nagai R. 2000 Mechanism of doxorubicin-induced inhibition of sarcoplasmic reticulum Ca(2+)-ATPase gene transcription. Circ Res 7-21;86:8-14.

Barton M and Prossnitz ER. 2015. Emerging roles of GPER in diabetes and atherosclerosis. Trends Endocrinol Metab 26:185-192.

Bopassa JC, Eghbali M, Toro L and Stefani E. 2010. A novel estrogen receptor GPER inhibits mitochondria permeability transition pore opening and protects the heart against ischemia-reperfusion injury. Am J Physiol Heart Circ Physiol 298:H16-23.

Carvalho FS, Burgeiro A, Garcia R, Moreno AJ, Carvalho RA and Oliveira PJ. 2014. Doxorubicin-induced cardiotoxicity: from bioenergetic failure and cell death to cardiomyopathy. Med Res Rev 34:106-135.

Cerra MC, De Iuri L, Angelone T, Corti A and Tota B. 2006. Recombinant N-terminal fragments of chromogranin-A modulate cardiac function of the Langendorff-perfused rat heart. Basic Res Cardiol 101:43-52.

De Francesco EM, Angelone T, Pasqua T, Pupo M, Cerra MC and Maggiolini M. 2013a. GPER mediates cardiotropic effects in spontaneously hypertensive rat hearts. PLoS One 8:e69322.

De Francesco EM, Lappano R, Santolla MF, Marsico S, Caruso A and Maggiolini M. 2013b. HIF-1α/GPER signaling mediates the expression of VEGF induced by hypoxia in breast cancer associated fibroblasts (CAFs). Breast Cancer Res 15:R64.

De Francesco EM, Pellegrino M, Santolla MF, Lappano R, Ricchio E, Abonante S and Maggiolini M. 2014. GPER mediates activation of HIF1α/VEGF signalling by estrogens. Cancer Res 74:4053-4064.

de Jonge N, Goumans MJ, Lips D, Hassink R, Vlug EJ, van der Meel R, Emmerson CD, Nijman J, de Windt L and Doevendans PA. 2006. Controlling cardiomyocyte survival. Novartis Found Symp 274:41-51; discussion 51-7,152-5, 272-6.

Delbeck M, Golz S, Vonk R, Janssen W, Hucho T, Isensee J, Schäfer S and Otto C. 2011. Impaired left-ventricular cardiac function in male GPR30-deficient mice. Mol Med Rep 4:37-40.

Dennis MK, Burai R, Ramesh C, Petrie WK, Alcon SN, Nayak TK, Bologa CG, Leitao A, Brailoiu E, Deliu E, et al. 2009. In vivo effects of a GPR30 antagonist. Nat Chem Biol 5:421-7. doi: 10.1038/nchembio.168.

Deschamps AM and Murphy E. 2009. Activation of a novel estrogen receptor, GPER, is cardioprotective in male and female rats. Am J Physiol Heart Circ Physiol 297:H1806-H1813.

Filice E, Recchia AG, Pellegrino D, Angelone T, Maggiolini M and Cerra MC. 2009. A new membrane G protein-coupled receptor (GPR30) is involved in the cardiac effects of 17beta-estradiol in the male rat. J Physiol Pharmacol 60:3-10.

Kanda N and Watanabe S. 2003. 17beta-estradiol inhibits oxidative stress-induced apoptosis in keratinocytes by promoting Bcl-2 expression. J Invest Dermatol 121:1500-1509.

Kabir ME, Singh H, Lu R, Olde B, Leeb-Lundberg LM, Bopassa JC. 2015. G Protein-Coupled Estrogen Receptor 1 Mediates Acute Estrogen-Induced Cardioprotection via MEK/ERK/GSK-3β Pathway after Ischemia/Reperfusion. PLoS One 10(9):e0135988.

Kooptiwut S, Mahawong P, Hanchang W, Semprasert N, Kaewin S, Limjindaporn T, Yenchitsomanus PT. 2014. Estrogen reduces endoplasmic reticulum stress to protect against glucotoxicity induced-pancreatic β-cell death. J Steroid Biochem Mol Biol.;139:25-32. doi: 10.1016/j.jsbmb.2013.09.018.

Lappano R, Rigiracciolo D, De Marco P, Avino S, Cappello AR, Rosano C, Maggiolini M and De Francesco EM. 2016. Recent Advances on the Role of G Protein-Coupled Receptors in Hypoxia-Mediated Signaling. 2016. AAPS J: 18:305-10. doi: 10.1208/s12248-016-9881-6.

Lindsey SH and Chappell MC. 2011. Evidence that the G protein-coupled membrane receptor GPR30 contributes to the cardiovascular actions of estrogen. Gend Med 8:343-354.

Lou H, Danelisen I and Singal PK. 2005. Involvement of mitogen activated protein kinases in adriamycin-induced cardiomyopathy. Am J Physiol Heart Circ Physiol 288:H1925-H1930.

Maggiolini M and Picard D. 2010. The unfolding stories of GPR30, a new membrane-bound estrogen receptor. J Endocrinol 204:105-114.

Mantawy EM, El-Bakly WM, Esmat A, Badr AM and El-Demerdash E. 2014. Chrysin alleviates acute doxorubicin cardiotoxicity in rats via suppression of oxidative stress, inflammation and apoptosis. Eur. J Pharmacol 728:107-118.

Meyer MR, Fredette NC, Howard TA, Hu C, Ramesh C, Daniel C, Amann K, Arterburn JB, Barton M and Prossnitz ER. 2014. G protein-coupled estrogen receptor protects from atherosclerosis. Sci Rep 4:7564. doi: 10.1038/srep07564.

Meyer MR, Prossnitz ER and Barton M. 2011. The G protein-coupled estrogen receptor GPER/GPR30 as a regulator of cardiovascular function. Vascul Pharmacol 55:17-25.

Octavia Y, Tocchetti CG, Gabrielson, KL, Janssens S, Crijns HJ and Moens AL. 2012. Doxorubicin-induced cardiomyopathy: from molecular mechanisms to therapeutic strategies. J Mol Cell Cardiol 52:1213-1225.

Pagliaro P, Mancardi D, Rastaldo R, Penna C, Gattullo D, Miranda KM, Feelisch M, Wink DA, Kass DA and Paolocci N. 2003. Nitroxyl affords thiol-sensitive myocardial protective effects akin to early preconditioning. Free Radic Biol Med 34:33-43.

Patel VH, Chen J, Ramanjaneya M, Karteris E, Zachariades E, Thomas P, Been M and Randeva HS. 2010. G-protein coupled estrogen receptor 1 expression in rat and human heart: Protective role during ischaemic stress. Int J Mol Med 26:193-199.

Penna C, Cappello S, Mancardi D, Raimondo S, Rastaldo R, Gattullo D, Losano G and Pagliaro P. 2006. Post-conditioning reduces infarct size in the isolated rat heart: role of coronary flow and pressure and the nitric oxide/cGMP pathway. Basic Res Cardiol 101:168-179.

Penna C, Pasqua T, Perrelli MG, Pagliaro P, Cerra MC, Angelone T. 2012. Postconditioning with glucagon like peptide-2 reduces ischemia/reperfusion injury in isolated rat hearts: role of survival kinases and mitochondrial KATP channels. Basic Res Cardiol 107:272-283.

Prossnitz ER and Barton M. 2011. The G-protein-coupled estrogen receptor GPER in health and disease. Nat Rev Endocrinol 7:715-726.

Recchia AG, De Francesco EM, Vivacqua A, Sisci D, Panno ML, Andò S, and Maggiolini M. 2011. The G protein-coupled receptor 30 is up-regulated by hypoxia-inducible factor-1alpha (HIF-1alpha) in breast cancer cells and cardiomyocytes. J Biol Chem 286:10773-10782.

Rigiracciolo DC, Scarpelli A, Lappano R, Pisano A, Santolla MF, De Marco P, Cirillo F, Cappello AR, Dolce V, Belfiore A, et al. 2015. Copper activates HIF-1α/GPER/VEGF signalling in cancer cells. Oncotarget 6:34158-77.

Rigiracciolo DC, Scarpelli A, Lappano R, Pisano A, Santolla MF, Avino S, De Marco P, Bussolati B, Maggiolini M and De Francesco EM. 2015. GPER is involved in the stimulatory effects of aldosterone in breast cancer cells and breast tumor-derived endothelial cells. Oncotarget 7:94-111.

Saad SY, Najjar TA and Alashari M. 2004. Cardiotoxicity of doxorubicin/paclitaxel combination in rats: effect of sequence and timing of administration. J Biochem Mol Toxicol 18:78-86.

Su HF, Samsamshariat A, Fu J, Shan YX, Chen YH, Piomelli D and Wang PH. 2006. Oleylethanolamide activates Ras-Erk pathway and improves myocardial function in doxorubicin-induced heart failure. Endocrinology 147:827-834.

Sun Z, Schriewer J, Tang M, Marlin J, Taylor F, Shohet RV, Konorev EA. The TGF-β pathway mediates doxorubicin effects on cardiac endothelial cells. 2016.J Mol Cell Cardiol; 90:129-38. doi: 10.1016/j.yjmcc.2015.12.010.

Tocchetti CG, Carpi A, Coppola C, Quintavalle C, Rea D, Campesan M, Arcari A, Piscopo G, Cipresso C, Monti MG, et al. 2014. Ranolazine protects from doxorubicin-induced oxidative stress and cardiac dysfunction. Eur J Heart Fail 16:358-366.

Tropea T, De Francesco EM, Rigiracciolo D, Maggiolini M, Wareing M, Osol G and Mandalà M. 2015. Pregnancy Augments G Protein Estrogen Receptor (GPER) Induced

Vasodilation in Rat Uterine Arteries via the Nitric Oxide - cGMP Signaling Pathway. PLoS One 10:e0141997.

Vejpongsa P and Yeh ET. 2014. Prevention of anthracycline-induced cardiotoxicity: challenges and opportunities. J Am Coll Cardiol 64:938-945.

Weil BR, Manukyan MC, Herrmann JL, Wang Y, Abarbanell AM, Poynter JA and Meldrum DR. 2010. Signaling via GPR30 protects the myocardium from ischemia/reperfusion injury. Surgery 148:436-443.

Young, RC, Ozols RF and Myers CE. 1981. The anthracycline antineoplastic drugs. N Engl J Med 305:139-153.

Zimmerman MA, Budish RA, Kashyap S, Lindsey SH. 2016. GPER-novel membrane oestrogen receptor. Clin Sci (Lond) 130:1005-16.

LEGENDS

Figure 1: Evaluation of IL-1β and TNFα plasma (A-B) and cardiac tissue (C-D) levels in saline, Dox, G-1, Dox + G-1, Dox + G-1 + G15 groups. Values are expressed as means ± SEM with respect to saline group. Significance of differences from control value and comparison between groups by one-way ANOVA followed by Newman-Keuls Multiple Comparation Test. (§), ($), (*), (#), (◊), (○), (●), (■), (□) $p < 0.05$.

Figure 2: Evaluation of LDH (A) and ROS (B) plasma levels in saline, Dox, G-1, Dox + G-1, Dox + G-1 + G15 groups. Values are expressed as means±SEM in respect to saline group. Significance of differences from control value and comparison between groups by one-way ANOVA followed by Newman-Keuls Multiple Comparation Test. (§), (◊), (#), (○), (●), (■), (□) $p < 0.05$.

Figure 3: GPER mRNA (A) and protein (B,C) expression in heart homogenates from rats treated with vehicle (-), Dox, G-1 alone and in combination with Dox or G-1 in the presence of Dox and G15, as evaluated by real-time PCR and immunoblotting, respectively. In RNA experiments, PCR amplification in absence of cDNA was used as a control (-) and each data point represents the mean ± SD of three independent experiments performed in triplicate. In immunoblotting experiments, protein levels were quantified by densitometry and normalized to the expression of β-tubulin. Percentage changes were evaluated as the mean ± SD of 6 experiments for each group. (D,E) ERK, AKT and c-jun phosphorylation in heart homogenates from rats treated with vehicle (-), Dox, G-1 alone and in combination with Dox or G-1 in the presence of both Dox and G15. The protein expression of pERK, pAKT and p-c-jun was quantified by densitometry and normalized to total ERK, AKT and c-jun, respectively. Changes were evaluated and expressed as the mean ± SD of 6 experiments for each group. (○),(●),(□) $p \leq 0.05$. (F,G) BAX and BCL2 expression in heart homogenates from rats treated with vehicle (-), Dox, G-1 alone and in combination with Dox or G-1 in the presence of both Dox and G15. The protein levels were quantified by densitometry and normalized to the expression of β-tubulin. Percentage changes were evaluated as the mean ± SD of 6 experiments for each group. (○), (●) $p < 0.05$. (H,I) iNOS, COX2 and CTGF expression in heart homogenates from rats treated with vehicle (-), Dox, G-1 alone and in combination with Dox or G-1 in the presence of Dox and G15. The protein levels were quantified by densitometry and normalized to the expression of β-tubulin. Percentage changes were evaluated as the mean ± SEM of 6 experiments for each group. (○), (●), (□) $p < 0.05$.

Significance of difference from control value and comparison between groups (one-way ANOVA followed by Newman-Keuls Multiple Comparation Test).

Figure 4. (A-C) Representative images of Tunel-positive cardiomyocyte on rat hearts sections. Nuclei are indicated by red arrows. A (vehicle), B (Dox), C (Dox + G-1). (D) Apoptotic index of the cardiac muscle. Data shown are representative of three experiments for each group. Differences were evaluated by non-parametric Mann Whitney-U test. (§) $p < 0,05$.

Figure 5: Evaluation of LVP and LVEDP in saline, Dox, G-1, Dox + G-1, Dox + G-1 + G15 groups. Values are expressed as means±SD in respect to saline group from the stabilization to the end of the 150 min of reperfusion with respect to the baseline values for each group. Vertical lines indicate ischemic administration. Significance of differences from control value and comparison between groups by one-way ANOVA followed by Newman-Keuls Multiple Comparation Test: (†), (‡), (◊), (□), (■), (○), (●) $p < 0,05$.

Figure 6: Infarct size (IS): the amount of necrotic tissue is expressed as percentage of the left ventricle (% IS/LV), which is considered the risk area. Significance of differences from control value and comparison between groups by ANOVA followed by Newman-Keuls Multiple Comparation Test, (n=6 for each group) with respect to I/R (saline group). (*), (#), (‡), (○), (●), (■), (□) $p < 0,05$.

TNFα and IL1β levels

Plasma

Tissue
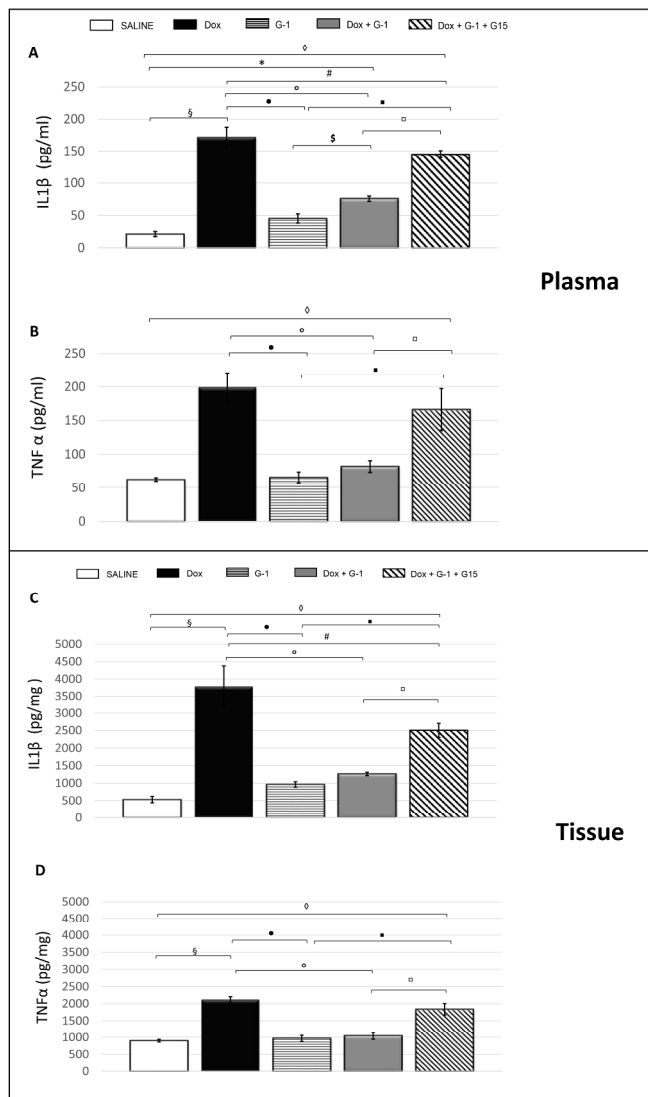
Figure 1

LDH and ROS plasma levels

Figure 2

Heart homogenate

Figure 3

Heart tissue

Figure 4

Isolated Langendorff Heart

Figure 5

Isolated Langendorff Heart
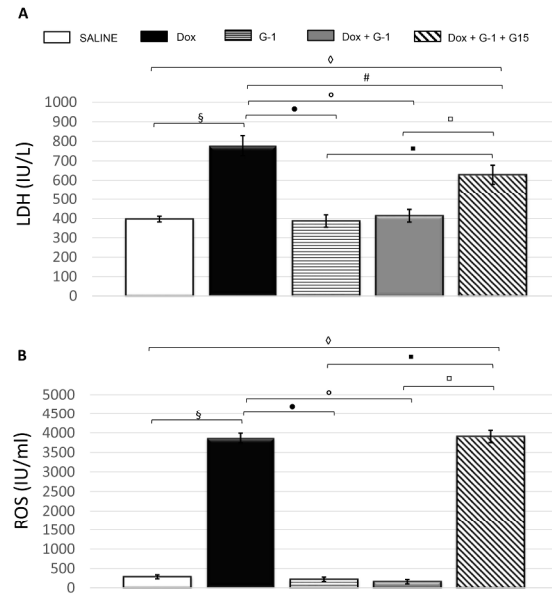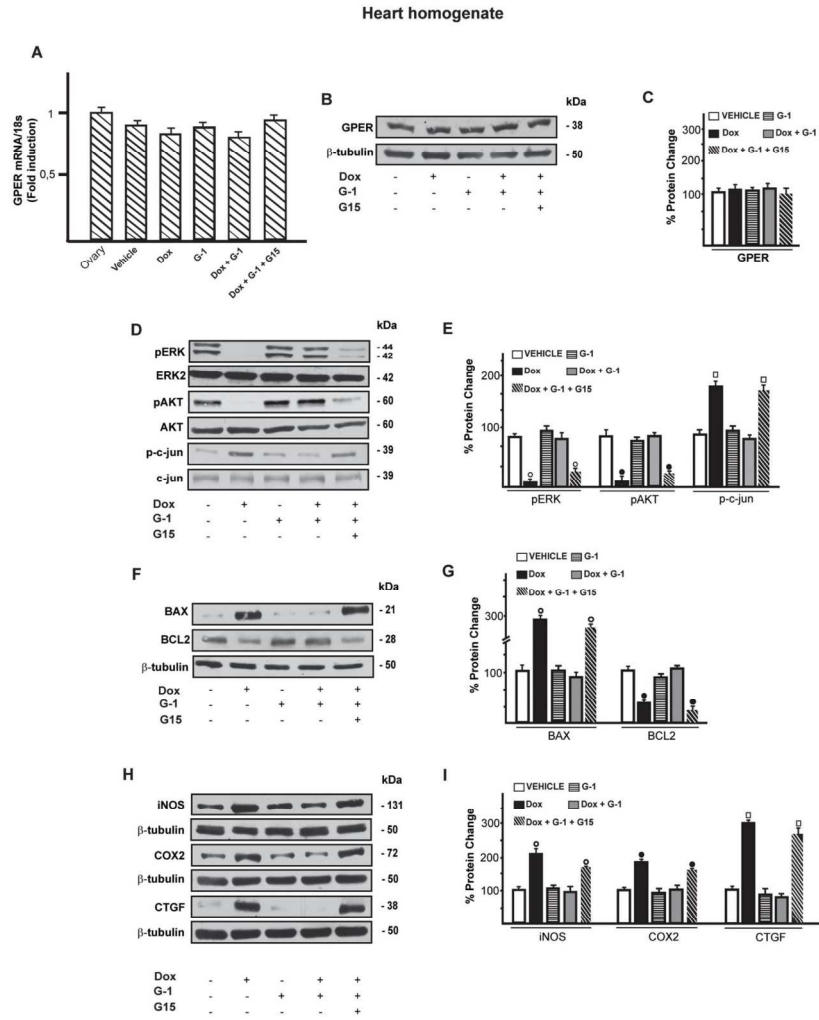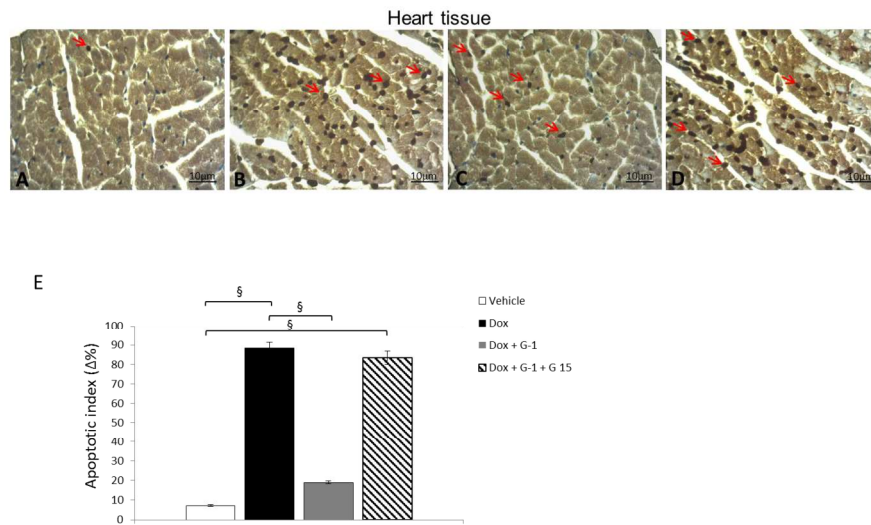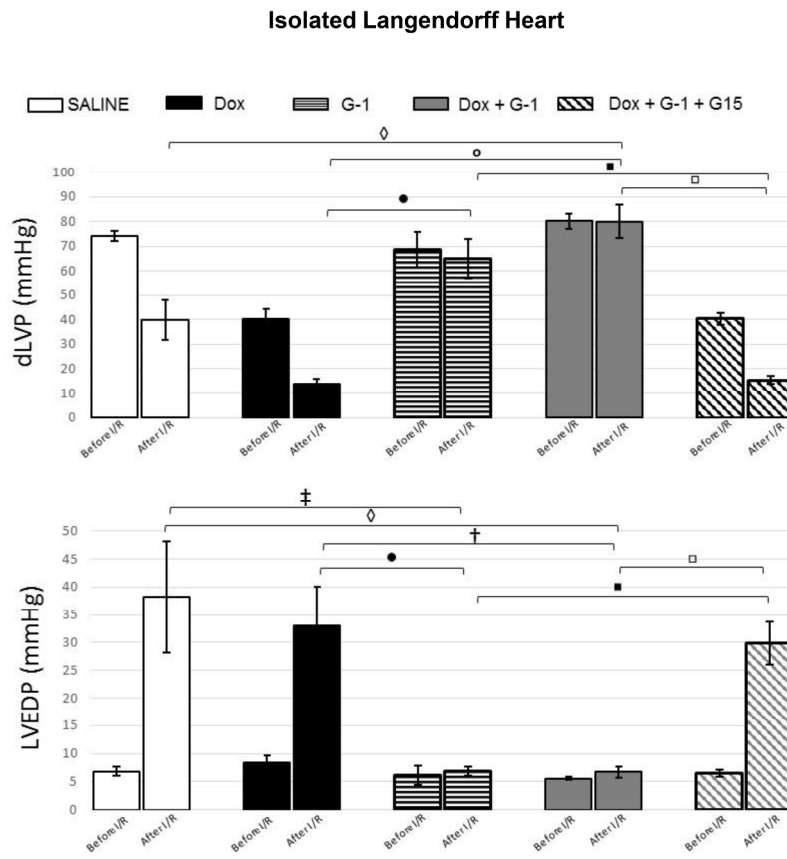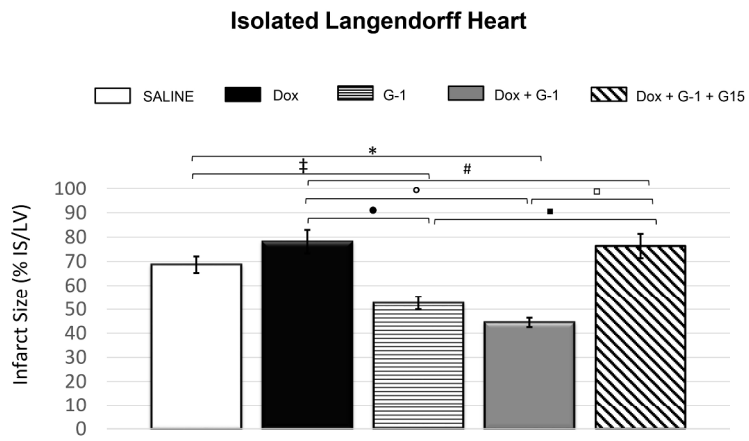

Legend: SALINE, Dox, G-1, Dox + G-1, Dox + G-1 + G15

Figure 6

SCIENTIFIC REP🝑RTS

GPER signalling in both cancer-associated fibroblasts and breast cancer cells mediates a feedforward IL1β/IL1R1 response

Paola De Marco[1,*], Rosamaria Lappano[1,*], Ernestina Marianna De Francesco[1], Francesca Cirillo[1], Marco Pupo[1,3], Silvia Avino[1], Adele Vivacqua[1], Sergio Abonante[2], Didier Picard[3] & Marcello Maggiolini[1]

Cancer-associated fibroblasts (CAFs) contribute to the malignant aggressiveness through secreted factors like IL1β, which may drive pro-tumorigenic inflammatory phenotypes mainly acting via the cognate receptor named IL1R1. Here, we demonstrate that signalling mediated by the G protein estrogen receptor (GPER) triggers IL1β and IL1R1 expression in CAFs and breast cancer cells, respectively. Thereby, ligand-activation of GPER generates a feedforward loop coupling IL1β induction by CAFs to IL1R1 expression by cancer cells, promoting the up-regulation of IL1β/IL1R1 target genes such as PTGES, COX2, RAGE and ABCG2. This regulatory interaction between the two cell types induces migration and invasive features in breast cancer cells including fibroblastoid cytoarchitecture and F-actin reorganization. A better understanding of the mechanisms involved in the regulation of pro-inflammatory cytokines by GPER-integrated estrogen signals may be useful to target these stroma-cancer interactions.

Cancer-associated fibroblasts (CAFs) as main players within the tumor microenvironment contribute to the growth, expansion and dissemination of cancer cells[1]. For instance, CAFs generate a dynamic signalling network through the secretion of several factors that stimulate adjacent malignant cells toward tumor progression[2]. In addition, CAFs may drive a worse cancer phenotype mostly via a paracrine action exerted by growth factors and chemokines released in the tumor microenvironment[2,3]. Increasing evidence have also assessed that CAFs act as mediators of neoplastic-promoting inflammation due to their production of pro-inflammatory cytokines[1,4,5]. The interleukin 1 (IL-1) family of cytokines plays an important role in diverse pathophysiological conditions, including the malignant disease[6]. In particular, IL1α and IL1β and the cognate receptors namely IL1R1 and IL1R2, are expressed in numerous types of cancer cells[7,8]. Accordingly, IL1α and IL1β knockout mice exhibited impaired skills to develop tumors and angiogenesis[9,10]. Likewise, the interleukin-1 receptor antagonist, named IL-1Ra, decreased the inflammatory response and inhibited tumor progression in mice[11]. High levels of IL1β within the tumor microenvironment have been associated with increased recurrence and metastasis in breast cancer[4,9,12,13]. In this regard, it has been shown that breast cancer cells exposed to IL1β may acquire an invasive phenotype through diverse structural changes as the loss of cell-cell contact, the acquisition of a fibroblastoid cytoarchitecture and cell scattering[14,15]. Moreover, a positive correlation between IL1β levels and estrogens was found in breast tissue biopsies and the ability of estrogens to stimulate IL1β production was recently reported both *in vitro* and in breast cancer xenografts[10,11].

Estrogens stimulate breast cancer progression mainly by binding to and activating the estrogen receptor (ER) α and ERβ, which regulate the expression of genes involved in the proliferation, migration and survival of tumor cells[16]. The G protein estrogen receptor (GPR30/GPER) can also mediates the action of estrogens in both normal and malignant cell contexts[17,18]. Ligand-activated GPER induces a network of signal transduction pathways

[1]Department of Pharmacy and Health and Nutritional Sciences, University of Calabria, 87036 Rende, Italy. [2]Breast Cancer Unit, Regional Hospital, 87100 Cosenza, Italy. [3]Department of Cell Biology, Faculty of Sciences, and Institute of Genetics and Genomics of Geneva, University of Geneva, Geneva Switzerland. *These authors contributed equally to the work. Correspondence and requests for materials should be addressed to M.M. (email: marcellomaggiolini@yahoo.it or marcello.maggiolini@unical.it)

including epidermal growth factor receptor (EGFR), intracellular cyclic AMP, calcium mobilization, MAPK and PI3K[19]. In addition, GPER mediates a specific gene signature associated with cell growth, migration and angio-genesis in estrogen-sensitive tumors[20–24]. The potential of GPER in mediating stimulatory effects has been also evidenced in CAFs derived from patients with breast cancer, suggesting that the action of GPER may involve a functional interaction between these components of the tumor microenvironment and cancer cells[20,25,26]. The role of GPER has been highlighted even in the cardiovascular, neurological and immunological systems as well as in the inflammatory state[27,28]. For instance, in knockout mice GPER was shown to be required for thymic atrophy and thymocyte apoptosis induced by estrogens and the selective GPER agonist G-1[29]. Moreover, estrogenic GPER signalling stimulated the invasion and migration of breast cancer cells through IL8-activated CXC receptor-1 (CXCR1)[30]. In endometrial cancer cells, GPER triggered the secretion of IL6, a pleiotropic cytokine that has been associated with both inflammation and cancer[31].

Here, we show that ligand-activated GPER triggers the EGFR/ERK/PKC signal transduction pathway generating a feedforward loop that couples IL1β induction by CAFs to IL1R1 expression by cancer cells. Our findings highlight the potential of GPER in contributing to the functional interplay between cancer cells and the surrounding stroma toward biological responses that drive the progression of breast cancer.

Results

GPER mediates induction of IL1β expression by E2 and G-1 in CAFs.   Previous studies have shown that the pro-inflammatory cytokine IL1β is regulated by estrogens in breast tissue and tumor xenografts, however the mechanisms involved remain to be elucidated[10,11]. In order to provide mechanistic insights into the IL1β response to estrogens within the tumor microenvironment, we began our study determining that IL1β is one of the most induced genes by ligand-activated GPER, as assessed in a nanostring analysis performed in CAFs (data not shown). In accordance with the aforementioned findings, we ascertained that E2 and G-1 induce IL1β expression in CAFs at both mRNA (Fig. 1A,B) and protein levels (Fig. 1C,D). Conversely, E2 and G-1 did not trigger IL1β stimulation in fibroblasts derived from noncancerous breast tissue (data not shown). As expected, E2 and G-1 stimulated the secretion of IL1β in CAFs medium, as determined by ELISA (Fig. 1E,F). Moreover, we established that IL1β protein induction upon E2 and G-1 exposure is no longer evident silencing GPER (Fig. 1G,H) or using the GPER antagonist G-15 (Fig. 1I). As agonist-stimulated GPER triggers the activation of diverse signal transduction pathways[19], we then assessed that the up-regulation of IL1β triggered by E2 and G-1 is prevented in the presence of EGFR tyrosine kinase inhibitor AG, MEK inhibitor PD and PKC inhibitor GF, but not using the PI3K inhibitor LY, the PKA inhibitor H89 and the p38 MAPK inhibitor SB (Fig. 1J,K). Overall, these data indicate that E2 and G-1 induce IL1β expression through GPER-mediated signalling in CAFs.

**IL1R1 expression is regulated by E2 and G-1 through GPER in breast cancer cells.**
Pro-inflammatory factors secreted within the breast tumor microenvironment mainly act via cognate receptors expressed by cancer cells[32]. On the basis of the abovementioned results and previous studies showing that estro-gens may regulate the levels of IL1R1[33], we evaluated whether GPER mediates IL1R1 expression in breast tumor cells. As shown in Fig. 2, E2 and G-1 up-regulated the mRNA (Fig. 2A,B) and protein expression (Fig. 2C–F) of IL1R1 in both SkBr3 and MCF-7 cells. Moreover, IL1R1 protein induction by E2 and G-1 was abolished knocking-down the expression of GPER as well as in the presence of the GPER antagonist G-15 in SkBr3 and MCF-7 cells (Fig. 3A–F). Next, the up-regulation of IL1R1 by E2 and G-1 was prevented using the EGFR inhibitor AG, the MEK inhibitor PD and the PKC inhibitor GF, while the inhibitors of PI3K, PKA and p38 transduction pathways namely LY, H89 and SB, respectively, did not show any effect (Fig. 3G–J) as observed using also the ER antagonist ICI (Supplementary Fig. 1). Altogether, these results suggest that E2 and G-1 trigger the up-regulation of IL1R1 in breast cancer cells through GPER-mediated signalling.

GPER and IL1R1 are involved in the induction of PTGES expression by E2 and G-1 in breast cancer cells.   In order to evaluate the transcriptional responses mediated by GPER through the up-regulation of IL1R1 in SkBr3 and MCF-7 cells, we assessed the changes of certain IL1β target genes[34,35]. For instance, the mRNA expression of ATP-binding cassette G2 (ABCG2), cyclooxygenase-2 (COX2), prostaglandin E synthase-1 (PTGES) and receptor for advanced glycation end products (RAGE) was stimulated only in SkBr3 and MCF-7 cells treated with E2 and G-1 before IL1β exposure (Fig. 4A,B). In accordance with these findings, we deter-mined that the protein levels of PTGES are up-regulated by IL1β only upon E2 and G-1 exposure in SkBr3 and MCF-7 cells (Fig. 5A–F), suggesting that the increase of IL1R1 by agonist-activated GPER does contribute to the aforementioned responses. Considering that E2 and G-1 trigger the expression of IL1β in CAFs (shown in Fig. 1) and IL1R1 in breast cancer cells (shown in Fig. 2), we then assessed that conditioned medium from CAFs exposed to E2 and G-1 does induce PTGES protein expression in SkBr3 (Fig. 5G–H) and MCF-7 (Fig. 5I,J) cells exposed to E2 or G-1. Using the IL1R1 antagonist, namely IL1R1a, the up-regulation of PTGES observed in the aforementioned experimental conditions was no longer evident (Fig. 5G–J). Moreover, an increased expression of PTGES was observed treating with IL1β both SkBr3 and MCF-7 cells exposed to E2 and G-1 (Fig. 5G–J). The up-regulation of PTGES in SkBr3 and MCF-7 cells treated with E2 and G-1 and cultured with conditioned medium from CAFs exposed to these ligands was not altered by increasing concentrations of the ER antagonist ICI up to 10 μM (data not shown). Collectively, these findings suggest that estrogenic GPER signalling generates a feedforward loop that couples IL1β induction in CAFs to IL1R1 expression by cancer cells, hence contributing to the functional cross-talk between the tumor microenvironment and breast cancer cells.

GPER and IL1β/IL1R1 signalling cooperate in breast cancer cells.   Upon IL1β stimulation, breast cancer cells acquire certain features of an invasive phenotype as the loss of cell-cell contact, the acquisition of a fibroblastoid cytoarchitecture and cell scattering[14,15,36]. Nicely recapitulating the abovementioned results, medium
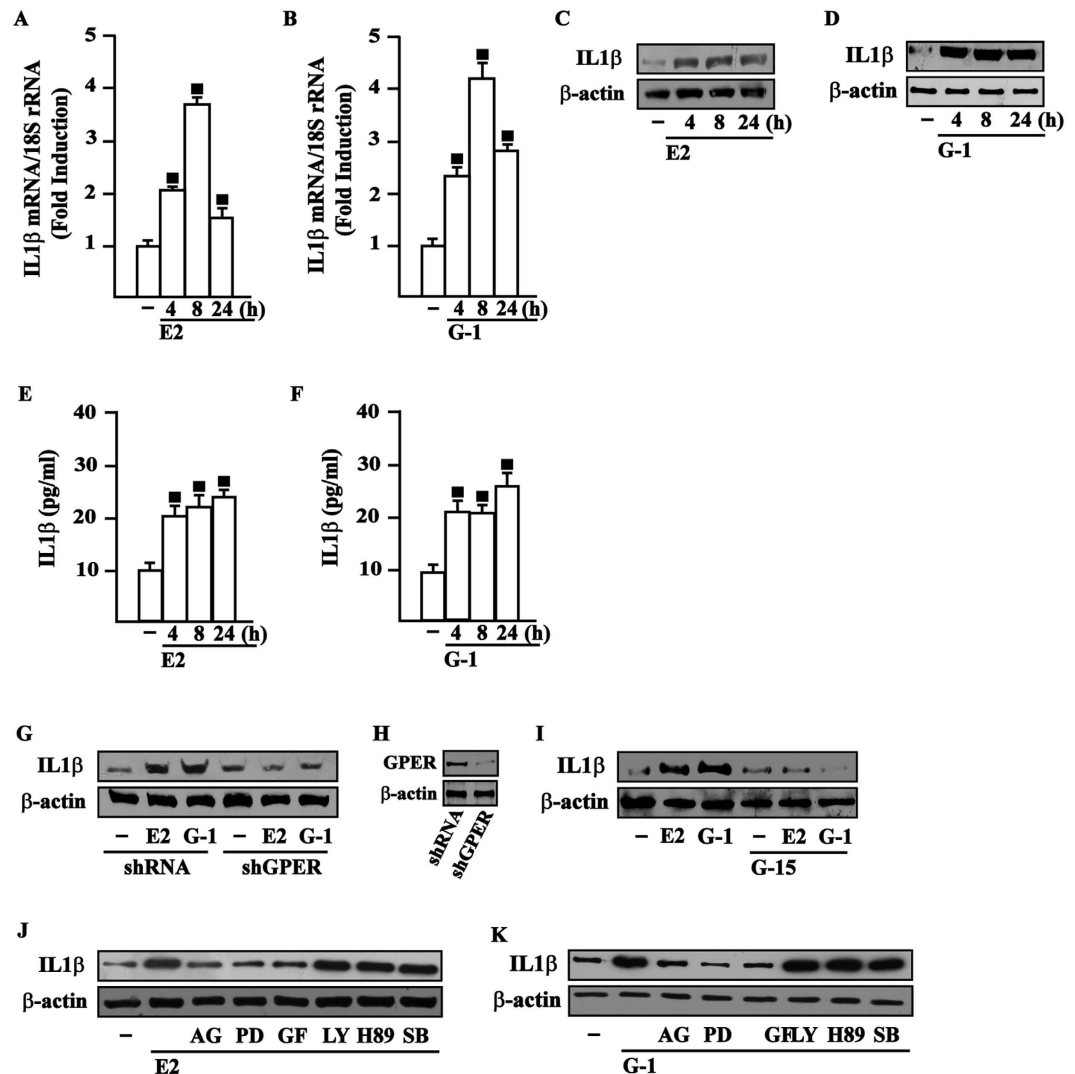
Figure 1. GPER mediates the up-regulation of IL1β expression by E2 and G-1 in CAFs. 10 nM E2 (**A**) and 100 nM G-1 (**B**) induce IL1β mRNA expression, as evaluated by real-time PCR. Data obtained in three independent experiments performed in triplicate were normalized to 18S expression and shown as fold changes of IL1β expression upon E2 and G-1 treatments respect to cells exposed to vehicle (−). (■) $p < 0.05$ for cells receiving treatments versus vehicle. 10 nM E2 (**C**) and 100 nM G-1 (**D**) up-regulate IL1β protein expression, as indicated. (**E,F**) ELISA of IL-1β in supernatants collected from E2 or G-1 treated CAFs. Data are representative of 5 independent experiments. (**G**) The up-regulation of IL1β protein levels induced by 10 nM E2 and 100 nM G-1 is abrogated in CAFs transfected for 24 h with shGPER and then treated for 8 h with vehicle (−), 10 nM E2 and 100 nM G-1. (**H**) Efficacy of GPER silencing. (**I**) The induction of IL1β protein expression observed upon treatments for 8 h with 10 nM E2 or 100 nM G-1 is abolished using 100 nM GPER antagonist G-15. (**J,K**) IL1β protein levels in CAFs treated for 8 h with vehicle (−), 10 nM E2 and 100 nM G-1 alone or in combination with 1 μM EGFR inhibitor AG1478 (AG), 1 μM MEK inhibitor PD98059 (PD), 1 μM PKC inhibitor GF109203X (GF), 1 μM PI3K inhibitor LY294,002 (LY), 1 μM PKA inhibitor H89 and 1 μM p38 MAPK inhibitor SB 203580 (SB). β-actin serves as a loading control. Results shown are representative of at least two independent experiments.

collected from E2 and G-1 treated CAFs induced a fibroblast-like phenotype (as evaluated by the polarity index) in SkBr3 cells transfected with a shRNA and exposed to E2 and G-1, but not in SkBr3 cells transfected with a shG-PER (Fig. 6A–D). Findings similar to those obtained using medium collected from E2 and G-1 treated CAFs were elicited in SkBr3 cells exposed to E2 and G-1 before IL1β treatment (data not shown). Then, SkBr3 cells were fixed and stained with rhodamine-phalloidin to visualize the F-actin pattern. Conditioned medium from E2 and G-1 treated CAFs triggered the F-actin reorganization in SkBr3 cells transfected with a shRNA and exposed to E2 and G-1, but not in SkBr3 cells transfected with a shGPER (Fig. 7A–H). Results comparable to those obtained using medium collected from E2 and G-1 treated CAFs were elicited in SkBr3 cells exposed to E2 and G-1 before IL1β
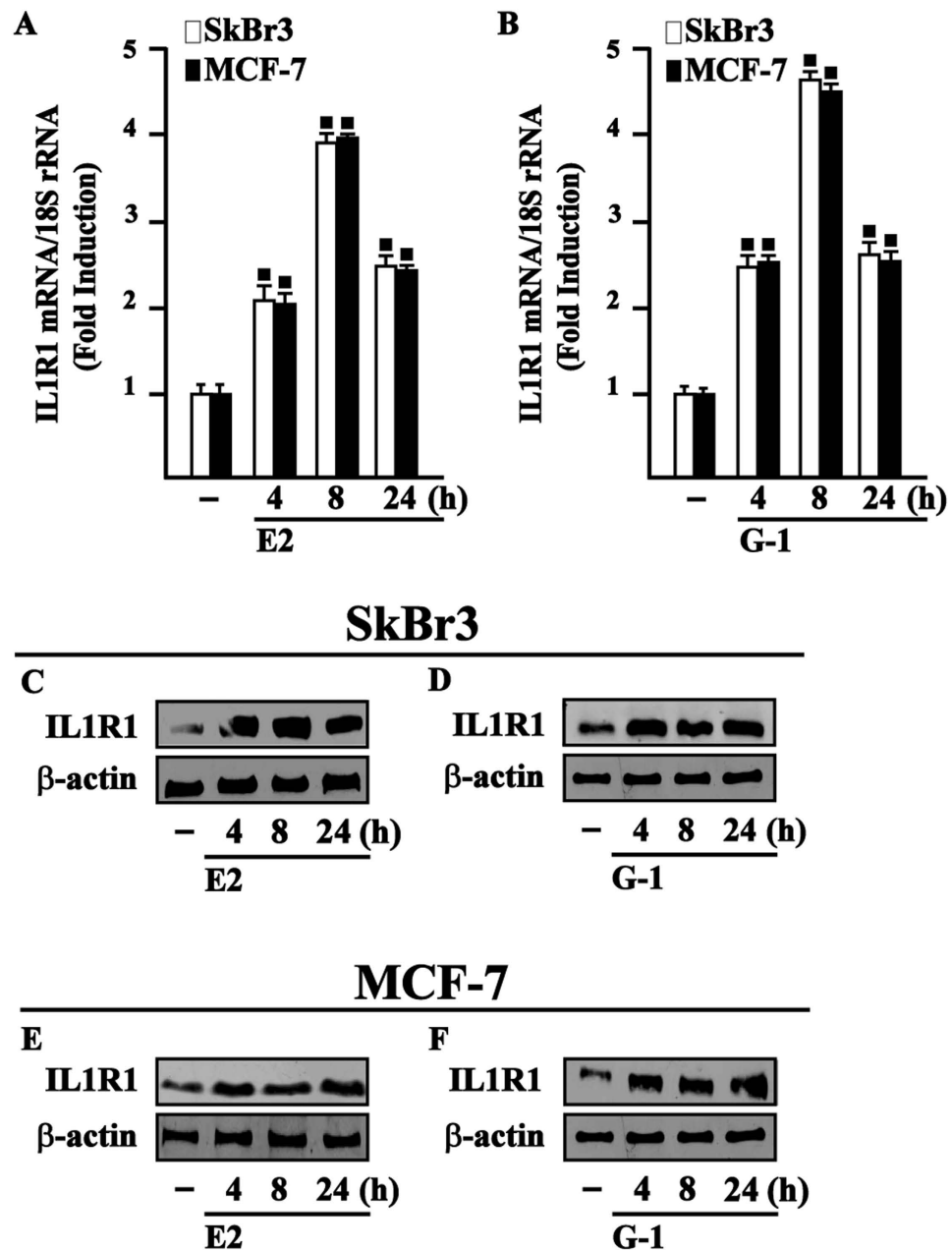
Figure 2. E2 and G-1 induce IL1R1 expression in SkBr3 and MCF-7 breast cancer cells. 10 nM E2 (**A**) and 100 nM G-1 (**B**) induce the mRNA expression of IL1R1, as evaluated by real-time PCR. Data obtained in three independent experiments performed in triplicate were normalized to 18S expression and shown as fold changes of IL1R1 expression upon E2 and G-1 treatments respect to cells exposed to vehicle (−). (■) $p < 0.05$ for cells receiving treatments versus vehicle. Evaluation of IL1R1 protein expression in SkBr3 (**C,D**) and MCF-7 cells (**E,F**) treated with 10 nM E2 and 100 nM G-1, as indicated. β-actin serves as a loading control. Results shown are representative of at least two independent experiments.

treatment (data not shown). The aforementioned findings were further supported by time-lapse video microscopy performed in MCF-7 cells treated with E2 and cultured with conditioned medium from CAFs exposed to E2 (videos 1–2). As previously shown[22], E2 and G-1 stimulated the migration of SkBr3 and MCF-7 cells. This effect was further potentiated culturing cells with medium collected from E2 and G-1 treated CAFs, while the response was no longer observed in both cell types transfected with a shGPER (Fig. 8).

GPER mediates IL1β up-regulation in CAFs derived from a cutaneous metastasis of breast cancer. The potential of GPER in regulating IL1β expression was also confirmed in CAFs derived from a cutaneous metastasis of an invasive mammary ductal carcinoma. In these cells lacking ERα and ERβ (data not shown) but expressing GPER mainly within the nuclear compartment (Supplementary Fig. 2A) as previously assessed in breast CAFs[25], E2 and G-1 induced IL1β expression at both mRNA (Supplementary Fig. 2B,C) and
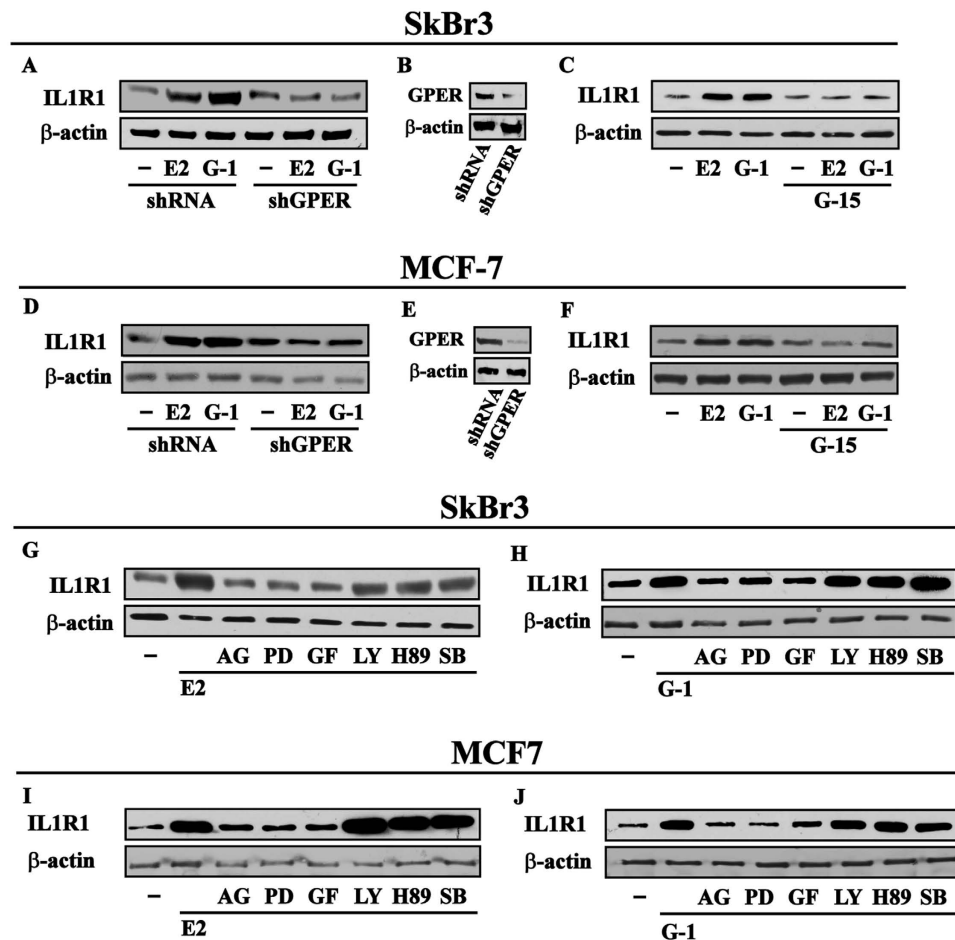
Figure 3. GPER mediates the up-regulation of IL1R1 expression by E2 and G-1 in SkBr3 and MCF-7 breast cancer cells. (**A**) The up-regulation of IL1R1 protein levels upon treatment for 8 h with 10 nM E2 and 100 nM G-1 is abrogated transfecting SkBr3 cells for 24 h with shGPER. (**B**) Efficacy of GPER silencing. (**C**) The induction of IL1R1 protein expression observed treating SkBr3 cells for 8 h with 10 nM E2 and 100 nM G-1 is abolished in the presence of 100 nM GPER antagonist G-15. (**D**) The up-regulation of IL1R1 protein levels upon treatment for 8 h with 10 nM E2 and 100 nM G-1 is abrogated transfecting MCF-7 cells for 24 h with shGPER. (**E**) Efficacy of GPER silencing. (**F**) The induction of IL1R1 protein expression observed treating MCF-7 cells for 8 h with 10 nM E2 and 100 nM G-1 is abolished in the presence of 100 nM GPER antagonist G-15. IL1R1 protein levels in SkBr3 cells treated for 8 h with 10 nM E2 (**G**) and 100 nM G-1 (**H**) alone or in combination with 1 μM EGFR inhibitor AG1478 (AG), 1 μM MEK inhibitor PD98059 (PD), 1 μM PKC inhibitor GF109203X (GF), 1 μM PI3K inhibitor LY294,002 (LY), 1 μM PKA inhibitor H89 and 1 μM p38 MAPK inhibitor SB 203580 (SB). IL1R1 protein levels in MCF-7 cells treated for 8 h with 10 nM E2 (**I**) and 100 nM G-1 (**J**) alone or in combination with 1 μM EGFR inhibitor AG, 1 μM MEK inhibitor PD, 1 μM PKC inhibitor GF, 1 μM PI3K inhibitor LY, 1 μM PKA inhibitor H89 and 1 μM p38 MAPK inhibitor SB. β-actin serves as a loading control. Results shown are representative of at least two independent experiments.

protein levels (Supplementary Fig. 2D,E). Next, we found that the induction of IL1β upon exposure to E2 and G-1 occurs through GPER as its silencing abrogated the response (Supplementary Fig. 2F,G). Together, these results show that estrogenic GPER signalling may regulate IL1β expression also in CAFs derived from a breast cancer metastasis.

Discussion

In the present study we have shown that estrogenic GPER signalling triggers a feedforward loop which couples IL1β induction by CAFs to IL1R1 expression by cancer cells, toward the up-regulation of IL1β/IL1R1 target genes like PTGES, COX2, RAGE and ABCG2 and invasive features of breast cancer cells such as fibroblastoid cytoarchitecture and F-actin reorganization (see the schematic representation in Fig. 9). The aforementioned findings were confirmed, at least in part, in CAFs derived from a cutaneous metastasis of a breast malignancy. Altogether, these data provide novel insights into the potential of ligand-activated GPER to contribute to the functional interplay between cancer cells and the surrounding stroma toward the malignant progression.

Numerous factors are involved in the crosstalk between tumor cells and the associated stroma that influences disease initiation, progression and patient prognosis[37]. In particular, key components of the tumor
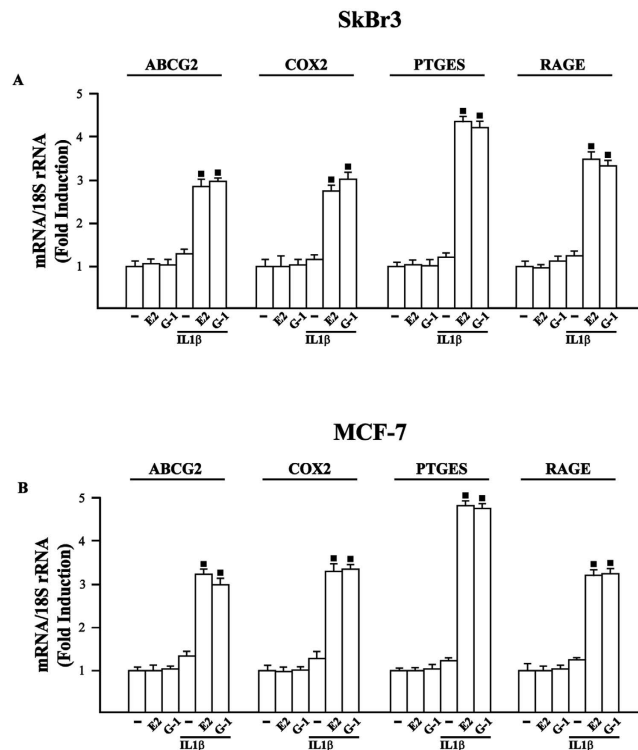
Figure 4. mRNA expression of ABCG2, COX2, PTGES and RAGE evaluated by real-time PCR in SkBr3 (**A**) and MCF-7 (**B**) cells treated for 8 h with vehicle (−), 10 nM E2, 100 nM G-1 and 10 ng/ml IL1β. Cells were also treated for 8 h with 10 nM E2 and 100 nM G-1 before the treatment for 8 h with 10 ng/ml IL1β, as indicated. Results obtained from three independent experiments performed in triplicate were normalized for 18S expression and shown as fold change of RNA expression respect to cells treated with vehicle. (■) $p < 0.05$ for cells receiving treatments versus vehicle.

microenvironment, namely CAFs, produce diverse secreted factors that sustain cancer aggressiveness targeting both cancer and stromal cells[38]. For instance, the pro-inflammatory cytokine CXCL12 produced by CAFs stimulate the proliferation and migration of tumor cells interacting with the cognate receptors expressed by cancer cells[39]. Other cytokines, chemokines and growth factors may also promote cancer-associated inflammation and metastasis inhibiting certain biological processes as the imbalance of oxidative stress, autophagy and angiogenesis[40]. Furthermore, CAFs can recruit immune cells responsible for the secretion of pro-inflammatory molecules, which contribute to tumor progression triggering immunosuppressive or ineffective host-antitumor responses[41].

The cytokine IL1β is secreted by mononuclear phagocytes, keratinocytes, lymphocytes and cellular components of the tumor microenvironment[7,8,42]. IL1β, which is produced as an inactive precursor (pro-IL1b), is cleaved by the interleukin-converting enzyme and secreted in its mature form following tissue damage, infection and inflammation[6]. IL1β binding to and activating the cognate receptor IL1R1, stimulates diverse pathways like JNK, MAPK and NFkB, that lead to the production of inflammatory mediators and the regulation of biological responses like tissue vascularity, adipogenesis, lipid metabolism and inflammation[7]. As it concerns breast cancer, IL1β has been involved in the initiation, progression and invasiveness of this malignancy[43–45]. For instance, IL1β/IL1R1 system has been shown to up-regulate PTGES, which is a key enzyme involved in the production of COX2 and prostaglandin E_2 that promote the motility of breast cancer cells[44]. Likewise, IL1β through IL1R1 stimulates the expression of genes linking inflammation and breast tumor, like RAGE and ABCG2[34,35,42]. Recapitulating these findings, we ascertained that IL1β/IL1R1 system mediates the transcription of the aforementioned genes induced by estrogenic GPER signalling in breast cancer cells. Moreover, our data may recall previous findings obtained either *in vitro* or *in vivo* showing that IL1β/IL1R1 axis plays a main role in the functional crosstalk between cancer cells and fibroblasts, leading to a pro-tumorigenic inflammatory phenotype[6,10,32].

IL1β/IL1R1 activation promotes the motility of breast cancer cells, at least in part, through the stimulation of matrix metalloproteinases activity and morphological changes as fibroblast-like cellular phenotype characterized by a dynamic actin-rich lamellae and peripheral ruffles[14,46]. Nicely extending these data, in the present study medium collected from E2 and G-1 treated CAFs triggered the acquisition of a fibroblastoid cytoarchitecture and the reorganization of F-actin in breast cancer cells exposed to these GPER agonists. On the basis of these results, it could be assumed that estrogenic GPER signalling couples the expression of both IL1β in CAFs and IL1R1 in breast cancer cells, thus generating a feedforward IL1beta/IL1R1 response. Together, these findings suggest that ligand-activated GPER may play a role toward the inflammatory processes driving the progression of breast cancer. Moreover, the potential of GPER in contributing to the stimulatory effects elicited by estrogens has been previously shown using either cancer cells or CAFs[17,19,20,25,47]. For instance, GPER signalling activated the HIF-1α/
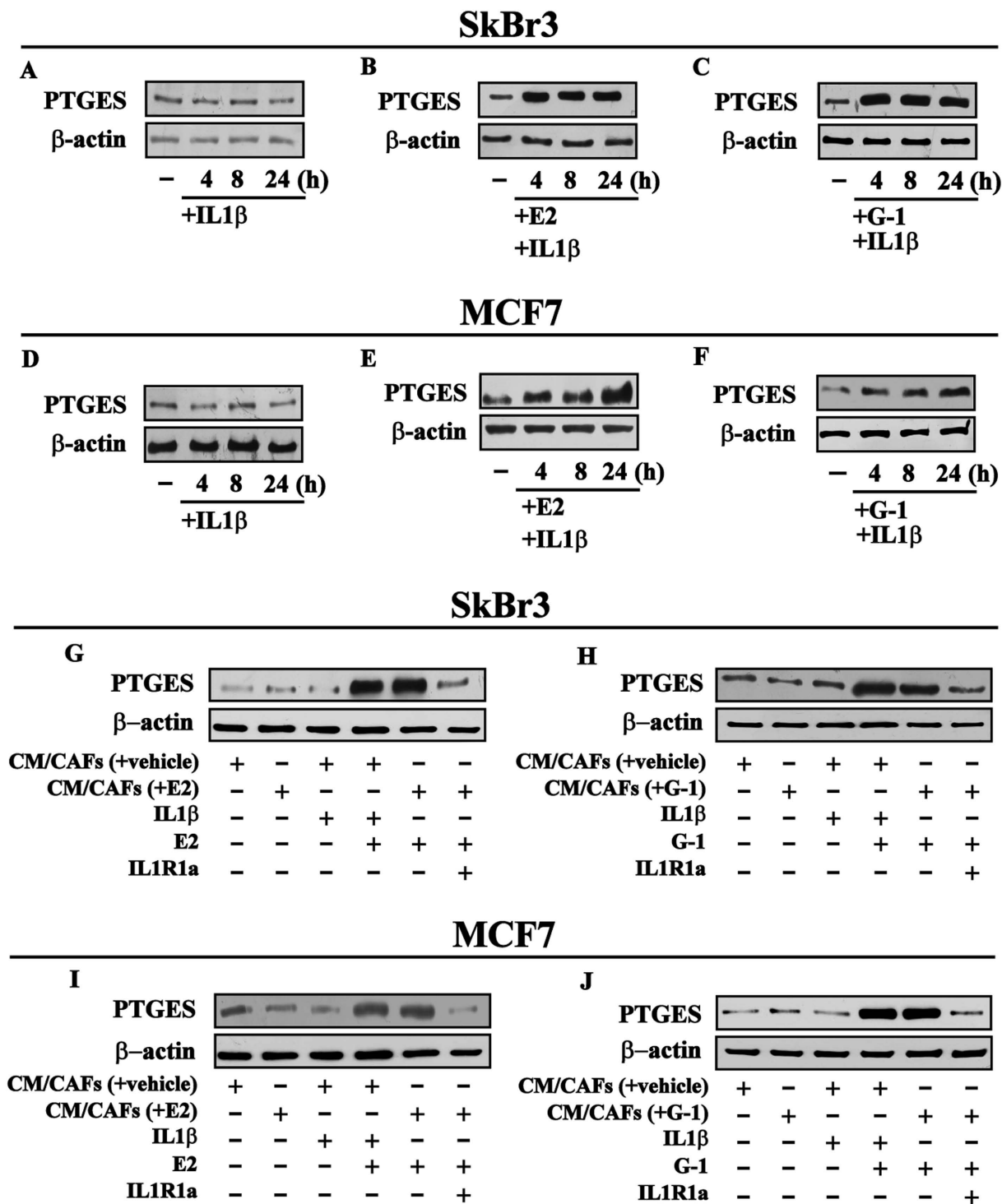
**Figure 5.** PTGES protein expression in SkBr3 (**A–C**) and MCF-7 (**D–F**) cells treated with 10 ng/ml IL1β alone or treated for 8 h with 10 nM E2 or 100 nM G-1 and then exposed to 10 ng/ml IL1β, as indicated. Protein levels of PTGES in SkBr3 (**G,H**) and MCF-7 (**I–J**) cells treated for 8 h with 10 nM E2 or 100 nM G-1 and then switched for additional 8 h to medium without serum in the presence of 10 ng/ml IL1β or conditioned medium collected from CAFs (CM/CAFs) treated for 8 h with vehicle [CM/CAFs (+vehicle)], 10 nM E2 [CM/CAFs (+E2)] and 100 nM G-1 [CM/CAFs (+G-1)]. SkBr3 and MCF-7 cells treated for 8 h with 10 nM E2 or 100 nM G-1 were also exposed to [CM/CAFs (+E2)] and [CM/CAFs (+G-1)] alone or in combination with 1 μM IL1R1 antagonist namely IL1R1a. β-actin serves as a loading control. Results shown are representative of at least two independent experiments.

VEGF signal transduction pathway leading to the stimulation of a main feature of tumor cells/stroma interaction such as hypoxia-induced angiogenesis[48,49]. To date, the multifaceted function of GPER in tumorigenesis is still a subject of deep debate. It should be mentioned that in previous studies GPER activation has been reported to
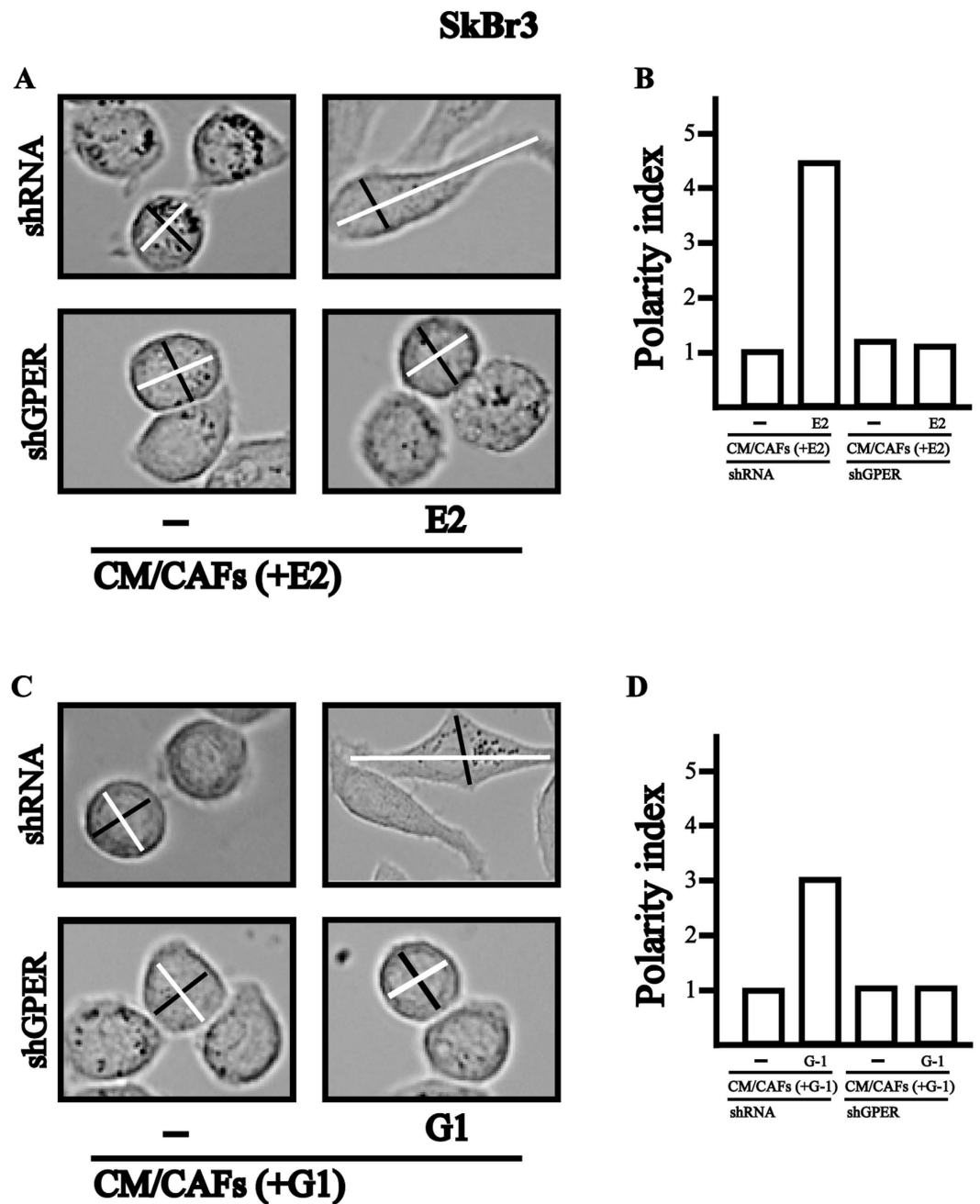
Figure 6. (**A–D**) SkBr3 cells were transfected for 24 h with shRNA or shGPER, treated for 8 h with vehicle (−), 10 nM E2 or 100 nM G-1 and then exposed for additional 8 h to conditioned medium collected from CAFs stimulated for 8 h with 10 nM E2 [CM/CAFs (+E2)] or 100 nM G-1 [CM/CAFs (+G-1)]. In panels (**A,C**) lines traced on cells were used to calculate the polarity index. White lines correspond to the migratory axis (MAx) and black lines to the transversal axis (TAx). In panels B and D, the polarity index (white migratory axis divided by black transversal axis) quantitatively defines the morphology of the migratory cell shown. Polarity Index = 1.0 defines a polygonal shape, whereas a value > 1.0 defines ranges of migratory shapes. Images shown are representative of 30 random fields obtained in three independent experiments.

inhibit cancer cell growth[50]. Further investigations have shown that high expression of GPER may be favorable for the survival of breast and ovarian cancer patients[51–53]. On the contrary, GPER mediated the expression of genes triggering tumor cell migration and proliferation both *in vitro* and *in vivo*[20,31,54]. In patients with endometrial and ovarian tumors, the expression of GPER was associated with aggressive features and lower survival rates[55,56]. Moreover, increased tumor size and metastasis of breast malignancies correlated with high levels of GPER expression[57]. GPER was also found increased and negatively correlated with relapse-free survival in patients treated with tamoxifen[53]. Next, the overexpression of GPER and its localization to the plasma membrane were suggested to be critical in breast cancer progression, whereas the absence of GPER in the plasma membrane predicted excellent
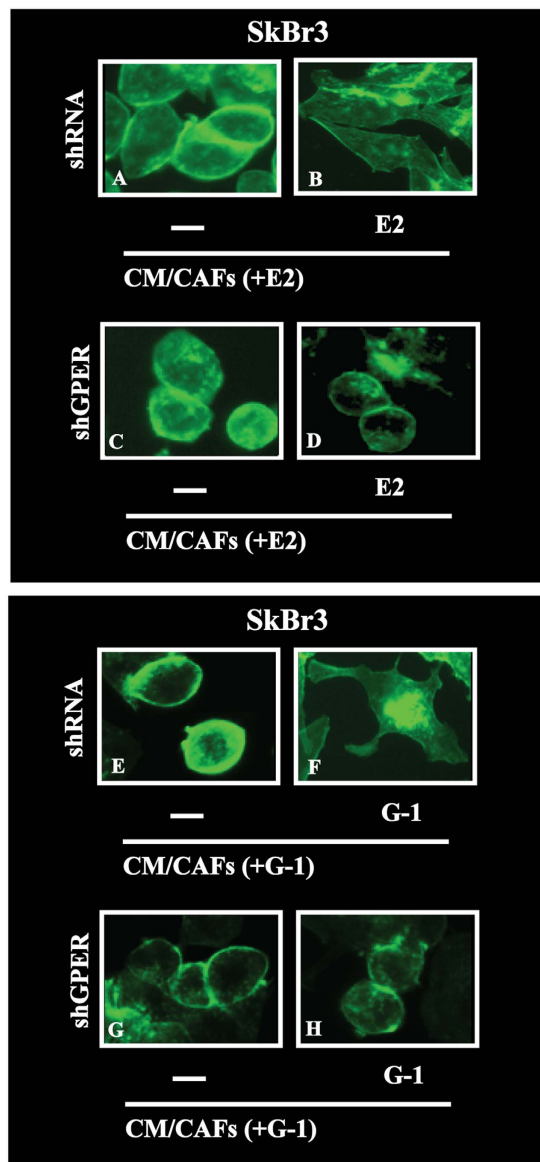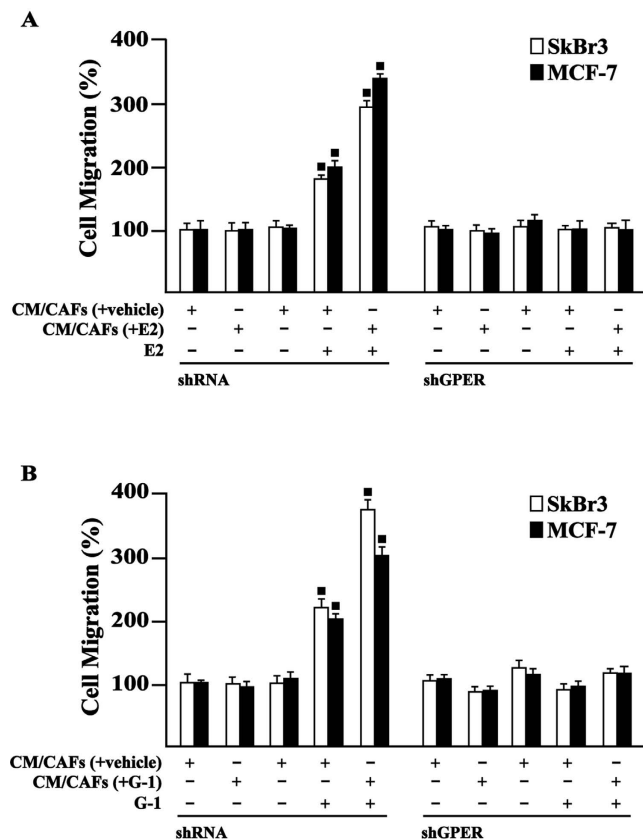
Figure 7. Actin cytoskeleton reorganization in SkBr3 cells transfected for 24 h with shRNA or shGPER and then treated for 8 h with vehicle (−) and 10 nM E2 (**A–D**) or vehicle (−) and 100 nM G-1 (**E–H**) before to be exposed for additional 8 h to conditioned medium collected from CAFs treated for 8 h with 10 nM E2 [CM/CAFs (+E2)] or 100 nM G-1 [CM/CAFs (+G-1)]. Cells were stained with Phalloidin-Fluorescent Conjugate (Santa Cruz Biotechnology) to visualize F-actin and analyzed using the Cytation 3 Cell Imaging Multimode Reader (BioTek, Winooski, VT). Images shown are representative of 30 random fields obtained in three independent experiments.

long-term prognosis in breast cancer patients treated with tamoxifen[58]. Collectively, the results of these studies indicate that further investigations are needed in order to better understand the biological role exerted by GPER in different pathophysiological conditions. Here, we have demonstrated that GPER may integrate a feedforward IL1beta/IL1R1 response linking the tumor microenvironment with tumor cells toward the stimulation of breast cancer, as recapitulated in Fig. 9. The regulation of pro-inflammatory cytokines by estrogenic GPER signalling may be useful in order to set novel comprehensive therapeutic strategies targeting breast malignancy.

Methods

Reagents.   17β-Estradiol (E2) was purchased from Sigma-Aldrich Srl (Milan, Italy). G-1 (1-[4-(-6-bromoben-zol[1,3]diodo-5-yl)-3a,4,5,9b-tetrahidro3H5cyclopenta[c]quinolin-8yl]-ethanone) and G-15 (3aS,4R,9bR)-4-(6-bromo-1,3-benzodioxol-5-yl)-3a,4,5,9b-3H-cyclopenta[c]quinolone were obtained from Tocris Bioscience (Bristol, UK). Tyrphostin AG1478 (AG) was purchased from Biomol Research Laboratories, Inc (Milan, Italy). PD98059 (PD), bisindolylmaleimide I (GF109203X) (GF), LY294,002 (LY) and SB202190 (SB) were obtained from Calbiochem (Milan, Italy). H89 was purchased from Sigma-Aldrich Corp. (Milan, Italy). All the

Figure 8. Migration assays performed by Boyden Chamber assay in SkBr3 and MCF-7 cells transfected for 24 h with shRNA or shGPER and then treated for 8 h with vehicle (−) and 10 nM E2 (**A**) or vehicle (−) and 100 nM G-1 (**B**) before to be exposed for additional 8 h to conditioned medium collected from CAFs treated for 8 h with vehicle, 10 nM E2 [CM/CAFs (+E2)] or 100 nM G-1 [CM/CAFs (+G-1)]. Each data point is the average ± SD of three independent experiments performed in triplicate. (■) p < 0.05 for cells receiving treatments versus vehicle.
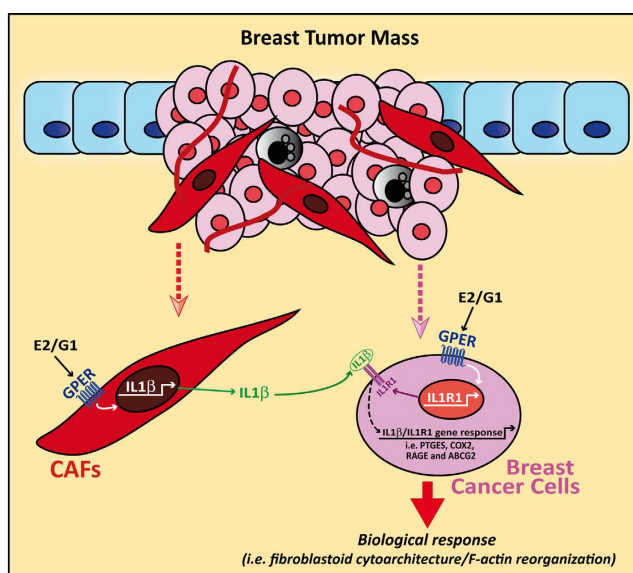
Figure 9. Schematic representation of ligand-activated GPER that generates a feedforward loop coupling IL1β induction by CAFs to IL1R1 expression by cancer cells, toward the induction of IL1β/IL1R1 target genes and biological responses as well as invasive features in breast cancer cells as fibroblastoid cytoarchitecture and F-actin reorganization.

afore-mentioned compounds were dissolved in DMSO, except E2 which was solubilized in ethanol. Recombinant human IL1β was purchased from Thermo Fisher Scientific Inc. (Monza, Italy) and solubilized in PBS. IL-1 receptor antagonist (IL1R1a) human recombinant protein was purchased from Thermo Fisher Scientific Inc. (Monza, Italy) and solubilized in 20 mM TBS, pH 8, with 50% glycerol.

Cell cultures.   SkBr3 and MCF-7 breast cancer cells were obtained by ATCC (Manassas, VA, USA) and used <6 months after resuscitation. SkBr3 breast cancer cells were maintained in RPMI-1640 (Life Technologies, Milan, Italy) without phenol red, supplemented with 10% fetal bovine serum (FBS) and 100 μg/ml penicillin/streptomycin. MCF-7 breast cancer cells were cultured in DMEM (Dulbecco's modified Eagle's medium) (Life Technologies, Milan, Italy) with phenol red, supplemented with 10% FBS and 100 μg/ml penicillin/streptomycin. CAFs obtained from breast malignancies were characterized and maintained as we previously described[59]. CAFs were extracted from six invasive mammary ductal carcinomas obtained from mastectomies. In each patient, a second population of fibroblasts was isolated from a noncancerous breast tissue at least 2 cm from the outer tumor margin. Metastasis-derived CAFs were obtained from biopsy of cutaneous metastasis in a patient with a primary invasive mammary ductal carcinoma, who previously had undergone surgery. Briefly, specimens were cut into smaller pieces (1–2 mm diameter), placed in digestion solution (400 IU collagenase, 100 IU hyaluronidase, and 10% serum, containing antibiotic and antimycotic solution) and incubated overnight at 37 °C. The cells were then separated by differential centrifugation at $90 \times g$ for 2 min. Supernatant containing fibroblasts was centrifuged at $485 \times g$ for 8 min; the pellet obtained was suspended in fibroblasts growth medium (Medium 199 and Ham's F12 mixed 1:1 and supplemented with 10% FBS) and cultured at 37 °C in 5% CO2. Primary cells cultures of metastasis-derived fibroblasts were characterized by immunofluorescence. Briefly cells were incubated with human anti-vimentin (V9) and human anti-cytokeratin 14 (LL001), both from Santa Cruz Biotechnology (DBA, Milan, Italy). To characterize fibroblasts activation, we used anti-fibroblast activated protein α (FAPα) antibody (H-56; Santa Cruz Biotechnology, DBA, Milan, Italy) (data not shown). CAFs and metastasis-derived CAFs were maintained in Medium 199 and Ham's F12 (mixed 1:1) supplemented with 10% FBS and 100 μg/ml penicillin/streptomycin and cultured at 37 °C in 5% CO2. Signed informed consent from all the patients was obtained and all samples were collected, identified and used in accordance with approval by the Institutional Ethical Committee Board (Regional Hospital, Cosenza, Italy). All cell lines were grown in a 37 °C incubator with 5% CO2. All cell lines to be processed for immunoblot and RT-PCR assays were switched to medium without serum and phenol red the day before treatments.

Gene expression studies.   Total RNA was extracted and cDNA was synthesized by reverse transcription as previously described[60]. The expression of selected genes was quantified by real-time PCR using platform Quant Studio7 Flex Real-Time PCR System (Life Technologies). Gene-specific primers were designed using Primer Express version 2.0 software (Applied Biosystems). For IL1β, IL1R1, PTGES, RAGE, ABCG2, COX2 and the ribosomal protein 18S, which was used as a control gene to obtain normalized values, the primers were: 5′-ACGATGCACCTGTACGATCA-3′ (IL1β forward) and 5′-TGCTTGAGAGGTGCTGATGT-3′ (IL1 β reverse); 5′-AACAGACAGGGCCTAGCTTT-3′ (IL1R1 forward) and 5′-TCAAAGGAAGTTCACGGGGA-3′ (IL1R1 reverse); 5′-CATCAACTTTCCGGGGGGTGA-3′ (ABCG2 forward) and 5′-ACCAACAGACCATCAT AAACACA-3′ (ABCG2 reverse); 5′-CCCTTCTGCCTGACACCTTT-3′ (COX2 forward) and 5′-GCCTGCTCT GGTCAATGGAA-3′ (COX2 reverse); 5′-CCAAGGTTTGAGTCCCTCC-3′ (PTGES forward) and 5′-CACATCTCAGGTCACGGGTC-3′ (PTGES reverse); 5′-CGTAAAGATGGGGGCTGGAG-3′ (RAGE forward) and 5′-ACCTTCCAAGCTTCTGTCCG-3′ (RAGE reverse); 5′-GGCGTCCCCCAACTTCTTA-3′ (18S forward) and 5′-GGGCATCACAGACCTGTTATT-3′ (18S reverse). Assays were performed in triplicate and the results were normalized for 18S expression and then calculated as fold induction of RNA expression.

Western Blot Analysis.   Cells were grown in 10-cm dishes, exposed to treatments and then lysed in 500 μL of 50 mmol/L NaCl, 1.5 mmol/L MgCl2, 1 mmol/L EGTA, 10% glycerol, 1% Triton X-100, 1% sodium dodecyl sulfate (SDS), and a mixture of protease inhibitors containing 1 mmol/L aprotinin, 20 mmol/L phenylmethylsulfonyl fluoride and 200 mmol/L sodium orthovanadate. Protein concentration was determined using Bradford reagent according to the manufacturer's recommendations (Sigma-Aldrich, Milan, Italy). Equal amounts of whole protein extract were resolved on a 10% SDS-polyacrylamide gel, transferred to a nitrocellulose membrane (Amersham Biosciences, GE Healthcare, Milan, Italy), probed overnight at 4 °C with antibodies against IL1β (R&D Systems, Inc. Celbio, Milan, Italy), IL1R1 (OriGene Technologies, TEMA ricerca srl, Bologna, Italy), GPER (N-15), PGE synthase (S-16) and β-actin (C-2) all purchased from Santa Cruz Biotechnology, DBA, Milan, Italy). Proteins were detected by horseradish peroxidase-linked secondary antibodies (Santa Cruz Biotechnology, DBA) and revealed using the ECL System (GE Healthcare).

Gene Silencing Experiments.   Cells were plated onto 10-cm dishes and transfected using X-treme GENE 9 DNA Transfection Reagent (Roche Diagnostics, Milan, Italy) for 24 hours before treatments with a control shRNA or a shRNA specific for GPER (shGPER). The silencing of GPER expression was obtained by the construct which we have previously described and used[60].

Enzyme-Linked Immunosorbent Assay.   The concentrations of IL-1β in supernatants from E2 and G-1 treated CAFs were evaluated by enzyme-linked immunosorbent assay (ELISA) according to the manufacturers' protocols (Thermo Fisher Scientific Inc.).

Conditioned medium.   CAFs were cultured in regular growth medium, switched to medium without serum and phenol red for 24 h and then treated for 8 h with E2 or G-1. Thereafter, the supernatants were collected and used as conditioned medium in SkBr3 and MCF-7 cells.

Polarization assay.   SkBr3 cells were serum deprived and transfected for 24 h with a control shRNA or shG-PER using X-tremeGene9 reagent (Roche Molecular Biochemical), as recommended by the manufacturer, and then treated for 8 h with vehicle (−), E2 (10 nM) or G-1 (100 nM) before to be exposed for additional 8 h to conditioned medium from CAFs treated for 8 h with E2 or G-1. Then cells were fixed in 4% paraformaldehyde. After washed with PBS, images were acquired using the Cytation 3 Cell Imaging Multimode Reader (BioTek, Winooski, VT). For each individual cell, the polarity index (PI) was calculated dividing the length of the long migration-defined axis by the perpendicular axis passing by the centroid of the cell[36].

F-actin staining.   Cells were transfected, treated and fixed as indicated above. Thereafter, cells were washed with PBS, incubated with Phalloidin-Fluorescent Conjugate (Santa Cruz Biotechnology, DBA) to visualize F-actin and analyzed using the Cytation 3 Cell Imaging Multimode Reader (BioTek, Winooski, VT).

Migration assay.   Migration assays were performed in triplicate using Boyden chambers (Costar Transwell, 8 mm polycarbonate membrane, Sigma Aldrich, Milan, Italy). SkBr3 and MCF-7 cells were transfected for 24 hours with shRNA or shGPER in regular growth medium. Thereafter, cells were treated with ligands for 8 h, then trypsinized and seeded in the upper chambers. Conditioned medium from CAFs treated with ligands was added in the bottom wells for 8 hours, then cells on the bottom side of the membrane were fixed and counted.

Immunofluorescence microscopy.   Metastasis-derived CAFs were seeded in Lab-Tek II chamber slides at a density of 1×10^5 per well and incubated for 24 h in the corresponding maintenance media. For immunofluorescence staining, cells were transfected for 24 h, fixed in 4% paraformaldehyde, permeabilized with 0.1% TWEEN three times for 5 min and then were blocked for 30 min at room temperature with PBS containing 10% normal donkey serum (Santa Cruz Biotechnology, DBA, Milan, Italy), 0.1% Triton X-100, and 0.05% TWEEN. Thereafter, cells were incubated overnight at 4 °C with a primary antibody against GPER (K-19) (1:100 purchased from Santa Cruz Santa Cruz Biotechnology, DBA, Milan, Italy) in PBS containing 0.05% TWEEN. After incubation, the slides were extensively washed with PBS and incubated with donkey anti-rabbit IgG-FITC (1:100, from Santa Cruz Biotechnology, DBA, Milan, Italy) and 4′,6-Diamidino-2-phenylindole dihydrochloride (DAPI) (1:1000, Sigma-Aldrich, Milan, Italy). The slides were imaged on the Cytation 3 Cell Imaging Multimode reader (BioTek, Winooski, VT) and analysed using the software Gen5 (BioTek, Winooski, VT).

Time-lapse microscopy.   MCF-7 cells (1×10^5) were seeded for 24 hours in 6-well plates in regular growth medium and cultured thereafter in medium without serum in the presence of E2 for 8 hours. Then, cells were cultured in conditioned medium from CAFs exposed to E2 for 8 hours. Cells were maintained at routine incubation settings (37 °C, 5% CO_2) using Cytation™3 Cell Imaging Multi-Mode Reader (Biotek, Winooski, VT). In order to evaluate the fibroblastoid cytoarchitecture and cell scattering, the images were recorded in 10 min intervals for 8 hours culturing MCF-7 cells in conditioned medium from CAFs (software Gen5, BioTek, Winooski, VT). The images that were processed as a movie using the software Adobe Creative Cloud Premier Pro CC. Frames, are displayed at a rate of 10 frames s-1.

Statistical analysis.   Statistical analysis was performed using ANOVA followed by Newman-Keuls' testing to determine differences in means. $p < 0.05$ was considered statistically significant.

References

1. Erez, N., Glanz, S., Raz, Y., Avivi, C. & Barshack, I. Cancer associated fibroblasts express pro-inflammatory factors in human breast and ovarian tumors. *Biochem Biophys Res. Commun.* **437,** 397–402 (2013).
2. Han, Y., Zhang, Y., Jia, T. & Sun, Y. Molecular mechanism underlying the tumor-promoting functions of carcinoma-associated fibroblasts. *Tumor Biol.* **36,** 1385–1394 (2015).
3. Kalluri, R. & Zeisberg, M. Fibroblasts in cancer. *Nature Rev Cancer* **6,** 392–401 (2006).
4. Ma, X. J., Dahiya, S., Richardson, E., Erlander, M. & Sgroi, D. C. Gene expression profiling of the tumor microenvironment during breast cancer progression. *Breast Cancer Res.* **11,** R7 (2009).
5. Servais, C. & Erez, N. From sentinel cells to inflammatory culprits: cancer-associated fibroblasts in tumour-related inflammation. *J. Pathol.* **229,** 198–207 (2013).
6. Weber, A., Wasiliew, P. & Kracht, M. Interleukin-1beta (IL-1beta) processing pathway. *Sci. Signal* **3** (2010).
7. Dinarello, C. Interleukin-1 in the pathogenesis and treatment of inflammatory diseases. *Blood* **117,** 3720–3732 (2011).
8. Dinarello, C. A. A clinical perspective of IL-1beta as the gatekeeper of inflammation. *Eur. J. Immunol.* **41,** 1203–1217 (2011).
9. Apte, R. N. *et al.* The involvement of IL-1 in tumorigenesis, tumor invasiveness, metastasis and tumor-host interactions. *Cancer Metastasis Rev.* **25,** 387–408 (2006).
10. Abrahamsson, A., Morad, V., Saarinen, N. M. & Dabrosin, C. Estradiol, tamoxifen, and flaxseed alter IL-1β and IL-1Ra levels in normal human breast tissue *in vivo*. *J. Clin. Endocrinol. Metab.* **97,** E2044–54 (2012).
11. Lindahl, G., Saarinen, N., Abrahamsson, A. & Dabrosin, C. Tamoxifen, flaxseed, and the lignan enterolactone increase stroma- and cancer cell-derived IL-1Ra and decrease tumor angiogenesis in estrogen-dependent breast cancer. *Cancer Res.* **71,** 51–60 (2011).
12. Elaraj, D. M. *et al.* The role of interleukin 1 in growth and metastasis of human cancer xenografts. *Clin. Cancer Res.* **12,** 1088–96 (2006).
13. Lewis, A. M., Varghese, S., Xu, H. & Alexander, H. R. Interleukin-1 and cancer progression: the emerging role of interleukin-1 receptor antagonist as a novel therapeutic agent in cancer treatment. *J. Transl. Med.* **4,** 48 (2006).
14. Franco-Barraza, J. *et al.* "Actin cytoskeleton participation in the Onset of IL-1β induction of an invasivemesenchymal-like phenotype in epithelial MCF-7 Cells". *Archives of Medical Research* **41,** 170–181 (2010).
15. Pérez-Yépez, E. A., Ayala-Sumuano, J. T., Reveles-Espinoza, A. M. & Meza, I. Selection of a MCF-7 Breast Cancer Cell Subpopulation with High Sensitivity to IL-1β: Characterization of and Correlation between Morphological and Molecular Changes Leading to Increased Invasiveness. *Int. J. Breast Cancer* **2012,** 609148 (2012).
16. Jia, M., Dahlman-Wright, K. & Gustafsson, J. Å. Estrogen receptor alpha and beta in health and disease. *Best Pract. Res. Clin. Endocrinol. Metab.* **29,** 557–68 (2015).
17. Prossnitz, E. R. & Maggiolini, M. Mechanisms of estrogen signaling and gene expression via GPR30. *Mol. Cell. Endocrinol.* **308,** 32–38 (2009).

18. Lappano, R. & Maggiolini, M. G protein-coupled receptors: novel targets for drug discovery in cancer. *Nat. Rev. Drug Discov.* **10,** 47–60 (2011).
19. Maggiolini, M. & Picard, D. The unfolding stories of GPR30, a new membrane-bound estrogen receptor. *J. Endocrinol.* **204,** 105–114 (2010).
20. Pandey, D. P. *et al.* Estrogenic GPR30 signalling induces proliferation and migration of breast cancer cells through CTGF. *EMBO J.* **28,** 523–32 (2009).
21. De Francesco, E. M. *et al.* GPER mediates activation of HIF1α/VEGF signaling by estrogens. *Cancer Res.* **15,** 4053–64 (2014).
22. Lappano, R. *et al.* MIBE acts as antagonist ligand of both estrogen receptor α and GPER in breast cancer cells. *Breast Cancer Res.* **14,** R12 (2012).
23. Lappano, R. *et al.* Two novel GPER agonists induce gene expression changes and growth effects in cancer cells. *Curr. Cancer Drug Targets* **12,** 531–42 (2012).
24. Vivacqua, A. *et al.* GPER mediates the Egr-1 expression induced by 17β-estradiol and 4-hydroxitamoxifen in breast and endometrial cancer cells. *Breast Cancer Res. Treat.* **133,** 1025–35 (2012).
25. Pupo, M. *et al.* The nuclear localization signal is required for nuclear GPER translocation and function in breast Cancer-Associated Fibroblasts (CAFs). *Mol. Cell. Endocrinol.* **376,** 23–32 (2013).
26. Santolla, M. F. *et al.* SIRT1 is involved in oncogenic signaling mediated by GPER in breast cancer. *Cell Death Dis.* **6,** e1834 (2015).
27. De Francesco, E. M. *et al.* GPER mediates cardiotropic effects in spontaneously hypertensive rat hearts. *Plos One* **8,** e69322 (2013).
28. Prossnitz, E. R. & Barton, M. Estrogen biology: New insights into GPER function and clinical opportunities. *Mol. Cell. Endocrinol.* **389,** 71–83 (2014).
29. Wang, C. *et al.* GPR30 contributes to estrogen-induced thymic atrophy. *Mol. Endocrinol.* **22,** 636–648 (2008).
30. Jiang, Q. F. *et al.* 17β-estradiol promotes the invasion and migration of nuclear estrogen receptor-negative breast cancer cells through cross-talk between GPER1 and CXCR1. *J. Steroid Biochem. Mol. Biol.* **138,** 314–24 (2013).
31. He, Y. Y., Cai, B., Yang, Y. X., Liu, X. L. & Wan, X. P. Estrogenic G protein-coupled receptor 30 signaling is involved in regulation of endometrial carcinoma by promoting proliferation, invasion potential, and interleukin-6 secretion via the MEK/ERK mitogen-activated protein kinase pathway. *Cancer Sci.* **100,** 1051–61 (2009).
32. Whipple, C. A. Tumor talk: understanding the conversation between the tumor and its microenvironment. *Cancer Cell Microenviron.* **2,** e773 (2015).
33. Tamm-Rosenstein, K., Simm, J., Suhorutshenko, M., Salumets, A. & Metsis, M. Changes in the transcriptome of the human endometrial Ishikawa cancer cell line induced by estrogen, progesterone, tamoxifen, and mifepristone (RU486) as detected by RNA-sequencing. *Plos One* **8,** e68907 (2013).
34. Mehrotra, S., Morimiya, A., Agarwal, B., Konger, R. & Badve, S. Microsomal prostaglandin E2 synthase-1 in breast cancer: a potential target for therapy. *J. Pathol.* **208,** 356–63 (2006).
35. Malekshah, O. M., Lage, H., Bahrami, A. R., Afshari, J. T. & Behravan, J. PXR and NF-κB correlate with the inducing effects of IL-1β and TNF-α on ABCG2 expression in breast cancer cell lines. *Eur. J. Pharm. Sci.* **47,** 474–80 (2012).
36. Vicente-Manzanares, M., Koach, M. A., Whitmore, L., Lamers, M. L. & Horwitz, A. F. Segregation and activation of myosin IIB creates a rear in migrating cells. *J. Cell. Biol.* **183,** 543–54 (2008).
37. Joyce, J. A. & Pollard, J. W. Microenvironmental regulation of metastasis. *Nat. Rev. Cancer* **9,** 239–52 (2009).
38. Cirri, P. & Chiarugi, P. Cancer associated fibroblasts: the dark side of the coin. *Am. J. Cancer Res.* **1,** 482–97 (2011).
39. Luker, K. E. & Luker, G. D. Functions of CXCL12 and CXCR4 in breast cancer. *Cancer Lett.* **238,** 30–41 (2006).
40. Madeddu, C. *et al.* Role of inflammation and oxidative stress in post-menopausal oestrogen-dependent breast cancer. *J Cell Mol Med.* **18,** 2519–2529 (2014).
41. Suman, S. *et al.* Current perspectives of molecular pathways involved in chronic Inflammation-mediated breast cancer. *Biochem Biophys Res Commun.* doi: 10.1016/j.bbrc.2015.10.133 (2015).
42. Hardaway, A. L. & Podgorski, I. IL-1β, RAGE and FABP4: targeting the dynamic trio in metabolic inflammation and related pathologies. *Future Med Chem.* **5,** 1089–108 (2013).
43. Ma, L. *et al.* Epidermal growth factor (EGF) and interleukin (IL)-1β synergistically promote ERK1/2-mediated invasive breast ductal cancer cell migration and invasion. *Mol Cancer.* **11,** 79 (2012).
44. Reed, J. R., Leon, R. P., Hall, M. K. & Schwertfeger, K. L. Interleukin-1beta and fibroblast growth factor receptor 1 cooperate to induce cyclooxygenase-2 during early mammary tumourigenesis. *Breast Cancer Res.* **11,** R21 (2009).
45. Perrier, S., Caldefie-Chézet, F. & Vasson, M. P. IL-1 family in breast cancer: Potential interplay with leptin and other adipocytokines. *FEBS Letters* **583,** 259–265 (2009).
46. Wang, F. M. *et al.* SHP-2 promoting migration and metastasis of MCF-7 with loss of E-cadherin, dephosphorylation of FAK and secretion of MMP-9 induced by IL-1β *in vivo* and *in vitro. Breast Cancer Res. Treat.* **89,** 5–14 (2005).
47. Madeo, A. & Maggiolini, M. Nuclear alternate estrogen receptor GPR30 mediates 17beta-estradiol-induced gene expression and migration in breast cancer-associated fibroblasts. *Cancer Res.* **70,** 6036–46 (2010).
48. De Francesco, E. M. *et al.* HIF-1α/GPER signaling mediates the expression of VEGF induced by hypoxia in breast cancer associated fibroblasts (CAFs). *Breast Cancer Res.* **15,** R64 (2014).
49. Rigiracciolo, D. C. *et al.* Copper activates HIF-1α/GPER/VEGF signalling in cancer cells. *Oncotarget* **6,** 34158–77 (2015).
50. Weißenborn, C. *et al.* GPER functions as a tumor suppressor in MCF-7 and SK-BR-3 breast cancer cells. *J. Cancer Res. Clin. Oncol.* **140,** 663–71 (2014).
51. Arias-Pulido, H. *et al.* GPR30 and estrogen receptor expression: new insights into hormone dependence of inflammatory breast cancer. *Breast Cancer Res. Treat.* **123,** 51–8 (2010).
52. Bartella, V., De Marco, P., Malaguarnera, R., Belfiore, A. & Maggiolini, M. New advances on the functional cross-talk between insulin-like growth factor-I and estrogen signalling in cancer. *Cell. Signal.* **24,** 1515–1521 (2012).
53. Ignatov, A. *et al.* G-protein-coupled estrogen receptor GPR30 and tamoxifen resistance in breast cancer. *Breast Cancer Res. Treat.* **128,** 457–66 (2011).
54. Marjon, N. A., Hu, C., Hathaway, H. J. & Prossnitz, E. R. G protein-coupled estrogen receptor regulates mammary tumorigenesis and metastasis. *Mol. Cancer Res.* **12,** 1644–54 (2014).
55. Smith, H. O. *et al.* GPR30 predicts poor survival for ovarian cancer. *Gynecol. Oncol.* **114,** 465–71 (2009).
56. Smith, H. O. *et al.* GPR30: a novel indicator of poor survival for endometrial carcinoma. *Am. J. Obstet. Gynecol.* **196,** 386 e1–9 (2007).
57. Filardo, E. J. *et al.* Distribution of GPR30, a seven membrane-spanning estrogen receptor, in primary breast cancer and its association with clinicopathologic determinants of tumor progression. *Clin. Cancer Res.* **12,** 6359–66 (2006).
58. Sjöström, M. *et al.* Lack of G protein-coupled estrogen receptor (GPER) in the plasma membrane is associated with excellent long-term prognosis in breast cancer. *Breast Cancer Res. Treat.* **145,** 61–71 (2014).
59. De Marco, P. *et al.* Insulin-like growth factor-I regulates GPER expression and function in cancer cells. *Oncogene* **32,** 678–88 (2013).
60. De Marco, P. *et al.* GPER1 is regulated by insulin in cancer cells and cancer-associated fibroblasts. *Endocr. Relat. Cancer.* **21,** 739–53 (2014).

Author Contributions

P.D.M. and R.L. designed and performed experiments, analysed the data, prepared figures and participated in writing the manuscript. E.M.D.F., F.C., M.P., S.A. and A.V. designed and performed some of the experiments. S.A. provided the breast cancer samples. D.P. and M.M. designed the experiments, analysed the data and wrote the manuscript.

Additional Information

Supplementary information accompanies this paper at http://www.nature.com/srep

Competing financial interests: The authors declare no competing financial interests.

How to cite this article: De Marco, P. *et al.* GPER signalling in both cancer-associated fibroblasts and breast cancer cells mediates a feedforward IL1β/IL1R1 response. *Sci. Rep.* **6**, 24354; doi: 10.1038/srep24354 (2016).

CrossMark

Review Article

Recent Advances on the Role of G Protein-Coupled Receptors in Hypoxia-Mediated Signaling

Rosamaria Lappano,[1] Damiano Rigiracciolo,[1] Paola De Marco,[1] Silvia Avino,[1] Anna Rita Cappello,[1] Camillo Rosano,[2] Marcello Maggiolini,[1,3] and Ernestina Marianna De Francesco[1]

Abstract. G protein-coupled receptors (GPCRs) are cell surface proteins mainly involved in signal transmission; however, they play a role also in several pathophysiological conditions. Chemically heterogeneous molecules like peptides, hormones, lipids, and neurotransmitters activate second messengers and induce several biological responses by binding to these seven transmembrane receptors, which are coupled to heterotrimeric G proteins. Recently, additional molecular mechanisms have been involved in GPCR-mediated signaling, leading to an intricate network of transduction pathways. In this regard, it should be mentioned that diverse GPCR family members contribute to the adaptive cell responses to low oxygen tension, which is a distinguishing feature of several illnesses like neoplastic and cardiovascular diseases. For instance, the G protein estrogen receptor, namely G protein estrogen receptor (GPER)/GPR30, has been shown to contribute to relevant biological effects induced by hypoxia via the hypoxia-inducible factor (HIF)-1α in diverse cell contexts, including cancer. Likewise, GPER has been found to modulate the biological outcome of hypoxic/ischemic stress in both cardiovascular and central nervous systems. Here, we describe the role exerted by GPCR-mediated signaling in low oxygen conditions, discussing, in particular, the involvement of GPER by a hypoxic microenvironment.

INTRODUCTION

G protein-coupled receptors (GPCRs) are seven transmembrane-spanning receptors that regulate many cellular functions upon ligand activation (1). The biological responses mediated by GPCRs involve the recruitment of proteins prompting the receptor internalization and desensitization, like arrestins and GPCR kinases (GRKs) as well as membrane-bound partners, namely heterotrimeric G proteins (1,2). In the inactive state, G proteins consist of a Gβγ monomer which maintains a high affinity for a guanine diphosphate (GDP)-bound Gα subunit (1,2). On the basis of the sequence identity, four subtypes of Gα subunit (Gαs, Gαi, Gαq, and Gα12) have been extensively characterized (1,2). Ligand binding promotes conformational modifications that result in the exchange of GDP for GTP on the Gα subunit, leading to a decreased affinity of Gα for the Gβγ subunit. The dissociation of the heterotrimer allows that both GTP-bound Gα and free Gβγ activate numerous transduction pathways like mitogen-activated protein kinase (MAPK), phosphatidylinositol 3-kinase (PI3-K), small GTP-binding proteins (Ras and Rho GTPases), and other mediators that contribute to various physiopathological responses (1,2). For instance, an aberrant expression of GPCRs and/or their activation have been associated to several types of tumors (3,4). Consequently, the pharmacological manipulation of certain GPCR-mediated signaling may represent a promising anti-cancer strategy (3,4). As demonstrated for many GPCRs (3,4), the G protein estrogen receptor (GPER, also known as GPR30) may trigger oncogenic signaling (5,6). GPER binds to estrogens, phyto- and xenoestrogens, and also estrogen receptor (ER) antagonists that may act as GPER agonists (7–12). GPER mediates the activation of a network of transduction pathways; however, the actual role elicited by GPER in tumorigenesis is still controversial. Previous studies have shown that GPER may induce cell cycle arrest and inhibition of cancer cell growth (13–16). Nevertheless, other *in vitro* and *in vivo* studies have revealed that GPER triggers cancer cell migration and proliferation (5,17). In addition, GPER expression was associated to inflammatory breast tumor (18), was found reduced during breast cancer tumorigenesis (19), and was related to a poor relapse-free survival in breast cancer patients treated with tamoxifen (20). The lack of GPER in the plasma membrane was linked to a

[1] Department of Pharmacy, Health and Nutritional Sciences, University of Calabria, Via Bucci, 87036, Rende, CS, Italy.
[2] UOS Proteomics IRCCS AOU San Martino-IST National Institute for Cancer Research, Largo R. Benzi 10, 16132, Genoa, Italy.
[3] To whom correspondence should be addressed. (e-mail: marcellomaggiolini@yahoo.it; marcello.maggiolini@unical.it)

favorable prognosis in breast cancer (21), whereas its expression was associated with aggressive features of breast, endometrial, and ovarian tumors (22–24). In this context, we have demonstrated that GPER is upregulated by EGF, insulin-like growth factor (IGF)-I, insulin, and a main factor contributing to tumor aggressiveness like hypoxia (25–31). A low oxygen tension characterizes the growth of solid tumors, where it promotes adaptive responses like anaerobic glycolysis, reduction of macromolecule synthesis, and angiogenesis (32). In addition, hypoxia is critical for the pathogenesis of heart disease and stroke, the major causes of human mortality (33). The effects of hypoxia are mainly mediated by hypoxia-inducible factor (HIF) family members, which orchestrate the complex responses to low oxygen tension (34). In particular, HIF-1α regulates the expression of several pro-angiogenic factors involved in tumor angiogenesis progression (34,35). Many signaling cascades are engaged by hypoxia toward HIF-1α activation such as receptor tyrosine kinases (RTKs) and GPCRs (30,31,36). Here, we discuss the involvement of certain GPCRs, including GPER, in hypoxia-mediated signaling toward cancer development and cardiovascular diseases.

GPCR INVOLVEMENT IN HYPOXIA-MEDIATED SIGNALING

A low oxygen tension characterizes relevant pathophysiological conditions like cancer and cardiovascular diseases (32–34). Multiple mechanisms for oxygen sensing have been developed and conserved in both prokaryotic and eukaryotic organisms (32–34). In particular, HIF-1 acts as a master regulator of the adaptive cell response to limited oxygen availability mainly by activating the transcription of genes that regulate physiological processes as glycolysis, survival, and angiogenesis (34–37). HIF-1 is a heterodimer of two helix-loop-helix-PAS proteins, namely HIF-1α and HIF-1β or ARNT (38). Upon hypoxia, HIF-1α and HIF-1β dimerize and bind to the hypoxia-responsive elements (HREs) located within the promoter region of target genes (38). Several factors contribute to HIF-1α-mediated action in hypoxic conditions, including diverse GPCRs (30,39). For instance, GPR41 was shown to be a hypoxia-induced receptor that drives p53-dependent apoptosis in rat cardiomyocytes subjected to ischemia and reoxygenation injury (40) whereas GPR22 was involved in cardioprotection as its ablation increased the susceptibility to functional decompensation following hemodynamic stress (41). The adrenergic signaling axis, consisting of catecholamines and their adrenergic receptors, has been included among GPCRs that play a primary role in oxygen-related diseases like hypertension, cardiac hypertrophy, and heart failure (42). Moreover, the adrenoreceptors have been shown to functionally interact with opioid receptors (43), which elicit protective actions in response to pre- and post-conditioning stimuli upon cardiac and cerebral damages (44,45). It is worth noting that certain ligand-activated GPCRs induce HIF-1 expression and function (46–48), thus mimicking hypoxic conditions. For instance, the recruitment of transcription factors to the promoter sequence of HIF-1 as well as the stabilization of HIF-1 protein levels may occur upon activation of GPCRs by endothelin-1 (ET-1), β-adrenoceptor agonists, and lysophosphatidic acid (46–48).

GPCR INVOLVEMENT IN TUMOR ANGIOGENESIS UPON HYPOXIA

Tumor microenvironment is often characterized by hypoxia, which is a distinguishing feature of an aggressive cancer phenotype and disease recurrence (32). The metabolic changes occurring in rapidly growing cells, the increasing diffusion distances between the blood vessels and certain tumor areas, and the compressive action elicited by the expanding mass on local blood vessels may cumulatively account for low intra-tumor oxygenation (32). The effects of hypoxia on the malignant progression are mediated by complex mechanisms that allow tumor cells to survive and/or escape their oxygen-deficient environment (32,34). Moreover, the adaptive responses to hypoxic stress in the tumor microenvironment trigger the formation of new blood vessels stimulated by pro-angiogenic factors (35,37). Along with the activation of endothelial cells (ECs) and the subsequent degradation of the basement membrane, the angiogenic response leads to the migration and proliferation of ECs, which then form tubes generating new blood vessels (49). Moreover, tumor angiogenesis prompts cancer cells to grow, evade the host surveillance, form the pre-metastatic niche, and invade distant sites (49); hence, the molecular players driving this complex process are intensively investigated toward effective anti-tumor strategies (49). To date, the major growth factors involved in the formation of blood vessels are members of the vascular endothelial growth factor (VEGF) family (50). It includes placental growth factor (PlGF), VEGF-A VEGF-B, VEGF-C, VEGF-D, and VEGF-E, which bind to the tyrosine kinase receptors, namely VEGF receptor (VEGFR)-1, VEGFR-2, and VEGFR-3 (50). VEGF-A mainly mediates new blood vessel formation within the tumor mass as its binding to VEGFR-2 promotes EC proliferation, migration, and vascular permeability (50). Hormones, cytokines, and growth factors have been shown to boost VEGF-dependent tumor angiogenesis; however, hypoxia represents the primary stimulus for VEGF production and release in the tumor microenvironment (50). Diverse members of the GPCR family are involved in the angiogenic action induced by thrombin, prostaglandins, lysophosphatidic acid, chemokines, and sphingosine 1-phosphate in different pathophysiological conditions, suggesting that certain GPCRs contribute to the development of blood vessels (51–54). In addition, the heterotrimeric G proteins Gαq and Gα11 may contribute to angiogenic responses by interacting with VEGFR-2 (55) and the G protein-coupled receptor kinase 2 (GRK2) has recently emerged as an integrative node toward the development of cancer-associated vascularization (56). In the tumor microenvironment, chemokines and their receptors elicit relevant paracrine actions, as suggested by the ability of CCL2, CCL5, and CXCL8/IL-8 to recruit within the tumor mass leukocytes and macrophages, which release VEGF and other angiogenic factors (57). Furthermore, cytokines may stimulate the production of prostaglandin E2 (PGE2), which increases the secretion of VEGF, CXCL8, and CXCL5 by tumor and stromal cells (57). Overall, these data suggest that GPCR-mediated signaling may modulate the angiogenic

process together with the VEGF/VEGFR axis. Further corroborating these observations, the anti-tumor activity exhibited by several GPCR antagonists has been correlated with their anti-angiogenic properties and anti-proliferative effects (58). Among the GPCRs contributing to the formation of new blood vessels in hypoxic conditions, the chemokine receptor CXCR4 that binds to the stromal cell-derived factor-1 (SDF-1)/CXCL12 has been shown to stimulate tumor outgrowth and metastasis as well as angiogenesis upon hypoxia (59). The angiogenic factor named adrenomedullin (ADM) signals through the calcitonin receptor-like receptor (CRLR), which is a GPCR expressed in several tumors like the high-vascular clear renal cell carcinoma (RCC) (60,61). A functional consensus HRE was identified within the promoter region of the human CRLR gene, thus corroborating the role of CRLR in the formation of new blood vessels upon hypoxic conditions (60,61). Among the vasoactive pro-angiogenic molecules, ET-1 and the cognate receptors (ETRs) are aberrantly activated in diverse malignancies and regulated by low oxygen tension through HIF-1α (62). In this regard, HIF-1α/VEGF signaling has been considered as a downstream transduction pathway activated by the ET-1 axis (62). For instance, in human chondrosarcoma cells, ET-1 promoted the expression of VEGF, angiogenesis, and cell migration by activating integrin-linked kinase (ILK), Akt, and HIF-1α-mediated signaling cascades (63). In ovarian carcinoma, in both normoxic and hypoxic conditions, ET-1 induced the transcription and accumulation of HIF-1α and the upregulation of VEGF, suggesting that ET-1 action may be linked to hypoxia and HIF-1α-dependent angiogenesis (64). In our recent study (65), we also found that ET-1 may trigger GPER expression and function leading to angiogenic responses. Recently, the adrenergic system has been shown to boost tumor angiogenesis and aggressive features through the upregulation of diverse angiogenic factors like VEGF, IL-6, IL-8, matrix metalloproteinase (MMP)-2, and MMP-9 (66,67). The involvement of HIF-1α in the aforementioned biological responses to catecholamine-mediated stress was also evidenced in other studies showing that the β2-adrenergic receptor (AR)/HIF-1α axis regulates angiogenesis and stress-induced pancreatic tumor growth in mouse models (68). In hypoxic melanoma cells, β3-ARs have been found to be upregulated and involved in the increase of VEGF, as evidenced by using two β3-AR blockers (69). Additionally, in ovarian cancer cells, the α1-AR blocker doxazosin prevented VEGF-mediated cell migration, proliferation, and capillary-like structure tube formation (70). These effects were dependent on the activation of VEGFR-2 and downstream signaling including HIF-1α (70). Altogether, these observations may suggest that the adrenergic system plays a role in tumor angiogenesis and progression, in particular through HIF-1α-mediated responses and VEGF expression in hypoxic conditions. Virally encoded GPCRs may also contribute to cancer angiogenesis and progression as evidenced by the human herpesvirus-8 (HHV-8 or Kaposi's sarcoma-associated herpesvirus (KSHV))-encoded G protein-coupled receptor (vGPCR) (71). In this regard, it has been demonstrated that KSHV stimulates the expression of the angiogenic factor angiopoietin-like 4 (71) as well as the production of

VEGF through HIF-1α (72). Accordingly, the expression of vGPCR in human umbilical vein endothelial cells (HUVECs) triggered cell immortalization together with a constitutive expression and activation of VEGFR-2, thus proposing a role for vGPCRs in the acquisition of the KS-angiogenic phenotype in the model system used (73).

GPER IS INVOLVED IN HYPOXIA-MEDIATED SIGNALING

GPER has been recently characterized toward its ability to mediate estrogen action in reproductive, immune, skeletal, cardiovascular, and central nervous systems (5). In addition, our and other studies have largely demonstrated the involvement of GPER in the stimulatory effects elicited by estrogens in cancer cells and tumor microenvironment (6,9–11). Significantly, several studies performed in different cell and animal models have ascertained the role exerted by GPER in certain pathological conditions characterized by oxygen deficiency (30,31,74–78). In this regard, it has been demonstrated that GPER activation may decrease myocardial damage and increase functional recovery after ischemia-reperfusion (I/R) injury, which often induces dangerous complications like arrhythmia in patients with myocardial infarction (74–78). Likewise, in rat hearts of both sexes exposed to I/R injury, the activation of GPER reduced myocardial inflammation and infarct size as well as improved immunosuppression and myocardial mechanical performance (79–81). Interestingly, the expression levels of both GPER and HIF-1α were found to be increased in spontaneously hypertensive rat hearts compared to normotensive controls, suggesting that HIF-1α/GPER signaling may represent a transduction mediator in certain conditions characterized by elevated blood pressure (74), which is tightly linked to hypoxia (82). Of note, the selective GPER agonist G-1 markedly lowered blood pressure in normotensive and hypertensive rats (83,84), thus supporting the hypothesis that GPER may be a valuable pharmacological target for the prevention/treatment of certain cardiovascular diseases. Further supporting the role elicited by GPER in hypoxic conditions, previous studies have reported that its activation may attenuate the detrimental effects induced by oxygen deficiency in some areas of the central nervous system like the hypothalamic-pituitary axis, hippocampal formation, brainstem autonomic nuclei, and spinal cord (85,86). For instance, GPER activation promoted neuronal survival after global ischemia through the activation of pro-survival and anti-apoptotic signaling cascades (86). An improvement in cerebral microvascular function upon hypoxia/reoxygenation injury was also observed upon GPER activation in male and female rats (87), although sex-dependent protective effects mediated by GPER have been also shown to influence the outcome of ischemic stroke (88). In this regard, it has been demonstrated that GPER expression increases after stroke in the brain of male but not female mice, thus suggesting that a gender-specific regulation of GPER may occur and influence the recovery from cerebral I/R (88). The regulation of GPER expression following hypoxia has been evaluated in breast cancer cells as well as in cancer-associated fibroblasts (CAFs) obtained from breast malignancies (30,31). In these cells, hypoxia-stimulated HIF-1α was found recruited to the HRE sequences located

within the promoter region of the human GPER gene (30,31). Accordingly, HIF-1α was required for both the transactivation of a GPER promoter reporter gene as well as for the upregulation of GPER expression upon hypoxia (30,31). These observations were further corroborated by the involvement of HIF-1α/GPER signaling in VEGF expression toward tumor angiogenesis and progression (31,89). In addition, HIF-1α/GPER/VEGF transduction pathway was triggered in cancer cells upon exposure to copper, which showed the ability to mimic the hypoxia-mediated signaling (90). Interestingly, the copper-chelating agent TEPA exerted an inhibitory action on the activation of the aforementioned pathway (90), in accordance with previous studies demonstrating that copper-chelating agents can exert anti-tumor effects (91). Altogether, these results indicate that diverse stimuli including hypoxia may trigger relevant biological responses through GPER, which was recently shown to be also involved in the stimulatory effects exerted by aldosterone in breast cancer cells and breast tumor-derived endothelial cells (92) as well as in pregnancy-induced vasodilation of rat uterine arteries (93).

GPCRS AND HYPOXIA: IMPLICATIONS FOR DRUG DISCOVERY

The multifaceted mechanisms of oxygen sensing mainly orchestrated by HIF-1 represent an essential response to cope with hypoxic stress, which often occurs in cancer, heart disease, and stroke (32,33). As many members of the GPCR family elicit a role in the intricate cell adaptation to oxygen deficiency, a cross talk between HIF-1 and GPCR-mediated pathways may be involved in the biological responses to hypoxia in the aforementioned pathological conditions. In recent years, the discovery and development of several different strategies to block HIF-1 action directly or indirectly has been suggested as a promising tool to overcome the resistance to conventional chemotherapeutic agents in hypoxic microenvironment (34,94). In this vein, HIF-1 inhibitors may be regarded as golden candidates in combination treatment targeting the molecular mediators activated by hypoxia. For instance, a further approach toward new therapeutic strategies may combine the pharmacological manipulation of both HIF-1- and GPCR-mediated signaling. In addition to the therapeutic purposes, GPCRs along with HIF-1 may be regarded as further hallmarks of hypoxia signature in different pathophysiological conditions. As it concerns GPER, on the basis of its involvement in biological responses to low oxygen tension, new GPER-targeted therapies might pioneer for innovative drug discovery strategies aimed to improve the efficacy of HIF blockers and conventional angiogenic inhibitors.

CONCLUSIONS

A significant progress has been made in the past few years toward the characterization of the molecular mechanisms involved in GPCR action. In particular, many members of the GPCR family have been shown to contribute to the adaptive cell responses to low oxygen tension, which is a distinguishing feature of tumor development and certain cardiovascular diseases. In this regard, GPER may be included among the HIF-1α target genes that drive cancer cell survival and malignant progression. In addition, HIF-1α/GPER signaling may play a relevant role toward VEGF stimulation, angiogenesis, and cancer development. Furthermore, the role elicited by GPER in heart failure, stroke, and hypertension has been largely elucidated, paving the way for novel therapeutic approaches in these relevant illnesses that are characterized by hypoxia and ischemia.

REFERENCES

1. Rosenbaum DM, Rasmussen SG, Kobilka BK. The structure and function of G-protein-coupled receptors. Nature. 2009;459:356–63.
2. Pierce KL, Premont RT, Lefkowitz RJ. Seven-transmembrane receptors. Nat Rev Mol Cell Biol. 2002;3:639–50.
3. Dorsam RT, Gutkind JS. G-protein-coupled receptors and cancer. Nat Rev Cancer. 2007;7:79–94.
4. Lappano R, Maggiolini M. G protein-coupled receptors: novel targets for drug discovery in cancer. Nat Rev Drug Discov. 2011;10:47–60.
5. Maggiolini M, Picard D. The unfolding stories of GPR30, a new membrane-bound estrogen receptor. J Endocrinol. 2010;204:105–14.
6. Lappano R, Pisano A, Maggiolini M. GPER function in breast cancer: an overview. Front Endocrinol (Lausanne). 2014;5:66.
7. Albanito L, Lappano R, Madeo A, Chimento A, Prossnitz ER, Cappello AR, *et al*. Effects of atrazine on estrogen receptor α- and G protein-coupled receptor 30-mediated signaling and proliferation in cancer cells and cancer-associated fibroblasts. Environ Health Perspect. 2015;5:493–9.
8. Maggiolini M, Vivacqua A, Fasanella G, Recchia AG, Sisci D, Pezzi V, *et al*. The G protein-coupled receptor GPR30 mediates c-fos up-regulation by 17beta-estradiol and phytoestrogens in breast cancer cells. J Biol Chem. 2004;279:27008–16.
9. Pandey DP, Lappano R, Albanito L, Madeo A, Maggiolini M, Picard D. Estrogenic GPR30 signalling induces proliferation and migration of breast cancer cells through CTGF. EMBO J. 2009;28:523–32.
10. Pupo M, Pisano A, Lappano R, Santolla MF, De Francesco EM, Abonante S, *et al*. Bisphenol A induces gene expression changes and proliferative effects through GPER in breast cancer cells and cancer-associated fibroblasts. Environ Health Perspect. 2012;120:1177–82.
11. Madeo A, Maggiolini M. Nuclear alternate estrogen receptor GPR30 mediates 17beta-estradiol-induced gene expression and migration in breast cancer-associated fibroblasts. Cancer Res. 2010;70:6036–46.
12. Lappano R, Rosano C, De Marco P, De Francesco EM, Pezzi V, Maggiolini M. Estriol acts as a GPR30 antagonist in estrogen receptor-negative breast cancer cells. Mol Cell Endocrinol. 2010;320:162–70.
13. Ariazi EA, Brailoiu E, Yerrum S, Shupp HA, Slifker MJ, Cunliffe HE, *et al*. The G protein-coupled receptor GPR30 inhibits proliferation of estrogen receptor-positive breast cancer cells. Cancer Res. 2010;70:1184–94.
14. Wei W, Chen ZJ, Zhang KS, Yang XL, Wu YM, Chen XH, *et al*. The activation of G protein-coupled receptor 30 (GPR30) inhibits proliferation of estrogen receptor-negative breast cancer cells in vitro and in vivo. Cell Death Dis. 2014;5, e1428.

15. Weißenborn C, Ignatov T, Ochel HJ, Costa SD, Zenclussen AC, Ignatova Z, et al. GPER functions as a tumor suppressor in triple-negative breast cancer cells. J Cancer Res Clin Oncol. 2014;140:713–23.

16. Weißenborn C, Ignatov T, Poehlmann A, Wege AK, Costa SD, Zenclussen AC, et al. GPER functions as a tumor suppressor in MCF-7 and SK-BR-3 breast cancer cells. J Cancer Res Clin Oncol. 2014;140:663–71.

17. Marjon NA, Hu C, Hathaway HJ, Prossnitz ER. G protein-coupled estrogen receptor regulates mammary tumorigenesis and metastasis. Mol Cancer Res. 2014;12:1644–54.

18. Arias-Pulido H, Royce M, Gong Y, Joste N, Lomo L, Lee SJ, et al. GPR30 and estrogen receptor expression: new insights into hormone dependence of inflammatory breast cancer. Breast Cancer Res Treat. 2010;123:51–8.

19. Ignatov T, Weißenborn C, Poehlmann A, Lemke A, Semczuk A, Roessner A, et al. GPER-1 expression decreases during breast cancer tumorigenesis. Cancer Invest. 2013;31:309–15.

20. Ignatov T, Ignatov A, Weissenborn C, Eggemann H, Bischoff J, Semczuk A, et al. G-protein-coupled estrogen receptor GPR30 and tamoxifen resistance in breast cancer. Breast Cancer Res Treat. 2011;128:457–66.

21. Sjöström M, Hartman L, Grabau D, Fornander T, Malmström P, Nordenskjöld B, et al. Lack of G protein-coupled estrogen receptor (GPER) in the plasma membrane is associated with excellent long-term prognosis in breast cancer. Breast Cancer Res Treat. 2014;145:61–71.

22. Smith HO, Leslie KK, Singh M, Qualls CR, Revankar CM, Joste NE, et al. GPR30: a novel indicator of poor survival for endometrial carcinoma. Am J Obstet Gynecol. 2007;196:386. e1-11.

23. Smith HO, Arias-Pulido H, Kuo DY, Howard T, Qualls CR, Lee SJ, et al. GPR30 predicts poor survival for ovarian cancer. Gynecol Oncol. 2009;114:465–71.

24. Filardo EJ, Graeber CT, Quinn JA, Resnick MB, Giri D, DeLellis RA, et al. Distribution of GPR30, a seven membrane-spanning estrogen receptor, in primary breast cancer and its association with clinicopathologic determinants of tumor progression. Clin Cancer Res. 2006;12:6359–66.

25. Albanito L, Sisci D, Aquila S, Brunelli E, Vivacqua A, Madeo A, et al. Epidermal growth factor induces G protein-coupled receptor 30 expression in estrogen receptor-negative breast cancer cells. Endocrinology. 2008;149:3799–808.

26. Vivacqua A, Lappano R, De Marco P, Sisci D, Aquila S, De Amicis F, et al. G protein-coupled receptor 30 expression is up-regulated by EGF and TGF alpha in estrogen receptor alpha-positive cancer cells. Mol Endocrinol. 2009;23:1815–26.

27. Bartella V, De Marco P, Malaguarnera R, Belfiore A, Maggiolini M. New advances on the functional cross-talk between insulin-like growth factor-I and estrogen signalling in cancer. Cell Signal. 2012;24:1515–21.

28. De Marco P, Bartella V, Vivacqua A, Lappano R, Santolla MF, Morcavallo A, et al. Insulin-like growth factor-I regulates GPER expression and function in cancer cells. Oncogene. 2013;32:678–88.

29. De Marco P, Romeo E, Vivacqua A, Malaguarnera R, Abonante S, Romeo F, et al. GPER1 is regulated by insulin in cancer cells and cancer-associated fibroblasts. Endocr Relat Cancer. 2014;21:739–53.

30. Recchia AG, De Francesco EM, Vivacqua A, Sisci D, Panno ML, Andò S, et al. The G protein-coupled receptor 30 is up-regulated by hypoxia-inducible factor-1alpha (HIF-1alpha) in breast cancer cells and cardiomyocytes. J Biol Chem. 2011;286:10773–82.

31. De Francesco EM, Lappano R, Santolla MF, Marsico S, Caruso A, Maggiolini M. HIF-1α/GPER signaling mediates the expression of VEGF induced by hypoxia in breast cancer associated fibroblasts (CAFs). Breast Cancer Res. 2013;15:R64.

32. Harris AL. Hypoxia—a key regulator factor in tumor growth. Nat Rev Cancer. 2002;2:38–47.

33. Bishop T, Ratcliffe PJ. HIF hydroxylase pathways in cardiovascular physiology and medicine. Circ Res. 2015;117:65–79.

34. Semenza GL. Hypoxia-inducible factors: mediators of cancer progression and targets for cancer therapy. Trends Pharmacol Sci. 2012;33:207–14.

35. Manalo DJ, Rowan A, Lavoie T, Natarajan L, Kelly BD, Ye SQ, et al. Transcriptional regulation of vascular endothelial cell responses to hypoxia by HIF-1. Blood. 2005;105:659–69.

36. Glück AA, Aebersold DM, Zimmer Y, Medová M. Interplay between receptor tyrosine kinases and hypoxia signaling in cancer. Int J Biochem Cell Biol. 2015;62:101–14.

37. Wang GL, Semenza GL. General involvement of hypoxia-inducible factor 1 in transcriptional response to hypoxia. Proc Natl Acad Sci U S A. 1993;90:4304–8.

38. Semenza GL, Aganì F, Booth G, Forsythe J, Iyer N, Jiang H, et al. Structural and functional analysis of hypoxia-inducible factor I. Kidney Int. 1997;51:553–5.

39. Guo M, Cai C, Zhao G, Qiu X, Zhao H, Ma Q, et al. Hypoxia promotes migration and induces CXCR4 expression via HIF-1α activation in human osteosarcoma. PLoS One. 2014;9, e90518.

40. Kimura M, Mizukami Y, Miura T, Fujimoto K, Kobayashi S, Matsuzaki M. Orphan G protein-coupled receptor, GPR41, induces apoptosis via a p53/Bax pathway during ischemic hypoxia and reoxygenation. J Biol Chem. 2001;276:26453–60.

41. Adams JW, Wang J, Davis JR, Liaw C, Gaidarov I, Gatlin J, et al. Myocardial expression, signaling, and function of GPR22: a protective role for an orphan G protein-coupled receptor. Am J Physiol Heart Circ Physiol. 2008;295:H509–21.

42. Corbi G, Conti V, Russomanno G, Longobardi G, Furgi G, Filippelli A, et al. Adrenergic signaling and oxidative stress: a role for sirtuins? Front Physiol. 2013;4:324.

43. Jordan BA, Gomes I, Rios C, Filipovska J, Devi LA. Functional interactions between mu opioid and alpha 2A-adrenergic receptors. Mol Pharmacol. 2003;64:1317–24.

44. Headrick JP, See Hoe LE, Du Toit EF, Peart JN. Opioid receptors and cardioprotection-opioidergic conditioning' of the heart. Br J Pharmacol. 2015;172:2026–50.

45. Gao CJ, Niu L, Ren PC, Wang W, Zhu C, Li YQ, et al. Hypoxic preconditioning attenuates global cerebral ischemic injury following asphyxial cardiac arrest through regulation of delta opioid receptor system. Neuroscience. 2012;202:352–62.

46. Caprara V, Scappa S, Garrafa E, Di Castro V, Rosanò L, Bagnato A, et al. Endothelin-1 regulates hypoxia-inducible factor-1α and -2α stability through prolyl hydroxylase domain 2 inhibition in human lymphatic endothelial cells. Life Sci. 2014;118:185–90.

47. Hu HT, Ma QY, Zhang D, Shen SG, Han L, Ma YD, et al. HIF-1alpha links beta-adrenoceptor agonists and pancreatic cancer cells under normoxic condition. Acta Pharmacol Sin. 2010;31:102–10.

48. Lee SJ, No YR, Dang DT, Dang LH, Yang VW, Shim H, et al. Regulation of hypoxia-inducible factor 1α (HIF-1α) by lysophosphatidic acid is dependent on interplay between p53 and Krüppel-like factor 5. J Biol Chem. 2013;288:25244–53.

49. Baeriswyl V, Christofori G. The angiogenic switch in carcinogenesis. Semin Cancer Biol. 2009;19:329–37.

50. Ferrara N, Gerber HP, LeCouter J. The biology of VEGF and its receptors. Nat Med. 2003;9:66–76.

51. Richard DE, Vouret-Craviari V, Pouyssegur J. Angiogenesis and G-protein-coupled receptors: signals that bridge the gap. Oncogene. 2001;20:1556–62.

52. Sumida H, Noguchi K, Kihara Y, Abe M, Yanagida K, Hamano F, et al. LPA4 regulates blood and lymphatic vessel formation during mouse embryogenesis. Blood. 2010;116:5060–70.

53. Moore BB, Keane MP, Addison CL, Arenberg DA, Strieter RM. CXC chemokine modulation of angiogenesis: the importance of balance between angiogenic and angiostatic members of the family. J Investig Med. 1998;46:113–20.

54. Liu Y, Wada R, Yamashita T, Mi Y, Deng CX, Hobson JP, et al. Edg-1, the G protein-coupled receptor for sphingosine-1-phosphate, is essential for vascular maturation. J Clin Invest. 2000;106:951–61.

55. Zeng H, Zhao D, Yang S, Datta K, Mukhopadhyay D. Heterotrimeric Gαq/Gα11 proteins function upstream of vascular endothelial growth factor (VEGF) receptor-2 (KDR) phosphorylation in vascular permeability factor/VEGF signaling. J Biol Chem. 2003;278:20738–45.

56. Rivas V, Carmona R, Muñoz-Chápuli R, Mendiola M, Nogués L, Reglero C, et al. Developmental and tumoral vascularization is

regulated by G protein-coupled receptor kinase 2. P J Clin Invest. 2013;123:4714–30.

57. Sarvaiya PJ, Guo D, Ulasov I, Gabikian P, Lesniak MS. Chemokines in tumor progression and metastasis. Oncotarget. 2013;4:2171–85.

58. Guha S, Eibl G, Kisfalvi K, Fan RS, Burdick M, Reber H, *et al*. Broad-spectrum G protein-coupled receptor antagonist, [D-Arg1, D-Trp5,7,9, Leu11]SP: a dual inhibitor of growth and angiogenesis in pancreatic cancer. Cancer Res. 2005;65:2738–45.

59. Jin F, Brockmeier U, Otterbach F, Metzen E. New insight into the SDF-1/CXCR4 axis in a breast carcinoma model: hypoxia-induced endothelial SDF-1 and tumor cell CXCR4 are required for tumor cell intravasation. Mol Cancer Res. 2012;10:1021–31.

60. Nikitenko LL, Leek R, Henderson S, Pillay N, Turley H, Generali D, *et al*. The G-protein-coupled receptor CRLR is upregulated in an autocrine loop with adrenomedullin in clear cell renal cell carcinoma and associated with poor prognosis. Clin Cancer Res. 2013;19:5740–8.

61. Nikitenko LL, Smith DM, Bicknell R, Rees MC. Transcriptional regulation of the CRLR gene in human microvascular endothelial cells by hypoxia. FASEB J. 2003;17:1499–501.

62. Yamashita K, Discher DJ, Hu J, Bishopric NH, Webster KA. Molecular regulation of the endothelin-1 gene by hypoxia. Contributions of hypoxia-inducible factor-1, activator protein-1, GATA-2, AND p300/CBP. J Biol Chem. 2001;276:12645–53.

63. Wu MH, Huang CY, Lin JA, Wang SW, Peng CY, Cheng HC, *et al*. Endothelin-1 promotes vascular endothelial growth factor-dependent angiogenesis in human chondrosarcoma cells. Oncogene. 2014;33:1725–35.

64. Spinella F, Rosanò L, Di Castro V, Natali PG, Bagnato A. Endothelin-1 induces vascular endothelial growth factor by increasing hypoxia-inducible factor-1alpha in ovarian carcinoma cells. J Biol Chem. 2002;277:27850–5.

65. Bartella V, De Francesco EM, Perri MG, Curcio R, Dolce V, Maggiolini M, *et al*. The G protein estrogen receptor (GPER) is regulated by endothelin-1 mediated signaling in cancer cells. Cell Signal. 2016;2:61–71.

66. Moretti S, Massi D, Farini V, Baroni G, Parri M, Innocenti S, *et al*. β-Adrenoceptors are upregulated in human melanoma and their activation releases pro-tumorigenic cytokines and metalloproteases in melanoma cell lines. Lab Invest. 2013;279.

67. Yang EV, Kim SJ, Donovan EL, Chen M, Gross AC, Webster Marketon JI, *et al*. Norepinephrine upregulates VEGF, IL-8, and IL-6 expression in human melanoma tumor cell lines: implications for stress-related enhancement of tumor progression. Brain Behav Immun. 2009;23:267–75.

68. Shan T, Ma J, Ma Q, Guo K, Guo J, Li X, *et al*. β2-AR-HIF-1α: a novel regulatory axis for stress-induced pancreatic tumor growth and angiogenesis. Curr Mol Med. 2013;13:1023–34.

69. Dal Monte M, Casini G, Filippi L, Nicchia GP, Svelto M, Bagnoli P. Functional involvement of β3-adrenergic receptors in melanoma growth and vascularization. J Mol Med (Berl). 2013;91:1407–19.

70. Park MS, Kim BR, Dong SM, Lee SH, Kim DY, Rho SB. The antihypertension drug doxazosin inhibits tumor growth and angiogenesis by decreasing VEGFR-2/Akt/mTOR signaling and VEGF and HIF-1α expression. Oncotarget. 2014;5:4935–44.

71. Ma T, Jham BC, Hu J, Friedman ER, Basile JR, Molinolo A, *et al*. Viral G protein-coupled receptor up-regulates angiopoietin-like 4 promoting angiogenesis and vascular permeability in Kaposi's sarcoma. Proc Natl Acad Sci U S A. 2010;107:14363–8.

72. Sodhi A, Montaner S, Patel V, Zohar M, Bais C, Mesri EA, *et al*. The Kaposi's sarcoma-associated herpes virus G protein-coupled receptor up-regulates vascular endothelial growth factor expression and secretion through mitogen-activated protein kinase and p38 pathways acting on hypoxia-inducible factor 1alpha. Cancer Res. 2000;60:4873–80.

73. Bais C, Van Geelen A, Eroles P, Mutlu A, Chiozzini C, Dias S, *et al*. Kaposi's sarcoma associated herpesvirus G protein-coupled receptor immortalizes human endothelial cells by activation of the VEGF receptor-2/ KDR. Cancer Cell. 2003;3:131–43.

74. De Francesco EM, Angelone T, Pasqua T, Pupo M, Cerra MC, Maggiolini M. GPER mediates cardiotropic effects in spontaneously hypertensive rat hearts. PLoS One. 2013;8, e69322.

75. Patel VH, Chen J, Ramanjaneya M, Karteris E, Zachariades E, Thomas P, *et al*. G-protein coupled estrogen receptor 1 expression in rat and human heart: protective role during ischaemic stress. Int J Mol Med. 2010;26:193–9.

76. Meyer MR, Prossnitz ER, Barton M. The G protein-coupled estrogen receptor GPER/GPR30 as a regulator of cardiovascular function. Vascul Pharmacol. 2011;55:17–25.

77. Deschamps AM, Murphy E, Sun J. Estrogen receptor activation and cardioprotection in ischemia reperfusion injury. Trends Cardiovasc Med. 2011;20:73–8.

78. Deschamps AM, Murphy E. Activation of a novel estrogen receptor, GPER, is cardioprotective in male and female rats. Am J Physiol Heart Circ Physiol. 2009;297:H1806–13.

79. Weil BR, Manukyan MC, Herrmann JL, Wang Y, Abarbanell AM, Poynter JA, *et al*. Signaling via GPR30 protects the myocardium from ischemia/reperfusion injury. Surgery. 2010;148:436–43.

80. Zhang B, Subramanian S, Dziennis S, Jia J, Uchida M, Akiyoshi K, *et al*. Estradiol and G1 reduce infarct size and improve immunosuppression after experimental stroke. J Immunol. 2010;18:4087–94.

81. Li WL, Xiang W, Ping Y. Activation of novel estrogen receptor GPER results in inhibition of cardiocyte apoptosis and cardioprotection. Mol Med Rep. 2015;12:2425–30.

82. Czibik G. Complex role of the HIF system in cardiovascular biology. J Mol Med (Berl). 2010;88:1101–1.

83. Lindsey SH, Cohen JA, Brosnihan KB, Gallagher PE, Chappell MC. Chronic treatment with the G protein-coupled receptor 30 agonist G-1 decreases blood pressure in ovariectomized mRen2.Lewis rats. Endocrinology. 2009;150:3753–8.

84. Meyer MR, Prossnitz ER, Barton M. GPER/GPR30 and regulation of vascular tone and blood pressure. Immunol, Endocr Metab Agents Med Chem. 2011;11:255–61.

85. Brailoiu E, Dun SL, Brailoiu GC, Mizuo K, Sklar LA, Oprea TI, *et al*. Distribution and characterization of estrogen receptor G protein-coupled receptor 30 in the rat central nervous system. J Endocrinol. 2007;193:311–21.

86. Chen J, Hu R, Ge H, Duanmu W, Li Y, Xue X, *et al*. G-protein-coupled receptor 30-mediated antiapoptotic effect of estrogen on spinal motor neurons following injury and its underlying mechanisms. Mol Med Rep. 2015;12:1733–40.

87. Murata T, Dietrich HH, Xiang C, Dacey Jr RG. G protein-coupled estrogen receptor agonist improves cerebral microvascular function after hypoxia/reoxygenation injury in male and female rats. Stroke. 2013;44:779–85.

88. Broughton BR, Brait VH, Guida E, Lee S, Arumugam TV, Gardiner-Mann CV, *et al*. Stroke increases G protein-coupled estrogen receptor expression in the brain of male but not female mice. Neurosignals. 2013;21:229–39.

89. De Francesco EM, Pellegrino M, Santolla MF, Lappano R, Ricchio E, Abonante S, *et al*. GPER mediates activation of HIF1α/VEGF signaling by estrogens. Cancer Res. 2014;74:4053–64.

90. Rigiracciolo DC, Scarpelli A, Lappano R, Pisano A, Santolla MF, De Marco P, *et al*. Copper activates HIF-1α/GPER/VEGF signalling in cancer cells. Oncotarget. 2015;33:34158–77.

91. Brewer GJ. Anticopper therapy against cancer and diseases of inflammation and fibrosis. Drug Discov Today. 2005;10:1103–19.

92. Rigiracciolo DC, Scarpelli A, Lappano R, Pisano A, Santolla MF, Avino S, et al. GPER is involved in the stimulatory effects of aldosterone in breast cancer cells and breast tumor-derived endothelial cells. Oncotarget. 2015 Dec 5. doi: 10.18632/oncotarget.6475.

93. Tropea T, De Francesco EM, Rigiracciolo D, Maggiolini M, Wareing M, Osol G, *et al*. Pregnancy augments G protein estrogen receptor (GPER) induced vasodilation in rat uterine arteries via the nitric oxide—cGMP signaling pathway. PLoS One. 2015;10(11), e0141997.

94. Xia Y, Choi HK, Lee K. Recent advances in hypoxia-inducible factor (HIF)-1 inhibitors. Eur J Med Chem. 2012;49:24–40.

GPER is involved in the stimulatory effects of aldosterone in breast cancer cells and breast tumor-derived endothelial cells

Damiano Cosimo Rigiracciolo[1], Andrea Scarpelli[1], Rosamaria Lappano[1], Assunta Pisano[1], Maria Francesca Santolla[1], Silvia Avino[1], Paola De Marco[1], Benedetta Bussolati[2], Marcello Maggiolini[1] and Ernestina Marianna De Francesco[1]

[1] Department of Pharmacy, Health and Nutritional Sciences, University of Calabria, Rende, Italy

[2] Department of Molecular Biotechnology and Health Sciences, University of Torino, Turin, Italy

Correspondence to: *Marcello Maggiolini*, **email**: *marcellomaggiolini@yahoo.it*

Rosamaria Lappano, **email**: *lappanorosamaria@yahoo.it*

ABSTRACT

Aldosterone induces relevant effects binding to the mineralcorticoid receptor (MR), which acts as a ligand-gated transcription factor. Alternate mechanisms can mediate the action of aldosterone such as the activation of epidermal growth factor receptor (EGFR), MAPK/ERK, transcription factors and ion channels. The G-protein estrogen receptor (GPER) has been involved in the stimulatory effects of estrogenic signalling in breast cancer. GPER has been also shown to contribute to certain responses to aldosterone, however the role played by GPER and the molecular mechanisms implicated remain to be fully understood. Here, we evaluated the involvement of GPER in the stimulatory action exerted by aldosterone in breast cancer cells and breast tumor derived endothelial cells (B-TEC). Competition assays, gene expression and silencing studies, immunoblotting and immunofluorescence experiments, cell proliferation and migration were performed in order to provide novel insights into the role of GPER in the aldosterone-activated signalling. Our results demonstrate that aldosterone triggers the EGFR/ERK transduction pathway in a MR- and GPER-dependent manner. Aldosterone does not bind to GPER, it however induces the direct interaction between MR and GPER as well as between GPER and EGFR. Next, we ascertain that the up-regulation of the Na$^+$/H$^+$ exchanger-1 (NHE-1) induced by aldosterone involves MR and GPER. Biologically, both MR and GPER contribute to the proliferation and migration of breast and endothelial cancer cells mediated by NHE-1 upon aldosterone exposure. Our data further extend the current knowledge on the molecular mechanisms through which GPER may contribute to the stimulatory action elicited by aldosterone in breast cancer.

INTRODUCTION

Aldosterone elicits multiple biological effects binding to the mineralcorticoid receptor (MR), which acts as a ligand-gated transcription factor [1]. In addition, rapid aldosterone signalling involves alternate mechanisms that include the activation of transduction pathways like tyrosine kinase c-Src, epidermal growth factor receptor (EGFR) and MAPK/ERK cascade [2-4]. Aldosterone is a key component of the renin-angiotensin-aldosterone system (RAAS), which is mainly implicated in maintaining salt and water balance toward the regulation of systemic blood pressure [5]. In addition, aldosterone activates ionic membrane transporters as the Na$^+$/H$^+$ exchanger (NHE-1) and Na$^+$/HCO$_3^-$ cotransporter (NBC), which regulate the cellular pH and volume [6-7]. Aldosterone has been also involved in diverse cardio-metabolic diseases as it triggers inflammatory and fibrotic responses in both heart and vessels [8-11]. Recent studies have suggested that aldosterone/MR signalling may contribute to the progression of certain types of tumor [12-13]. For instance, it has been shown that aldosterone stimulates

the survival and proliferation of renal carcinoma cells by upregulating K-RAS and the activation of the Akt and Raf pathways [12]. Moreover, an aldosterone blocker inhibited the growth of hepatocellular carcinoma and angiogenesis both *in vitro* and *in vivo* [13].

The G-protein estrogen receptor namely GPER mediates several pathophysiological functions in the cardiovascular, immune and central nervous systems, glucose and fat metabolism [14]. In addition, our and other previous studies have largely demonstrated that estrogenic GPER signalling elicits stimulatory effects in cancer cells and tumor microenvironment toward cancer progression [14-19]. In this regard, it has been reported that GPER activation triggers diverse transduction pathways involved in the proliferation, invasion and migration of tumor cells, including the epidermal growth factor receptor (EGFR), the MAPK/ERK and PI3K/AKT transduction cascades, Ca^{2+} mobilization and cAMP production [20-27]. Numerous endogenous, environmental and newly synthesized molecules have been shown to trigger relevant GPER-mediated responses in different cell contexts [28-36]. Aldosterone has been recently suggested to act through GPER in diverse models, including the cardiovascular and renal systems [6, 37-40]. For instance, it was demonstrated that GPER is involved in important effects exerted by aldosterone on vascular endothelial cells, cardiac vagal tone and connecting tubule glomerular feedback [37-40]. These observations have pointed out the potential of GPER to contribute to the aldosterone action, however the effective role played by GPER and the molecular mechanisms implicated are controversial as pharmacologic criteria for considering GPER as an aldosterone receptor have been not adequately fulfilled [41-43].

In the framework of the aforementioned observations, the current study provides novel insights into the role of GPER in mediating the action of aldosterone in breast tumor. In particular, our data show that a functional cross-talk between MR and GPER may occur upon aldosterone treatment leading to stimulatory effects in both breast cancer cells and endothelial cells obtained from breast malignancies.

RESULTS

Aldosterone activates the EGFR/ERK transduction pathway and induces the interaction between MR and GPER

We began our study evaluating whether aldosterone could be able to activate the EGFR/ERK transduction signalling in SkBr3 breast cancer cells and B-TEC breast tumor-derived endothelial cells, which were used as model systems. Both cell types express MR and GPER but not

ERα (Supplementary Figure 1). Of note, pM aldosterone concentrations induced the phosphorylation of EGFR and ERK1/2 in both SkBr3 cells and B-TEC (Figure 1A-1D), though these effects were no longer evident silencing the expression of MR (Figure 1E-1J). Recently, it has been reported that GPER contributes to aldosterone action although the mechanisms involved remain to be fully understood [6, 38-44]. In this vein, we therefore performed saturation curves and scatchard plot analyses using as radiotracers the GPER ligand [³H]E2 [28, 31-32, 34-36] and the MR ligand [³H]aldosterone. [³H]E2 showed an estimated Bmax corresponding to 6799 ± 707.8 cpm/1 × 10^5 SkBr3 cells and an estimated Kd corresponding to 8.16 ± 1.70 nM (Figure 2A), whereas [³H]aldosterone showed an estimated Bmax corresponding to 2159 ± 229.2 cpm/1 × 10^5 SkBr3 cells and an estimated Kd corresponding to 0.42 ± 0.08 nM (Figure 2B). In competition assays, E2 but not aldosterone displaced [³H]E2 (Figure 2C), while aldosterone but not E2 displaced [³H]Aldosterone (Figure 2D). Collectively, these findings argue that in SkBr3 cells aldosterone is not able to displace [³H]E2, which was used as a GPER radioligand.

In order to gain further insights into the role of GPER in certain biological responses to aldosterone, we then evaluated the possible interaction of GPER and MR and EGFR. Our immunoprecipitation data indicated that aldosterone triggers a direct interaction between GPER and MR as well as GPER and EGFR (Figure 2E-2L). Immunofluorescence experiments performed in SkBr3 cells further corroborated the aforementioned results as an increased merged (orange) signal of MR and GPER was observed upon a short (15 min) aldosterone treatment (Figure 2M-2O). Altogether, these data suggest that GPER may contribute to aldosterone/MR-activated EGFR signalling.

GPER is involved in the aldosterone-mediated signalling

On the basis of the abovementioned observations, we performed gene silencing experiments in order to assess whether GPER is involved in the rapid signalling induced by aldosterone. Interestingly, the activation of both EGFR and ERK1/2 by aldosterone was no longer evident silencing GPER in both SkBr3 cells and B-TEC (Figure 3A-3F). In accordance with these findings, the GPER antagonist G15 prevented the EGFR/ERK phosphorylation upon aldosterone exposure (Figure 3G-3I). Next, the EGFR tyrosine kinase inhibitor AG1478 (AG) but not the MEK inhibitor PD98059 (PD) blocked EGFR phosphorylation by aldosterone (Figure 3G-3I), while ERK1/2 activation was prevented in the presence of both AG and PD. Hence, the MEK/ERK transduction pathway is activated afterward the engagement of EGFR upon aldosterone treatment in our model system.
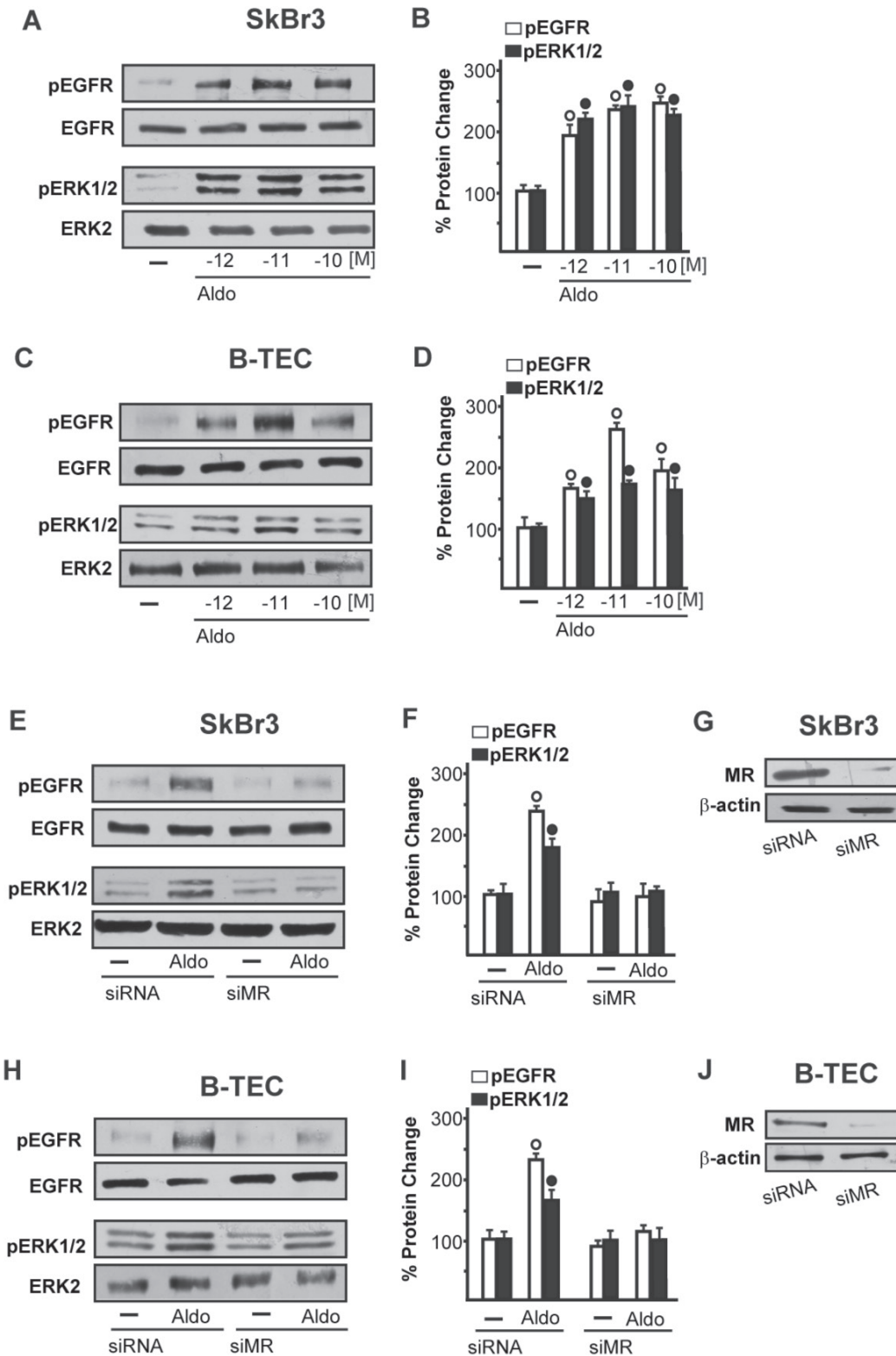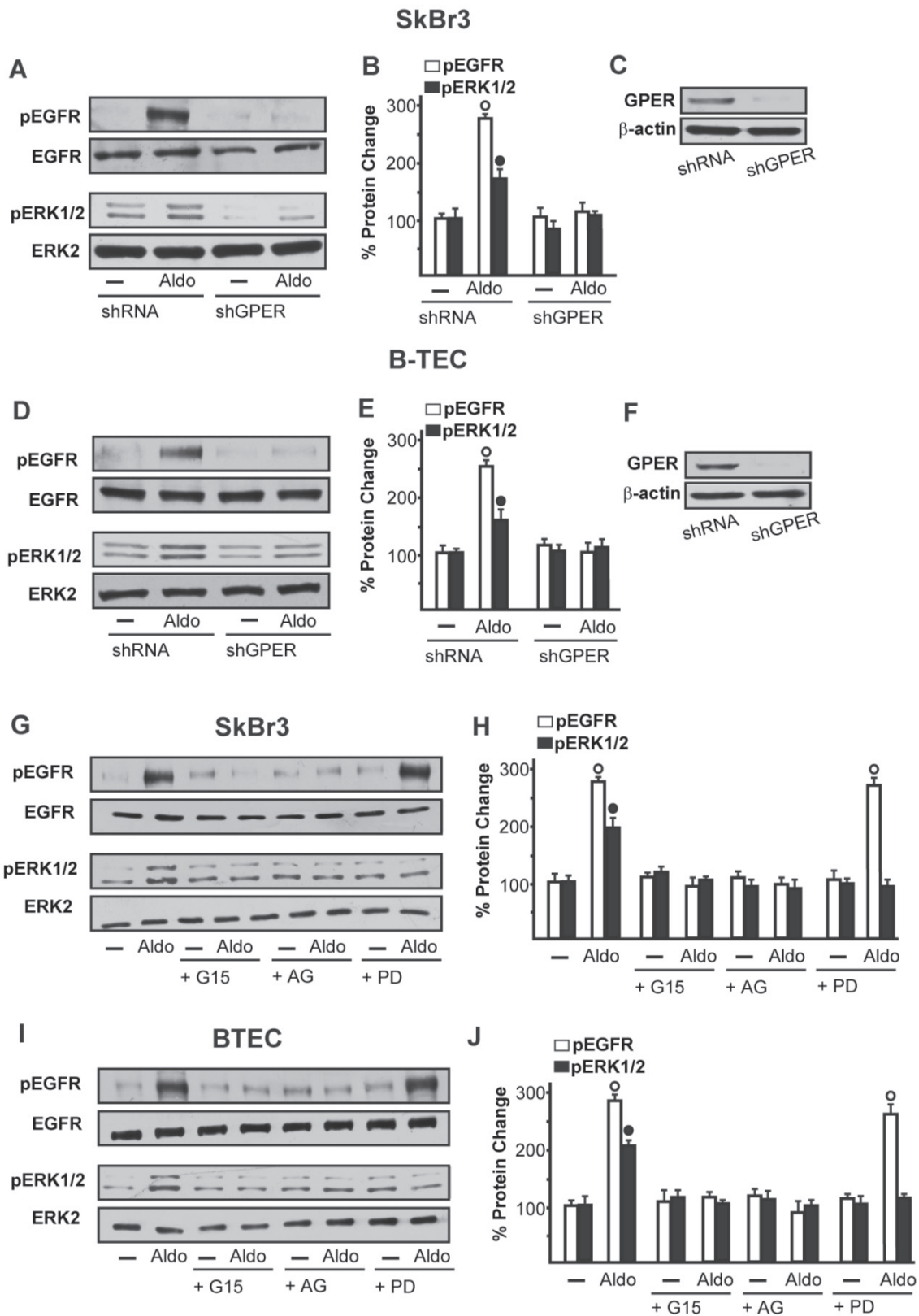
Figure 1: EGFR and ERK1/2 phosphorylation in SkBr3 cells. A., **B.** and B-TEC **C.**, **D.** treated with Aldosterone (Aldo) for 15 min. EGFR and ERK1/2 phosphorylation in SkBr3 cells **E.**, **F.** and B-TEC **H.**, **I.** transfected for 24 h with siRNA or siMR and then treated with 10 pM Aldo for 15 min. **G.**, **J.** Efficacy of MR silencing. The blots were normalized to EGFR or ERK2 and each data point represents the mean ± SD of three independent experiments. (○) and (●) indicate $p < 0.05$ for cells receiving vehicle (-) *versus* Aldo treatment.
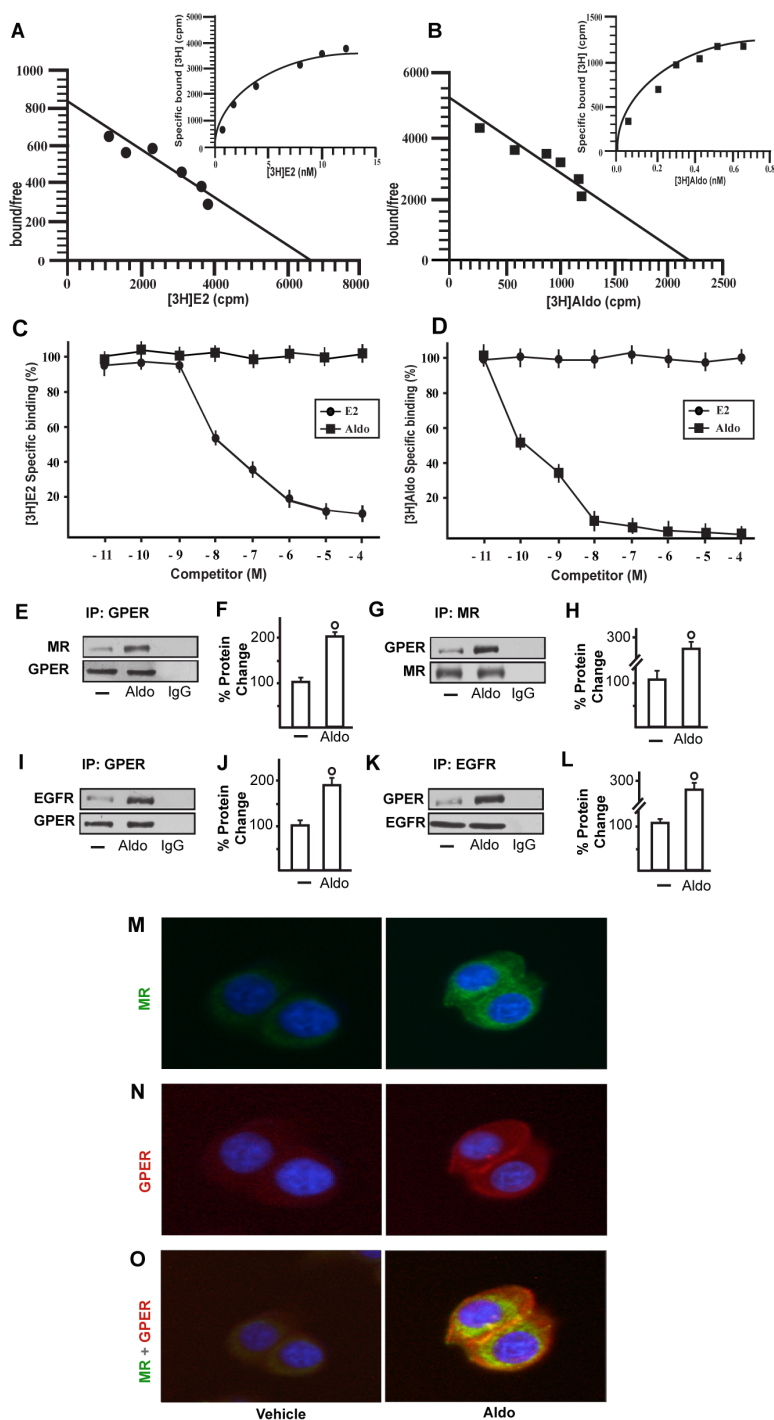
Figure 2: Representative saturation curve and Scatchard plot of [³H]17β-estradiol (E2) binding. A. and [³H]Aldosterone (Aldo) binding **B.** in SkBr3 cells. Each value represents the mean ± SEM of three determinations. Ligand binding assay in SkBr3 cells incubated with [³H]E2 and exposed to increasing concentrations of E2 and Aldo for 2 hours **C.**. Ligand binding assay in SkBr3 cells incubated with [³H]Aldo and exposed to increasing concentrations of E2 and Aldo for 2 hours **D.**. Competition curves are expressed as a percentage of maximum specific [³H]E2 or [³H]Aldo binding. Each data point represents the mean ± SEM of three independent experiments performed in triplicate. The co-immunoprecipitation of MR with GPER increases upon treatment with 10 pM Aldo for 15 min in SkBr3 cells **E.-H.** The blots were normalized to GPER or MR, respectively. The interaction between GPER and EGFR increases upon treatment with 10 pM Aldo for 15 min in SkBr3 cells **I.-L.** The blots were normalized to GPER or EGFR, respectively. In control samples, nonspecific IgG was used instead of the primary antibody, as indicated. Each data point represents the mean ± SD of three independent experiments. (○) indicates $p < 0.05$ for cells receiving vehicle (-) *versus* Aldo treatment. Localization of MR **M.** and GPER **N.** alone or in combination **O.**, as evaluated by immunofluorescence in SkBr3 cells treated with 10 pM Aldo for 15 min. Green signal: MR; Red signal: GPER; Blue signal: Nuclei. Images shown are representative of ten random fields from three independent experiments.

Figure 3: EGFR and ERK1/2 phosphorylation in SkBr3 cells. A., B. and B-TEC **D., E.** transfected for 24 h with shRNA or shGPER and then treated with 10 pM Aldo for 15 min. **C., F.** Efficacy of GPER silencing. EGFR and ERK1/2 activation in SkBr3 cells **G., H.** and B-TEC **I., J.** treated for 15 min with 10 pM Aldo alone and in combination with 10 µM EGFR inhibitor AG1478 (AG), 10 µM MEK inhibitor PD98059 (PD) and 100 nM GPER antagonist G15. The blots were normalized to EGFR or ERK2 and each data point represents the mean ± SD of three independent experiments. (○) and (●) indicate $p < 0.05$ for cells receiving vehicle (-) *versus* Aldo treatment.

Aldosterone/MR signalling stimulates the activity and expression of NHE-1, which has been involved in tumor cell migration, invasion and metastasis particularly in breast cancer [6-7, 45]. In this regard, we assessed that aldosterone prompts NHE-1 activity in both SkBr3 cells and B-TEC as evaluated by a fluorescent indicator of cytoplasmic pH changes (Figure 4A). In addition, aldosterone up-regulated NHE-1 at both the mRNA and protein levels as determined by real time PCR (Figure 4B) and immunofluorescence studies performed in SkBr3 cells and B-TEC (Figure 4C-4F). Next, the stimulatory effects induced by aldosterone on NHE-1 protein expression were abolished silencing MR (Figure 5) as well as GPER (Figure 6). Collectively, these findings suggest that NHE-1 regulation by aldosterone requires MR along with GPER.

Aldosterone induces biological responses through both MR and GPER

Functionally, we studied the role of MR and GPER in the proliferative effects of aldosterone in breast tumor cells as well as in the migration of tumor endothelial cells. Indeed, aldosterone triggered growth effects in SkBr3 cells, as assessed by cell counting (Figure 7A) and evidenced by time-lapse video microscopy (Videos 1-2). Cell proliferation stimulated by 10pM aldosterone was no longer evident silencing MR (Figure 7B-7C) or knocking-down GPER expression (Figure 7D-7E) and using the NHE-1 inhibitor cariporide (Figure 7F). Similar results were obtained using aldosterone concentrations up to 10 nM (data not shown). Furthermore, aldosterone promoted the migration of B-TEC as evidenced by time-lapse video microscopy (Videos 3-4) and scratch assay (Figure 8). The observed aldosterone-induced motility was abrogated silencing MR (Figure 8A, 8B, 8F) or GPER (Figure 8C-8D, 8G) and in the presence of cariporide (Figure 8E). Overall, these results indicate that the functional interaction between MR and GPER is involved in the aforementioned stimulatory action of aldosterone in both SkBr3 cells and B-TEC.

DISCUSSION

In the present study we provide novel evidence regarding the molecular mechanisms by which GPER may contribute to the biological responses induced by aldosterone in breast cancer cells and breast tumor-derived endothelial cells. In particular, we have demonstrated that aldosterone activates the EGFR/ERK transduction signalling through the classic MR and the involvement of GPER, as evidenced by gene silencing experiments and pharmacological inhibitors. In addition, we have shown that both MR and GPER mediate the aldosterone-induced up-regulation of Na$^+$/H$^+$ exchanger-1 (NHE-1), a well-known MR target involved in cancer progression

[7, 45]. We have also evidenced that aldosterone does not bind to GPER in accordance with previous studies [44], however it triggers the direct interaction between MR and GPER as well as GPER and EGFR. Interestingly, we have determined that both MR and GPER are required for the proliferation and migration of breast cancer cells and B-TEC mediated by NHE-1 upon aldosterone exposure.

Aldosterone elicits important biological effects in several physio-pathological conditions, spanning from electrolyte and fluid homeostasis to the regulation of fibrotic, inflammatory, proliferative and angiogenic responses in cardiovascular, metabolic diseases and cancer [12-13, 46-49]. As it concerns the breast tissue, it has been demonstrated that aldosterone potentiates prolactin stimulation of casein synthesis in pregnant rabbit mammary gland and contributes to mammary gland development and differentiation [50].

The actions exerted by aldosterone mainly occur through the binding to MR, a ligand-inducible transcription factor that belongs to the nuclear receptor superfamily [1]. The enzyme 11β-hydroxysteroid dehydrogenase type II (11βHSD2), which catalyzes the conversion of 11β-hydroxycorticosteroids like cortisol and corticosterone to the respective 11-keto metabolites namely cortisone and 11-dehydrocorticosterone, does allow the aldosterone binding to MR [51]. 11βHSD2 is mainly expressed in mineralcorticoid target tissues like kidney, colon, salivary glands and placenta [51]. In addition, immunohistochemical studies have detected in normal and malignant breast tissues high levels of 11β-HSD2 that co-localize with MR [52]. Previous studies have also evaluated the 11β-HSD2 activity in breast cancer cells, suggesting that this enzyme may play a regulatory role of aldosterone action in breast malignancy [53]. According to the classical model of MR signalling, the interaction between aldosterone and un-liganded receptor promotes the dissociation of the heat shock proteins from MR, which translocates into the nucleus [1]. Then, the aldosterone/MR complex binds to specific response elements located within the regulatory region of target genes, hence resulting in gene expression changes [1]. In addition, aldosterone induces rapid effects through alternate mechanisms including the activation of the EGFR/ERK transduction pathway, as demonstrated in different animal and cell models [3-4]. The existence of aldosterone receptors structurally unrelated to the classic MR paved also the way for analyzing the role of further mediators of the multifaceted action elicited by aldosterone [49].

GPER has been largely demonstrated to mediate estrogenic signalling in a wide number of physio-pathological conditions, including cancer [54-64]. GPER has been also involved in functional responses to aldosterone in various experimental contexts [37-40]. For instance, the ability of aldosterone in activating ERK1/2 in vascular smooth muscle cells and sensitizing
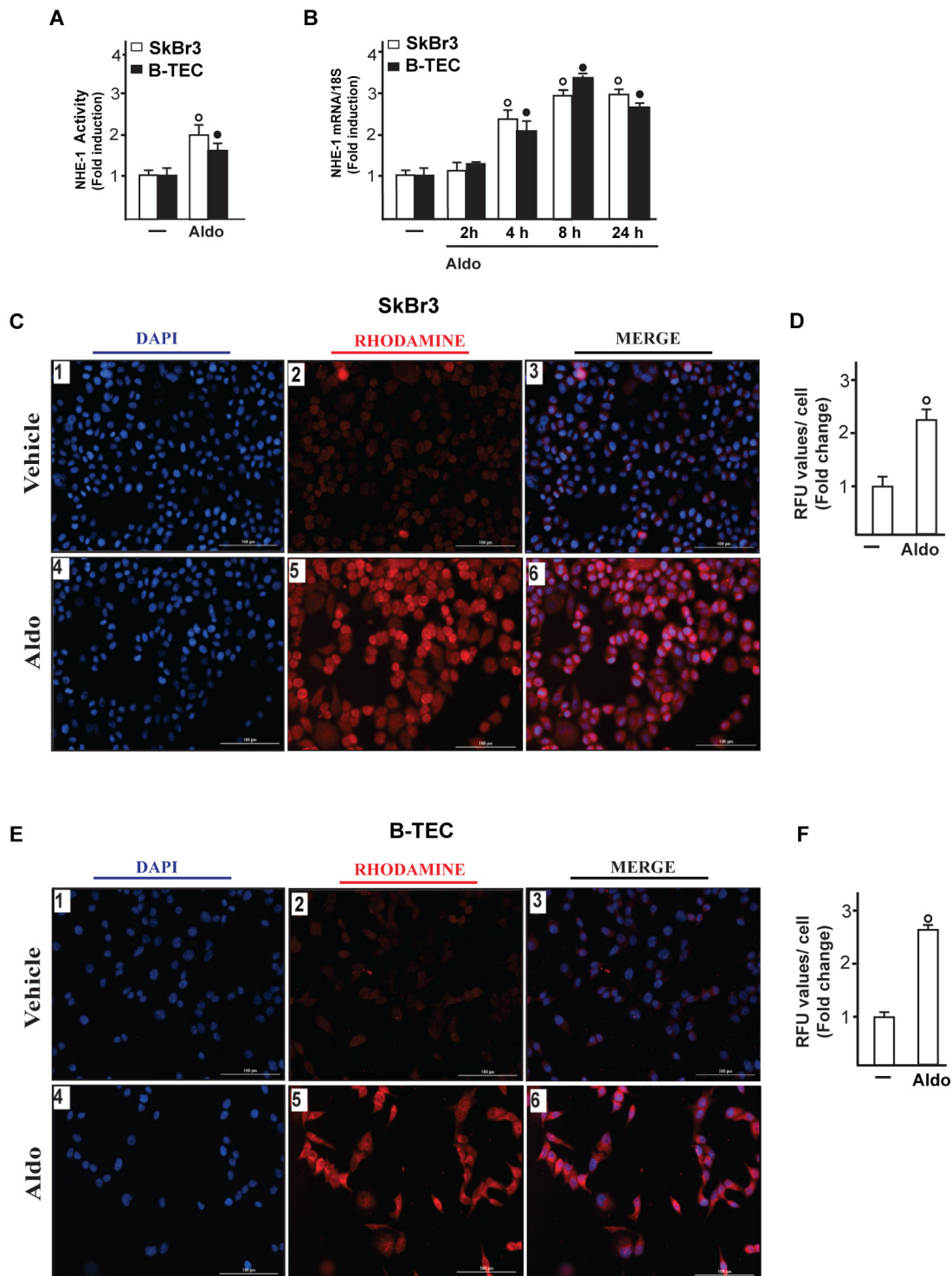
Figure 4: Na⁺/H⁺ Exchanger 1 (NHE-1) activity in SkBr3 cells and B-TEC treated with 10 pM Aldo, as evaluated by fluorescence intensity measurement. A. Each data point represents the mean ± SD of three independent experiments. mRNA expression of NHE-1 in SkBr3 cells and B-TEC treated with 10 pM Aldo, as evaluated by real-time PCR **B.**. Values are normalized to the 18S expression and shown as fold changes of the mRNA expression induced by Aldo respect to cells treated with vehicle (-). NHE-1 expression as evaluated by immunofluorescence in SkBr3 cells **C.** and B-TEC **E.** treated with ethanol as vehicle or 10 pM Aldo for 8 hours. NHE-1 accumulation is shown by the red signal, nuclei were stained by DAPI (blue signal). Images shown are representative of three independent experiments. **D.**, **F.** Fluorescence intensities for the red channel were quantified in 10 random fields for each condition and results are expressed as fold change of relative fluorescence units (RFU) over the vehicle-treated cells. (○) and (●) indicate $p < 0.05$ for cells receiving vehicle (-) *versus* Aldo treatment.
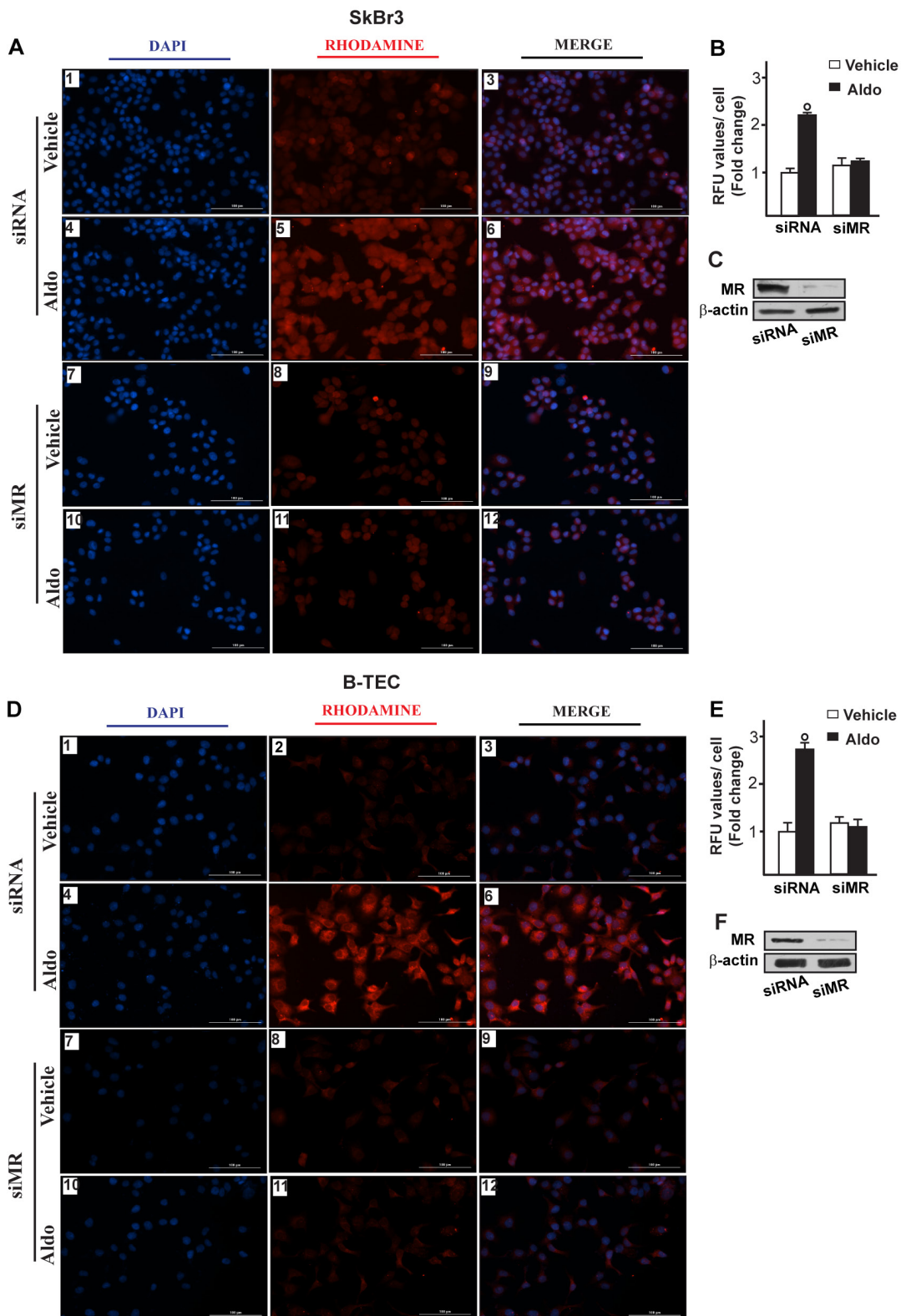
Figure 5: Na⁺/H⁺ Exchanger 1 (NHE-1) expression as evaluated by immunofluorescence in SkBr3 cells. A. and B-TEC **D.** transfected for 24 hours with siRNA (panels 1-6) or siMR (panels 7-12) and then treated with ethanol as vehicle or 10 pM Aldosterone (Aldo) for 8 hours. NHE-1 accumulation is shown by the red signal, nuclei were stained by DAPI (blue signal). Images shown are representative of three independent experiments. **B.**, **E.** Fluorescence intensities for the red channel were quantified in 10 random fields for each condition and results are expressed as fold change of relative fluorescence units (RFU) over the vehicle-treated cells. **C.**, **F.** Efficacy of MR silencing. (○) indicates $p < 0.05$ for cells receiving vehicle *versus* Aldo treatment.
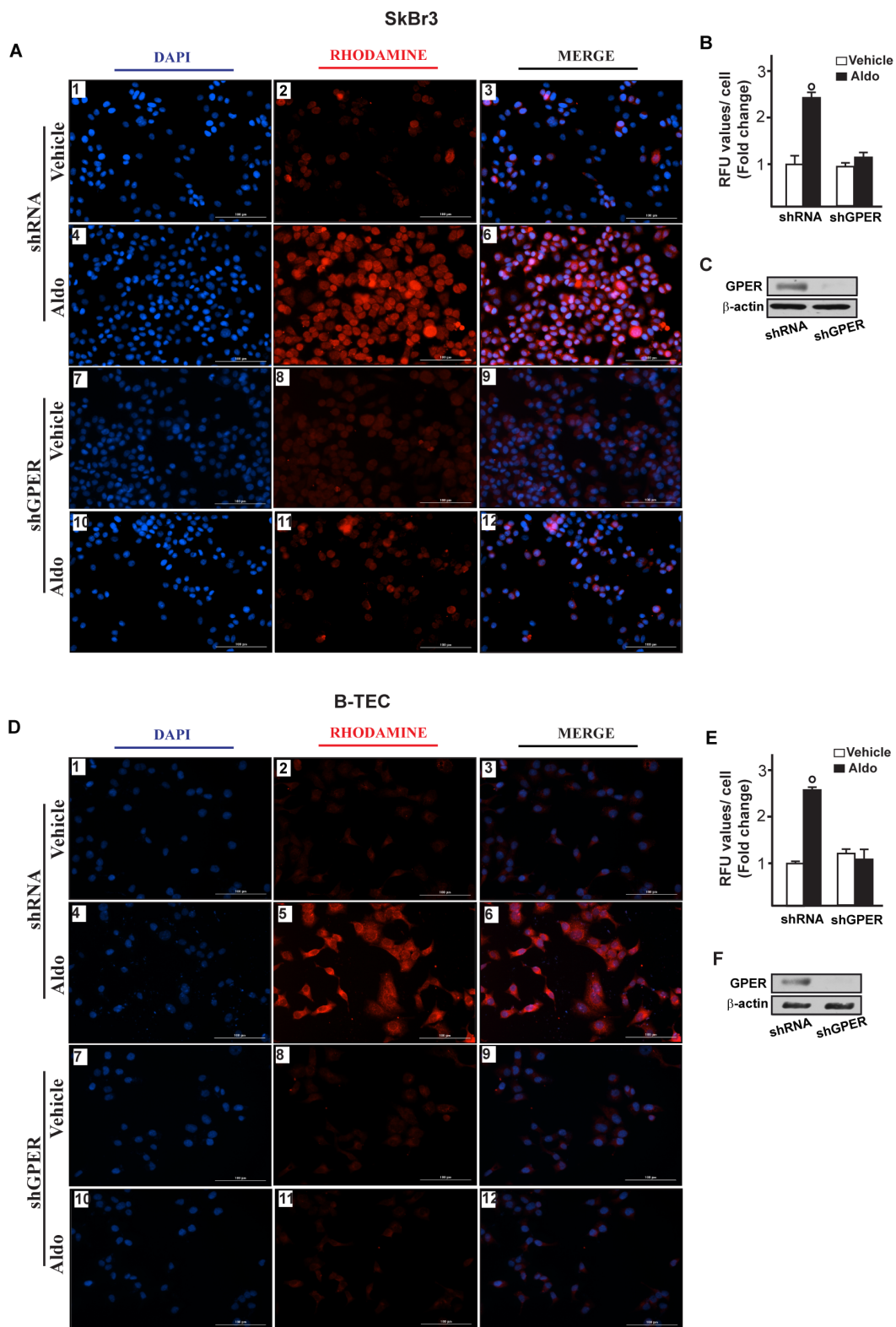
Figure 6: Na$^+$/H$^+$ Exchanger 1 (NHE-1) expression as evaluated by immunofluorescence in SkBr3 cells. A. and B-TEC **D.** transfected for 24 hours with shRNA (panels 1-6) or shGPER (panels 7-12) and then treated with ethanol as vehicle or 10 pM aldosterone (Aldo) for 8 hours. NHE-1 accumulation is shown by the red signal, nuclei were stained by DAPI (blue signal). Images shown are representative of three independent experiments. **B.**, **E.** Fluorescence intensities for the red channel were quantified in 10 random fields for each condition and results are expressed as fold change of relative fluorescence units (RFU) over the vehicle-treated cells. **C.**, **F.** Efficacy of GPER silencing. (○) indicates $p < 0.05$ for cells receiving vehicle (-) *versus* Aldo treatment.

the connecting tubule glomerular feedback in afferent arterioles was prevented using both MR and GPER blockers [38-40]. Other studies evidenced that the increase of cardiac vagal tone observed upon aldosterone treatment is abolished in the presence of the GPER antagonist G36 but not using the MR antagonists spironolactone and eplerenone [39]. In rat aortic endothelial cells devoid of MR, the biological effects triggered by aldosterone were mimicked by the GPER agonist G-1 and prevented using pharmacological inhibitors of GPER as well as knocking down its expression [38]. The aforementioned observations suggest that GPER is involved in the effects exerted by aldosterone either through MR or acting as an alternate aldosterone receptor. However, it should be pointed out that diverse controversies argue against the last conclusion, as pharmacologic criteria for GPER to be considered as an aldosterone-responsive receptor are not still adequately fulfilled [41-43]. Indeed, binding studies performed in HEK cells overexpressing GPER (HEK-GPER-1) showed that aldosterone and the MR antagonists, spironolactone and eplerenone, do not compete for specific [³H]E2 binding to membrane of HEK-GPER-1 cells [44].
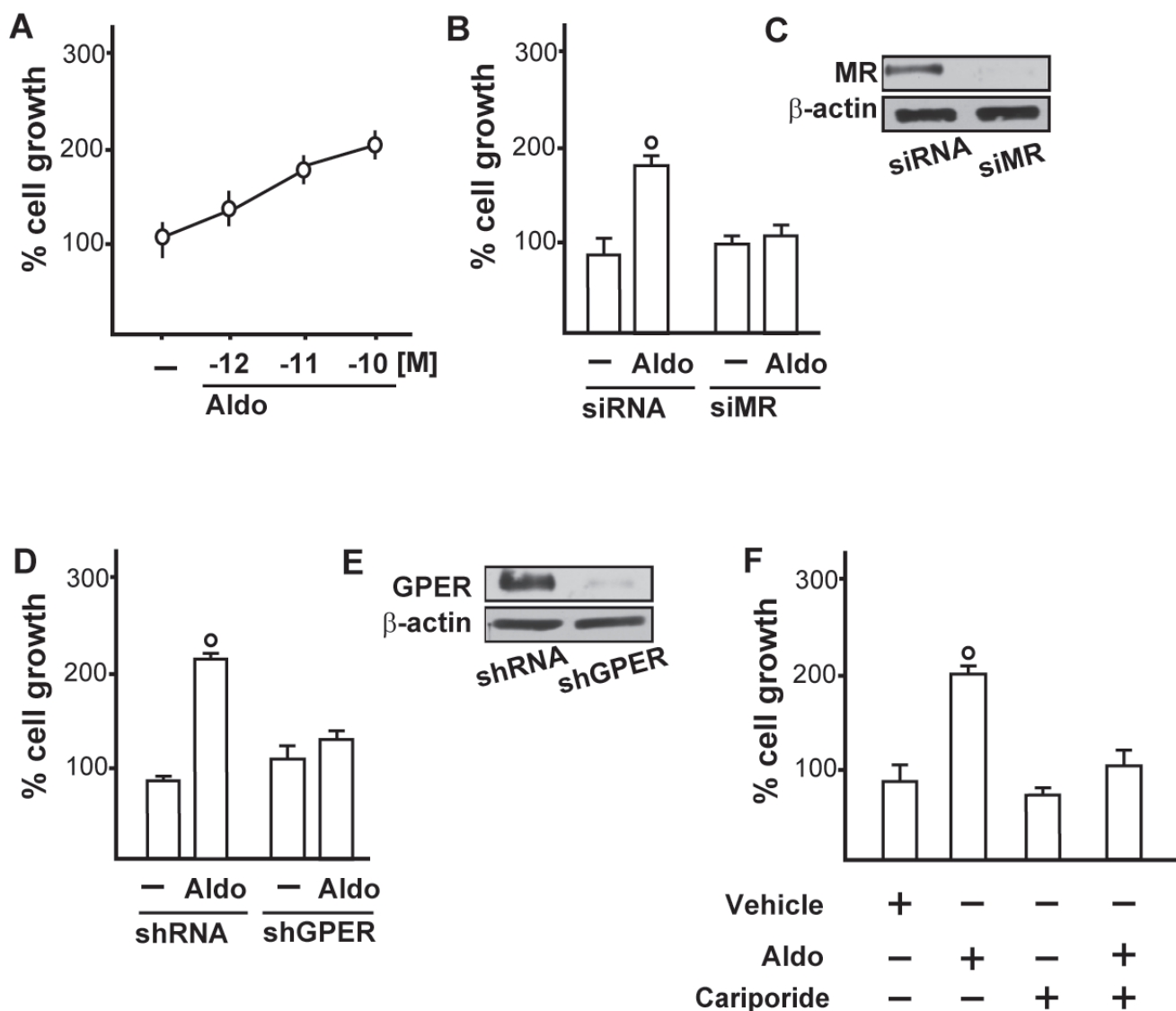
Figure 7: A. SkBr3 cell proliferation upon treatment for 5 days with increasing concentrations of Aldosterone (Aldo). Proliferation of SkBr3 cells transfected with siMR **B.**, **C.** and shGPER **D.**, **E.** and treated for 5 days with 10 pM Aldo. SkBr3 cell proliferation stimulated by 10 pM Aldo in the presence of 50 μM Na$^+$/H$^+$ Exchanger 1 (NHE-1) inhibitor named cariporide **F.**. Values shown are mean ± SD of three independent experiments performed in triplicate. (○) indicates $p < 0.05$ for cells receiving vehicle (-) *versus* Aldo treatment.

In accordance with these findings, in the present study aldosterone failed to bind to GPER in competition assays based on experimental approaches used in previous investigations in order to characterize the binding properties of GPER ligands [28, 31-32, 34-36]. Worthy, we found that aldosterone stimulates the interaction of GPER with MR and EGFR, thus suggesting a further mechanism through which ligand-activated MR triggers EGFR signalling [49, 65-67]. Nicely supporting the functional cross-talk between MR and GPER, we ascertained that both receptors are required for the aldosterone-induced expression of NHE-1 which is considered as a molecular sensor of MR activation [45]. In this respect, our data are reminiscing of previous findings showing that EGFR and GPER cooperate toward the regulation of NHE-1 function upon aldosterone treatment [40, 66]. Importantly, we found that the stimulatory effects elicited by aldosterone on the proliferation and migration of breast cancer cells and breast tumor-derived endothelial cells are mediated by NHE-1 and involve both GPER and MR. Hence, the current results further extend the well-known action played by NHE-1 toward negative biological features, in particular in breast cancer [7, 68]. In this regard, it is worth mentioning that in tumor metabolic microenvironment
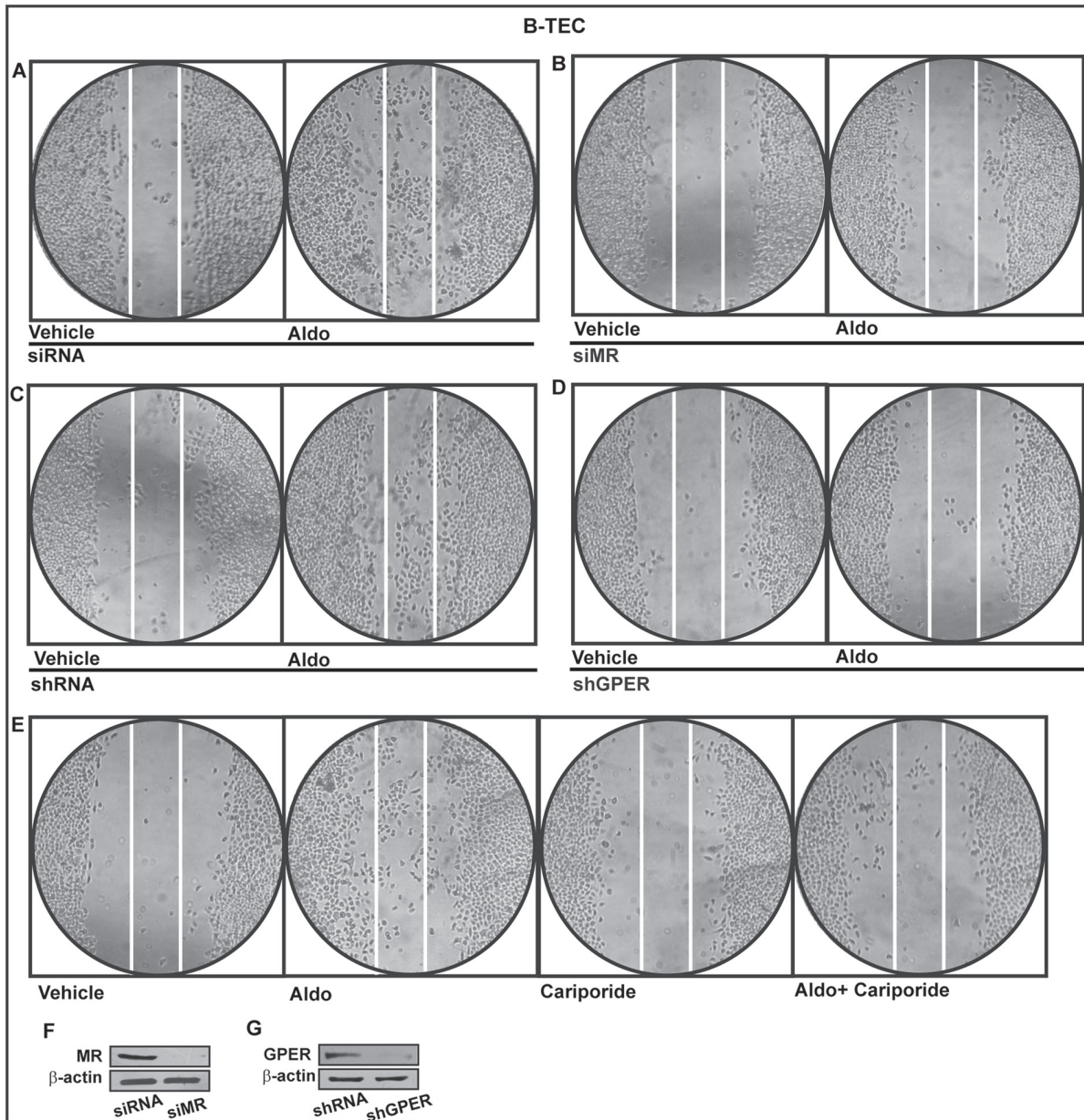
Figure 8: Cell migration in B-TEC transfected for 24 h with siRNA. A., siMR **B.**, shRNA **C.** or shGPER **D.** and then treated for 48 hours with ethanol as vehicle or 10 pM Aldosterone (Aldo). **E.** Cell migration stimulated by 10 pM Aldo in B-TEC in the presence of 50 μM Na+/H+ Exchanger 1 (NHE-1) inhibitor cariporide. **F.**, **G.** Efficacy of MR and GPER silencing. Data are representative of three independent experiments performed in triplicate.

characterized by hypoxic-acidic milieu [69], the dysregulation of pH homeostasis mediated by NHE-1 may actually contribute to key steps in tumor progression like increased cell proliferation, loss of cell-cell contact and detachment from the extracellular matrix [68]. In breast cancer cells and breast cancer associated fibroblasts exposed to hypoxia, we have previously assessed that GPER cooperates with hypoxia inducible factor-1 (HIF-1) toward the regulation of vascular endothelial growth factor (VEGF) and tumor angiogenesis [70-73]. Hence, the present findings suggest further mechanisms through which GPER may play a role in the complex adaptive responses to hypoxic-acidic tumor microenvironment. Additionally, our results indicate that GPER contributes to the effects mediated by aldosterone/MR signalling, as evidenced by other ligand-activated steroid receptors [74-75].

Collectively, our findings provide novel insights into the controversial mechanisms through which GPER contributes to aldosterone-mediated signalling. On the basis of our data showing that the functional interaction between MR and GPER triggers certain stimulatory effects exerted by aldosterone, GPER may be considered as a further target within the intricate transduction network activated by aldosterone in particular in breast cancer.

MATERIALS AND METHODS

Reagents

Aldosterone (Aldo), 17β-estradiol (E2) and Cariporide were purchased from Sigma Aldrich (Milan, Italy). G15 ((3aS,4R,9bR)-4-(6-bromo-1,3-benzodioxol-5-yl)-3a,4,5,9b-3H-cyclopenta[c]quinolone) was obtained from Tocris Bioscience (distributed by Space, Milan, Italy). Tyrphostin AG1478 (AG) was purchased from DBA (Milan, Itay). PD98059 (PD) was obtained from Calbiochem (DBA, Milan, Italy). All compounds were dissolved in dimethyl sulfoxide (DMSO) except Aldosterone and E2 which were solubilized in ethanol.

Cell cultures

SkBr3 breast cancer cells were maintained in RPMI-1640 without phenol red, supplemented with 10% fetal bovine serum (FBS) and 100 μg/ml penicillin/streptomycin (Life Technologies, Milan, Italy). Breast tumor-derived endothelial cells (B-TEC) were obtained from human breast carcinomas and characterized as previously described [76]. B-TEC showed constant expression of endothelial markers and increased angiogenic properties, migration and drug resistance in respect to normal microendothelial cells [76-78]. Briefly, specimens were finely minced with scissors and

then digested by incubation for 1 h at 37˚C in DMEM containing collagenase IV (Sigma Aldrich, Milan, Italy). After washings in medium plus 10% FCS (Life Technologies, Milan, Italy), the cell suspension was forced through a graded series of meshes to separate the cell components from stroma and aggregates. Endothelial cells were isolated from cells suspension using anti-CD105 Ab coupled to magnetic beads, by magnetic cell-sorting using the MACS system (Miltenyi Biotech, Auburn, CA). B-TEC were seeded on collagen-coated flasks (Sigma-Aldrich Srl, Milan, Italy) and cultured in Endothelial Growth Medium (EGM) (Lonza, Milan, Italy), supplemented with 5% FBS (Lonza, Milan, Italy). MCF-7 breast cancer cells were maintained in DMEM F12 supplemented with 10% FBS and 100 μg/mL penicillin/streptomycin (Life Technologies, Milan, Italy). All cell lines were grown in a 37° C HeraCell incubator (ThermoScientific-Heraeus, Milan, Italy) with 5% CO_2. Cells were switched to medium without serum the day before experiments.

Saturation curve and scatchard plot analysis

SkBr3 cells were grown in 10-cm cell culture dishes and incubated with increasing concentrations of [2, 4, 6, 7-3H] E2 (89 Ci/mmol; GE Healthcare) or [1, 2, 6, 7-3H] Aldosterone (85 Ci/mmol; Perkinelmer). Cells were then washed with ice-cold phosphate-buffered saline (PBS); after 100% ethanol extraction of cells, radioactivity was measured by liquid scintillation counting. The plot of the bound radioactivity (cpm) *versus* the concentration of the radiotracer (nM) was fitted to the saturation binding curve using Prism GraphPad program (GraphPad Software, San Diego, CA), which was used to calculate the binding dissociation constant (Kd) and binding capacity (Bmax).

Ligand binding assay

SkBr3 cells were grown in 10-cm cell culture dishes and incubated with 4 nM [2, 4, 6, 7-3H] E2 (89 Ci/mmol; GE Healthcare) or 100 pM [1, 2, 6, 7-3H] Aldosterone (85 Ci/mmol; Perkinelmer) in the presence or absence of increasing concentrations of nonlabeled E2 or aldosterone for 2 hours at 37°C. Cells were then washed with ice-cold PBS; after 100% ethanol extraction of cells, radioactivity was measured by liquid scintillation counting. The displacement of [3H]E2 or [3H]Aldo binding by the competitors was expressed as a percentage of the maximum specific binding of E2 or Aldo.

Na^+/H^+ Exchanger 1 (NHE-1) activity assay

SkBr3 cells and B-TEC were grown in 10-cm cell culture dishes and then shifted for 24h to medium

lacking serum. Then, 4×10^7 cells/ml were suspended in HEPES buffer solution 1M (Sigma Aldrich, Milan, Italy) and incubated with a membrane-permeable fluorescent indicator for the measurement of cytoplasmic pH namely SPIRO(ISOBENZOFURAN-1(3H),9'-(9H)XANTHENE)-2',7'-DIPROPANOIC ACID (BCECF-AM) (0,3μM) (Santa Cruz Biotechnology, Milan, Italy) for 30 min at 37°C. Then, cells were washed with HEPES buffer saline and a cell suspension of 3×10^6 cells/ml was prepared. Fluorescence ratio from the dye was measured using an FLX-800 micro plate fluorimeter (Bio-Tek Instruments, Inc., Winooski, VT, USA).

Gene expression studies

Total RNA was extracted from cell cultures using the TRIzol commercial kit (Life Technologies, Milan, Italy) according to the manufacturer's protocol. RNA was quantified spectrophotometrically and quality was checked by electrophoresis through agarose gels stained with ethidium bromide. Only samples that were not degraded and showed clear 18 S and 28 S bands under UV light were used for RT-PCR. Total cDNA was synthesized from the RNA by reverse transcription using the murine leukemia virus reverse transcriptase (Life Technologies, Milan, Italy), following the protocol provided by the manufacturer. The expression of selected genes was quantified by real-time PCR using Step One (TM) sequence detection system (Applied Biosystems Inc, Milan, Italy), following the manufacturer's instructions. Gene-specific primers were designed using Primer Express version 2.0 software (Applied Biosystems. Inc., Milan, Italy) and are as follows: GPER Fwd: 5'-ACACACCTGGGTGGACACAA-3' and Rev: 5'-GGAGCCAGAAGCCACATCTG-3'; MR Fwd: 5'-GCTTTGATGGTAACTGTGAAGG-3' and Rev: 5'- TGTGTTGCCCTTCCACTGCT-3'; ERα Fwd: 5'-AGAGGGCATGGTGGAGATCTT-3' and Rev: 5'-CAAACTCCTCTCCCTGCAGATT-3'; NHE-1 Fwd: 5':- AAGGACCAGTTCATCATCGC-3' and Rev:5'- TTCTTCACAGCCAACAGGTC-3'; 18S Fwd: 5'-GGCGTCCCCCAACTTCTTA-3 and Rev: 5'-GGGCATCACAGACCTGTTATT-3'. Assays were performed in triplicate and the RNA expression values were normalized using 18S expression and then calculated as fold induction.

Gene silencing experiments

For the silencing of GPER expression, cells were plated onto 10-cm dishes and transfected using X-treme GENE 9 DNA Transfection Reagent (Roche Diagnostics, Milan, Italy) for 24 hours with two shRNA and two different shGPER. The silencing of GPER expression was obtained by using constructs which we have previously described and used [79]. For knocking down MR expression, cells were seeded in six-well multidishes and transiently transfected the consecutive day at 50% confluence. For transfection, X-treme GENE 9 DNA Transfection Reagent (Roche Diagnostics, Milan, Italy) was mixed with two small interfering RNAs (siRNA) specific for silencing MR or two siRNA controls (Origene, distributed by Tema Ricerca, Milan, Italy) for 24 hours, prior to treatments.

Western blot analysis

SkBr3 cells and B-TEC were processed according to a previously described protocol [80-81] to obtain protein lysate that was electrophoresed through a reducing SDS/10% (w/v) polyacrylamide gel, electroblotted onto a nitrocellulose membrane and probed with primary antibodies against MR (PA1594) (Boster Immunoleader, distributed by Tema Ricerca, Milan, Italy), phosphorylated ERK 1/2 (E-4), ERK2 (C-14), EGFR (1005), pEGFR^{Tyr} ^{1173} (sc-12351-R), GPER (N15), ERα (F10) and β-actin (C2), all purchased from DBA (Milan, Italy). Proteins were detected by horseradish peroxidase-linked secondary antibodies (DBA, Milan, Italy) and revealed using the ECL System (GE Healthcare). Precision Plus Protein™ Dual Color Standard (Bio-Rad Laboratories, Milan, Italy) was used to estimate molecular weights and then antigen specificity.

Coimmunoprecipitation

After stimulation with 10 pM Aldo, SkBr3 breast cancer cells were washed with PBS and lysed using 500 μl RIPA buffer with a mixture of protease inhibitors containing 1.7 mg/ml aprotinin, 1mg/ml leupeptin, 200 mmol/liter phenylmethylsulfonyl fluoride, 200 mmol/liter sodium orthovanadate, and 100 mmol/liter sodium fluoride. Samples were then centrifuged at 13,000 rpm for 10 min, and protein concentrations were determined using Bradford reagent. Protein (250 μg) was then incubated for 2 hours with 900 μl of immunoprecipitation buffer with inhibitors, 2 μg of GPER, MR or EGFR antibody and 20 μl of Protein A/G agarose immunoprecipitation reagent (DBA, Milan, Italy). Samples were then centrifuged at 13,000 rpm for 5 min at 4° C to pellet beads. Pellets were washed four times with 500 μl of PBS and centrifuged at 13,000 rpm for 5 min at 4° C. Supernatants were collected, resuspended in 20 μl RIPA buffer with protease inhibitors, 2X SDS sample buffer (40 mM Tris-HCl; 4% glycerol; 2% SDS) and β-mercaptoethanol and heated to 95° C for 5 min. Samples were then run on 10% SDS-PAGE, transferred to nitrocellulose, and probed with rabbit anti-GPER, rabbit anti-MR or rabbit anti-EGFR antibody. Western blot analysis and ECL detection were performed as described above.

Immunofluorescence and colocalization studies

50 % confluent cultured SkBr3 cells and B-TEC grown on coverslips were serum deprived and then treated for 8 hours with 10 pM Aldo, as indicated. Where required, cells previously transfected for 24 hours with shGPER or siMR and respective control (as described above) and then treated for 8 hours with 10 pM Aldo. Then cells were fixed in 4% paraformaldehyde, permeabilized with 0.2% Triton X-100, washed three times with PBS and incubated overnight with a goat primary antibody against NHE-1 (C20) (DBA, Milan, Italy). After incubation, the slides were extensively washed with PBS and incubated with 4′,6-diamidino-2-phenylindole dihydrochloride (DAPI), (1:1000), (Sigma-Aldrich, Milan, Italy) and donkey anti-goat IgG-Rhodamine (1:100; purchased from DBA, Milan, Italy). The slides were imaged on the Cytation 3 Cell Imaging Multimode reader (BioTek, Winooski, VT) and analysed using the software Gen5 (BioTek, Winooski, VT).

For colocalization studies SkBr3 cells seeded on chamber slides were serum deprived for 24 hours and then treated for 15 min with 10 pM Aldo. Next, cells were fixed, permeabilized and incubated overnight with anti-rabbit GPER (N15) and anti-mouse MR (H10E4C9F) antibodies (DBA, Milan, Italy) alone and in combination. Slides were then incubated with secondary antibodies (donkey anti-rabbit IgG-Rhodamine, DBA, Milan, Italy) and donkey anti-mouse IgG-Fitch (Alexa Fluor, Life Technologies, Milan, Italy), stained by DAPI and then imaged on the Cytation 3 Cell Imaging Multimode reader (BioTek, Winooski, VT).

Proliferation assay

For quantitative proliferation assay, SkBr3 cells (1×10^5) were seeded in 24-well plates in regular growth medium. Cells were washed once they had attached and then incubated in medium containing 2.5% charcoal-stripped FBS, transfected for 24 hours, and then treated, as indicated, with transfection and treatments renewed every 2 days. Cells were counted on day 5 using the Countess Automated Cell Counter, as recommended by the manufacturer's protocol (Life Technologies, Milan, Italy).

Migration assay

Twelve-well plates were coated with 500 μL fibronectin for 2 hours at 37°C (Sigma Aldrich, Milan, Italy). B-TEC were allowed to grow in regular growth medium until they reached a 70% to 80% confluence. Next, cells were incubated in medium containing 2.5% charcoal-stripped FBS and transfected for 24 hours, as indicated. To create a scratch of the cell monolayer, a p200 pipette tip was used. Cells were then washed twice with PBS and treated. The migration assay was evaluated after 48 hours of treatment.

Time-lapse microscopy

SkBr3 cells and B-TEC (1×10^5) were seeded in 24-well plates in regular growth medium until they reached a 70% to 80% confluence. The culture wells were then incubated in medium containing 2.5% charcoal-stripped FBS, treated and transferred into a time-lapse microscopy platform, equipped with a heated stage chamber (Cytation™3 Cell Imaging Multi-Mode Reader, Biotek, Winooski, VT). Cells were maintained at routine incubation settings (37 °C, 5% CO_2) using temperature and gas controllers. To evaluate cell proliferation and motility, the images were recorded using Cytation 3 Cell Imaging Multimode Reader and the software Gen5 (BioTek, Winooski, VT) in 10 min intervals for 24 hours (cell proliferation) and 10 hours (cell motility). Then, the images were processed as a movie using the software Adobe Creative Cloud Premier Pro CC. Frames collected every 10 minutes are displayed at a rate of 10 frames s-[1].

Statistical analysis

Statistical analysis was performed using ANOVA followed by Newman-Keuls' testing to determine differences in means. $p < 0.05$ was considered as statistically significant.

COMPETING INTERESTS

The authors declare that they have no competing interests.

REFERENCES

1. Arriza JL, Weinberger C, Cerelli G, Glaser TM, Handelin BL, Housman DE, Evans RM. Cloning of human mineralocorticoid receptor complementary DNA: structural and functional kinship with the glucocorticoid receptor. Science. 1987; 237: 268-275.

2. Meinel S, Gekle M, Grossmann C. Mineralocorticoid receptor signaling: crosstalk with membrane receptors and other modulators. Steroids. 2014; 91: 3-10.

3. Williams JS. Evolving research in nongenomic actions of aldosterone. Curr Opin Endocrinol Diabetes Obes. 2013; 20: 198-203.

4. Krug AW, Grossmann C, Schuster C, Freudinger R, Mildenberger S, Govindan MV, Gekle M. Aldosterone stimulates epidermal growth factor receptor expression. J Biol Chem. 2003; 278: 43060-43066.

5. Paul M, Poyan Mehr A, Kreutz R. Physiology of local renin-angiotensin systems. Physiol Rev. 2006; 86: 747-803.

6. De Giusti VC, Orlowski A, Ciancio MC, Espejo MS, Gonano LA, Caldiz CI, Vila Petroff MG, Villa-Abrille MC, Aiello EA. Aldosterone stimulates the cardiac sodium/bicarbonate cotransporter via activation of the g protein-coupled receptor gpr30. J Mol Cell Cardiol. 2015; [Epub ahead of print] PMID: 26497404.

7. Amith SR, Fliegel L. Regulation of the Na+/H+ Exchanger (NHE-1) in Breast Cancer Metastasis. Cancer Res. 2013; 73: 1259-1264.

8. Luther JM, Brown NJ. The renin-angiotensin-aldosterone system and glucose homeostasis. Trends Phamacol Sci. 2011; 32: 734-739.

9. Briet M, Schiffrin EL. Vascular actions of aldosterone. J Vasc Res. 2013; 50: 89-99.

10. Calvier L, Miana M, Reboul P, Cachofeiro V, Martinez-Martinez E, de Boer RA, Poirier F, Lacolley P, Zannad F, Rossignol P, López-Andrés N. Galectin-3 mediates aldosterone-induced vascular fibrosis. Arterioscler Thromn Vasc Biol. 2013; 33: 67-75.

11. Bienvenu LA1, Morgan J, Rickard AJ, Tesch GH, Cranston GA, Fletcher EK, Delbridge LM, Young MJ. Macrophage mineralocorticoid receptor signaling plays a key role in aldosterone-independent cardiac fibrosis. Endocrinology. 2012; 153: 3416-3425.

12. King S, Bray S, Galbraith S, Christie L, Fleming S. Evidence for aldosterone-dependent growth of renal cell carcinoma. Int J Exp Pathol. 2014; 95: 244-250.

13. Kaji K, Yoshiji H, Kitade M, Ikenaka Y, Noguchi R, Shirai Y, Yoshii J, Yanase K, Namisaki T, Yamazaki M, Tsujimoto T, Kawaratani H, Fukui H. Selective aldosterone blocker, eplerenone, attenuates hepatocellular carcinoma growth and angiogenesis in mice. Hepatol Res. 2010; 40: 540-549.

14. Maggiolini M, Picard D. The unfolding stories of GPR30, a new membrane-bound estrogen receptor. J Endocrinol. 2010; 204: 105-114.

15. Prossnitz ER, Barton M. The G-protein-coupled estrogen receptor GPER in health and disease. Nat Rev Endocrinol. 2011; 7: 715-726.

16. Barton M. Position paper: The membrane estrogen receptor GPER—Clues and questions. Steroids. 2012; 77: 935-942.

17. Filardo EJ, Thomas P. Minireview: G protein-coupled estrogen receptor-1, GPER-1: its mechanism of action and role in female reproductive cancer, renal and vascular physiology. Endocrinology. 2012; 153: 2953-2962.

18. Meyer MR, Prossnitz ER, Barton M. The G protein-coupled estrogen receptor GPER/GPR30 as a regulator of cardiovascular function. Vascul Pharmacol. 2011; 55: 17-25.

19. Lindsey SH, Chappell MC. Evidence that the G protein-coupled membrane receptor GPR30 contributes to the cardiovascular actions of estrogen. Gend Med. 2011; 8: 343-354.

20. Prossnitz ER, Maggiolini M. Mechanisms of estrogen signaling and gene expression via GPR30. Molecular and Cellular Endocrinology. 2009; 308: 32-38.

21. Filardo EJ, Quinn JA, Bland KI, Frackelton AR Jr. Estrogen-induced activation of Erk-1 and Erk-2 requires the G protein-coupled receptor homolog, GPR30, and occurs via trans-activation of the epidermal growth factor receptor through release of HB-EGF. Mol Endocrinol. 2000; 14: 1649-1660.

22. Revankar CM, Cimino DF, Sklar LA, Arterburn JB, Prossnitz ER. A transmembrane intracellular estrogen receptor mediates rapid cell signaling. Science. 2005; 307: 1625-1630.

23. Pandey DP, Lappano R, Albanito L, Madeo A, Maggiolini M, Picard D. Estrogenic GPR30 signalling induces proliferation and migration of breast cancer cells through CTGF. EMBO J. 2009; 28: 523-532.

24. Santolla MF, Lappano R, De Marco P, Pupo M, Vivacqua A, Sisci D, Abonante S, Iacopetta D, Cappello AR, Dolce V, Maggiolini M. G protein-coupled estrogen receptor mediates the up-regulation of fatty acid synthase induced by 17β-estradiol in cancer cells and cancer-associated fibroblasts. J Biol Chem. 2012; 287: 43234-43245.

25. Vivacqua A, De Marco P, Santolla MF, Cirillo F, Pellegrino M, Panno ML, Abonante S, Maggiolini M. Estrogenic gper signalling regulates mir144 expression in cancer cells and cancer-associated fibroblasts (cafs). Oncotarget. 2015; 6: 16573-16587. Doi: 10.18632/oncotarget.4117.

26. Lappano R, Pisano A, Maggiolini M. GPER Function in Breast Cancer: An Overview. Front Endocrinol (Lausanne). 2014; 5:66.

27. Santolla MF, Avino S, Pellegrino M, De Francesco EM, De Marco P, Lappano R, Vivacqua A, Cirillo F, Rigiracciolo DC, Scarpelli A, Abonante S, Maggiolini M. SIRT1 is involved in oncogenic signaling mediated by GPER in breast cancer. Cell Death and Disease. 2015; 6:e1834.

28. Santolla MF, De Francesco EM, Lappano R, Rosano C, Abonante S, Maggiolini M. Niacin activates the G protein estrogen receptor (GPER)-mediated signalling. Cell Signal. 2014; 26: 1466-1475.

29. Lappano R, Rosano C, De Marco P, De Francesco EM, Pezzi V, Maggiolini M. Estriol acts as a GPR30 antagonist in estrogen receptor-negative breast cancer cells. Mol Cell Endocrinol. 2010; 320: 162-170.

30. Pupo M, Pisano A, Lappano R, Santolla MF, De Francesco EM, Abonante S, Rosano C, Maggiolini M. Bisphenol A induces gene expression changes and proliferative effects through GPER in breast cancer cells and cancer-associated fibroblasts. Environ Health Perspect. 2012; 120: 1177-1182.

31. Lappano R, Santolla MF, Pupo M, Sinicropi MS, Caruso A, Rosano C, Maggiolini M. MIBE acts as antagonist ligand of both estrogen receptor α and GPER in breast cancer cells. Breast Cancer Res. 2012; 14:R12.

32. Maggiolini M, Santolla MF, Avino S, Aiello F, Rosano C, Garofalo A, Grande F. Identification of two benzopyrroloxazines acting as selective GPER antagonists in breast cancer cells and cancer-associated fibroblasts. Future Med Chem. 2015; 7: 437-448.

33. Sinicropi MS, Lappano R, Caruso A, Santolla MF, Pisano A, Rosano C, Capasso A, Panno A, Lancelot JC, Rault S, Saturnino C, Maggiolini M. (6-bromo-1,4-dimethyl-9H-carbazol-3-yl-methylene)-hydrazine (carbhydraz) acts as a GPER agonist in breast cancer cells. Curr Top Med Chem. 2015; 15: 1035-1042.

34. Lappano R, Rosano C, Pisano A, Santolla MF, De Francesco EM, De Marco P, Dolce V, Ponassi M, Felli L, Cafeo G, Kohnke FH, Abonante S, Maggiolini M. A calixpyrrole derivative acts as a GPER antagonist: mechanisms and models. Dis Model Mech. 2015; 8: 1237-1246.

35. Albanito L, Lappano R, Madeo A, Chimento A, Prossnitz ER, Cappello AR, Dolce V, Abonante S, Pezzi V, Maggiolini M. Effects of Atrazine on Estrogen Receptor α- and G Protein-Coupled Receptor 30-Mediated Signalling and Proliferation in Cancer Cells and Cancer-Associated Fibroblasts. Environ Health Perspect. 2015; 123: 493-499.

36. Lappano R, Rosano C, Santolla MF, Pupo M, De Francesco EM, De Marco P, Ponassi M, Spallarossa A, Ranise A, Maggiolini M. Two novel GPER agonists induce gene expression changes and growth effects in cancer cells. Curr Cancer Drug Targets. 2012; 12: 531-542.

37. Funder JW. GPR30, mineralocorticoid receptors, and the rapid vascular effects of aldosterone. Hypertension. 2011; 57: 370-372.

38. Gros R, Ding Q, Liu B, Chorazyczewski J, Feldman RD. Aldosterone mediates its rapid effects in vascular endothelial cells through GPER activation. Am J Physiol Cell Physiol. 2013; 304: C532-540.

39. Brailoiu GC, Benamar K, Arterburn JB, Gao E, Rabinowitz JE, Koch WJ, Brailoiu E. Aldosterone increases cardiac vagal tone via G protein-coupled oestrogen receptor activation. J Physiol. 2013; 591: 4223-4235.

40. Ren Y, D'Ambrosio MA, Garvin JL, Leung P, Kutskill K, Wang H, Peterson EL, Carretero OA. Aldosterone sensitizes connecting tubule glomerular feedback via the aldosterone receptor GPR30. Am J Physiol Renal Physiol. 2014; 307: F427-434.

41. Wendler A, Wehling M. Is GPR30 the membrane aldosterone receptor postulated 20 years ago? Hypertension. 2011; 57:e16.

42. Barton M, Meyer MR. Nicolaus Copernicus and the rapid vascular responses to aldosterone. Trends Endocrinol Metab. 2015; 26: 396-398.

43. Feldman RD, Limbird LE. Copernicus Revisited: Overturning Ptolemy's View of the GPER Universe. Trends Endocrinol Metab. 2015; 26: 592-594.

44. Cheng SB, Dong J, Pang Y, LaRocca J, Hixon M, Thomas P, Filardo EJ. Anatomical location and redistribution of G protein-coupled estrogen receptor-1 during the estrus cycle in mouse kidney and specific binding to estrogens but not aldosterone. Mol Cell Endocrinol. 2014; 382: 950-959.

45. Karmazyn M, Liu Q, Gan XT, Brix BJ, Fliegel L. Aldosterone increases NHE-1 expression and induces NHE-1-dependent hypertrophy in neonatal rat ventricular myocytes. Hypertension. 2003; 42: 1171-1176.

46. Bruder-Nascimento T, da Silva MA, Tostes RC. The involvement of aldosterone on vascular insulin resistance: implications in obesity and type 2 diabetes. Diabetol Metab Syndr. 2014; 6:90.

47. Brown NJ. Contribution of aldosterone to cardiovascular and renal inflammation and fibrosis. Nat Rev Nephrol. 2013; 9: 459-469.

48. Queisser N, Oteiza PI, Link S, Hey V, Stopper H, Schupp N. Aldosterone activates transcription factor Nrf2 in kidney cells both *in vitro* and *in vivo*. Antioxid Redox Signal. 2014; 21: 2126-2142.

49. Grossmann C, Husse B, Mildenberger S, Schreier B, Schuman K, Gekle M. Colocalization of mineralocorticoid and EGF receptor at the plasma membrane. Biochim. Biophys. Acta. 2010; 1803: 584-590.

50. Jahn GA, Moguilewsky M, Houdebine LM, Djiane J. Binding and action of glucocorticoids and mineralocorticoids in rabbit mammary gland. Exclusive participation of glucocorticoid type II receptors for stimulation of casein synthesis. Mol Cell Endocrinol. 1987; 52: 205-212.

51. Rabbitt EH, Gittoes NJ, Stewart PM, Hewison M. 11beta-hydroxysteroid dehydrogenases, cell proliferation and malignancy. J Steroid Biochem Mol Biol. 2003; 85: 415-421.

52. Sasano H, Frost AR, Saitoh R, Matsunaga G, Nagura H, Krozowski ZS, Silverberg SG. Localization of mineralocorticoid receptor and 11 beta-hydroxysteroid dehydrogenase type II in human breast and its disorders.

Anticancer Res. 1997; 17: 2001-2007.

53. Kim CH, Cho YS. Selection and optimization of MCF-7 cell line for screening selective inhibitors of 11beta-hydroxysteroid dehydrogenase 2. Cell Biochem Funct. 2010; 28: 440-447.

54. De Francesco EM, Angelone T, Pasqua T, Pupo M, Cerra MC, Maggiolini M. GPER mediates cardiotropic effects in spontaneously hypertensive rat hearts. PLoS One. 2013; 8: e69322.

55. Filice E, Angelone T, De Francesco EM, Pellegrino D, Maggiolini M, Cerra MC. Crucial role of phospholamban phosphorylation and S-nitrosylation in the negative lusitropism induced by 17β-estradiol in the male rat heart. Cell Physiol Biochem. 2011; 28: 41-52.

56. Lappano R, Maggiolini M. G protein-coupled receptors: novel targets for drug discovery in cancer. Nat Rev Drug Discov. 2011; 10: 47-60.

57. Lappano R, Maggiolini M. GPCRs and cancer. Acta Pharmacol Sin. 2012; 33: 351-362.

58. Vivacqua A, Romeo E, De Marco P, De Francesco EM, Abonante S, Maggiolini M. GPER mediates the Egr-1 expression induced by 17β-estradiol and 4-hydroxitamoxifen in breast and endometrial cancer cells. Breast Cancer Res Treat. 2012; 133: 1025-1035.

59. Lappano R, De Marco P, De Francesco EM, Chimento A, Pezzi V, Maggiolini M. Cross-talk between GPER and growth factor signalling. J Steroid Biochem Mol Biol. 2013; 137: 50-56.

60. De Marco P, Cirillo F, Vivacqua A, Malaguarnera R, Belfiore A, Maggiolini M. Novel Aspects Concerning the Functional Cross-Talk between the Insulin/IGF-I System and Estrogen Signalling in Cancer Cells. Front Endocrinol (Lausanne). 2015; 6:30.

61. Bartella V, De Marco P, Malaguarnera R, Belfiore A, Maggiolini M. New advances on the functional cross-talk between insulin-like growth factor-I and estrogen signalling in cancer. Cell Signal. 2012; 24: 1515-1521.

62. Madeo A, Maggiolini M. Nuclear alternate estrogen receptor GPR30 mediates 17beta-estradiol-induced gene expression and migration in breast cancer-associated fibroblasts. Cancer Res. 2010; 70: 6036-6046.

63. Pupo M, Pisano A, Abonante S, Maggiolini M, Musti AM. GPER activates Notch signalling in breast cancer cells and cancer-associated fibroblasts (CAFs). Int J Biochem Cell Biol. 2014; 46: 56-67.

64. Pupo M, Vivacqua A, Perrotta I, Pisano A, Aquila S, Abonante S, Gasperi-Campani A, Pezzi V, Maggiolini M. The nuclear localization signal is required for nuclear GPER translocation and function in breast Cancer-Associated Fibroblasts (CAFs). Mol Cell Endocrinol. 2013; 376: 23-32.

65. McEneaney V, Harvey BJ, Thomas W. Aldosterone rapidly activates protein kinase D via a mineralocorticoid receptor/EGFR trans-activation pathway in the M1 kidney CCD cell line. J Steroid Biochem Mol Biol. 2007; 107: 180-190.

66. De Giusti VC, Nolly MB, Yeves AM, Caldiz CI, Villa-Abrille MC, Chiappe de Cingolani GE, Ennis IL, Cingolani HE, Aiello EA. Aldosterone stimulates the cardiac Na(+)/H(+) exchanger via transactivation of the epidermal growth factor receptor. Hypertension. 2011; 58: 912-919.

67. Morgado-Pascual JL, Rayego-Mateos S, Valdivielso JM, Ortiz A, Egido J, Ruiz-Ortega M. Paricalcitol Inhibits Aldosterone-Induced Proinflammatory Factors by Modulating Epidermal Growth Factor Receptor Pathway in Cultured Tubular Epithelial Cells. Biomed Res Int. 2015; 2015:783538.

68. Fang JS, Gillies RD, Gatenby RA. Adaptation to hypoxia and acidosis in carcinogenesis and tumor progression. Semin Cancer Biol. 2008; 18: 330-337.

69. Martinez-Outschoorn U, Sotgia F, Lisanti MP. Tumor microenvironment and metabolic synergy in breast cancers: critical importance of mitochondrial fuels and function. Semin Oncol. 2014; 41: 195-216.

70. De Francesco EM, Lappano R, Santolla MF, Marsico S, Caruso A, Maggiolini M. HIF-1α/GPER signalling mediates the expression of VEGF induced by hypoxia in breast cancer associated fibroblasts (CAFs). Breast Cancer Res. 2013; 15:R64.

71. De Francesco EM, Pellegrino M, Santolla MF, Lappano R, Ricchio E, Abonante S, Maggiolini M. GPER mediates activation of HIF1α/VEGF signalling by estrogens. Cancer Res. 2014; 74: 4053-4064.

72. Recchia AG, De Francesco EM, Vivacqua A, Sisci D, Panno ML, Andò S, Maggiolini M. The G protein-coupled receptor 30 is up-regulated by hypoxia-inducible factor-1alpha (HIF-1alpha) in breast cancer cells and cardiomyocytes. J Biol Chem. 2011; 286: 10773-10782.

73. Rigiracciolo DC, Scarpelli A, Lappano R, Pisano A, Santolla MF, De Marco P, Cirillo F, Cappello AR, Dolce V, Belfiore A, Maggiolini M, De Francesco EM. Copper activates HIF-1α/GPER/VEGF signalling in cancer cells. Oncotarget. 2015; 6:34158-77. doi: 10.18632/oncotarget.5779.

74. Barton M, Prossnitz ER. Emerging roles of GPER in diabetes and atherosclerosis. Trends Endocrinol Metab. 2015; 26: 185-192.

75. Feldman RD, Gros R. scular effects of aldosterone: sorting out the receptors and the ligands. Clin Exp Pharmacol Physiol. 2013; 40: 916-921.

76. Brossa A, Grange C, Mancuso L, Annaratone L, Satolli MA, Mazzone M, Camussi G, Bussolati B. Sunitinib but not VEGF blockade inhibits cancer stem cell endothelial differentiation. Oncotarget. 2015; 6: 11295-11309. doi: 10.18632/oncotarget.3123.

77. Grange C, Bussolati B, Bruno S, Fonsato V, Sapino A, Camussi G. Isolation and characterization of human breast tumor-derived endothelial cells. Oncol Rep. 2006; 15: 381-386.

78. Fiorio Pla A, Ong HL, Cheng KT, Brossa A, Bussolati B,

Lockwich T, Paria B, Munaron L, Ambudkar IS. TRPV4 mediates tumor-derived endothelial cell migration via arachidonic acid-activated actin remodeling. Oncogene. 2012; 31: 200-212.

79. Albanito L, Sisci D, Aquila S, Brunelli E, Vivacqua A, Madeo A, Lappano R, Pandey DP, Picard D, Mauro L, Andò S, Maggiolini M. Epidermal growth factor induces G protein-coupled receptor 30 expression in estrogen receptor-negative breast cancer. Endocrinology. 2008; 149: 3799-3808.

80. De Marco P, Bartella V, Vivacqua A, Lappano R, Santolla MF, Morcavallo A, Pezzi V, Belfiore A, Maggiolini M. Insulin-like growth factor-I regulates GPER expression and function in cancer cells. Oncogene. 2013; 32: 678-688.

81. De Marco P, Romeo E, Vivacqua A, Malaguarnera R, Abonante S, Romeo F, Pezzi V, Belfiore A, Maggiolini M. GPER1 is regulated by insulin in cancer cells and cancer-associated fibroblasts. Endocr Relat Cancer. 2014; 21: 739-753.

npg

ORIGINAL ARTICLE

Inactivating mutations in *GNA13* and *RHOA* in Burkitt's lymphoma and diffuse large B-cell lymphoma: a tumor suppressor function for the Gα₁₃/RhoA axis in B cells

M O'Hayre[1], A Inoue[2,3], I Kufareva[4], Z Wang[1], CM Mikelis[5], RA Drummond[6], S Avino[1,7], K Finkel[1], KW Kalim[8], G DiPasquale[9], F Guo[8], J Aoki[2,10], Y Zheng[8], MS Lionakis[6], AA Molinolo[1] and JS Gutkind[1,11]

G proteins and their cognate G protein-coupled receptors (GPCRs) function as critical signal transduction molecules that regulate cell survival, proliferation, motility and differentiation. The aberrant expression and/or function of these molecules have been linked to the growth, progression and metastasis of various cancers. As such, the analysis of mutations in the genes encoding GPCRs, G proteins and their downstream targets provides important clues regarding how these signaling cascades contribute to malignancy. Recent genome-wide sequencing efforts have unveiled the presence of frequent mutations in *GNA13*, the gene encoding the G protein Gα₁₃, in Burkitt's lymphoma and diffuse large B-cell lymphoma (DLBCL). We found that mutations in the downstream target of Gα₁₃, RhoA, are also present in Burkitt's lymphoma and DLBCL. By multiple complementary approaches, we now show that that these cancer-specific *GNA13* and *RHOA* mutations are inhibitory in nature, and that the expression of wild-type Gα₁₃ in B-cell lymphoma cells with mutant *GNA13* has limited impact *in vitro* but results in a remarkable growth inhibition *in vivo*. Thus, although Gα₁₃ and RhoA activity has previously been linked to cellular transformation and metastatic potential of epithelial cancers, our findings support a tumor suppressive role for Gα₁₃ and RhoA in Burkitt's lymphoma and DLBCL.

INTRODUCTION

G protein-coupled receptors (GPCRs) represent the largest class of cell-surface receptors and when activated by extracellular ligands, they transmit signals involved in cell growth, proliferation, survival, differentiation and motility.[1] GPCRs initiate signal transduction cascades by coupling to and activating heterotrimeric G proteins. Depending on the coupling specificity, a given GPCR may couple to one or more different Gα proteins, which are grouped into four main families: Gα₁₂ (including Gα₁₃), Gαₛ, Gαᵢ and Gαq (including Gα₁₁). Each family of G proteins activates distinct sets of second messenger and kinase signaling cascades.[1]

Heterotrimeric G proteins are major cellular signaling hubs, and they are activated upon binding to GPCRs or non-receptor guanine nucleotide exchange factors (GEFs).[2] Because of their important roles in regulating cell survival, proliferation and movement, it is not surprising that tumors often harbor mutations in or exhibit aberrant expression of G proteins and their GEFs.[3] For example, activating mutations in *GNA11* and *GNAQ*, encoding Gα₁₁ and Gαq respectively, were recently discovered to be the key oncogenic drivers in uveal melanoma.[4–6] Gαₛ is the most frequently mutated G protein in human cancers; and activating mutations in the gene, *GNAS,* have been found in a variety of

neoplasms including pituitary, thyroid, pancreatic, biliary tract, colon and small intestine and a variety of other tumors.[3] Furthermore, constitutively active mutants of genes encoding Gαᵢ, Gα₀, Gαq Gα₁₂ and Gα₁₃ were found to induce cellular transformation in experimental systems (reviewed in Dorsam and Gutkind[1] and Dhanasekaran *et al.*[7]).

Despite the transforming capacity of constitutive Gα₁₂ and Gα₁₃ activity in experimental systems and numerous implications of this G-protein family and downstream targets in cancer metastasis,[8–13] activating mutations in the *GNA13* and *GNA12* genes in patient tumor samples have not been described. However, recent large-scale sequencing efforts have revealed the presence of *GNA13* mutations in Burkitt's lymphoma and diffuse large B- cell lymphoma (DLBCL).[14,15] Interestingly, recent studies in mouse models demonstrated that conditional B-cell deficiency in Gα₁₃- or the Gα₁₃-coupled sphingosine 1 phosphate receptor 2 (S1P2) result in DLBCL-like phenotypes.[16,17] On the basis of the analysis of deposited sequencing data from tumors in the Catalog of Somatic Mutations in Cancer (COSMIC), mutations in *GNA13* in human Burkitt's lymphoma and DLBCL are highly statistically significant over background cancer mutation rate, with *P*-value and *q*-value scores approaching 0,[3] suggesting that these

[1]Oral and Pharyngeal Cancer Branch, National Institute of Dental and Craniofacial Research, National Institutes of Health, Bethesda, MD, USA; [2]Graduate School of Pharmaceutical Sciences, Tohoku University, Sendai, Miyagi, Japan; [3]PRESTO, Japan Science and Technology Agency (JST), Kawaguchi, Saitama, Japan; [4]Skaggs School of Pharmacy and Pharmaceutical Sciences, University of California, San Diego, La Jolla, CA, USA; [5]Department of Biomedical Sciences, School of Pharmacy, Texas Tech University Health Sciences Center, Amarillo, TX, USA; [6]Fungal Pathogenesis Unit, Laboratory of Clinical Infectious Diseases, National Institute of Allergy and Infectious Diseases, National Institutes of Health, Bethesda, MD, USA; [7]Department of Pharmacy, Health and Nutritional Sciences, University of Calabria, Rende (Cs), Italy; [8]Division of Experimental Hematology and Cancer Biology, Cincinnati Children's Hospital Medical Center, Cincinnati, OH, USA; [9]Molecular Physiology and Therapeutics Branch, National Institute of Dental and Craniofacial Research, National Institutes of Health, Bethesda, MD, USA; [10]Japan Agency for Medical Research and Development, Core Research for Evolutional Science and Technology (AMED-CREST), AMED, Chiyoda-ku, Tokyo, Japan and [11]Department of Pharmacology, UC San Diego Moores Cancer Center, La Jolla, CA, USA. Correspondence: Dr JS Gutkind, Department of Pharmacology, UC San Diego Moores Cancer Center, 3855 Health Sciences Drive, #0803, La Jolla, CA 92093, USA.
E-mail: sgutkind@ucsd.edu
Received 22 July 2015; revised 15 September 2015; accepted 15 October 2015

mutations are likely not random. However, unlike the activating GTPase domain mutations found in other G proteins in cancers, including Gα$_q$ and Gα$_s$, the mutations in *GNA13* are distributed throughout the gene. Furthermore, we identified additional mutations in the gene of the major downstream effector of Gα$_{13}$ signaling, RhoA.

In this study, we characterize the mutations identified in *GNA13* and *RHOA* in Burkitt's lymphoma and DLBCL tumor samples to determine how these mutations affect protein function and signaling capacity. We also evaluated the effects of mutations and wild-type (WT) Gα$_{13}$ expression on tumor growth and progression in xenograft models. Overall, our results support a tumor suppressive role for the Gα$_{13}$/RhoA axis in Burkitt's lymphoma and DLBCL. Our data also extend recent findings supporting the presence of disruptive *RHOA* mutations in peripheral T-cell lymphomas, suggesting that disruption of RhoA function may have a broad impact in multiple hematological malignancies.[18-22]

RESULTS

Mutations in GNA13 and RHOA are frequent in Burkitt's lymphoma and DLBCL tumors

Data from genome-wide sequencing analyses collected through the Catalog of Somatic Mutations in Cancer (COSMIC v72) database reveal the presence of *GNA13* mutations in nearly 2% of all hematopoietic and lymphoid malignancies (Figure 1a). Previous statistical analyses of these mutations indicated *P*-value and *q*-value (for false discovery rate) scores approaching 0, suggesting that they are unlikely to be random, but rather could have important driver mutation functions.[3] Of the hematopoietic and lymphoid malignancies evaluated in COSMIC, most of the *GNA13* mutations are present in B-cell lymphomas, primarily DLBCL and Burkitt's lymphoma, for which mutations are harbored in approximately 10% of patient tumor samples (Figure 1a). Mutations in *GNA13* found in Burkitt's lymphoma and DLBCL appeared likely to result in loss of function because nearly 22% (5/23) of the DLBCL mutations (17% of overall in both lymphomas)
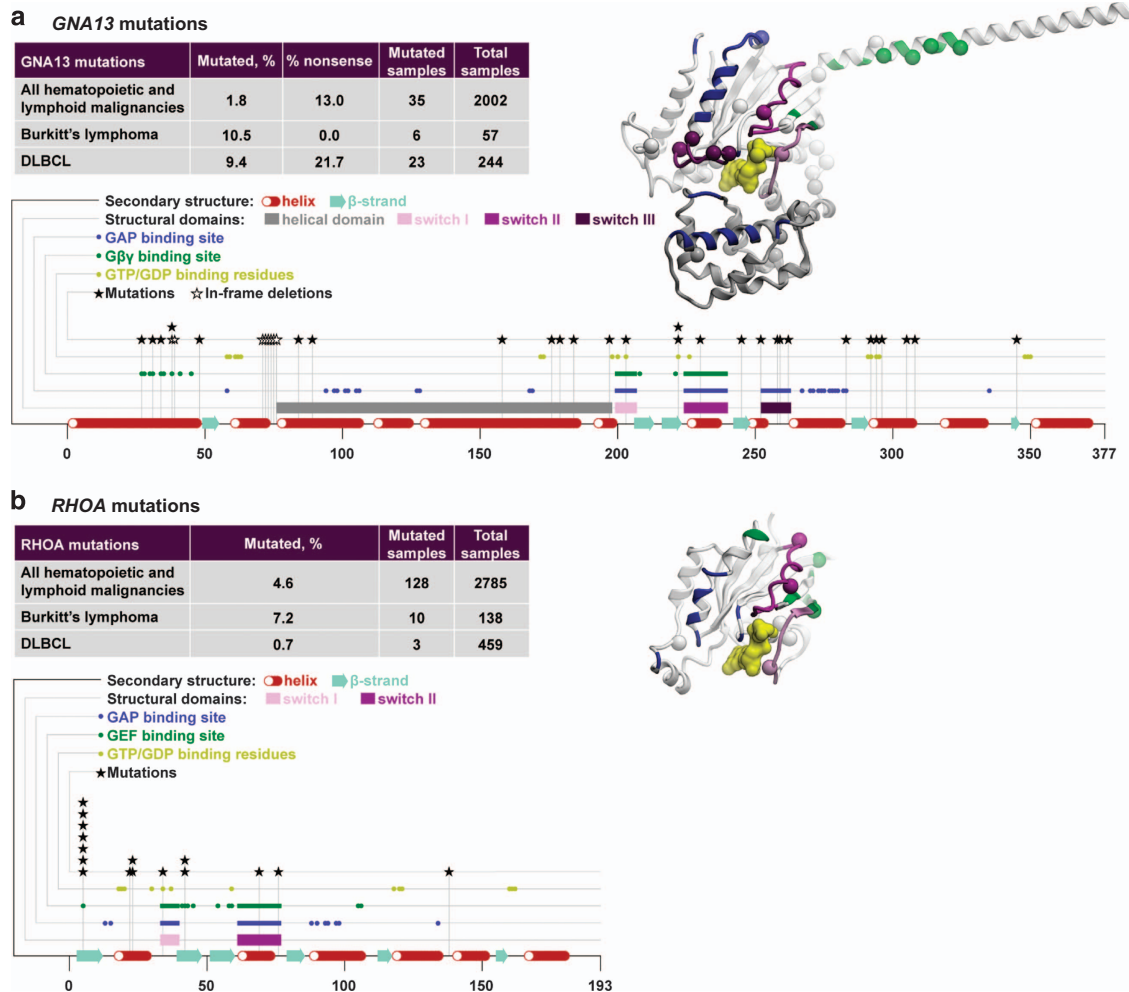
Figure 1. Sequence and structure localization of mutations in *GNA13* and *RHOA* that are observed in Burkitt's Lymphoma and DLBCL tumors. (**a**) Table of the number and percentage of *GNA13* mutations in hematopoietic malignancies overall and in Burkitt's lymphoma and DLBCL based on data from COSMIC v72 (top). Linear diagram of mutations along the *GNA13* gene and the functional and structural domains of the protein Gα$_{13}$ (bottom). (**b**) Table of the number and percentage of *RHOA* mutations in haematopoietic malignancies overall and in Burkitt's Lymphoma and DLBCL based on data from COSMIC v72 (top). Linear diagram of mutations along the *RHOA* gene and the functional and structural domains of the protein and the ribbon diagram of RhoA crystal structure (bottom). Structural and functional domains of both proteins are color-coded and indicated on separate lines above the linear diagram and mapped onto the 3D structures. The mutated residue positions are shown as stars on over the corresponding residues of the linear diagrams and as spheres in the 3D structure representation. The nucleotide is shown as yellow skin.

were non-sense, resulting in a premature STOP codon and all other mutations were non-synonymous (Figure 1a). When mapped onto the crystal structure of GNA13, the mutations clustered into multiple regions including the binding interface for the Gβ/γ subunits, the helical domain, conformational switches 1 and 2 (important for nucleotide binding as well as interaction with regulators and effectors), conformational switch 3, the GPCR interface and directly in the nucleotide pocket (Figure 1a, Supplementary Table 1). An interesting in-frame deletion was observed in the loop connecting the GTPase and the helical domain that can dramatically impair the relative mobility of the two domains. Mutations are therefore not localized into one region and so they could exert a broad influence on the protein function or stability.

RhoA is the main downstream effector of Gα$_{13}$ signaling,[23–25] therefore we searched the COSMIC database to determine whether there were mutations in RHOA in Burkitt's lymphoma and DLBCL tumors as well. Although less frequent than the GNA13 mutations, non-redundant RHOA mutations were observed in nearly 6% of Burkitt's lymphoma and almost 1% of DLBCL tumors (Figure 1b), as these RHOA mutations were present in separate tumor samples from those with GNA13 mutations. Taken together, the Gα$_{13}$/RhoA axis is disrupted in >10% of these B-cell lymphomas. Interestingly, there was a recurrent R5Q mutation,

observed in 7/16 RHOA mutations identified in these tumors. Structural analysis of RhoA suggests that R5 is important for GEF binding. Several of the other mutations in RHOA also localized to GEF binding residues, indicating that these mutations could influence RhoA activation due to changes in RhoA–GEF interactions (Figure 1b, Supplementary Table 2).

Characterization of GNA13 mutations indicates loss of function

To determine the consequences of the GNA13 mutations on Gα$_{13}$ protein function, we prepared and characterized nine of the mutations from the COSMIC data repository, representing a variety of the structural and functional domains. Plasmids encoding empty vector, Gα$_{13}$ WT and Gα$_{13}$ mutants based on Burkitt's lymphoma and DLBCL tumor samples and an established constitutively active Q226L mutant were transfected into HEK293 cells; and Gα$_{13}$ protein expression was assessed by western blotting (Figure 2a). Although most of the Gα$_{13}$ mutants were expressed at similar levels to WT, there were a few including L197Q and F245S that had reduced protein expression. Because the Gα$_{13}$ antibody recognizes an epitope in the C-terminus of Gα$_{13}$, disrupted antibody recognition is unlikely to fully explain the relatively low protein expression observed in the L197Q and F245S mutants. Rather, it could be that these mutants affect protein stability, thus reducing expression.
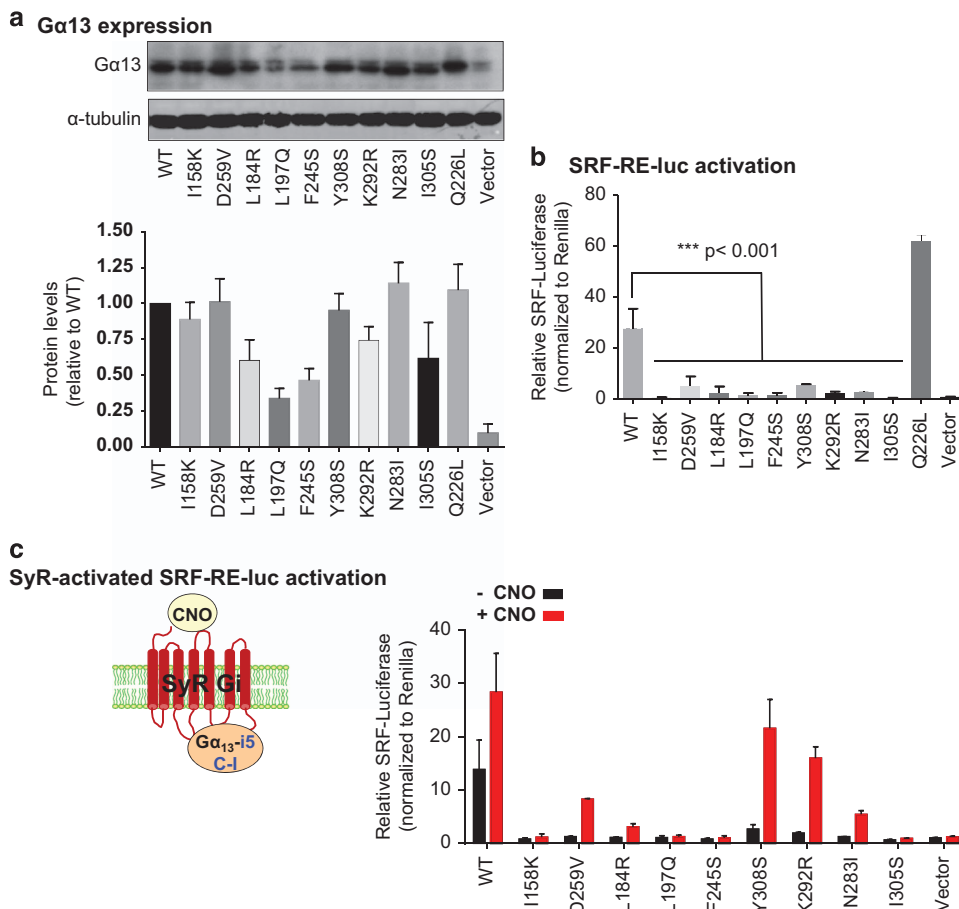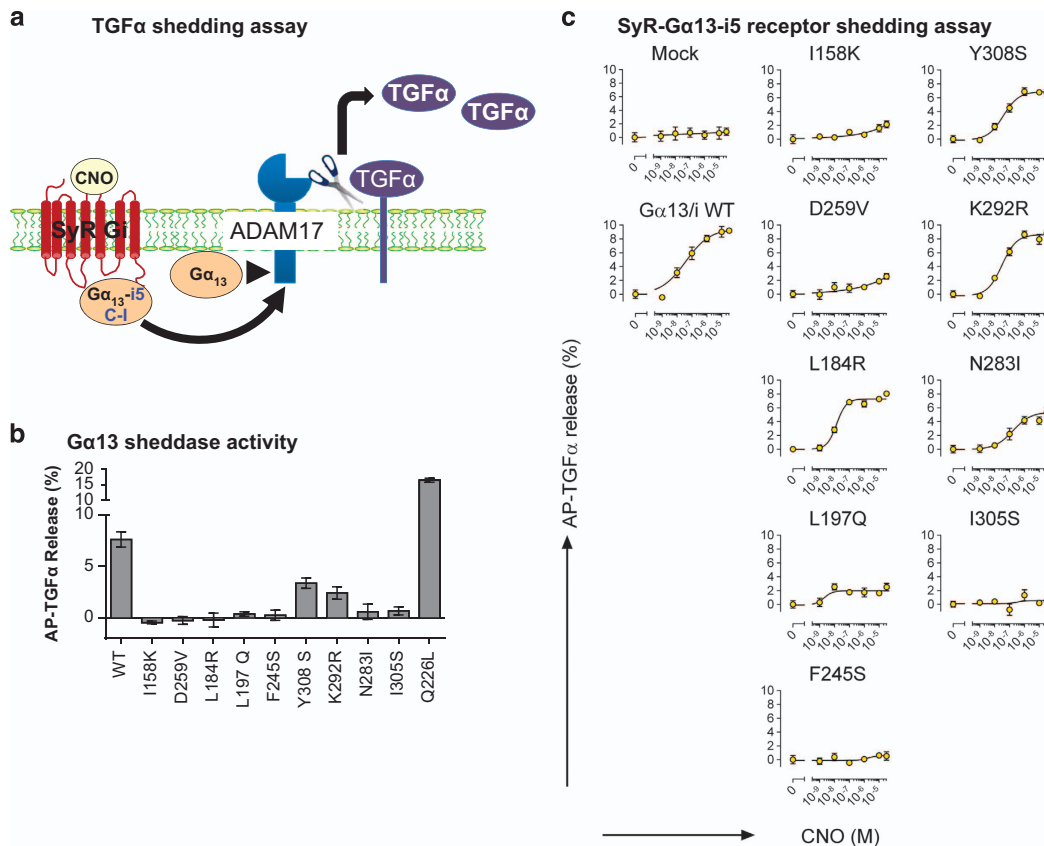

Figure 2. GNA13 mutations in Burkitt's lymphoma and DLBCL tumor samples result in loss of downstream transcriptional activity based on SRF-RE luciferase assay. (**a**) Representative western blot for Gα$_{13}$ expression of cells transfected with Gα$_{13}$ WT, mutants based on COSMIC data, constitutively active Q226L mutant or vector control. Antibody detection of α-tubulin was used as a loading control (top). Densitometry quantification of Gα$_{13}$ protein expression of the mutants relative to WT (bottom) as an average of three independent western blots. Error bars indicate standard deviation. (**b**) SRF-RE luciferase assay of spontaneous activity of cells transfected with Gα$_{13}$ WT, mutants, constitutively active Q226L mutant or vector control. Error bars indicate standard deviation. (**c**) SRF-RE luciferase activity of cells expressing SyR-Gi transfected with WT or mutant Gα$_{13-i5}$ chimeras, in the presence (+) and absence (−) of CNO stimulation. Error bars indicate standard deviation.

To evaluate the functional consequences of these mutants, we tested their activity in a serum response factor response element (SRF-RE) luciferase assay, which is used to selectively monitor gene transcription downstream of $G\alpha_{13}$-RhoA signaling. The SRF-RE luciferase assay demonstrated that all nine $G\alpha_{13}$ mutants had significantly reduced basal transcriptional activity relative to WT and constitutively active (Q226L) $G\alpha_{13}$ (Figure 2b). Due to promiscuity of most $G\alpha_{13}$-coupled GPCRs, which often also couple to other G proteins and/or have ligands that target other GPCRs, a synthetic biology approach was employed to determine the effects of the $G\alpha_{13}$ mutants on ligand-activated $G\alpha_{13}$ signaling events. The synthetic GPCR (SyR), also known as DREADD,[26] is activated by an otherwise biologically inert ligand, clozapine N-oxide (CNO). Because no $G\alpha_{13}$-SyR is currently available, an SyR that couples to $G\alpha_i$ was used in combination with a chimeric G protein that has $G\alpha_i$-coupling specificity (based on the last 5 amino acids at the C-terminus) but retains $G\alpha_{13}$ signaling response. Additionally, in order to ensure that the responses observed were due to $G\alpha_{13}$ activity and not influenced by potential $G\alpha_i$ signaling, a C-I mutation was made in the last five amino acids of the $G\alpha_{13-i5}$ chimeras to make them pertussis toxin (PTX) insensitive and the assay was performed in the presence of PTX. The SRF-RE assay demonstrated that some of the $G\alpha_{13}$ mutants were completely dead, whereas others still retained some ligand-activated response (Figure 2c). Nevertheless, overall SRF-RE activity was lower in all the mutants compared with WT (and basal activity was again lower in all the mutants). A recently developed transforming growth factor-α (TGF-α) shedding assay was used as another measurement of $G\alpha_{13}$ activity.[27] $G\alpha_{13}$ and $G\alpha_q$ activity is known to induce the shedding of tethered TGF-α, and so we could monitor the release of alkaline phosphatase-fused TGF-α (AP-TGF-α) into media as a measurement of $G\alpha_{13}$ signaling (Figure 3a). Similar to the SRF-RE results, the spontaneous (or basal) activities of all the $G\alpha_{13}$ mutants were significantly lower than WT or the Q226L constitutively active mutant (Figure 3b, Supplementary Table 3), whereas a few of the mutants still retained some ligand-induced signaling response as determined using the synthetic receptor system, SyR-Gi with the $G\alpha_{13-i5}$ chimeras (Figure 3c, Supplementary Table 4) and using another receptor that couples to $G\alpha_{13}$, the dopamine D2 receptor (Supplementary Figure 1, Supplementary Table 5).

GNA13 and RHOA mutations impair RhoA activity

RhoA is the main downstream effector of $G\alpha_{13}$ signaling, thus we sought to analyze the effects of the *GNA13* mutations on RhoA activity and to determine the effect of the recurrent RhoA R5Q mutation. We monitored active GTP-bound RhoA using a pull-down assay for three of the $G\alpha_{13}$ mutants and controls. In line with the previous experiments, the $G\alpha_{13}$ mutants had considerably reduced levels of active RhoA compared with WT $G\alpha_{13}$, constitutively active $G\alpha_{13}$ Q226L and the thrombin-stimulated positive control (Figure 4a). Next, we evaluated the activity of the R5Q RhoA mutant that had been identified in several DLBCL and Burkitt's lymphoma tumors. The R5Q mutant exhibited reduced activity compared with WT RhoA and the constitutively active Q63L RhoA mutant in both an active RhoA pull-down assay (Figure 4b) and an SRF-RE luciferase assay (Figure 4c). However, the RhoA R5Q mutant appeared to retain a little activity compared

Figure 3. *GNA13* mutations in Burkitt's lymphoma and DLBCL tumor samples result in loss of function based on a TGFα shedding assay. (**a**) Schematic representation of the AP-TGFα shedding assay used to monitor activity of the $G\alpha_{13}$ mutants. (**b**) AP-TGFα shedding assay for spontaneous/basal activity of $G\alpha_{13}$ WT and mutants. Error indicates standard deviation. (**c**) AP-TGFα shedding assay dose response curves of CNO stimulation of cells expressing SyR-Gi transfected with WT or mutant $G\alpha_{13-i5}$ chimeras.
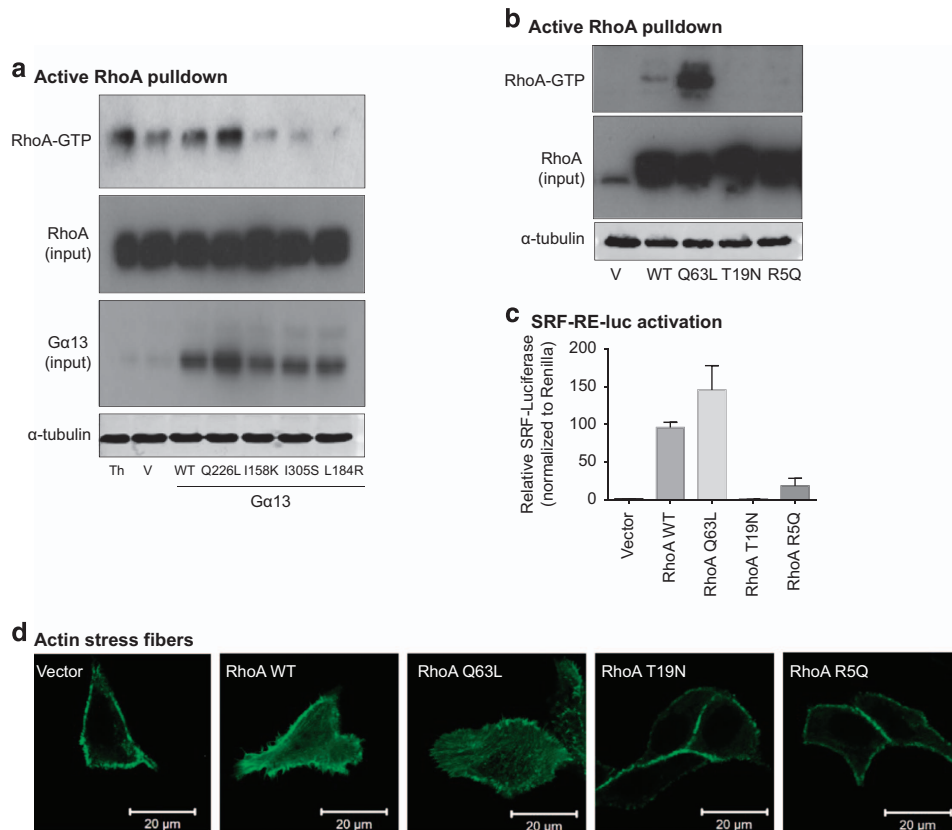
Figure 4. Burkitt's lymphoma and DLBCL GNA13 and RHOA mutations impair RhoA activity. (a) GST-Rhotekin-RBD pull-down assay to monitor RhoA activity in HEK293 cells transfected with vector control (V), WT, constitutively active Q226L or mutant $G\alpha_{13}$ plasmids. Thrombin (Th) stimulation was used as a positive control. Input lysates were probed for $G\alpha_{13}$ and for total RhoA and α-tubulin as loading controls. (b) GST-Rhotekin-RBD pull-down assay to monitor RhoA activity in HEK293 cells transfected with vector control (V) or RhoA WT, constitutively active Q63L, dominant-negative T19N or R5Q mutant plasmids. (c) SRF-RE luciferase assay detecting spontaneous activity of cells transfected with vector control, RhoA WT, constitutively active Q63L, dominant-negative T19N and the R5Q mutant plasmids. Error bars indicate standard deviation. (d) Immunofluorescence images of actin stress fibers in MDCK cells co-transfected with LifeActin GFP and vector control or RhoA WT, constitutively active Q63L, dominant-negative T19N or R5Q mutant plasmids.

with the dominant-negative T19N RhoA mutant (Figure 4c). Formation of actin stress fibers is often used as another indication of RhoA activity, so we performed a stress fiber formation assay using LifeActin GFP in Madin-Darby Canine Kidney (MDCK) cells. Consistent with the SRF and RhoA pull-down results, we observed significant actin stress fiber formation in WT and Q63L constitutively active RhoA-transfected MDCK cells, but not with the R5Q mutant or the dominant-negative T19N mutant (Figure 4d). Overall, these data indicate that the GNA13 and RHOA mutations observed in DLBCL and Burkitt's lymphoma tumors result in loss of function of RhoA activity and downstream signaling events.

Restoration of $G\alpha_{13}$ WT suppresses tumor growth
The COSMIC sequencing data indicated the presence of a GNA13 mutation at L184R in the frequently used Raji Burkitt's lymphoma cell line. Therefore, in order to determine whether mutation and thus loss of $G\alpha_{13}$ activity provides the cells with a growth or survival advantage, we expressed $G\alpha_{13}$ WT in the cells. First, we verified the COSMIC sequencing data in the Raji cell line and confirmed the presence of a heterozygous L184R mutation (Figure 5a). Then, we transduced Raji cells using MSCV puro IRES GFP retrovirus with $G\alpha_{13}$ WT or vector control. After cell sorting, we were able to achieve a highly GFP-enriched population of cells and verified the expression of $G\alpha_{13}$ (Figure 5b). B-cell lines are notorious for their difficulties in terms of feasibility of genetic manipulations, which prevented us from deploying similar or

complementary strategies to express $G\alpha_{13}$ WT in additional relevant cellular systems. Regarding $G\alpha_{13}$ function, it was previously reported that $G\alpha_{13}$ activity has suppressive effects on Akt phosphorylation.[17] Thus, we measured basal Akt phosphorylation at S473, and found that $G\alpha_{13}$ WT expression in the Raji cells reduced phosphorylated Akt (Figure 5c). Using in vitro viability and proliferation assays, we did not observe any differences between the control and $G\alpha_{13}$ WT-expressing Raji cells (data not shown). In a methocellulose clonogenic assay, WT $G\alpha_{13}$-expressing cells showed only a slight reduction in the number of colonies; however, the difference in cell morphology was striking (Figures 5d and e). Although the majority of the control Raji cells formed spheroid colonies in the methocellulose, the Raji cells expressing $G\alpha_{13}$ WT tended to exhibit a more flattened morphology (Figure 5e). Next, we tested the Raji control cells and Raji $G\alpha_{13}$ WT-transduced cells in a tumor xenograft model using NSG (NOD SCID gamma) mice. In line with the role of a tumor suppressor, the restoration of $G\alpha_{13}$ WT to the Raji cells resulted in significantly delayed and impaired tumor growth and smaller tumor masses and volumes (Figures 5f and h). Histological evaluation of the cells indicated that the Raji cells with $G\alpha_{13}$ WT expressed were considerably smaller and more necrotic than the control Raji cells (Figures 5i and j). In addition, the Raji cells expressing $G\alpha_{13}$ WT were significantly less proliferative, based on Ki67 staining and analysis of tumor sections (Figure 5k). These data indicate that restoration and/or overexpression of $G\alpha_{13}$ WT

influences the survival and/or proliferation of the Raji cells within the tumor microenvironment, which may be the mechanism by which it suppresses tumor growth *in vivo*.

DISCUSSION

Burkitt's lymphoma and DLBCL are aggressive and prevalent B-cell malignancies.[28] Although some genetic alterations have been identified and associated with malignancy of these B-cell

lymphomas, much is still unknown about the majority of the genetic mutations and how these alterations may affect the development and progression of disease.[14,29] Previous genome-wide sequencing studies unveiled frequent mutations in *GNA13*, the gene encoding the G protein, $G\alpha_{13}$,[14,15] and these mutations were found to be highly statistically significant over background cancer mutation rates.[3] Although activity of $G\alpha_{13}$ has previously been linked to cellular transformation in fibroblasts as well as tumor cell invasion in several cancers including breast cancer and
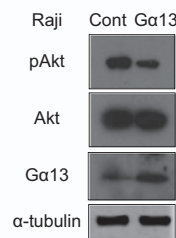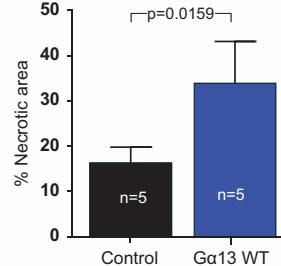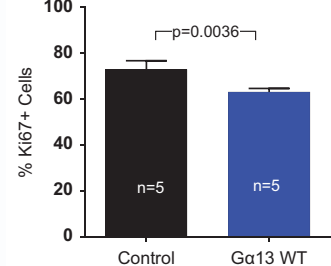
prostate cancer,[7,30–32] our characterization of the GNA13 mutations present in human Burkitt's lymphoma and DLBCL tumors indicates that these mutations rather result in loss of function and/or reduced protein stability. Furthermore, we demonstrated that expression of wild-type Gα$_{13}$ to Burkitt's lymphoma cells with mutated GNA13 results in reduced tumor growth in xenograft models and altered cell morphology and growth in a methocellulose colony assay.

Recent elegant genetic mouse models support our loss-of-function characterization of GNA13 mutations present in DLBCL and Burkitt's lymphoma, as mice deficient in lymphoid lineage for Gα$_{13}$ or the Gα$_{13}$-coupled receptor, S1P2, exhibited an increase in total T-cell and B-cell numbers and resulted in an outgrowth of cells classified as DLBCL.[16,17,33] Specifically, these studies identified a migration defect and an increase in phosphorylated Akt in germinal center (GC) B cells caused by S1P2 or Gα$_{12}$/Gα$_{13}$ deficiency. Thus, signaling through the Gα$_{12}$/Gα$_{13}$ axis via GPCRs, including S1P2 and the recently characterized P2Ry8, is proposed to help confine B cells to the GC and limit B-cell expansion.[17] Loss of this axis would therefore allow cells to escape the GC and populate lymph nodes as is characteristic of DLBCL. However, in addition to the migration defects observed in these previous studies, our data indicate a direct role for Gα$_{13}$ in growth suppression of B cells in vivo and suggest that Gα$_{13}$ may influence their survival and/or differentiation state.

Previous sequencing of non-Hodgkin's lymphomas reported frequent GNA13 mutations that were enriched in GC B-cell type DLBCL.[34] Of interest, DLBCL have been recently classified in multiple distinct groups based on their histological and biological characteristics and morphological features.[35] Thus, based on our findings it is possible that DLBCL harboring RHOA or GNA13 mutations may exhibit particular characteristics. Indeed, further characterization of RHOA and GNA13 mutations in relation to subgroup, stage and patient survival is warranted once more information becomes available.

To evaluate the mechanisms by which the GNA13 mutations may alter signaling that could affect the growth and morphology of the B cells, we first investigated possible effects on the major downstream effector, RhoA. The constitutive/basal activity of RhoA was found to be significantly reduced in all nine of the Gα$_{13}$ mutants tested compared with WT Gα$_{13}$. Although a few of the mutants still had some ligand-induced signaling responses, the overall levels of activity were reduced compared with WT. Furthermore, these ligand-induced signaling assays were performed with receptor overexpression systems, so it is possible that these ligand responses may not be as pronounced in more physiological systems.

Because the Gα$_{13}$ mutants critically impacted RhoA activity, we investigated whether independent mutations in RHOA were present in DLBCL and Burkitt's lymphoma tumors by searching the COSMIC database. Indeed, mutations in RHOA were identified in several patient tumors that were independent from those with GNA13 mutations. Intriguingly, a recurrent glutamine substitution at R5 of RhoA was observed in several patient tumors, aligned with the recent description of RHOA mutations, including a recurrent R5Q mutation, in 8.5% of pediatric Burkitt's lymphoma cases studied.[36] Correlating with the loss of function data observed with the Gα$_{13}$ mutations, our data indicate that the activity of R5Q is significantly impaired compared with WT RhoA in active RhoA pull-down, SRF-RE luciferase and actin stress fiber formation assays. Based on structural modeling and known interactions, R5 appears to be directly involved in the interaction with RhoGEFs (particularly RhoGEFs 11, 12 and DBS). Although no mutations were found in the RhoGEFs most frequently activated by Gα13, p115 (ARHGEF1), LARG (ARHGEF12) or PDZ RhoGEF (ARHGEF11), this is not surprising due to the redundancy of the RhoGEFs and the opportunities for compensation.[37,38] Interestingly, inactivating or dominant-negative mutations in RhoA were recently identified in 50–70% of peripheral T-cell lymphomas,[18–22] suggesting that the Gα$_{13}$/RhoA pathway may have tumor suppressive functions in other hematological malignancies as well.

Although Gα$_{13}$ and RhoA have been associated with cellular transformation and characterized as growth promoting in fibroblasts and some epithelial cancer models, this axis appears to have the opposite effect in B-cell lymphomas. This sort of duality in function based on cellular context is not unheard of and has been observed with other key pathways, including JNK and transforming growth factor beta signaling pathways.[39,40] Although the precise mechanism by which Gα$_{13}$/RhoA axis may inhibit cell growth in B cells requires further exploration, the reduction in phosphorylated Akt (Ser473) associated with Gα$_{13}$ activity could in part affect the growth and survival of B cells.[16,17] In addition, we observed distinct morphological changes in the cells with mutant Gα$_{13}$ compared with WT Gα$_{13}$ both in the methocelluolose clonogenic assay and in the histology analysis from tumor xenografts, suggesting that other factors may have a role. Nevertheless, the reasons why Gα$_{13}$ and RhoA may exhibit pro-tumorigenic effects in some cancers while having tumor suppressive functions in other cancers requires further investigation. In this regard, once better tools become available for manipulation of B cells and B-cell lines, it will be possible to determine how disruption of GNA13 or RHOA in normal human B cells and other Burkitt's lymphoma and DLBCL lines influences their growth and morphology, thereby helping to elucidate fully the repertoire of tumor suppressive signals induced by Gα$_{13}$/RhoA in B cells.

Characterization of tumor mutations provides valuable information for how to precisely identify causes of disease and best

Figure 5. Gα$_{13}$ WT expression has tumor suppressive effects on Raji Burkitt's lymphoma xenograft tumor growth. (**a**) Sequence chromatogram of Raji cell DNA validating the presence of a heterozygous T → G mutation resulting in the L184R mutation. (**b**) Immunofluorescence imaging for GFP expression of Raji cells transduced with MSCV PIG vector control or expressing Gα$_{13}$ WT. (**c**) Western blot of Raji cells transduced with MSCV PIG vector control or expressing Gα$_{13}$ WT. Lysates were probed for Gα$_{13}$ and pAkt S473 expression and for total Akt and α-tubulin as loading controls. (**d**) Number of colonies formed in a methocellulose clonogenic assay of Raji control and Gα$_{13}$ WT-expressing cells. Data represent the averages of three independent experiments performed in duplicate or triplicate. Error indicates standard deviation and a two-tailed t-test was used to determine statistical significance. (**e**) Percentage of colonies exhibiting spheroid, flat or mixed morphologies (representative images on right) in Raji control and Gα$_{13}$ WT-expressing cells. (**f**) Tumor volume measurements (error bars represent standard error of the mean (s.e.m.)) of Raji control (n = 9) and Gα$_{13}$ WT-expressing (G13 WT, n = 10) tumor xenografts over time, starting with injections of the tumor cells at day 0. (**g**) Graphs of the mean (error bars represent s.e.m.) of final tumor masses (left) and final tumor volumes (right) of Raji control and Gα$_{13}$ WT (G13 WT) tumors. (**h**) Representative image of Raji control and Gα$_{13}$ WT tumors. A two-tailed t-test was used to determine statistical significance. (**i**) H&E staining of tissue sections from Raji control and Gα$_{13}$ WT tumors. H&E shows viable round atypical cells infiltrating skeletal muscle, aberrant mitotic figures (arrowhead) and apoptotic cells (star) in the Raji control image. H&E shows that the Raji Gα$_{13}$ WT tumor is highly necrotic with numerous ghost cells, eosinophilic cell bodies lacking nuclear structure (star) and chromatin dust (arrowhead) observed. (**j**) Quantification of necrotic area in Raji control (n = 5) and Raji Gα$_{13}$ WT (n = 5) tumors analyzed. Statistics were based on a Mann–Whitney test. (**k**) Quantification of Ki67 immunohistochemistry staining in Raji control (n = 5) and Raji Gα$_{13}$ WT (n = 5) tumors. Statistics were based on a t-test.

treatment options. Our data suggest that the mutations identified in the Gα13 signaling pathway in Burkitt's lymphoma and DLBCL tumors result in loss of function, and that restoration and/or activation of this signaling pathway may help reduce tumor growth and progression. Overall, the characterization of these mutations may enable more precise treatment in the > 10% of patients with mutations in *GNA13* and *RHOA* in DLBCL and Burkitt's lymphoma.

MATERIALS AND METHODS

Identification of interaction interfaces for mapping and structural characterization of mutations

Structures of RhoA protein and its complexes were retrieved from the PDB. Per-residue contact strengths of RhoA with each of the available co-crystallized binding partners were measured as described in Qin *et al*.[41] and Kufareva *et al*.[42] for residue side-chains only and averaged over multiple structures of homologous complexes. On the basis of this analysis, residues were classified as a part of GAP interface, GEF interface or nucleotide binding pocket. Conformational switches I and II were found to be extensively involved in binding of both GAPs and GEFs. The analysis for Gα13 was conducted similarly; however, because there are no structures of trimeric α/β/γ complexes for Gα13 and because the N-terminal helix is absent from all available structures, this part of the protein was modeled and Gβ/γ interface was mapped by homology with bovine Gαt (transducin, PDB 1got), rat Gαi1 (PDB 1gp2) and mouse Gαq (PDB 3ah8).

DNA constructs and site-directed mutagenesis

MSCV puro IRES GFP (PIG) and pBABE puro retroviral vectors were obtained from Addgene (Cambridge, MA, USA).[43,44] The SyR-Gi plasmid (also known as Gi-DREADD) was originally provided by Dr Bryan Roth, and was subcloned into the pBABE retroviral vector. Gα13 and N-terminally tagged AU5-RhoA were cloned into our in-house pCEFL vector, and mutations as indicated were prepared by site-directed mutagenesis using the Quik-Change Lightning Kit (Agilent, Santa Clara, CA, USA). Gα13-i5 chimeras were prepared by PCR substitution of the last five amino acids of Gα13 with the Gαi1 sequence including a C-I mutation to make the plasmid PTX insensitive (the last five amino acids were as follows: DIGLF). Sequences were confirmed by DNA sequence analysis (NIDCR shared resource facility). A plasmid for AP-TGFα[45] was kindly provided by Prof. Shigeki Higashiyama, Ehime University, Japan. A human dopamine D2 receptor (D2R, long isoform) was inserted into the pCAGGS expression plasmid as previously described.[27]

Genomic DNA isolation and sequencing

Raji cells were obtained from ATCC (ATCC CCL-86). Genomic DNA was isolated from 5×10^6 Raji cells using the QiaAmp DNA isolation kit (Qiagen, Valencia, CA, USA), and PCR was performed on the genomic DNA in the region surrounding the 184 amino-acid position using AccuPrime Pfx Supermix (Life Technologies, Grand Island, NY, USA). PCR primer details are included in Supplementary information.

Retrovirus production and infection

Retrovirus from MSCV PIG empty vector and expressing Gα13 WT was produced by transfection of HEK293t/17 cells in a poly-lysine coated 6-well plate with 1 μg of MSCV plasmid DNA, 0.67 μg of gag/pol and 0.33 μg of VSV-G using Turbofect transfection reagent (Life Technologies). Virus for pBABE SyR-Gi was similarly prepared by transfecting 1 μg of pBABE SyR-Gi, 0.67 μg of gag/pol and 0.33 μg of VSV-G. Viral supernatants were collected at 48 h and 72 h post transfection and filtered with 0.45 μm PVDF filters onto target cells. For HEK293 cells transduced with pBABE SyR-Gi, 6 μg/ml of polybrene was added with the viral supernatants; cells were then selected with 1 μg/ml puromycin (Life Technologies) to generate a stable line. For transduction of Raji cells with MSCV virus, Raji cells were seeded onto retronectin-coated plates (Takara, Madison, WI, USA) and centrifuged with viral supernatants at 2000 r.p.m. for 2 h and then incubated overnight at 37 °C/5% CO2. MSCV-transduced Raji cells were allowed to recover before fluorescence-activated cell sorting (FASCS) for GFP expression using a BD FACSAria III Cell Sorter (NIDCR Shared Resource Facility). Raji cells were cultured in RPMI media (Sigma, St Louis, MO, USA) supplemented with 10% fetal bovine serum.

SRF-RE luciferase assay

A SRF-RE luciferase assay was performed by seeding HEK293 cells in a poly-lysine coated 24-well plate and culturing in DMEM supplemented with 10% fetal bovine serum for 24 h. Cells were then co-transfected with 100 ng Gα13 plasmid DNA or control, 50 ng pSRF-RE-firefly luciferase reporter DNA and 20 ng pRL-renilla luciferase using lipofectamine 2000 (Life Technologies) transfection reagent. For stimulated SRF response, HEK293 cells stably transduced with SyR-Gi were similarly transfected. The day after transfection, cells were serum starved overnight in the presence of 50 ng/ml PTX (List Biological Laboratories, Campbell, CA, USA) and then stimulated for 6 h with CNO before harvesting the cells. For all SRF-luciferase assays, cells were lysed and luciferase activity was determined using Dual-Glo Luciferase Assay Kit (Promega, Madison, WI, USA). Chemiluminescence was measured using a BioTek Synergy Neo plate reader (Winooski, VT, USA), and the SRF-RE activation was calculated as the ratio of firefly to renilla luciferase levels. The assays were performed three times in duplicates and results are presented as the mean ± s.d.

Rho-GTP pull-down assay and western blot

Antibodies to RhoA (catalog #2117), pAkt (Ser473) (catalog #4060), Akt (catalog #9272) and α-tubulin (catalog #3873) were obtained from Cell Signaling Technology (Danvers, MA, USA). Gα13 antibody was obtained from Santa Cruz (Santa Cruz, CA, USA; catalog #sc-26788). Cells for western blot lysates were lysed on ice in RIPA buffer (Sigma) containing protease and phosphatase inhibitors (Thermo Scientific, Pittsburgh, PA, USA) and clarified by centrifugation at 13 000 r.p.m. for 10 min at 4 °C. The relative Gα13 protein expression levels were quantified by densitometry using ImageJ and normalized to α-tubulin; data represent an average of three independent western blots (mean ± standard deviation). GST-tagged Rhotekin RBD beads were purchased from Millipore (Billerica, MA, USA) for pull-down assays to detect active RhoA. HEK293 cells were seeded in 6-cm plates and transfected with Lipofectamine 2000 for 48 h with 4 μg of plasmid DNAs. Cells were serum starved overnight and harvested for pull downs with 350 μl of recommended lysis buffer. Lysates were clarified, and 50 μl of lysate was saved for input and the remaining lysate was rotated in tubes with the GST-tagged Rhotekin RBD beads. zA 3-min thrombin (Sigma) stimulation (1 U/ml) was used as a positive control. Lysates were resolved on SDS–PAGE gels, transferred onto PVDF membranes (Millipore), probed with appropriate antibodies and developed with ECL and film (GE Healthcare, Piscataway, NJ, USA) or scanned on an Odyssey Imager (Licor, Lincoln, NE, USA).

Tumor xenograft model and tissue analysis

Ten-week-old female NOD-*scid* IL2Rgamma[null] (NOD.Cg-*Prkdc*[scid] *Il2rg*[tm1Wjl]/SzJ) mice were obtained from the Jackson Laboratory (Bar Harbor, ME, USA) and randomly assigned for injection with tumor cells. Raji cells transduced with MSCV PIG control or MSCV PIG Gα13 WT were resuspended in phosphate-buffered saline (PBS), and 5×10^6 cells in a 200-μl volume were injected into the right and left flanks of five mice for each group (ten tumors in total for each group. One injection was excluded from the Raji control group due to an injection error). Tumors were monitored 2–3 times a week, and mice were killed all together once the largest tumors reached approximately 1 cm^3 volume. Tumor measurements were performed by a blinded individual and the measurements were recorded by an unblinded person. An initial pilot study was performed with four tumors in each group, which was used to determine the appropriate sample size. This study was then expanded and repeated two more times; data trends were the same in all three experiments. Necropsies were performed and tumors were weighed, measured and imaged and tumor sections were cut and fixed in z-fix and embedded in paraffin for histology and immunohis-tochemistry analysis as previously described[46] and elaborated in Supplementary information. Individual data points are shown in the scatter dot plots to indicate variance in the data and indicate the mean ± s.e.m. These animal studies were carried out according to National Institutes of Health (NIH) approved protocols (ASP #13-695) in compliance with the NIH Guide for the Care and Use of Laboratory Mice.

TGFα shedding assay

TGFα shedding assay was performed as described previously[27] and as detailed in Supplementary information. Briefly, HEK293A cells were seeded in 12-well plates and transfected using lipofectamine 2000 (Life Technologies) with a combination of the following plasmids: AP-TGFα-

encoding plasmid, a GPCR-encoding plasmid and a Gα-encoding plasmid. After 24 h, cells were harvested with a trypsin-EDTA solution, washed with D-PBS, suspended in Hank's balanced salt solution containing 5 mM HEPES (pH 7.4), seeded in a 96-well plate and incubated for 30 min. The seeded cells were treated with various concentrations of a GPCR ligand (10 μl/well) and incubated for 1 h. Conditioned media (CM, 80 μl/well) was transferred into a blank 96-well plate. Alkaline phosphatase (AP) solution was added to both the conditioned media plate and the cell plate (80 μl/well). Absorbance at 405 nm of the two plates was measured before and after 1 h incubation at room temperature, using a SpectraMax 340PC384 microplate reader (Molecular Devices, Sunnyvale, CA, USA). TGFα shedding data are shown as the mean ± s.d.

Spontaneous activity of Gα$_{13}$ was measured by a previously described method with a slight modification.[47] Briefly, HEK293A cells were seeded in 96-well plates in Opti-MEM (80 μl/well), transfected with lipofectamine 2000 reagent (0.1 μl/well), the AP-TGFα-encoding plasmids (20 ng/well), Gα$_{13}$-encoding plasmid (5–20 ng/well) and the pCEFL vector plasmid, which was used to adjust total volume of transfected plasmid. After adding the transfection solution, the cells were incubated for 24 h and then AP-TGFα release was measured as described above.

Actin stress fiber formation and confocal imaging

MDCK cells were seeded onto poly-lysine coated glass coverslips (Fisher, Hanover Park, IL, USA) in a 6-well plate and transfected with 1 μg LifeActin GFP and 1 μg of pCEFL RhoA plasmid or vector control using lipofectamine 2000. Cells for immunofluorescence imaging were washed with PBS and fixed with 2% formaldehyde–PBS solution for 12 min at room temperature. Fixed cells were washed twice with PBS and then mounted onto glass slides (Thermo Scientific/Fisher) with Fluorosave (Millipore/Calbiochem) mounting solution. Confocal images were collected on a Zeiss LSM-700 laser scanning microscope (Thornwood, NY, USA) with a ×40 oil immersion lens using 488 nm excitation for the LifeActin GFP.

Methocellulose clonogenic assay

Methocult (H4434) was purchased from Stem Cell Technologies (Vancouver, BC, Canada) and a clonogenic assay was performed by seeding 2000 Raji cells in 1 ml of Methocult in triplicate in a 6-well plate. Colonies were allowed to grow for 14 days, and then number of colonies per well and morphology of the colonies were analyzed. Results are shown as the mean ± s.d. Statistics were calculated using GraphPad Prism 6 (Graph Pad Software, San Diego, CA, USA) using a paired *t*-test.

REFERENCES

1 Dorsam RT, Gutkind JS. G-protein-coupled receptors and cancer. *Nat Rev Cancer* 2007; **7**: 79–94.

2 Garcia-Marcos M, Ghosh P, Farquhar MG. GIV/Girdin transmits signals from multiple receptors by triggering trimeric G protein activation. *J Biol Chem* 2015; **290**: 6697–6704.

3 O'Hayre M, Vazquez-Prado J, Kufareva I, Stawiski EW, Handel TM, Seshagiri S *et al*. The emerging mutational landscape of G proteins and G-protein-coupled receptors in cancer. *Nat Rev Cancer* 2013; **13**: 412–424.

4 Feng X, Degese MS, Iglesias-Bartolome R, Vaque JP, Molinolo AA, Rodrigues M *et al*. Hippo-independent activation of YAP by the GNAQ uveal melanoma oncogene through a trio-regulated rho GTPase signaling circuitry. *Cancer Cell* 2014; **25**: 831–845.

5 Van Raamsdonk CD, Bezrookove V, Green G, Bauer J, Gaugler L, O'Brien JM *et al*. Frequent somatic mutations of GNAQ in uveal melanoma and blue naevi. *Nature* 2009; **457**: 599–602.

6 Van Raamsdonk CD, Griewank KG, Crosby MB, Garrido MC, Vemula S, Wiesner T *et al*. Mutations in GNA11 in uveal melanoma. *N Engl J Med* 2010; **363**: 2191–2199.

7 Dhanasekaran N, Heasley LE, Johnson GL. G protein-coupled receptor systems involved in cell growth and oncogenesis. *Endocr Rev* 1995; **16**: 259–270.

8 Kelly P, Moeller BJ, Juneja J, Booden MA, Der CJ, Daaka Y *et al*. The G12 family of heterotrimeric G proteins promotes breast cancer invasion and metastasis. *Proc Natl Acad Sci USA* 2006; **103**: 8173–8178.

9 Kelly P, Stemmle LN, Madden JF, Fields TA, Daaka Y, Casey PJ. A role for the G12 family of heterotrimeric G proteins in prostate cancer invasion. *J Biol Chem* 2006; **281**: 26483–26490.

10 Gutkind JS, Coso OA, Xu NG12 and G13 α subunits of heterotrimeric G proteins: a novel family of oncogenesIn:SA Med. *G Proteins, Receptors, and Disease*. Humana Press: Totowa, NJ, USA, 1998, pp 101–117.

11 Juneja J, Casey PJ. Role of G12 proteins in oncogenesis and metastasis. *Br J Pharmacol* 2009; **158**: 32–40.

12 Xu N, Bradley L, Ambdukar I, Gutkind JS. A mutant alpha subunit of G12 potentiates the eicosanoid pathway and is highly oncogenic in NIH 3T3 cells. *Proc Natl Acad Sci USA* 1993; **90**: 6741–6745.

13 Xu N, Voyno-Yasenetskaya T, Gutkind JS. Potent transforming activity of the G13 alpha subunit defines a novel family of oncogenes. *Biochem Biophys Res Commun* 1994; **201**: 603–609.

14 Love C, Sun Z, Jima D, Li G, Zhang J, Miles R *et al*. The genetic landscape of mutations in Burkitt lymphoma. *Nat Genet* 2012; **44**: 1321–1325.

15 Lohr JG, Stojanov P, Lawrence MS, Auclair D, Chapuy B, Sougnez C *et al*. Discovery and prioritization of somatic mutations in diffuse large B-cell lymphoma (DLBCL) by whole-exome sequencing. *Proc Natl Acad Sci USA* 2012; **109**: 3879–3884.

16 Green JA, Suzuki K, Cho B, Willison LD, Palmer D, Allen CD *et al*. The sphingosine 1-phosphate receptor S1P(2) maintains the homeostasis of germinal center B cells and promotes niche confinement. *Nat Immunol* 2011; **12**: 672–680.

17 Muppidi JR, Schmitz R, Green JA, Xiao W, Larsen AB, Braun SE *et al*. Loss of signalling via Galpha13 in germinal centre B-cell-derived lymphoma. *Nature* 2014; **516**: 254–258.

18 Yoo HY, Sung MK, Lee SH, Kim S, Lee H, Park S *et al*. A recurrent inactivating mutation in RHOA GTPase in angioimmunoblastic T cell lymphoma. *Nat Genet* 2014; **46**: 371–375.

19 Sakata-Yanagimoto M, Enami T, Yoshida K, Shiraishi Y, Ishii R, Miyake Y *et al*. Somatic RHOA mutation in angioimmunoblastic T cell lymphoma. *Nat Genet* 2014; **46**: 171–175.

20 Cools J. RHOA mutations in peripheral T cell lymphoma. *Nat Genet* 2014; **46**: 320–321.

21 Manso R, Sanchez-Beato M, Monsalvo S, Gomez S, Cereceda L, Llamas P *et al*. The RHOA G17V gene mutation occurs frequently in peripheral T-cell lymphoma and is associated with a characteristic molecular signature. *Blood* 2014; **123**: 2893–2894.

22 Palomero T, Couronne L, Khiabanian H, Kim MY, Ambesi-Impiombato A, Perez-Garcia A *et al*. Recurrent mutations in epigenetic regulators, RHOA and FYN kinase in peripheral T cell lymphomas. *Nat Genet* 2014; **46**: 166–170.

23 Fromm C, Coso OA, Montaner S, Xu N, Gutkind JS. The small GTP-binding protein Rho links G protein-coupled receptors and Galpha12 to the serum response element and to cellular transformation. *Proc Natl Acad Sci USA* 1997; **94**: 10098–10103.

24 Hart MJ, Jiang X, Kozasa T, Roscoe W, Singer WD, Gilman AG *et al*. Direct stimulation of the guanine nucleotide exchange activity of p115 RhoGEF by Galpha13. *Science* 1998; **280**: 2112–2114.

25 Kozasa T, Jiang X, Hart MJ, Sternweis PM, Singer WD, Gilman AG *et al*. p115 RhoGEF, a GTPase activating protein for Galpha12 and Galpha13. *Science* 1998; **280**: 2109–2111.

26 Armbruster BN, Li X, Pausch MH, Herlitze S, Roth BL. Evolving the lock to fit the key to create a family of G protein-coupled receptors potently activated by an inert ligand. *Proc Natl Acad Sci USA* 2007; **104**: 5163–5168.

27 Inoue A, Ishiguro J, Kitamura H, Arima N, Okutani M, Shuto A *et al*. TGFalpha shedding assay: an accurate and versatile method for detecting GPCR activation. *Nat Methods* 2012; **9**: 1021–1029.

28 Jaffe ES, Pittaluga S. Aggressive B-cell lymphomas: a review of new and old entities in the WHO classification. *Hematology* 2011; **2011**: 506–514.

29 Roschewski M, Staudt LM, Wilson WH. Diffuse large B-cell lymphoma-treatment approaches in the molecular era. *Nat Rev Clin Oncol* 2014; **11**: 12–23.

30 Rasheed SA, Teo CR, Beillard EJ, Voorhoeve PM, Casey PJ. MicroRNA-182 and microRNA-200a control G-protein subunit alpha-13 (GNA13) expression and cell invasion synergistically in prostate cancer cells. *J Biol Chem* 2013; **288**: 7986–7995.

31 Kelly P, Casey PJ, Meigs TE. Biologic functions of the G12 subfamily of heterotrimeric g proteins: growth, migration, and metastasis. *Biochemistry* 2007; **46**: 6677–6687.

32 Yagi H, Tan W, Dillenburg-Pilla P, Armando S, Amornphimoltham P, Simaan M *et al*. A synthetic biology approach reveals a CXCR4-G13-Rho signaling axis driving transendothelial migration of metastatic breast cancer cells. *Science Signal* 2011; **4**: ra60.

33 Cattoretti G, Mandelbaum J, Lee N, Chaves AH, Mahler AM, Chadburn A *et al*. Targeted disruption of the S1P2 sphingosine 1-phosphate receptor gene leads to diffuse large B-cell lymphoma formation. *Cancer Res* 2009; **69**: 8686–8692.

34 Morin RD, Mendez-Lago M, Mungall AJ, Goya R, Mungall KL, Corbett RD *et al*. Frequent mutation of histone-modifying genes in non-Hodgkin lymphoma. *Nature* 2011; **476**: 298–303.

35 Menon MP, Pittaluga S, Jaffe ES. The histological and biological spectrum of diffuse large B-cell lymphoma in the World Health Organization classification. *Cancer J* 2012; **18**: 411–420.

36 Rohde M, Richter J, Schlesner M, Betts MJ, Claviez A, Bonn BR *et al*. Recurrent RHOA mutations in pediatric Burkitt lymphoma treated according to the NHL-BFM protocols. *Genes Chromosomes Cancer* 2014; **53**: 911–916.

37 Fukuhara S, Chikumi H, Gutkind JS. RGS-containing RhoGEFs: the missing link between transforming G proteins and Rho? *Oncogene* 2001; **20**: 1661–1668.

38 Mikelis CM, Palmby TR, Simaan M, Li W, Szabo R, Lyons R *et al*. PDZ-RhoGEF and LARG are essential for embryonic development and provide a link between thrombin and LPA receptors and Rho activation. *J Biol Chem* 2013; **288**: 12232–12243.

39 Liu J, Lin A. Role of JNK activation in apoptosis: a double-edged sword. *Cell Res* 2005; **15**: 36–42.

40 Bachman KE, Park BH. Duel nature of TGF-beta signaling: tumor suppressor vs. tumor promoter. *Curr Opin Oncol* 2005; **17**: 49–54.

41 Qin L, Kufareva I, Holden LG, Wang C, Zheng Y, Zhao C *et al*. Structural biology. Crystal structure of the chemokine receptor CXCR4 in complex with a viral chemokine. *Science* 2015; **347**: 1117–1122.

42 Kufareva I, Rueda M, Katritch V, Stevens RC, Abagyan R. Status of GPCR modeling and docking as reflected by community-wide GPCR Dock 2010 assessment. *Structure* 2011; **19**: 1108–1126.

43 Mayr C, Bartel DP. Widespread shortening of 3'UTRs by alternative cleavage and polyadenylation activates oncogenes in cancer cells. *Cell* 2009; **138**: 673–684.

44 Morgenstern JP, Land H. Advanced mammalian gene transfer: high titre retroviral vectors with multiple drug selection markers and a complementary helper-free packaging cell line. *Nucleic Acids Res* 1990; **18**: 3587–3596.

45 Tokumaru S, Higashiyama S, Endo T, Nakagawa T, Miyagawa JI, Yamamori K *et al*. Ectodomain shedding of epidermal growth factor receptor ligands is required for keratinocyte migration in cutaneous wound healing. *J Cell Biol* 2000; **151**: 209–220.

46 Wang Z, Martin D, Molinolo AA, Patel V, Iglesias-Bartolome R, Degese MS *et al*. mTOR co-targeting in cetuximab resistance in head and neck cancers harboring PIK3CA and RAS mutations. *J Natl Cancer Inst* 2014; **106**: 1–11.

47 Inoue A, Arima N, Ishiguro J, Prestwich GD, Arai H, Aoki J. LPA-producing enzyme PA-PLA(1)alpha regulates hair follicle development by modulating EGFR signalling. *EMBO J* 2011; **30**: 4248–4260.

Supplementary Information accompanies this paper on the Oncogene website (http://www.nature.com/onc)

npg

SIRT1 is involved in oncogenic signaling mediated by GPER in breast cancer

MF Santolla[1], S Avino[1], M Pellegrino[1], EM De Francesco[1], P De Marco[1], R Lappano[1], A Vivacqua[1], F Cirillo[1], DC Rigiracciolo[1], A Scarpelli[1], S Abonante[2] and M Maggiolini*,[1]

A number of tumors exhibit an altered expression of sirtuins, including NAD$^+$-dependent histone deacetylase silent information regulator 1 (SIRT1) that may act as a tumor suppressor or tumor promoter mainly depending on the tumor types. For instance, in breast cancer cells SIRT1 was shown to exert an essential role toward the oncogenic signaling mediated by the estrogen receptor-α (ERα). In accordance with these findings, the suppression of SIRT1 led to the inhibition of the transduction pathway triggered by ERα. As the regulation of SIRT1 has not been investigated in cancer cells lacking ER, in the present study we ascertained the expression and function of SIRT1 by estrogens in ER-negative breast cancer cells and cancer-associated fibroblasts obtained from breast cancer patients. Our results show that 17β-estradiol (E2) and the selective ligand of GPER, namely G-1, induce the expression of SIRT1 through GPER and the subsequent activation of the EGFR/ERK/c-fos/AP-1 transduction pathway. Moreover, we demonstrate that SIRT1 is involved in the pro-survival effects elicited by E2 through GPER, like the prevention of cell cycle arrest and cell death induced by the DNA damaging agent etoposide. Interestingly, the aforementioned actions of estrogens were abolished silencing GPER or SIRT1, as well as using the SIRT1 inhibitor Sirtinol. In addition, we provide evidence regarding the involvement of SIRT1 in tumor growth stimulated by GPER ligands in breast cancer cells and xenograft models. Altogether, our data suggest that SIRT1 may be included in the transduction network activated by estrogens through GPER toward the breast cancer progression.
Cell Death and Disease (2015) 6, e1834; doi:10.1038/cddis.2015.201; published online 30 July 2015

Estrogens are involved in multiple patho-physiological processes, including the development of diverse types of tumors.[1,2] For instance, in breast cancer cells 17β-estradiol (E2) triggers stimulatory effects binding to the estrogen receptor-α (ERα) and ERβ that regulate the expression of genes which contribute to cell proliferation, migration and survival.[3,4] In the last few years, increasing evidence have demonstrated that the G-protein ER (GPER, formerly known as GPR30), can mediate the action of estrogens and certain antiestrogens in both normal and malignant cells.[5–9] The ligand binding to GPER induces the release of the membrane-tethered heparin-bound epidermal growth factor, which binds to and activate the epidermal growth factor receptor (EGFR).[10,11] Then, the transactivation of EGFR stimulates a transduction network which includes calcium mobilization, MAPK and PI3-K activation in cancer cells and cancer-associated fibroblasts (CAFs), suggesting that GPER may trigger a functional interaction between tumor cells and important components of the tumor micro-environment.[10,11–13] As ascertained by microarray analysis,[10] GPER regulates a peculiar gene signature involved in the stimulation of estrogen-sensitive malignancies.[7,10,14,15] In accordance with these findings, GPER has been associated with negative clinical features and poor survival rates in patients with breast, endometrial and ovarian carcinomas.[5]

Recent studies have linked an altered expression of sirtuins family members with several diseases, including different types of tumors.[16] In particular, the NAD$^+$-dependent histone deacetylase silent information regulator 1 (SIRT1) deacetylates several histone and non-histone proteins, leading to the inactivation of tumor-suppressor genes and further target proteins.[16] SIRT1 influences many hallmarks of longevity, gene silencing, cell cycle progression, differentiation and apoptosis and was found upregulated in a variety of malignancies.[17,18] The role of SIRT1 in cancer has been extensively evaluated, however, its potential to act as tumor promoter or suppressor remains controversial.[19–21] For instance, SIRT1-mediated deacetylation repressed the functions of several tumor suppressors like p53, p73 and HIC1, suggesting that SIRT1 may be involved in tumor progression.[22,23] In contrast, SIRT1 exerted anti-proliferative effects through the inhibition of NF-κB,[24,25] a transcription factor having a central role in the regulation of the immune response and carcinogenesis.[26] As it concerns breast cancer, tumor samples displayed elevated levels of SIRT1 with respect to non-transformed counterparts and the expression of SIRT1 was upregulated by estrogens through ERα.[17,18] In addition, it was demonstrated that ERα physically interacts and functionally cooperates with SIRT1 toward the stimulation of breast tumor cells.[18] In accordance with these findings, the inhibition of SIRT1 led to the inhibition of ER-mediated signaling, thus

[1]Department of Pharmacy, Health and Nutritional Sciences, University of Calabria, Rende, Italy and [2]Breast Cancer Unit, Regional Hospital, Cosenza, Italy
*Corresponding author: M Maggiolini, Department of Pharmacy, Health and Nutritional Sciences, University of Calabria, Rende 87036, Italy. Tel: +39 09 8449 3076; Fax: +39 09 8449 3458; E-mail: marcellomaggiolini@yahoo.it
Abbreviations: GPER, G-protein estrogen receptor; CAFs, cancer-activated fibroblasts; SIRT1, silent information regulator 1; EGFR, epidermal growth factor receptor; ERK, extracellular signal-regulated kinase; AP-1, activator protein 1; HDACs, histone deacetylases

indicating that SIRT1 may act as a co-activator of ERα.[27] In the present study, using the GPER-positive and ER-negative SkBr3 breast cancer cells and CAFs obtained from breast cancer patients, we demonstrate that estrogens upregulate SIRT1 expression through the GPER/EGFR/ERK/c-fos/AP-1 transduction pathway. Moreover, we disclose that GPER and SIRT1 have an important role in the pro-survival effects prompted by E2 and the selective GPER ligand G-1 in cancer cells and CAFs treated with etoposide. Noteworthy, SIRT1 contributes to tumor growth elicited by ligand-activated GPER as assessed both *in vitro* as well as in breast tumor xenografts. Collectively, our data provide novel insights into the multifaceted action triggered by estrogenic GPER signaling, which engages also SIRT1, toward breast cancer progression.

Results

E2 and G-1 induce SIRT1 expression in ER-negative SkBr3 cells and CAFs.

Previous studies have reported that SIRT1 expression is upregulated by estrogens through ERα in breast cancer cells.[10,18] Hence, we aimed to evaluate whether estrogens may regulate SIRT1 levels also in ER-negative cancer cells. To this end, we used as a model system the SkBr3 breast cancer cells and CAFs, that are both ER-negative and GPER-positive (Supplementary Figure 1). In time course experiments, E2 and G-1 upregulated SIRT1

expression at both mRNA and protein levels, as determined by real-time PCR (Figures 1a and b) and confirmed by a semi-quantitative PCR evaluation (data not shown).[28] In line with these results, immunoblotting studies revealed that SIRT1 protein levels are also induced by E2 and G-1 in SkBr3 cells (Figures 1c and d) and CAFs (Figures 1e and f).

SIRT1 expression is regulated by estrogens through GPER along with the EGFR/ERK/c-fos/AP-1 transduction pathway.

These findings prompted us to evaluate the molecular mechanisms involved in the upregulation of SIRT1 elicited by estrogens in our experimental models. Silencing GPER through a specific short-hairpin GPER construct (shGPER) in SkBr3 cells and CAFs, E2 and G-1 lost the ability to increase SIRT1 expression (Figures 2a and d), suggesting that GPER mediates this effect in both cell types. Next, we found that the upregulation of SIRT1 upon E2 and G-1 treatments is abrogated in the presence of the EGFR inhibitor AG1478 (AG) or the MEK inhibitor PD98059 (PD), whereas the PKA and PI3-K inhibitors, namely H89 and LY294002 (LY), respectively, had no effect (Figures 2e and h). In accordance with these data, E2 and G-1 induced a rapid activation of both EGFR and ERK in SkBr3 cells and CAFs (Figures 2i and j). As the GPER/EGFR/ERK transduction signaling triggers c-fos expression,[6,13,15] we determined the occurrence of this response to E2 and G-1 in both SkBr3 cells
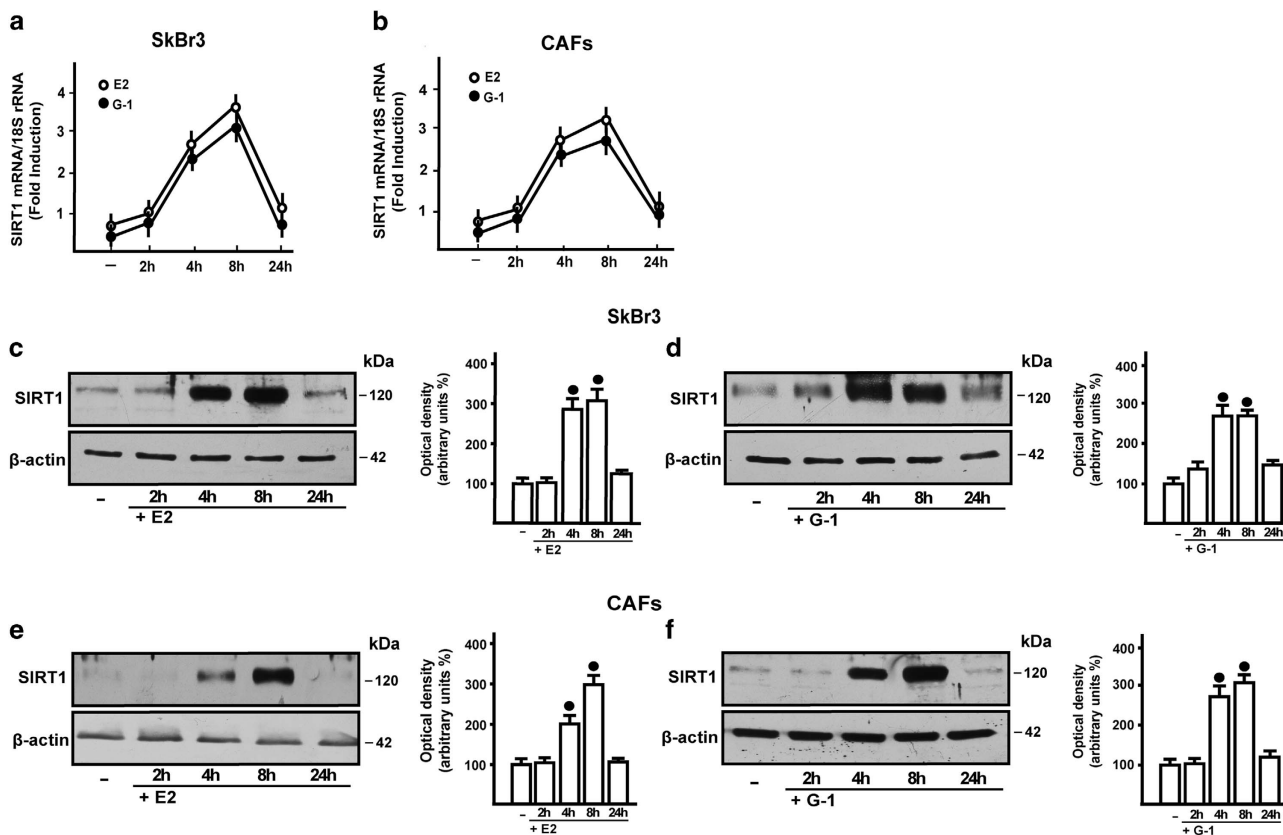
Figure 1 E2 and G-1 induce SIRT1 expression. In SkBr3 cells and CAFs, 100 nM E2 and 1 μM G-1 upregulate the mRNA (**a** and **b**) and protein levels (**c–f**) of SIRT1, as evaluated respectively by real-time PCR and immunoblotting. In RNA experiments, gene expression was normalized to 18 S expression and results are shown as fold changes of mRNA expression compared with the cells treated with vehicle (−). Side panels show densitometric analyses of the blots normalized to β-actin. Each data point represents the mean ± S.D. of three independent experiments. • indicates $P < 0.05$ for cells receiving vehicle (−) *versus* treatments
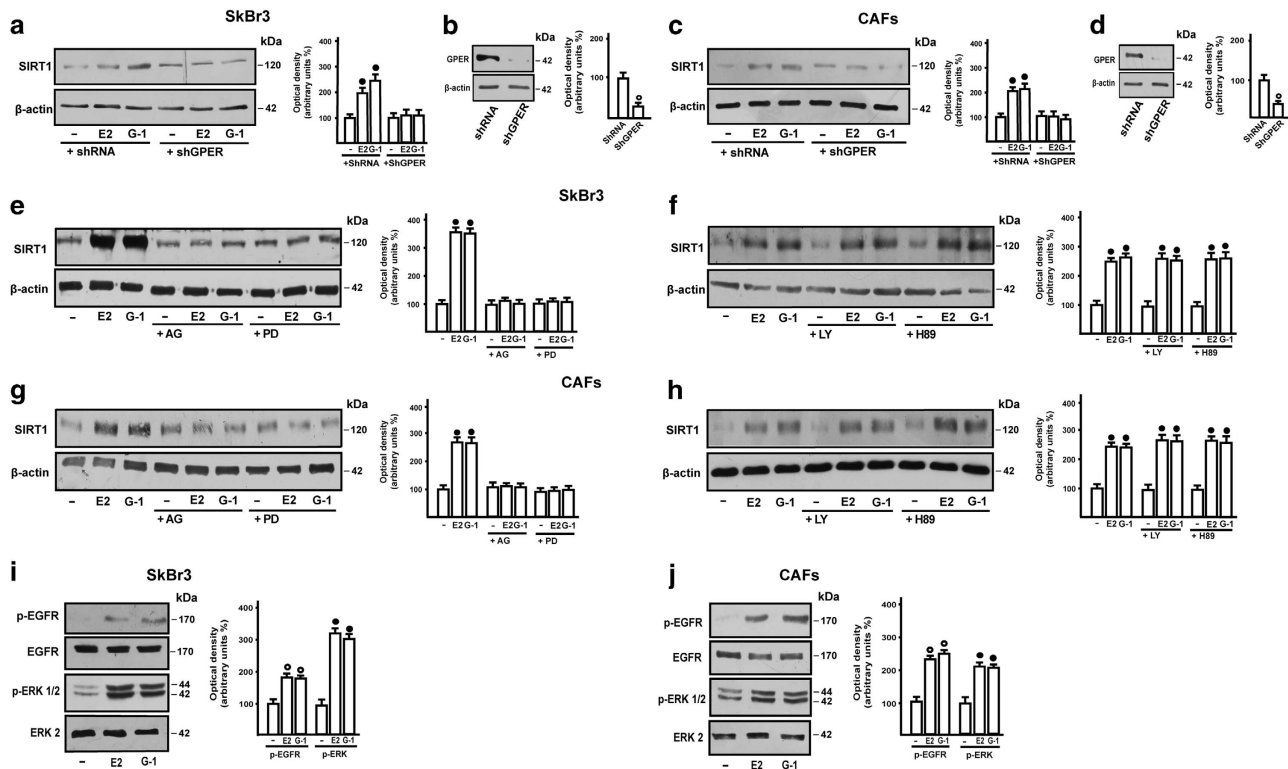
Figure 2 The upregulation of SIRT1 protein levels by E2 and G-1 is mediated by the GPER/EGFR/ERK transduction pathway. SIRT1 protein expression induced by 100 nM E2 and 1 μM G-1 is abolished in SkBr3 cells (**a**) and CAFs (**c**) by silencing GPER with a shGPER construct (**b** and **d**). SIRT1 protein expression in SkBr3 cells (**e** and **f**) and CAFs (**g** and **h**) treated for 8 h with vehicle (−), 100 nM E2 and 1 μM G-1 alone and in combination with 10 μM EGFR inhibitor AG1478 (AG), 10 μM MEK inhibitor PD98089 (PD), 10 μM PKA inhibitor H89, 10 μM PI3-K inhibitor LY294002 (LY), as indicated. ERK1/2 activation and EGFR^{Tyr1173} phosphorylation in SkBr3 cells (**i**) and CAFs (**j**) treated with vehicle (−), 100 nM E2 and 1 μM G-1 for 15 min. Side panels show densitometric analyses of the blots normalized to β-actin for SIRT1 expression, ERK2 for p-ERK1/2, EGFR for p-EGFR. Each data point represents the mean $\pm$ S.D. of three independent experiments. •, ° indicate $P < 0.05$ for cells receiving vehicle (−) versus treatments

and CAFs (Figures 3a and b), then establishing that both ligands prompt the recruitment of c-fos to the AP-1 site located within the promoter sequence of SIRT1 (Figures 3c and d). Further supporting these results, the transactivation of the SIRT1 promoter construct by E2 and G-1 was abolished co-transfecting a dominant negative form of c-fos (DN/c-fos; Figures 3e and f). Taken together, the aforementioned findings suggest that GPER along with the EGFR/ERK/c-fos/AP-1 transduction pathway mediate SIRT1 expression induced by E2 and G-1.

SIRT1 is involved in the pro-survival effects elicited by estrogens through GPER. Previous studies have reported that E2 through ERα protects breast cancer cells from oxidative stress and DNA injury.[29] DNA damage triggers p53 protein acetylation which leads to cell cycle arrest.[30] This process is mediated by many mechanisms and factors, including the increased expression of the cell cycle inhibitor p21, which facilitates cell accumulation in G0/G-1 phase in order to allow the repair of the damaged DNA.[31] As p21 expression is controlled by p53 which is regulated by SIRT1, for instance through deacetylation at Lys382 residue,[23] we investigated the role of SIRT1 in the pro-survival effects elicited by E2 and G-1 via GPER. In this regard, we performed western blot analysis to examine the p53 acetylation at residue Lys382 and the expression levels of p21 in SkBr3 cells and CAFs upon treatment with the DNA

damaging agent etoposide (ETO), which was also used in combination with E2 and G-1. As shown in Figures 4a–d, the treatment with E2 and G-1 prevented the activation of p53 and the increase of p21 protein levels triggered by ETO. Of note, this effect was abrogated in both cell types silencing GPER expression by a shGPER construct (Figures 4a and d and Supplementary Figure 2) or treating cells with the SIRT1 inhibitor namely Sirtinol (Figures 4e and h). Next, we performed cell cycle analysis determining that E2 prevents cell cycle arrest induced by ETO in SkBr3 cells and CAFs, however, this effect was no longer evident silencing GPER or in the presence of Sirtinol (Figures 5a and d). Then, we analyzed by TUNEL assay the involvement of GPER and SIRT1 in the pro-survival effects elicited by E2 in ETO-induced apoptosis. The DNA fragmentation induced by ETO was prevented treating with E2 both SkBr3 cells (Figure 6) and CAFs (Supplementary Figure 3), however the effect of E2 was abrogated silencing GPER, using the SIRT1 inhibitor Sirtinol or silencing SIRT1 expression with shSIRT1 (Supplementary Figure 4). Collectively, these findings suggest that GPER and SIRT1 contribute to the protective effects of estrogens upon exposure to the DNA damaging agent ETO.

GPER and SIRT1 promote tumor growth both *in vitro* and *in vivo*. In order to evaluate the potential of GPER along with SIRT1 to stimulate growth effects, we first assessed that in
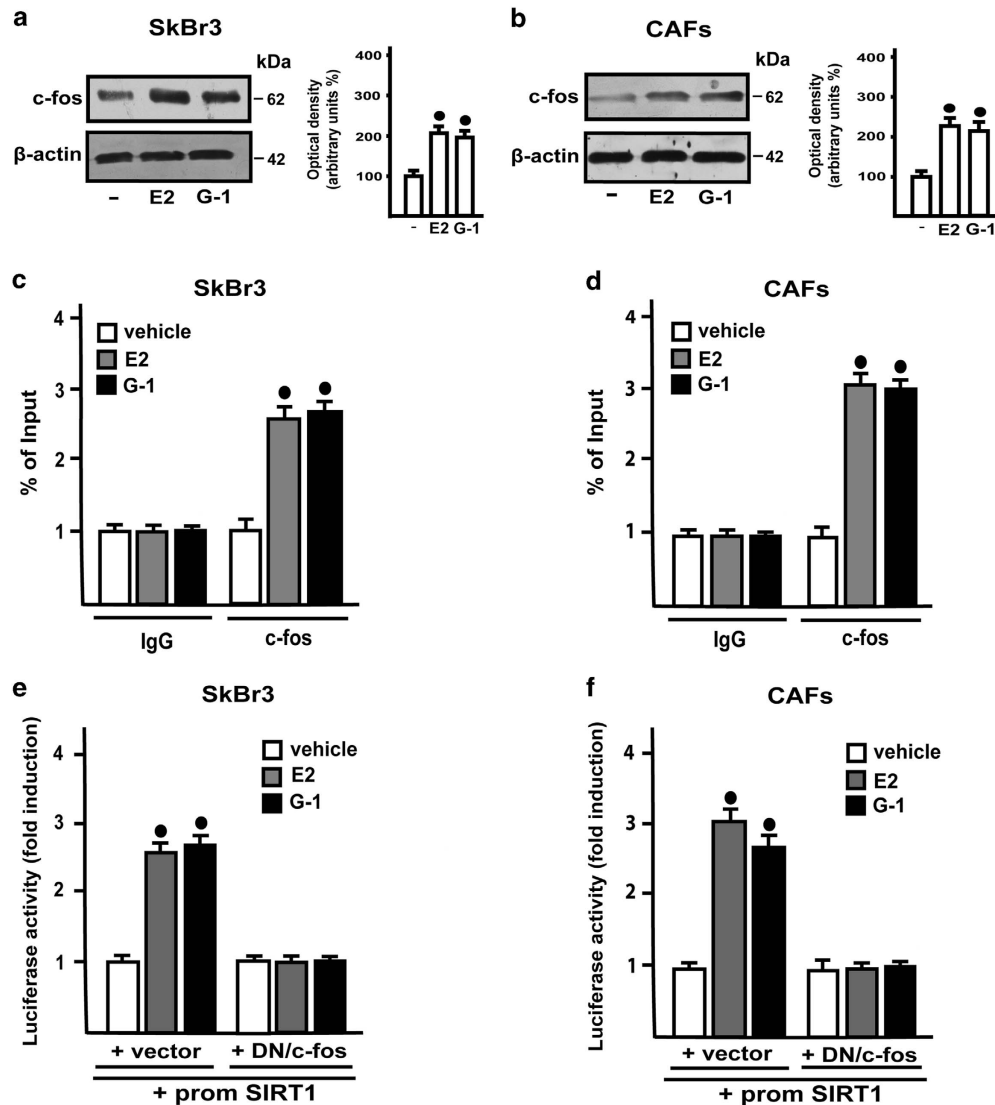
Figure 3 E2 and G-1 induce the expression of c-fos which is recruited to the AP-1 site located within the SIRT1 promoter sequence. In SkBr3 cells (**a**) and CAFs (**b**), the treatment with 100 nM E2 and 1 μM G-1 for 2 h upregulate c-fos, which is recruited to the AP-1 site located within the SIRT1 promoter sequence (**c** and **d**), as ascertained by ChiP assay. The transactivation of the SIRT1 promoter construct induced by an 18 h treatment with 100 nM E2 and 1 μM G-1 is prevented transfecting cells with a construct encoding for a dominant negative form of c-fos (DN/c-fos) (**e** and **f**). In immunoblotting, side panels show densitometric analyses of the blots normalized to β-actin. Each data point represents the mean $\pm$ S.D. of three independent experiments. $^\bullet$ indicates $P < 0.05$ for cells receiving vehicle ($-$) *versus* treatments. Each transfection experiment was performed in triplicate, the luciferase activities from three independent experiments were normalized to the internal transfection control and values for cells receiving vehicle were set as 1 fold induction upon which the activities induced by treatments were calculated

SkBr3 cells the induction of Cyclin D1 by E2 and G-1 is abolished silencing GPER expression, as well as in the presence of the DN/c-fos construct or Sirtinol (Figures 7a and e). In agreement with these results, the proliferation of SkBr3 cells upon exposure to E2 and G-1 was no longer evident of knocking down GPER expression (Figure 7f), in the presence of the DN/c-fos construct (Figure 7g) or Sirtinol (Figure 7h), as well as silencing SIRT1 expression (Figure 7i). Afterward, we evaluated the influence of SIRT1 on tumor growth *in vivo* in 45-day-old female nude mice bearing into the intrascapular region the SkBr3 cells. Tumor xenografts were treated with vehicle, G-1 at 0.5 mg/kg/day alone and in combination with Sirtinol at 10 mg/kg/day.[32–34] These administrations were well tolerated as no change in body weight or in food and water

consumption was observed together with no evidence of reduced motor function. No significant difference in the mean weights or histologic features of the major organs (liver, lung, spleen and kidney) was also detected after killing among vehicle and ligand-treated mice, thus indicating a lack of toxic effects. After 40 days of treatment, histologic examination of SkBr3 xenografts revealed that tumors explanted were primarily composed of human epithelial cells (Supplementary Figure 5). Moreover, we assessed that tumor growth induced by G-1 is prevented by Sirtinol (Figures 8a and b). Of note, increased Cyclin D1, Ki-67 and SIRT1 protein levels were found in tumor homogenates obtained from G-1 stimulated mice with respect to mice treated with vehicle, however, these stimulatory effects were prevented in the group of animals
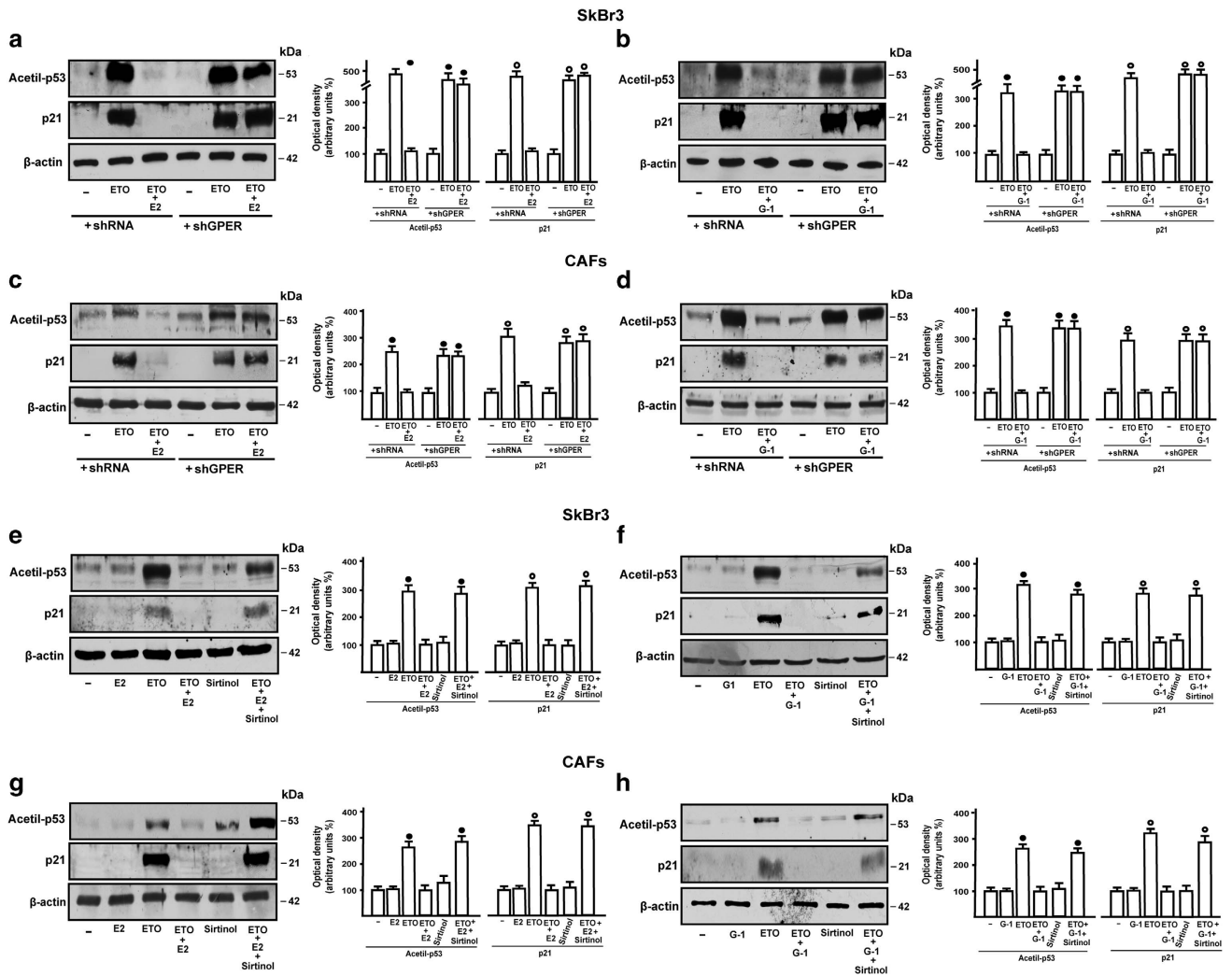
Figure 4 p53 acetylation and p21 upregulation induced by etoposide (ETO) are prevented by E2 and G-1 through GPER and SIRT1. SkBr3 cells (**a** and **b**) and CAFs (**c** and **d**) were transfected with shRNA or shGPER and then treated for 6 h with vehicle (−), 20 μM ETO alone and in combination with 100 nM E2 and 1 μM G-1. Immunoblots showing p53 acetylation at residue Lys382 and p21 protein expression in SkBr3 cells (**e** and **f**) and CAFs (**g** and **h**) treated for 6 h with vehicle (−), 20 μM ETO alone and in combination with 100 nM E2, 1 μM G-1 and 25 μM Sirtinol. Side panels show densitometric analysis of the blots normalized to β-actin. Each data point represents the mean $\pm$ S.D. of three independent experiments. •, ° indicate $P < 0.05$ for cells receiving vehicle (−) *versus* treatments

receiving G-1 in combination with Sirtinol (Figure 8c). Taken together, these results indicate that SIRT1 is also involved in tumor growth prompted by G-1 *in vivo*.

Discussion

In the present study, we provide novel insights into the regulation and function of SIRT1 by estrogens in ER-negative breast cancer cells and CAFs. In particular, we demonstrate that E2 and the selective GPER agonist G-1 induce SIRT1 expression through the rapid activation of the EGFR/ERK1/2 signaling and the stimulation of c-fos expression which is recruited to the AP-1 site located within the SIRT1 promoter sequence. Noteworthy, GPER mediates the upregulation of SIRT1 by E2 and G-1, as ascertained by silencing experiments. Using the DNA damaging agent ETO, we also disclose that GPER along with SIRT1 are involved in the pro-survival effects elicited by these ligands, as demonstrated knocking

down GPER expression and using the SIRT1 inhibitor Sirtinol. Biologically, we show that GPER and SIRT1 contribute to the growth effects triggered by E2 and G-1 *in vitro*, as well as in breast tumor xenografts. In accordance with these findings, Sirtinol abrogated the increase of both Cyclin D1 and the proliferative index Ki-67 upon G-1 treatment, as assessed in tumor homogenates. Collectively, our data reveal that SIRT1 may be engaged by GPER signaling toward tumor progression and pro-survival effects elicited by estrogens in cancer cells and main components of the tumor microenvironment like CAFs.

Sirtuins have drawn increasing attention due to their action in various patho-physiological processes as lifespan extension, aging, neurodegeneration, obesity, heart disease, inflammation and cancer.[16] In mammals, the sirtuins family includes seven members (SIRT1-7) that show distinct structure, distribution and functions.[35] SIRT1 is the mammalian homolog of the yeast silent information regulator 2 (sir2)

a

SkBr3

b

CAFs

c

SkBr3

d

CAFs
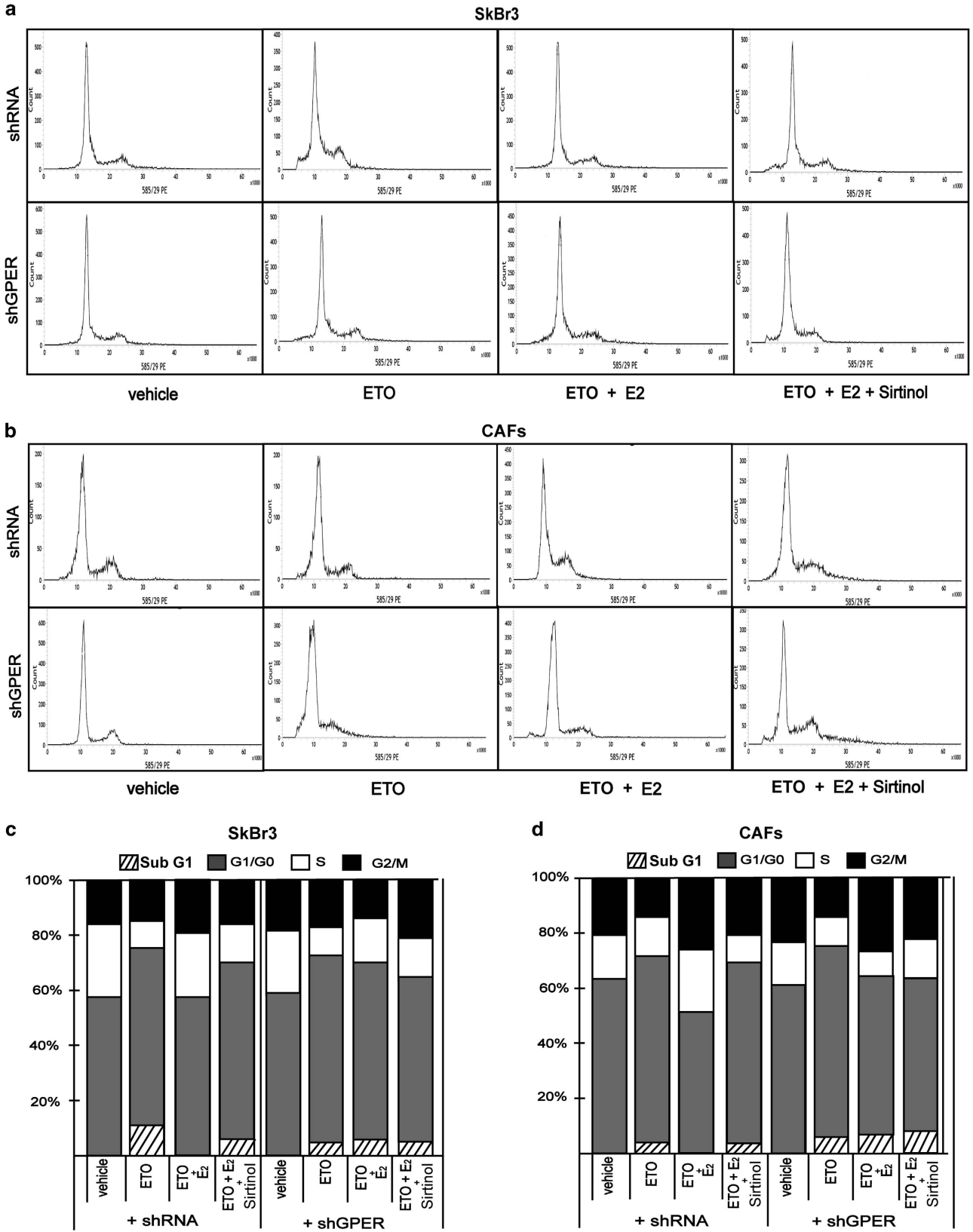
and the most extensively studied sirtuins member.[16] SIRT1 deacetylates several histone and non-histone proteins involved in the regulation of numerous cellular and metabolic processes including gene silencing, cell cycle progression, differentiation, apoptosis and aging.[17,36,37] For instance, SIRT1 inactivates the tumor suppressor p53 deacetylating the Lys382 residue.[38,39] Inactive p53 then leads to a defective apoptotic response to DNA damage, suggesting that SIRT1 may contribute to cancer initiation and progression.[40] Other SIRT1 downstream targets include NF-κB, PPAR-γ, p63, p73, FOXO, Ku70 and the androgen receptor.[22,39,41–43] To date, the function of SIRT1 remains controversial as previous data suggest that SIRT1 can act as a tumor promoter or a tumor suppressor likely depending on cell type, its distribution and biological targets.[19–21] SIRT1-deficient mice developed tumors in many tissues[44] and the overexpression of SIRT1 prevented intestinal tumorigenesis in transgenic mice,[45] nevertheless SIRT1 activity was suggested to have a role in breast and prostate cancer cell growth.[46,47] In addition, SIRT1 was involved in oncogenic signaling in mammary epithelial cancer cells[48] and SIRT1 knockout mice exhibited p53 hyperacetylation and increased apoptosis upon radiation exposure.[49] SIRT1 was also shown to suppress senescence and apoptosis indicating that its inhibition may be beneficial in diverse types of cancer.[50,51] Consequently, a number of SIRT1 inhibitors have been identified in order to interfere with cell proliferation in various types of tumors.[19,52–55]

Estrogens exert diverse patho-physiological functions, including the development and maintenance of female reproductive system and the progression of breast cancer.[56] The action of estrogens is mainly mediated by the classical ER, however, these steroids act also through GPER in both normal and malignant cell contexts, like breast cancer cells and CAFs that are main factors of the tumor microenvironment.[5,8,10,11,56,57] In particular, the stromal contribution to the development of a wide variety of tumors has been extensively assessed using both *in vitro* and *in vivo* model systems.[58–60] For instance, it has been shown that malignant cells may recruit into the tumor mass diverse components of the microenvironment like CAFs, inflammatory and vascular cells that actively cooperate toward cancer progression.[58] Increasing evidence has suggested that CAFs contribute to cancer aggressiveness through the production of secreted factors, which target numerous stromal components and cancer cell types.[59,61] In breast carcinoma ~80% of stromal fibroblasts exhibit the activated features of CAFs that stimulate the proliferation of cancer cells also at the metastatic sites.[62] CAFs may also promote the local production of estrogens, which largely contribute to the development of breast carcinomas through an intricate cross-talk with many transduction pathways activated by growth factors.[63] In addition, the ER antagonist tamoxifen was shown to upregulate the aromatase expression through GPER in both breast cancer cells and CAFs, suggesting that GPER may be involved in the tamoxifen resistance in breast cancer.[64] In this context, our current results provide evidence regarding a novel mechanism by which estrogens through GPER engages SIRT1 toward the stimulation of breast cancer cells, CAFs and breast tumor xenografts. Previous studies have demonstrated that ERα is involved in cell survival and oncogenic transformation triggered by E2 via activation of anti-oxidative enzymes, MAPK, PI3-K and p53 inhibition.[18,29] In addition, it has been shown that ERα and SIRT1 actively cooperate in mediating the protection elicited by E2 against DNA damaging agents.[18] Further extending these mechanisms of estrogen action, the current results indicate that E2 through GPER protect ER-negative breast cancer cells and CAFs from the DNA damage occurring upon ETO treatment. For instance, we have found that GPER and SIRT1 are involved in the prevention of cell cycle arrest and apoptosis prompted by ETO. Hence, GPER targets SIRT1 as ERα toward cell survival and tumor growth, suggesting that appropriate combination therapies could offer more effective interventions according to the ER expression pattern in breast cancer.

Materials and Methods

Materials. Tyrphostin AG1478 (AG) was purchased from Biomol Research Laboratories (Milan, Italy). PD98059 (PD) and Sirtinol were obtained from Calbiochem (Milan, Italy). 1-[4-(-6-Bromobenzol1,3diodo-5-yl)-3a,4,5,9btetrahydro-3H-cyclopenta[c −] quinolin8yl] ethanone (G-1) was purchased from Tocris Bioscience (Bristol, UK). E2, H89, LY294002 (LY) and ETO were purchased from Sigma-Aldrich Srl (Milan, Italy). All compounds were solubilized in dimethyl sulfoxide (DMSO), except E2 and PD which were dissolved in ethanol.

Cell culture. SkBr3 and MCF-7 breast cancer cells and LNCaP prostate cancer cells were obtained by ATCC (Manassas, VA, USA) and used <6 months after resuscitation. SkBr3 and LNCaP were maintained in RPMI-1640 without phenol red, MCF-7 was maintained in DMEM medium, with a supplement of 10% fetal bovine serum (FBS; Sigma-Aldrich Srl) and 100 μg/ml of penicillin/streptomycin (Life Technologies, Milan, Italy). CAFs obtained from breast cancer patients, were characterized and maintained as we previously described.[57,65] Signed informed consent from all the patients was obtained and all samples were collected, identified and used in accordance with approval by the Institutional Ethical Committee Board (Regional Hospital, Cosenza, Italy). All cell lines were grown in a 37 °C incubator with 5% CO2. Cells were switched to medium without serum 24 h before experiments.

Gene silencing experiments and plasmids. Cells were plated onto 10-cm dishes and transfected by X-treme GENE 9 DNA transfection reagent (Roche Molecular Biochemicals, Milan, Italy) for 24 h before treatments with a control vector, a specific shRNA sequence for each target gene, the DN/c-fos construct which encodes for c-fos mutant that heterodimerizes with c-fos dimerization partners but not allowing DNA binding (kindly obtained from Dr C Vinson, NIH, Bethesda, MD, USA). The silencing of GPER expression was obtained by a construct (shGPER) previously described,[66] whereas the silencing of SIRT1 expression was obtained by a construct (shSIRT1) kindly provided by Dr H Cha, (Sogang University, Seoul, Korea).

Gene expression studies. Total RNA was extracted and cDNA was synthesized by reverse transcription as previously described.[13] The expression of selected genes was quantified by real-time PCR using Step One sequence detection system (Applied Biosystems, Milan, Italy). Gene-specific primers were

---

Figure 5 The cell cycle arrest induced by etoposide (ETO) is blunted by E2 via GPER and SIRT1. Cell-cycle analysis performed in SkBr3 cells (**a**) and CAFs (**b**) transfected with shRNA or shGPER for 24 h and then treated for 12 h with 20 μM ETO alone and in combination with 100 nM E2 and 25 μM Sirtinol. (**c** and **d**) histograms show the percentages of cells in subG1, G0/G-1, S and G2/M phases of the cell cycle, as determined by flow cytometry analysis. Values represent the mean ± S.D. of three independent experiments
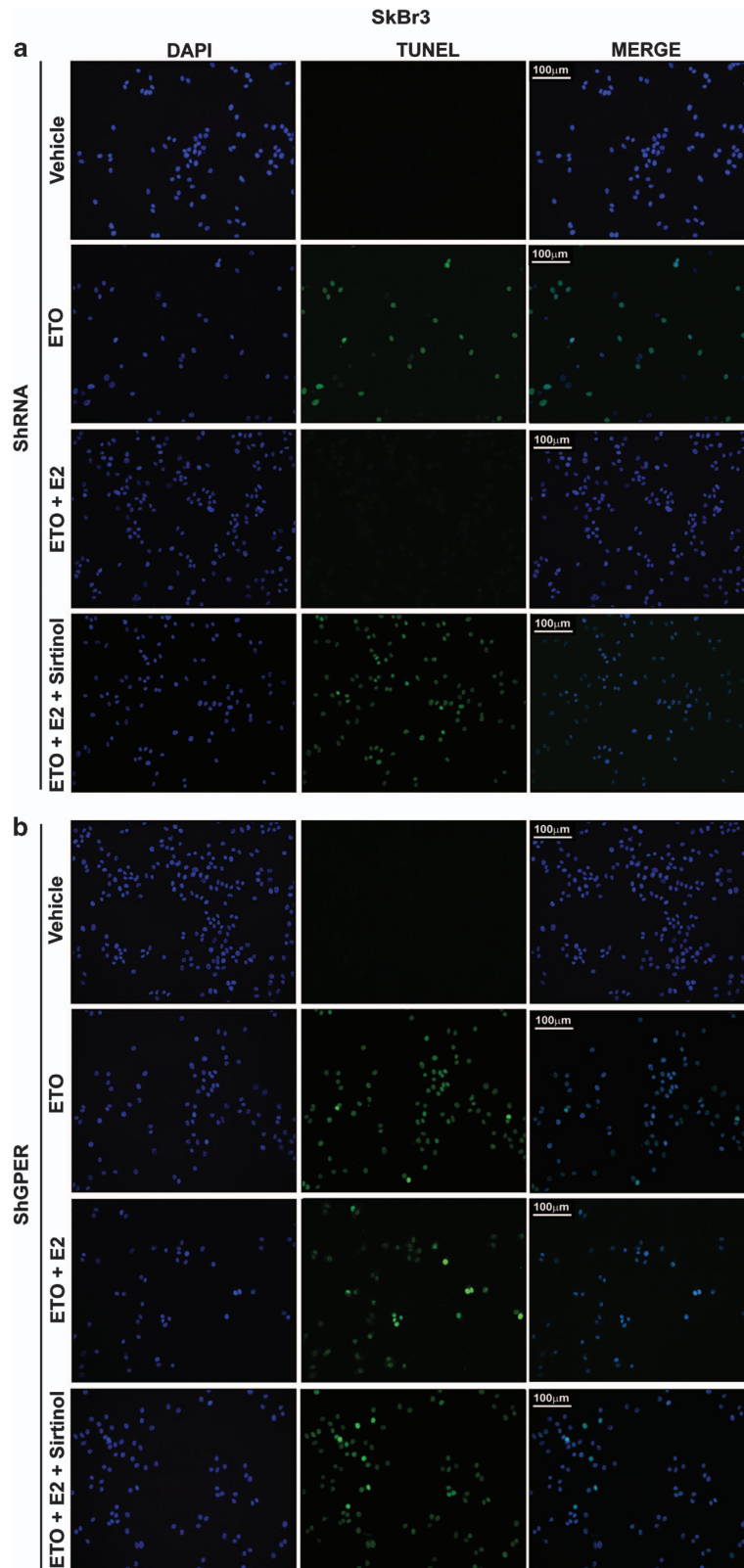
Figure 6 Apoptosis induced by etoposide (ETO) is prevented by E2 via GPER and SIRT1. In SkBr3 cells transfected with shRNA (**a**) or shGPER (**b**), apoptotic changes were detected using Tunel (green) and DAPI (blue) staining after 24 h of treatment with 20 μM ETO alone and in combination with 100 nM E2 and 25 μM Sirtinol. Each experiment shown is representative of 20 random fields. Data are representative of three independent experiments
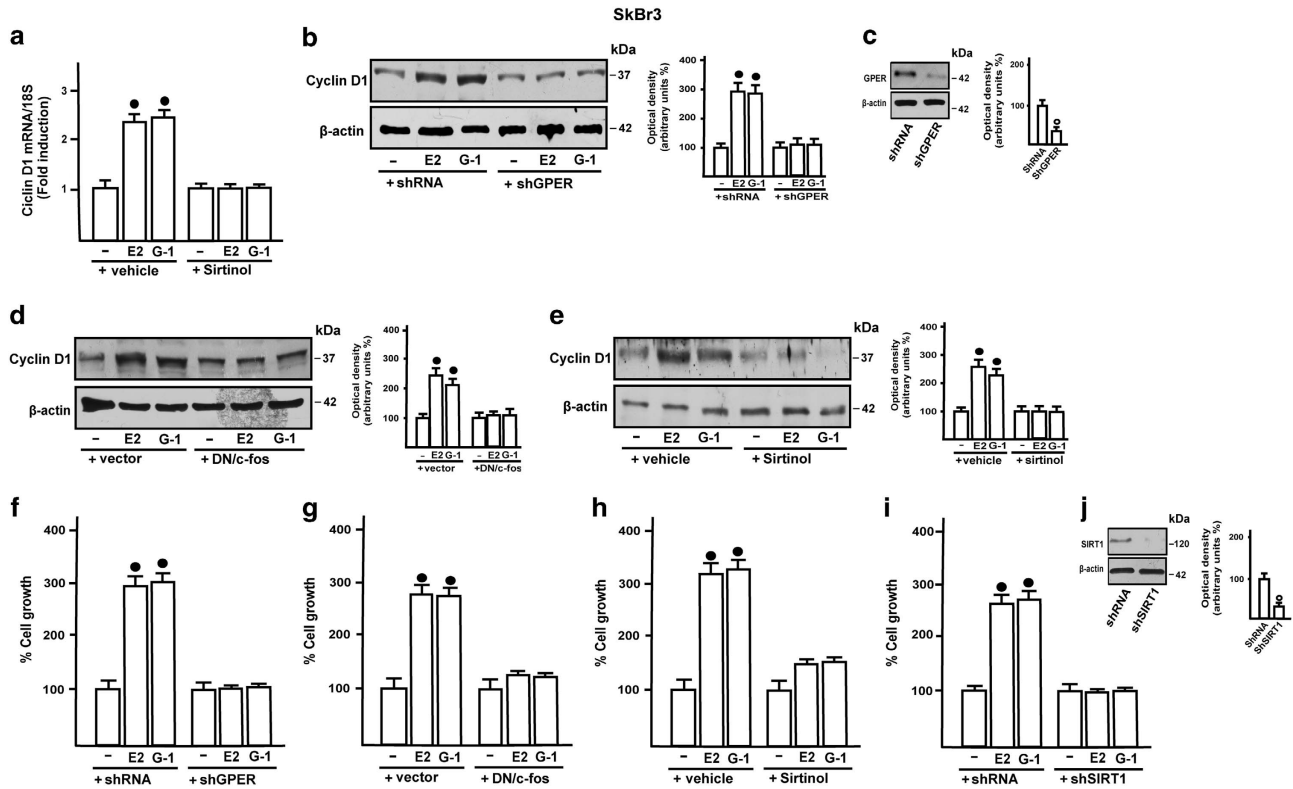
Figure 7 SIRT1 mediates the proliferative effects induced by E2 and G-1 in SkBr3 cells. (**a**) Evaluation of Cyclin D1 mRNA expression upon exposure to 100 nM E2 and 1 μM G-1 alone and in combination with 25 μM Sirtinol. The upregulation of Cyclin D1 protein levels by 100 nM E2 and 1 μM G-1 was abolished transfecting cells with shGPER (**b** and **c**), with the DN/c-fos construct (**d**) or treating cells also with 25 μM Sirtinol (**e**). Cell proliferation induced by 100 nM E2 and 100 nM G-1 was abrogated transfecting cells with shGPER (**f**), with the DN/c-fos construct (**g**), treating cells with 25 μM Sirtinol (**h**) or transfecting cells with shSIRT1 (**i**). In RNA experiments, gene expression was normalized to 18 S expression and results are shown as fold changes of mRNA expression induced by treatments with respect to cells treated with vehicle (−). In immunoblots experiments side panels show densitometric analyses of the blots normalized to β-actin. Each data point represents the mean ± S.D. of three independent experiments. •, ° indicate $P < 0.05$ for cells receiving vehicle (−) *versus* treatments

designed using Primer Express version 2.0 software (Applied Biosystems). For SIRT1, Cyclin D1 and the ribosomal protein 18 S, which was used as a control gene to obtain normalized values, the primers were: 5′-CTCTAGTGACTGGACTCC AAGG-3′ (SIRT1 forward), 5′-AAGATCTGGGAAGTCTACAGCA-3′ (SIRT1 reverse), 5′-GTCTGTGCATTTCTGGTTGCA-3′ (Cyclin D1 forward), 5′-GCTGGAAAC ATGCCGGTTA-3′ (Cyclin D1 reverse), 5′-GGCGTCCCCCAACTTCTTA-3′ (18 S forward) and 5′-GGGCATCACAGACCTGTTATT-3′ (18 S reverse). Assays were performed in triplicate and the results were normalized for 18 S expression and then calculated as fold induction of RNA expression.

Western blot analysis. SkBr3 cells, CAFs and tumor homogenates obtained from nude mice were processed according to the previously described protocol.[67–69] Protein lysates were electrophoresed through a reducing SDS/10% (w/v) polyacrylamide gel, electroblotted onto a nitrocellulose membrane probed with primary antibodies against SIRT1 (D739) and acetyl-p53 (Lys382) purchased from Cell Signaling Technology, Euroclone (Milan, Italy), c-fos (H-125), phosphorylated ERK1/2 (E-4), ERK2 (C-14), EGFR (1005), p-EGFR[Tyr1173] (sc-12351), p21 (H164), GPER (N-15), Cyclin D1 (M-20), Ki-67 (H-300) and β-actin (C2) purchased from Santa Cruz Biotechnology (DBA, Milan, Italy). The levels of proteins and phosphoproteins were detected, after incubation with the horseradish peroxidase-linked secondary antibodies (Santa Cruz Biotechnology), by the ECL System (GE Healthcare, Milan, Italy).

Chromatin immunoprecipitation (ChIP) assay. Cells grown in 10-cm plates were shifted for 24 h to medium lacking serum and then treated with vehicle, 100 nM E2 and 1 μM G-1. Chip assay was performed as previously described.[70] In brief, the immune-cleared chromatin was immunoprecipitated with anti-c-fos (H-125) or nonspecific IgG (Santa Cruz Biotecnology). A 4-μl volume of each immunoprecipitated DNA sample was used as template to amplify, by real-time

PCR, a region containing an AP-1 site located into the SIRT1 promoter region. The primers used to amplify this fragment were: 5′-GCTCACGCTAGAAAGGAAGG-3′ (forward) and 5′-GGAAGACCTTTGACGTGGAG-3′ (reverse). The data were normalized with respect to unprocessed lysates (input DNA). Inputs DNA quantification was performed by using 4 μl of the template DNA. The relative antibody-bound fractions were normalized to a calibrator that was chosen to be the basal, untreated sample. Final results were expressed as percent differences with respect to the relative input.

Gene reporter assays. The 2.2 kb SIRT1 promoter-luciferase construct containing full-length SIRT1 promoter sequence used in luciferase assays was a kind gift from Dr M Thangaraju, (Georgia Health Sciences University, Augusta, GA, USA). SkBr3 cells and CAFs (1×10^5) were plated into 24-well dishes with 500 μl/ well culture medium containing 10% FBS and transfected for 24 h with control vector and DN/c-fos construct. A mixture containing 0.5 μg of reporter plasmid and 10 ng of pRL-TK was then transfected by using X-treme GENE 9 DNA transfection reagent, as recommended by the manufacturer (Roche Diagnostics). After 8 h, cells were treated for 18 h with E2 and G-1 in serum-free medium. Luciferase activity was measured with Dual Luciferase Kit (Promega, Milan, Italy) and normalized to the internal transfection control provided by Renilla luciferase. The normalized relative light unit values obtained from cells treated with vehicle were set as onefold induction, upon which the activity induced by treatments was calculated.

FACS analysis. Around 1×10^5 cells per well were seeded into 12-well plates and maintained in medium for 24 h. For knockdown experiments, cells were transfected for 48 h with shRNA constructs directed against GPER and with an unrelated shRNA construct (3 μg DNA/well transfected with X-treme GENE 9 DNA transfection reagent in medium without serum). Cells were then treated with 20 μM ETO alone and in combination with 100 nM E2, as well as in presence of 25 μM
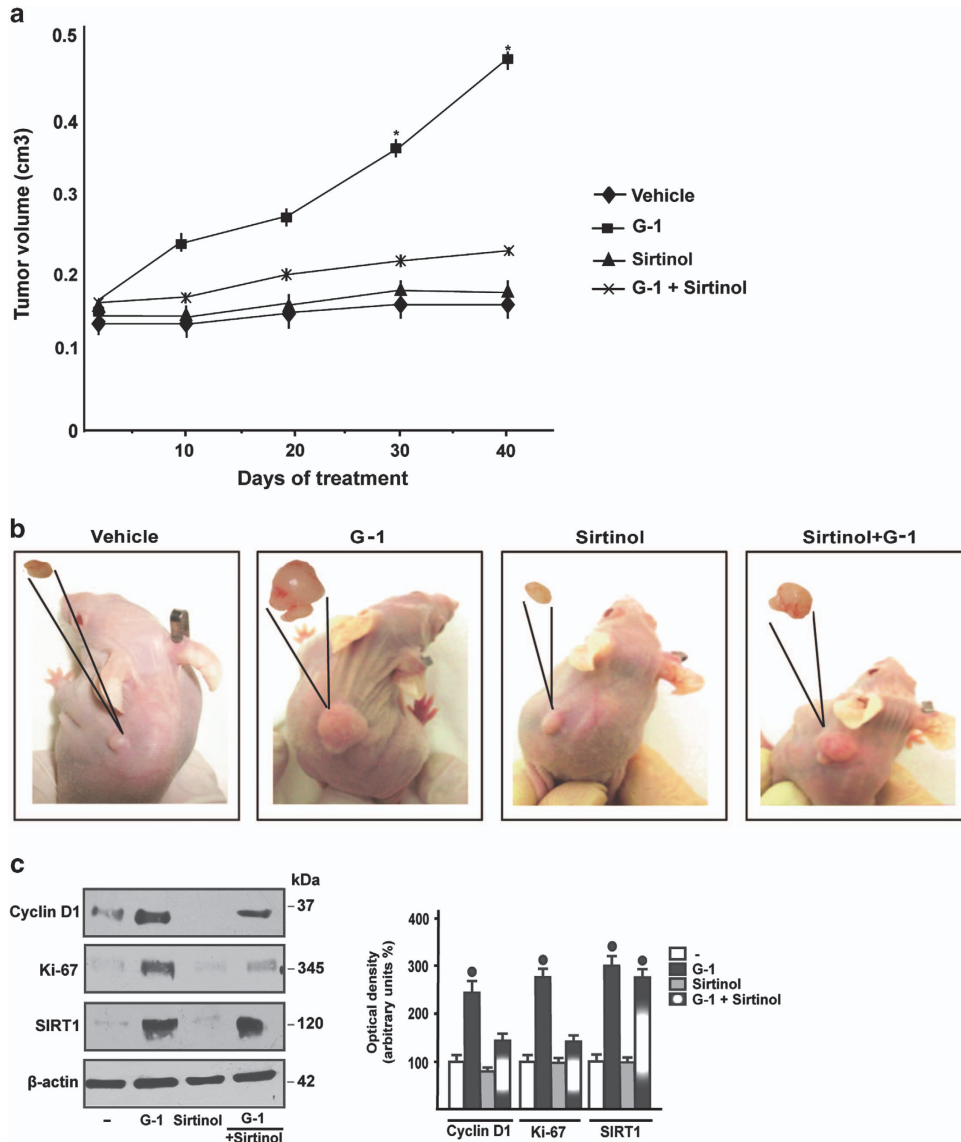
Figure 8 SIRT1 is involved in the growth of SkBr3 xenografts. (**a**) Tumor volume from SkBr3 xenografts implanted in female athymic nude mice treated for 40 days with vehicle, G-1 (0.50 mg/kg/die), Sirtinol (10 mg/kg/die) or a combination of these agents, as indicated. * indicates $P < 0.05$ for animals treated with G-1 *versus* animals treated with vehicle. (**b**) Representative images of mice and relative explanted tumors at day 40, scale bar, 0.3 cm. (**c**) Cyclin D1, Ki-67 and SIRT1 protein levels in tumor homogenates from SkBr3 xenografts treated as reported above. Side panels show densitometric analysis of the blots normalized to β-actin. • indicates $P < 0.05$ for G-1-treated animals *versus* vehicle-treated animals

Sirtinol. After 8 h, cells were pelleted, washed once with phosphate buffered saline (PBS) and resuspended in 0.5 ml of a 50 μg/ml propidium iodide in 1 × PBS (PI) solution containing 20 U/ml RNAse-A and 0.1% triton and incubated for 1 h (Sigma-Aldrich). Cells were analyzed for DNA content by FACS (BD, FACS JAZZ). Cell phases were estimated as a percentage of a total of 10 000 events.

Tunel assay. SkBr3 cells and CAFs were seeded into coverslips and maintained in medium for 24 h. Next, cells were serum-deprived, transfected and treated as indicated. Therefore, cells were fixed in 4% buffered paraformaldehyde for 15 min. Slides were rinsed twice in PBS, pH 7.4. For the detection of DNA fragmentation at the cellular level, cells were stained using DeadEnd Fluorometric Tunel System (Promega) following the manufacturer's instructions. Nuclei of cells were stained with 4′,6-Diamidino-2-phenylindole dihydrochloride (DAPI; 1 : 1000; Sigma-Aldrich). The Leica AF6000 Advanced Fluorescence Imaging System supported by quantification and image processing software Leica Application Suite

Advanced Fluorescence (Leica Microsystems CMS, GmbH Mannheim, Germany) was used for the microscopy evaluation.

Proliferation assay. For quantitative proliferation assay, SkBr3 cells (1×10^5) were seeded in 24-well plates in regular growth medium. Cells were washed once they had attached and then incubated in medium containing 2.5% charcoal-stripped FBS with the indicated treatments; medium was renewed every 2 days (with treatments) and cells were counted using the Countess Automated Cell Counter, as recommended by the manufacturer's protocol (Life Technologies).

***In vivo* studies.** Female 45-day-old athymic nude mice (nu/nu Swiss; Harlan Laboratories, Milan, Italy) were maintained in a sterile environment. At day 0, exponentially growing SkBr3 cells (8.0×10^6 per mouse) were inoculated into the intrascapular region in 0.1 ml of Matrigel (Cultrex, Trevigen, Gaithersburg, MD, USA). When the tumors reached average ~ 0.15 cm^3 (i.e., in about 1 week after implantation), mice were randomized and divided into four groups, according to

treatments administered by intramuscular injection for 40 days. The first group of mice ($n=7$) was treated daily with vehicle (0.9% NaCl with 0.1% albumin and 0.1% Tween-20), (Sigma-Aldrich), the second group of mice ($n=7$) was treated daily with G-1 (0.5 mg/kg/die), the third group of mice ($n=7$) was treated daily Sirtinol (10 mg/kg/die) and the fourth group of mice ($n=7$) was treated daily with G-1 in combination with Sirtinol (at the concentrations described above). G-1 and Sirtinol were dissolved in DMSO at 1 mg/ml. SkBr3 xenograft tumor growth was monitored twice a week by caliper measurements, along two orthogonal axes: length (L) and width (W). Tumor volumes (in cubic centimeters) were estimated by the following formula: $TV = L \times (W2)/2$. At 40 days of treatment, the animals were killed following the standard protocols and tumors were dissected from the neighboring connective tissue. Specimens of tumors were frozen in nitrogen and stored at –80 °C; the remaining tumor tissues of each sample were fixed in 4% paraformaldehyde and embedded in paraffin for the histologic analyses. Animal care, death and experiments were done in accordance with the US National Institutes of Health Guide for the Care and Use of Laboratory Animals (NIH Publication No 85–23, revised 1996) and in accordance with the Italian law (DL 116, 27 January 1992).

Histologic analysis. Morphologic analyses were carried out on formalin-fixed, paraffin-embedded sections of tumor xenografts were cut at 5 μm and allowed to air dry. Deparaffinized, rehydrated sections were stained with hematoxylin and eosin (Bio-Optica, Milan, Italy) or immunolabeled with human cytocheratin 18 (Santa Cruz Biotechnology) to verify that the tumors explanted will be primarily composed of human epithelial cells. Sections were then dehydrated, cleared with xylene, and mounted with resinous mounting medium.

Statistical analysis. Statistical analysis was performed using ANOVA followed by Newman-Keuls' testing to determine differences in means. Statistical comparisons for *in vivo* studies were made using the Wilcoxon–Mann–Whitney test. $P < 0.05$ was considered statistically significant.

Conflict of Interest
The authors declare no conflict of interest.

1. Hall JM, Couse JF, Korach KS. The multifaceted mechanisms of estradiol and estrogen receptor signalling. *J Biol Chem* 2001; **276**: 36869–36872.
2. Pearce ST, Jordan VC. The biological role of estrogen receptors alpha and beta in cancer. *Crit Rev Oncol Hematol* 2004; **50**: 3–22.
3. Sanchez R, Nguyen D, Rocha W, White JH, Mader S. Diversity in the mechanisms of gene regulation by estrogen receptors. *Bioessays* 2002; **24**: 244–254.
4. Métivier R, Penot G, Hübner MR, Reid G, Brand H, Koš M et al. Estrogen receptor-alpha directs ordered, cyclical, and combinatorial recruitment of cofactors on a natural target promoter. *Cell* 2003; **115**: 751–763.
5. Maggiolini M, Picard D. The unfolding stories of GPR30, a new membrane-bound estrogen receptor. *J Endocrinol* 2010; **204**: 105–114.
6. Lappano R, Maggiolini M. G protein-coupled receptors: novel targets for drug discovery in cancer. *Nat Rev Drug Discov* 2011; **10**: 47–60.
7. Maggiolini M, Vivacqua A, Fasanella G, Recchia AG, Sisci D, Pezzi V et al. The G protein-coupled receptor GPR30 mediates c-fos up-regulation by 17beta-estradiol and phytoestrogens in breast cancer cells. *J Biol Chem* 2004; **279**: 27008–27016.
8. Albanito L, Madeo A, Lappano R, Vivacqua A, Rago V, Carpino A et al. G protein-coupled receptor 30 (GPR30) mediates gene expression changes and growth response to 17beta-estradiol and selective GPR30 ligand G-1 in ovarian cancer cells. *Cancer Res* 2007; **67**: 1859–1866.
9. Prossnitz ER, Maggiolini M. Mechanisms of estrogen signalling and gene expression via GPR30. *Mol Cell Endocrinol* 2009; **308**: 32–38.
10. Pandey DP, Lappano R, Albanito L, Madeo A, Maggiolini M, Picard D. Estrogenic GPR30 signalling induces proliferation and migration of breast cancer cells through CTGF. *EMBO J* 2009; **28**: 523–532.
11. Madeo A, Maggiolini M. Nuclear alternate estrogen receptor GPR30 mediates 17β-estradiol - Induced gene expression and migration in breast cancer–associated fibroblasts. *Cancer Res* 2010; **70**: 6036–6046.
12. Pupo M, Vivacqua A, Perrotta I, Pisano A, Aquila S, Abonante S et al. The nuclear localization signal is required for nuclear GPER translocation and function in breast cancer-associated fibroblasts (CAFs). *Mol Cell Endocrinol* 2013; **376**: 23–32.
13. Santolla MF, Lappano R, De Marco P, Pupo M, Vivacqua A, Sisci D et al. G protein-coupled estrogen receptor mediates the up-regulation of fatty acid synthase induced by 17β-estradiol in cancer cells and cancer-associated fibroblasts. *J Biol Chem* 2012; **287**: 43234–43245.
14. Lappano R, Rosano C, De Marco P, De Francesco EM, Pezzi V, Maggiolini M. Estriol acts as a GPR30 antagonist in estrogen receptor-negative breast cancer cells. *Mol Cell Endocrinol* 2010; **320**: 162–170.
15. Lappano R, Santolla MF, Pupo M, Sinicropi MS, Caruso A, Rosano C et al. MIBE acts as antagonist ligand of both estrogen receptor α and GPER in breast cancer cells. *Breast Cancer Res* 2012; **14**: R12.
16. Moore RL, Dai Y, Faller D V. Sirtuin 1 (SIRT1) and steroid hormone receptor activity in cancer. *J Endocrinol* 2012; **213**: 37–48.
17. Liu T, Liu PY, Marshall GM. The critical role of the class III histone deacetylase SIRT1 in cancer. *Cancer Res* 2009; **69**: 1702–1705.
18. Elangovan S, Ramachandran S, Venkatesan N, Ananth S, Gnana-Prakasam JP, Martin PM et al. SIRT1 is essential for oncogenic signalling by estrogen/ estrogen receptor α in breast cancer. *Cancer Res* 2011; **71**: 6654–6664.
19. Lain S, Hollick JJ, Campbell J, Staples OD, Higgins M, Aoubala M et al. Discovery, in vivo activity, and mechanism of action of a small-molecule p53 activator. *Cancer Cell* 2008; **13**: 454–463.
20. Di Sante G, Pestell TG, Casimiro MC, Bisetto S, Powell MJ, Lisanti MP et al. Loss of Sirt1 promotes prostatic intraepithelial neoplasia, reduces mitophagy, and delays Park2 translocation to mitochondria. *Am J Pathol* 2015; **185**: 266–279.
21. Deng CX. SIRT1, is it a tumor promoter or tumor suppressor?. *Int J Biol Sci* 2009; **5**: 147–152.
22. Jin MD, Zhi YW, Dao CS, Ru XL, Sheng QW. SIRT1 interacts with p73 and suppresses p73-dependent transcriptional activity. *J Cell Physiol* 2007; **210**: 161–166.
23. Wen YC, Wang DH, RayWhay CY, Luo J, Gu W, Baylin SB. Tumor suppressor HIC1 directly regulates SIRT1 to modulate p53-dependent DNA-damage responses. *Cell* 2005; **123**: 437–448.
24. Kong S, Kim SJ, Sandal B, Lee SM, Gao B, Zhang DD et al. The type III histone deacetylase Sirt1 protein suppresses p300-mediated histone H3 lysine 56 acetylation at Bclaf1 promoter to inhibit T cell activation. *J Biol Chem* 2011; **286**: 16967–16975.
25. Yeung F, Hoberg JE, Ramsey CS, Keller MD, Jones DR, Frye RA et al. Modulation of NF-kappaB-dependent transcription and cell survival by the SIRT1 deacetylase. *EMBO J* 2004; **23**: 2369–2380.
26. Kiernan R, Brès V, Ng RWM, Coudart MP, El Messaoudi S, Sardet C et al. Post-activation turn-off of NF-κB-dependent transcription is regulated by acetylation of p65. *J Biol Chem* 2003; **278**: 2758–2766.
27. Yao Y, Brodie AMH, Davidson NE, Kensler TW, Zhou Q. Inhibition of estrogen signalling activates the NRF2 pathway in breast cancer. *Breast Cancer Res Treat* 2010; **124**: 585–591.
28. Maggiolini M, Donzé O, Picard D. A non-radioactive method for inexpensive quantitative RT-PCR. *Biol Chem* 1999; **380**: 695–697.
29. Viña J, Borrás C, Gambini J, Sastre J, Pallardó F V. Why females live longer than males? Importance of the upregulation of longevity-associated genes by oestrogenic compounds. *FEBS Lett* 2005; **579**: 2541–2545.
30. Dai Y, Faller D V. Transcription regulation by class III histone deacetylases (HDACs)-sirtuins. *Transl Oncogenomics* 2008; **3**: 53–65.
31. Brugarolas J, Chandrasekaran C, Gordon JI, Beach D, Jacks T, Hannon GJ. Radiation-induced cell cycle arrest compromised by p21 deficiency. *Nature* 1995; **377**: 552–557.
32. Huffman DM, Grizzle WE, Bamman MM, Kim JS, Eltoum IA, Elgavish A et al. SIRT1 is significantly elevated in mouse and human prostate cancer. *Cancer Res* 2007; **67**: 6612–6618.
33. Brooks CL, Gu W. How does SIRT1 affect metabolism, senescence and cancer? *Nat Rev Cancer* 2009; **9**: 123–128.
34. Gong D-J, Zhang J-M, Yu M, Zhuang B, Guo Q-Q. Inhibition of SIRT1 combined with gemcitabine therapy for pancreatic carcinoma. *Clin Interv Aging* 2013; **8**: 889–897.
35. Inoue T, Hiratsuka M, Osaki M, Oshimura M. The molecular biology of mammalian SIRT proteins: SIRT2 in cell cycle regulation. *Cell Cycle* 2007; **6**: 1011–1018.
36. Houtkooper RH, Pirinen E, Auwerx J. Sirtuins as regulators of metabolism and healthspan. *Nat Rev Mol Cell Biol* 2012; **13**: 225–238.
37. Zschoernig B, Mahlknecht U. SIRTUIN 1: regulating the regulator. *Biochem Biophys Res Commun* 2008; **376**: 251–255.
38. Rufini A, Tucci P, Celardo I, Melino G. Senescence and aging: the critical roles of p53. *Oncogene* 2013; **32**: 5129–5143.
39. Lane DP, Cheok CF, Lain S. p53-based cancer therapy. *Cold Spring Harb Perspect Biol* 2010; **2**: a001222.
40. Vaziri H, Dessain SK, Eaton EN, Imai SI, Frye RA, Pandita TK et al. hSIR2SIRT1 functions as an NAD-dependent p53 deacetylase. *Cell* 2001; **107**: 149–159.
41. Saunders LR, Verdin E. Sirtuins: critical regulators at the crossroads between cancer and aging. *Oncogene* 2007; **26**: 5489–5504.
42. Motta MC, Divecha N, Lemieux M, Kamel C, Chen D, Gu W et al. Mammalian SIRT1 represses forkhead transcription factors. *Cell* 2004; **116**: 551–563.
43. Cohen HY, Lavu S, Bitterman KJ, Hekking B, Imahiyerobo TA, Miller C et al. Acetylation of the C terminus of Ku70 by CBP and PCAF controls Bax-mediated apoptosis. *Mol Cell* 2004; **13**: 627–638.

44. Wang RH, Sengupta K, Li C, Kim HS, Cao L, Xiao C *et al*. Impaired DNA damage response, genome instability, and tumorigenesis in SIRT1 mutant mice. *Cancer Cell* 2008; **14**: 312–323.

45. Firestein R, Blander G, Michan S, Oberdoerffer P, Ogino S, Campbell J *et al*. The SIRT1 deacetylase suppresses intestinal tumorigenesis and colon cancer growth. *PLoS One* 2008; **3**: e2020.

46. Ota H, Tokunaga E, Chang K, Hikasa M, Iijima K, Eto M *et al*. Sirt1 inhibitor, Sirtinol, induces senescence-like growth arrest with attenuated Ras-MAPK signalling in human cancer cells. *Oncogene* 2006; **25**: 176–185.

47. Jung-Hynes B, Nihal M, Zhong W, Ahmad N. Role of sirtuin histone deacetylase SIRT1 in prostate cancer: a target for prostate cancer management via its inhibition? *J Biol Chem* 2009; **284**: 3823–3832.

48. Ford J, Jiang M, Milner J. Cancer-specific functions of SIRT1 enable human epithelial cancer cell growth and survival. *Cancer Res* 2005; **65**: 10457–10463.

49. Fang Y, Nicholl MB. Sirtuin 1 in malignant transformation: friend or foe? *Cancer Lett* 2011; **306**: 10–14.

50. Yao Y, Li H, Gu Y, Davidson NE, Zhou Q. Inhibition of SIRT1 deacetylase suppresses estrogen receptor signalling. *Carcinogenesis* 2010; **31**: 382–387.

51. Zhao W, Kruse J-P, Tang Y, Jung SY, Qin J, Gu W. Negative regulation of the deacetylase SIRT1 by DBC1. *Nature* 2008; **451**: 587–590.

52. Solomon JM, Pasupuleti R, Xu L, McDonagh T, Curtis R, DiStefano PS *et al*. Inhibition of SIRT1 catalytic activity increases p53 acetylation but does not alter cell survival following DNA damage. *Mol Cell Biol* 2006; **26**: 28–38.

53. Heltweg B, Gatbonton T, Schuler AD, Posakony J, Li H, Goehle S *et al*. Antitumor activity of a small-molecule inhibitor of human silent information regulator 2 enzymes. *Cancer Res* 2006; **66**: 4368–4377.

54. Lara E, Mai A, Calvanese V, Altucci L, Lopez-Nieva P, Martinez-Chantar ML *et al*. Salermide, a Sirtuin inhibitor with a strong cancer-specific proapoptotic effect. *Oncogene* 2009; **28**: 781–791.

55. Peck B, Chen C-Y, Ho K-K, Di Fruscia P, Myatt SS, Coombes RC *et al*. SIRT inhibitors induce cell death and p53 acetylation through targeting both SIRT1 and SIRT2. *Mol Cancer Ther* 2010; **9**: 844–855.

56. Deroo BJ, Korach KS. Estrogen receptors and human disease. *J Clin Invest* 2006; **116**: 561–570.

57. Pupo M, Pisano A, Lappano R, Santolla MF, de Francesco EM, Abonante S *et al*. Bisphenol A induces gene expression changes and proliferative effects through GPER in breast cancer cells and cancer-associated fibroblasts. *Environ Health Perspect* 2012; **120**: 1177–1182.

58. Kalluri R, Zeisberg M. Fibroblasts in cancer. *Nat Rev Cancer* 2006; **6**: 392–401.

59. Calon A, Lonardo E, Berenguer-llergo A, Espinet E, Hernando-momblona X, Iglesias M *et al*. Stromal gene expression defines poor-prognosis subtypes in colorectal cancer. *Nat Genet* 2015; **47**: 320–329.

60. Isella C, Terrasi A, Bellomo SE, Petti C, Galatola G, Muratore A *et al*. Stromal contribution to the colorectal cancer transcriptome. *Nat Genet* 2015; **47**: 312–319.

61. Bhowmick NA, Neilson EG, Moses HL. Stromal fibroblasts in cancer initiation and progression. *Nature* 2004; **432**: 332–337.

62. Orimo A, Gupta PB, Sgroi DC, Arenzana-Seisdedos F, Delaunay T, Naeem R *et al*. Stromal fibroblasts present in invasive human breast carcinomas promote tumor growth and angiogenesis through elevated SDF-1/CXCL12 secretion. *Cell* 2005; **121**: 335–348.

63. Yamaguchi Y, Hayashi S. Estrogen-related cancer microenvironment of breast carcinoma. *Endocr J* 2009; **56**: 1–7.

64. Catalano S, Giordano C, Panza S, Chemi F, Bonofiglio D, Lanzino M *et al*. Tamoxifen through GPER upregulates aromatase expression: a novel mechanism sustaining tamoxifen-resistant breast cancer cell growth. *Breast Cancer Res Treat* 2014; **146**: 273–285.

65. Santolla MF, De Francesco EM, Lappano R, Rosano C, Abonante S, Maggiolini M. Niacin activates the G protein estrogen receptor (GPER)-mediated signalling. *Cell Signal* 2014; **26**: 1466–1475.

66. Albanito L, Sisci D, Aquila S, Brunelli E, Vivacqua A, Madeo A *et al*. Epidermal growth factor induces G protein-coupled receptor 30 expression in estrogen receptor-negative breast cancer cells. *Endocrinology* 2008; **149**: 3799–3808.

67. De Francesco EM, Pellegrino M, Santolla MF, Lappano R, Ricchio E, Abonante S *et al*. GPER mediates activation of HIF1/VEGF signalling by estrogens. *Cancer Res* 2014; **74**: 4053–4064.

68. Maggiolini M, Santolla MF, Avino S, Aiello F, Rosano C, Garofalo A *et al*. Identification of two benzopyrroloxazines acting as selective GPER antagonists in breast cancer cells and cancer-associated fibroblasts. *Future Med Chem* 2015; **7**: 437–448.

69. Vivacqua A, De Marco P, Santolla MF, Cirillo F, Pellegrino M, Panno ML *et al*. Estrogenic gper signaling regulates mir144 expression in cancer cells and cancer-associated fibroblasts (cafs). *Oncotarget*; e-pub ahead of print 12 May 2015.

70. De Marco P, Bartella V, Vivacqua A, Lappano R, Santolla MF, Morcavallo A *et al*. Insulin-like growth factor-I regulates GPER expression and function in cancer cells. *Oncogene* 2013; **32**: 678–688.

Supplementary Information accompanies this paper on Cell Death and Disease website (http://www.nature.com/cddis)

Identification of two benzopyrroloxazines acting as selective GPER antagonists in breast cancer cells and cancer-associated fibroblasts

Background: G-protein coupled estrogen receptor (GPER) is involved in numerous intracellular physiological and pathological events including cancer cell migration and proliferation. Its characterization is yet incomplete due to the limited number of specific ligands. **Results**: Two novel selective GPER antagonists, based on a benzo[*b*]pyrrolo[1,2-*d*][1,4]oxazin-4-one structure, have been designed and synthesized. Their binding to the receptor was confirmed by a competition assay, while the antagonist effects were ascertained by their capability to prevent the ligand-stimulated action of GPER. The transcription mediated by the classical estrogen receptor was not influenced, demonstrating selectivity for GPER. **Conclusion**: These novel compounds may be considered useful leads toward the dissection of the GPER signaling and the development of new pharmacological treatments in breast cancer.

Marcello Maggiolini[‡,1], Maria Francesca Santolla[1], Silvia Avino[1], Francesca Aiello[1], Camillo Rosano[2], Antonio Garofalo[1] & Fedora Grande*[,‡,1]
[1]Department of Pharmacy, Health & Nutritional Sciences, University of Calabria, via P Bucci, 87036 Rende (Cs), Italy
[2]U.O.S.Biopolymers and Proteomics, IRCCS A.O.U. San Martino – IST, National Institute for Cancer Research, Largo R. Benzi 10, 16132 Genova, Italy.
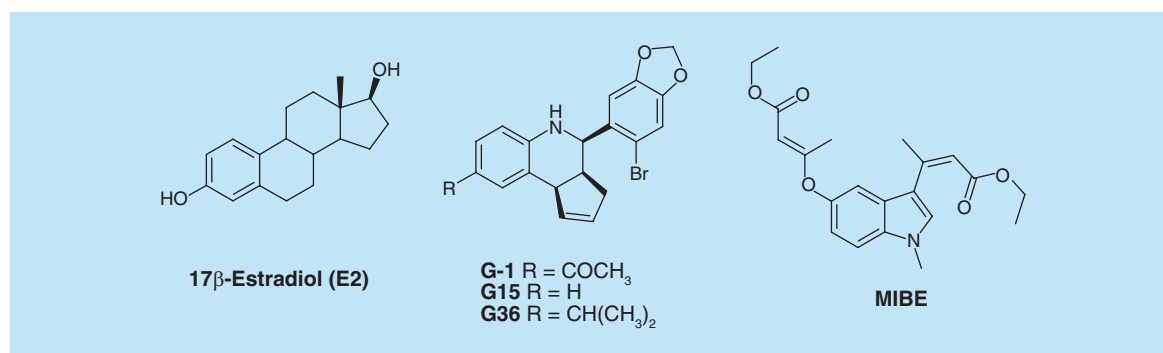*Author for correspondence:
Tel.: +39 0984 493 019
Fax: +39 0984 493 118
fedora.grande@unical.it
[‡]Authors contributed equally

17β-Estradiol (E2) exerts multiple biological actions binding to and activating the classical estrogen receptor (ER)α and ERβ [1]. In addition, the G-protein estrogen receptor (GPER) has been shown to be involved in diverse physiological processes regulated by E2 [2]. In particular, the release of the membrane-joined HB-EGF which binds to EGFR may result from the interaction of E2 with GPER [3]. The GPER-mediated transactivation of EGFR generates numerous intracellular events like the activation of MAPK ERK1/2, PI3K and PLC, together with the increase of the cAMP levels and the mobilization of intracellular calcium, that cumulatively lead to gene expression changes, cancer cell migration and proliferation [4]. A considerable progress in the evaluation of distinct actions mediated by GPER over those induced by the classical ER has been succeeded thanks to the discovery of a specific GPER agonist namely G-1, which is a tetrahydro-3*H*-cyclopenta[*c*]quinoline derivative [5,6]. A role for GPER in pathological conditions including cancer, metabolic and immune disorders, osteoporosis, cognitive and behavioral alterations and neurodegenerative diseases has been reported, along with

its potential involvement in the cardiovascular protection exerted by estrogens [7–11]. On the basis of the aforementioned observations, GPER may be considered a valuable therapeutic target worth to be thoroughly investigated. While specific agonists, chemically unrelated to G-1, were successively identified [12,13], only two selective GPER antagonists (named G15 and G36), close structural analogues of G-1, have been so far discovered [14] (Figure 1).

These compounds structurally differ from G-1 only for the lack of an ethanone moiety involved in the instauration of a H-bonding with GPER. The presence of such an interaction seems necessary either for the receptor activation and the selectivity toward GPER over the classical ER [15]. The tetrahydro-3*H*-cyclopenta[*c*]quinoline scaffold of G15 and G36 has been then conjugated with a series of organometallic complexes for the production of imaging agents useful as diagnostic tools [16]. Recently, a further antagonist (termed MIBE) showing the unique property to act as an antagonist for both GPER and ER, has been also identified [17]. The low number of available compounds acting selectively on GPER, either as agonists and even

Figure 1. GPER agonists (E2 and G-1) and antagonists (G15, G36 and MIBE).

more as antagonists, yet does not allow a wide characterization of GPER-mediated responses. Therefore, we focused our attention on the search of new lead compounds, which may act as GPER ligands endowed with antagonist activity, hence potentially suitable in the treatment of estrogen-sensitive tumors.

Herein, we describe two novel compounds, termed PBX1 and PBX2 (Figure 2) that were synthesized by an original procedure. Interestingly, PBX1 and PBX2 based on a pyrroloquinoxaline structure, showed the ability to inhibit the GPER-dependent signaling as selective antagonist ligands in breast cancer cells and cancer-associated fibroblasts (CAFs) that are main players of the tumor microenvironment [18]. The properties elicited by these novel compounds may result of great value in order to gain further insights into the characterization of GPER-mediated responses, particularly towards more comprehensive pharmacological approaches in many pathophysiological conditions.

Materials & methods
Molecular modeling & docking simulations
The molecular modeling and docking simulations relative to the interaction between GPER and PBX1 or PBX2 were essentially carried out as described in

ref. [19–22], using the same programs therein described. The protein active site center was identified in atom Phe208 O, on the basis of our previous studies carried over the same receptor [20,23,24]. Furthermore, atoms located within 20 Å from this point were considered as the active site atoms. Side chains of residues Asn118, Gln138, Met141, Phe206, Phe208, Glu275, His302 and Met309 of GPER were assumed to be able to freely rotate. Corresponding figures were drawn with the program Chimera [25].

Chemical synthesis
General experimental information and the synthetic procedures of intermediates **2** and **3** (Figure 3) are reported in the Supplementary Material. The purity of PBX1 and PBX2 was > 95%, as determined by HPLC.

7-(Quinoxalin-2-ylamino)-4H-benzo[b] pyrrolo[1,2-d][1,4]oxazin-4-one (PBX1)
A mixture of 7-amino-4*H*-pyrrolo[2,1-*c*][1,4]benzoxazin-4-one **3** (0.04 g, 0.20 mmol), 2-chloroquinoxaline (0.03 g, 0.20 mmol) and triethylamine (61 µl, 0.44 mmol) in dry dichloromethane (3 ml) was heated to reflux for 24 h. The solid obtained was washed sequentially with water, cold methanol and diethyl ether to give the compound PBX1 in 91% yield. Mp 228°C (dichloromethane/petroleum ether).^{1}H-NMR (CD$_3$OD) δ 8.80 (s, 1H), 8.15 (m, 1H), 8.02 (m, 1H), 7.91–7.82 (m, 3H), 7.61 (d, 1H, *J* = 9.0 Hz), 7.23 (dd, 1H, *J* = 4.1, 1.4 Hz), 6.60–6.70 (m + s, 3H).^{13}C-NMR (CD$_3$OD) δ 155.5, 147.4, 147.2, 144.9, 143.8, 141.7, 140.7, 131.2, 130.2, 128.7, 127.9, 118.8, 116.0, 115.9, 115.1, 113.5, 112.8, 111.5, 102.1. HRMS calcd for C$_{19}$H$_{12}$N$_4$O$_2$ 328.0960, found 328.0977. IR (KBr) υ$_{max}$: 1705 cm^{-1}.
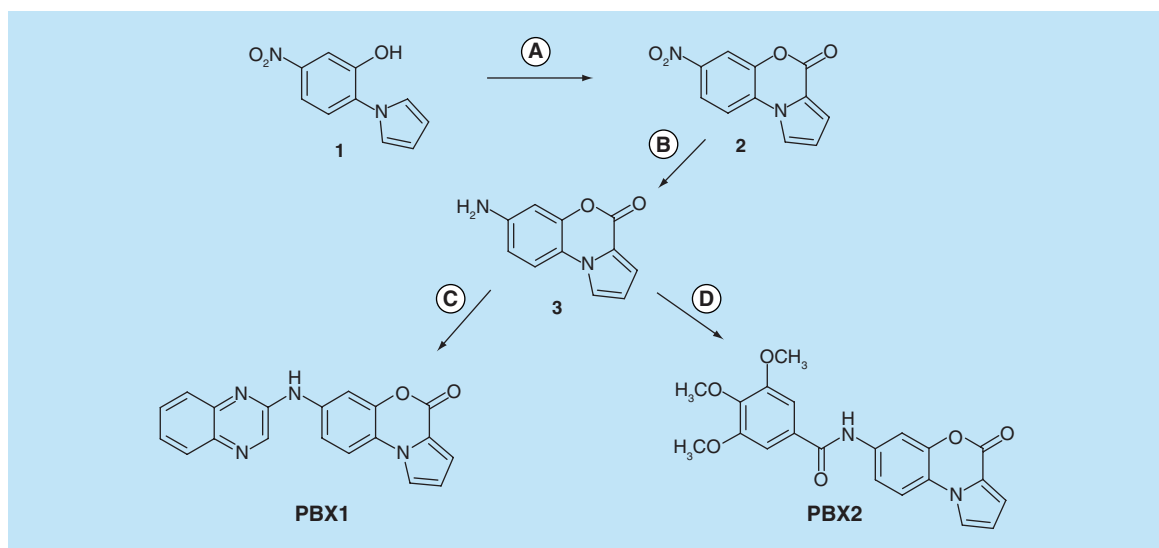
3,4,5-Trimethoxy-N-(4-oxo-4H-benzo[b] pyrrolo[1,2-d][1,4]oxazin-7-yl)benzamide(PBX2)
A solution of 3,4,5-trimethoxybenzoyl chloride (0.05 g, 0.20 mmol) in dry dichloromethane (1 ml) was added dropwise to a mixture of 7-amino-4*H*-pyrrolo[2,1-*c*] [1,4]benzoxazin-4-one **3** (0.04 g, 0.20 mmol) and
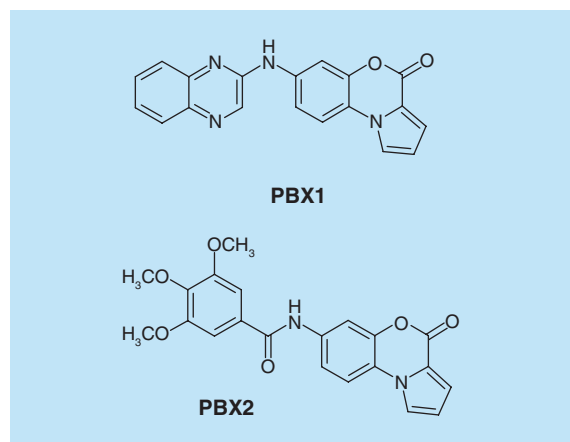
PBX1

PBX2

Figure 2. Studied compounds.

Figure 3. Synthesis of PBX1 and PBX2. Reagents and conditions: **(A)** $CO(OCCl_3)_2$, toluene, reflux (72%); **(B)** $NaBH_4$-$BiCl_3$, dry ethanol, rt (83%); **(C)** 2-chloroquinoxaline, Et_3N, dichloromethane, reflux (91%); **(D)** 3,4,5-trimethoxybenzoil chloride, Et_3N, dichloromethane, reflux (89%).

triethylamine (61 µl, 0.44 mmol) in dichloromethane (2 ml). The resulting suspension was stirred for 48 h under reflux. The solid obtained was sequentially washed with water, cold methanol and diethyl ether to give the compound PBX2 in 89% yield. Mp 299°C (dec.) (methanol).^{1}H-NMR (DMSO-d_6) δ 10.40 (s, 1H), 8.24 (s, 1H), 8.12 (d, 1H, J = 8.9 Hz), 7.92 (d, 1H, J = 2.1 Hz), 7.72 (dd, 1H, J = 8.9, 2.1 Hz), 7.29 (m, 1H), 6.75 (m, 1H), 3.85 (s, 6H), 3.70 (s, 3H).^{13}C-NMR (DMSO-d_6) δ 165.5, 153.6, 153.1 (2 × C), 142.9, 141.9, 137.9, 136.5, 130.1, 120.9, 118.7, 117.3, 116.8, 115.9, 114.3, 109.3, 105.8 (2 × C), 60.6, 56.6 (2 × C). HRMS calcd for $C_{21}H_{18}N_2O_6$ 394.1165, found 394.1178. IR (KBr) υ_{max}: 1721, 1667 cm^{-1}.

Biological methods
Reagents
17β-Estradiol (E2) was supplied by Sigma-Aldrich (Milan, Italy). 1-(4-(6-Bromobenzo[d][1,3]dioxol-5-yl)-3a,4,5,9b-tetrahydro-3H-cyclopenta[c]quinolin-8-yl)ethanone (G-1) was purchased by Merck KGaA (Frankfurt, Germany). Ethyl 3-[5-(2-ethoxycarbonyl-1-methylvinyloxy)-1-methyl-1H-indol-3-yl]but-2-enoate (MIBE) was synthesized as previously described [12]. ICI 182,780 (ICI) was purchased from Tocris Chemicals. MIBE, G-1, ICI were dissolved in dimethyl sulfoxide (DMSO). E2 was dissolved in ethanol.

Cell culture
MCF7 and SkBr3 breast cancer cells and human embryonic kidney Hek293 cells were obtained by ATCC (Manassas, USA) and cultured as previously described [12,17]. 100 µg/ml Penicillin/streptomycin (Life Technologies, Milan, Italy) were added to RPMI

medium. CAFs were obtained from breast cancer patients as previously described [13]. CAFs were maintained in a mixture of MEDIUM 199 and HAM'S F-12 (1:1) added with 10% FBS and 100 µg/ml penicillin/streptomycin.

Ligand binding assays
The **ligand binding** assay for GPER was performed using SkBr3 cells in the presence or absence of increas-
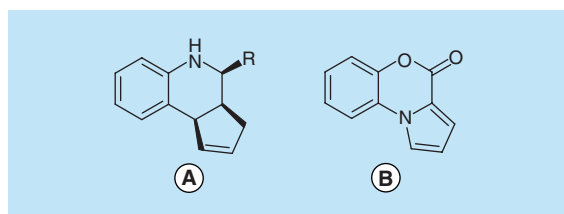

Figure 4. Tricyclic backbones of known GPER ligands (A) and new compounds (B).

Key terms

Tumor microenvironment: Neoplastic epithelial cells coexist in carcinomas with several types of stromal cells that generate the microenvironment of the cancer cells. Among the stromal components, one important type of cells recruited into the tumor mass is represented by fibroblasts, which acquire an activated phenotype, triggering thereafter paracrine signals between stromal and cancer cells.

Docking simulation: Computational simulation technique used to predict the binding orientation of a candidate ligand into the active site of protein targets.

Ligand binding: Detection method used to evaluate the interaction between two molecules. In particular, this assay is employed to determine the presence and extent of ligand–receptor complexes.
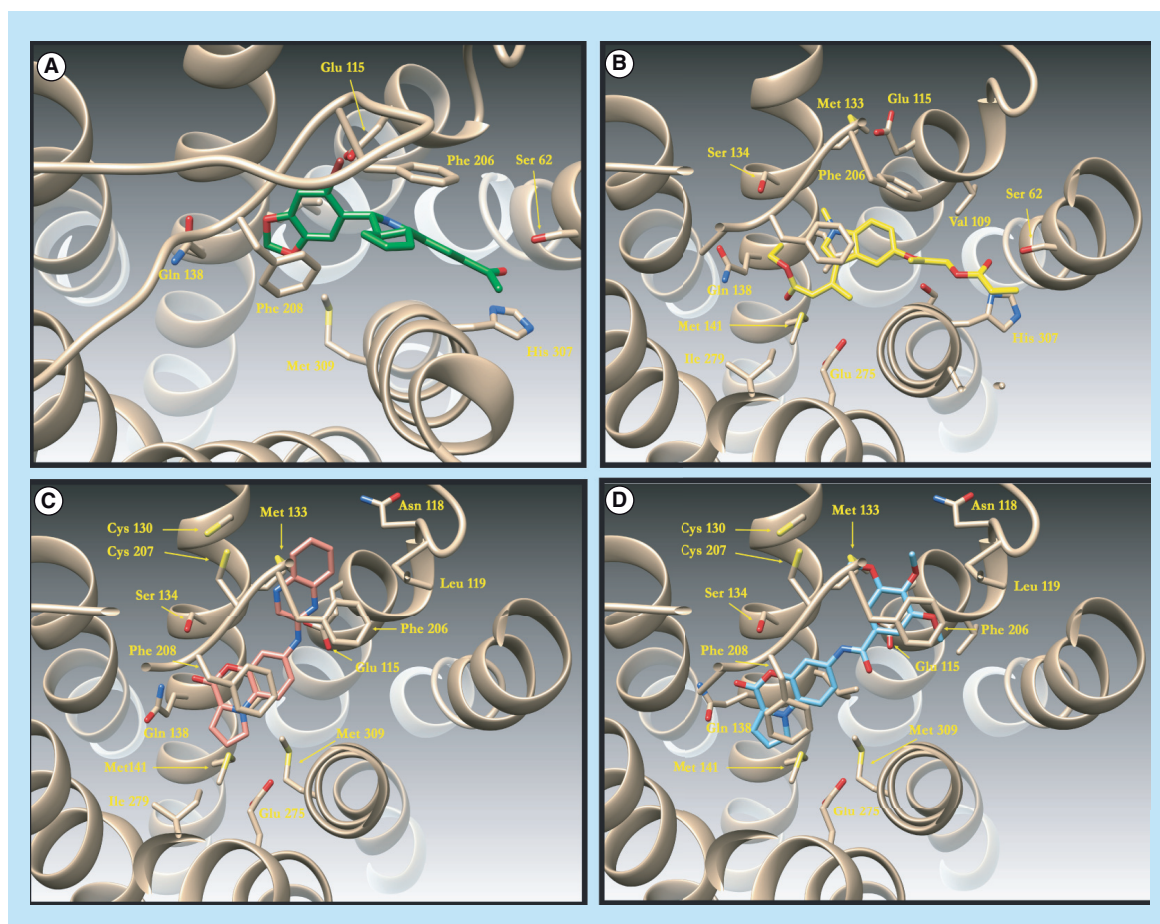
Figure 5. GPER docking simulations. The GPER ligand binding pocket. Ribbons representing protein structural elements are drawn in tan; residues involved in hydrophobic and polar interaction with ligands are drawn as sticks. Different ligand binding modes are reported: panel **(A)** G-1 (acting as agonist) is reported in green, panel **(B)** MIBE (acting as antagonist) is drawn in yellow, panel **(C)** PBX1 binding mode is represented in salmon and panel **(D)** PBX2 is drawn as cyan sticks.

ing concentrations of non labeled competitors (E2, G-1, PBX1 and PBX2), following the method reported in ref. [12]. Each value given is the mean of three observations.

Cell viability assay

Cell viability was determined by using the 3-(4,5-dimethylthiazol-2-yl)-2,5-diphenyltetrazolium (MTT) assay. Cells (3 × 10⁴ cells/ml) were plated in 24 well plates in regular growth medium. The next day cells were washed once and further incubated in a medium supplemented with 5% FBS before the addition of PBX1 and PBX2 for 48 h. For the MTT assay, 100 μl of MTT (2 mg/ml) Sigma-Aldrich (Milan, Italy) were added to each well and the plates were incubated for 3 h at 37°C. Then, 500 μl of DMSO Sigma-Aldrich (Milan, Italy) were added to solubilize the cells. The absorbance was measured using a FLX-800 microplate fluorimeter (Bio-Tek Instruments, Inc., Winooski, VT, USA) at a test wavelength of 570 nm.

Cytotoxicity was expressed as the concentration giving 50% inhibition respect to cells treated with the vehicle (IC$_{50}$). The absorbance readings were used to determine the IC$_{50}$ using GraphPad Prism 4 (GraphPad Software, Inc, San Diego, CA). Briefly, values were log transformed, normalized, and nonlinear regression analysis was used to generate a sigmoidal dose-response curve to calculate the IC$_{50}$ values.

Gene expression studies

Total RNA was extracted using Trizol commercial kit (Life Technologies, Milan, Italy) following the manufacturer's protocol as previously described [13]. The expression of selected genes was quantified by real-time PCR using Step One (TM) sequence detection system (Applied Biosystems Inc, Milano, Italy). Gene-specific primers were designed using Primer Express version 2.0 software (Applied Biosystems. Inc.). For *c-fos*, *CTGF*, and the ribosomal protein *18S*, which was used as a control gene to obtain normalized values, the primers

were: 5'-CGAGCCCTTTGATGACTTCCT-3' (*c-fos* forward), 5'-GGAGCGGGCTGTCTCAGA-3' (*c-fos* reverse); 5'-ACCTGTGGGATGGGCATCT-3' (*CTGF* forward), 5'-CAGGCGGCTCTGCTTCTCTA-3' (*CTGF* reverse); 5'- GGCGTCCCCCAACTTCTTA -3' (*18S* forward) and 5'- GGGCATCACAGACCT-GTTATT -3' (*18S* reverse), respectively.

Western blot analysis

Western blot analysis was essentially carried out as described in ref. [17]. Equal amounts (10–50 μg) of whole cell lysates were electrophoresed through a reducing SDS/10% (w/v) polyacrylamide gel, electroblotted onto a nitrocellulose membrane probed with primary antibodies against phosphorylated EGFR^{Tyr1173} (sc-12351), EGFR (1005), phosphorylated ERK1/2 (E-4), ERK2 (C-14), were used at a dilution of 1:4000, 1:2000, 1:1000 and 1:2000, respectively.

Proliferation assay

The proliferation assays were performed following the experimental conditions previously described [17].

Migration assay

Migration assays were carried out using Boyden chambers (Costar Transwell, 8 mm polycarbonate membrane) according to the experimental settings previously described [13].

Luciferase assays & plasmids

Luciferase assays and plasmids were used as previously described [17,26].

Results & discussion

Design & synthesis

The mode of interaction of several ligands with GPER was assessed by a **protein-based approach** drawn from an already available 3D model of the receptor [22]. Taken into consideration both the inspection of the active site of the protein and the structure of the tetrahydro-3*H*-cyclopenta[*c*]quinoline-based G-ligands **(Figure 4A)**, the design of new potential antagonists, derived from an alternative tricyclic backbone, was undertaken. **Random screening** of our internal compound library led to the identification of benzo[*b*]pyrrolo[1,2-*d*][1,4]oxazin-4-one **(Figure 4B)** as a base for the production of the new ligands. Due to the overall asset and dimension, this rigid skeleton closely resembles that of G-ligands. A noteworthy difference between the two systems consists in a flat shape of B if compared with A of G-derivatives that are all *endo* forms constrained in a bended arrangement. This particular feature could help the new compounds to more favorably enter the receptor binding site cleft,
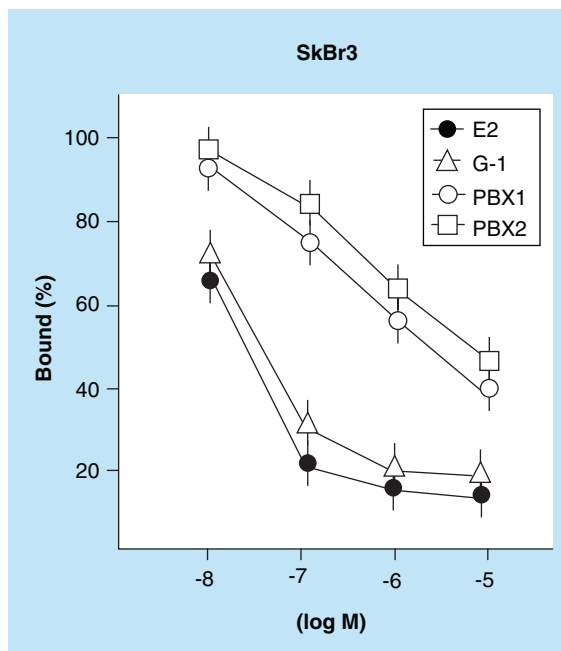
Figure 6. PBX1 and PBX2 compete with [3H]E2 for the binding to GPER. Competition curves of increasing concentrations of unlabeled E2, G-1, PBX1 and PBX2 expressed as a percentage of specific [3H]E2 binding in SkBr3 cells. Each data point represents the mean ±SD of three separate experiments performed in triplicate. The amount of tracer bound in the absence of competitor was arbitrarily set to 100%.

still maintaining the opportunity of forming hydrogen bonds through the oxygen atoms of lactone moiety.

Further attempted alterations consisted of the removal of the bromobenzo[*d*][1,3]dioxole moiety and the substituent at position 8 of G-series agonist and antagonists, with the concomitant introduction of bulky substituents at position 7 of the benzo-fused ring in order to shift the activity towards a marked antagonism, as stated for a previously reported ligand [16]. Two original compounds were then designed and synthesized. In particular, the first compound termed PBX1 **(Figure 2)** shows a 2-quinoxalinyl residue linked to the tricyclic benzo[*b*]pyrrolo[1,2-*d*][1,4]oxazine system at position 7 through an amino group. This should allow the quinoxaline system to assume a suitable orientation to better accommodating into the receptor active site, offering further possibility to form hydrogen, hydrophobic or charge transfer interactions with the key amino acids resi-

---

Key terms

Protein-based approach: Design of drugs based on the inspection of protein binding site features.

Random screening: One of the most used approach for the identification of lead compounds.
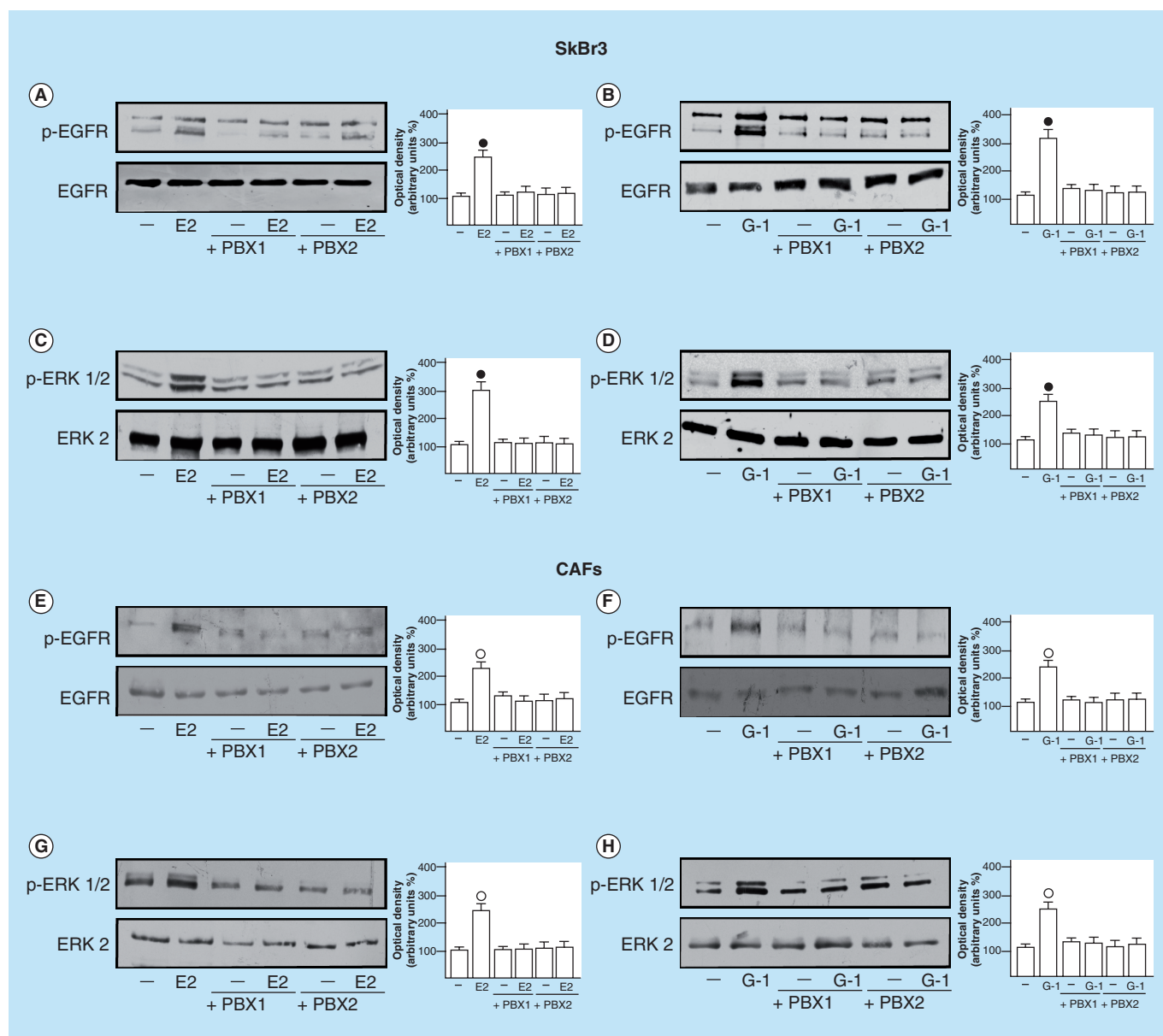

Figure 7. PBX1 and PBX2 prevent the phosphorylation of EGFR and ERK1/2. EGFR^{Tyr1173} phosphorylation in SkBr3 cells **(A&E)** and CAFs **(B&F)** treated for 10 min with vehicle (-), 100 nM E2 or 1 μM G-1 alone and in combination with 10 μM PBX1 or 10 μM PBX2. ERK1/2 activation in SkBr3 cells **(C&G)** and CAFs **(D&H)** treated for 10 min with vehicle (-) or 100 nM E2 or 1 μM G-1 alone and in combination with 10 μM PBX1 or 10 μM PBX2. Side panels show densitometric analysis of the blots normalized to EGFR and ERK2, as indicated. Each data point represents the mean ±SD of three independent experiments. (•,o) indicate $p < 0.05$ for cells receiving vehicle (-) versus treatments.
CAF: Cancer-associated fibroblast.

dues. The second compound named PBX2 is characterized by the same tricyclic scaffold linked at position 7 to a bulky 3,4,5-trimethoxyphenyl nucleus through an amide tether, which should limit flexibility of the entire molecule. For both compounds, the steric hindrance of substituents appended to the planar tricyclic structure may contrast a correct alignment for the receptor-bound complex formation so resulting in an eventual antagonist effect.

The synthesis of PBX1 and PBX2 was accomplished starting from the same intermediate 7-nitro-4*H*-pyrrolo[2,1-*c*][1,4]benzoxazin-4-one **2** [27], in turn obtained from reaction of 5-nitro-2-(1*H*-pyrrol-1-yl) phenol **1** and triphosgene, by a method previously described for similar compounds **(Figure 3)** [28]. The compound **2** was then subjected to selective reduction of nitro group to the corresponding amine derivative **3**, by means of NaBH$_4$/BiCl$_3$ [29]. Reaction of 7-amino-
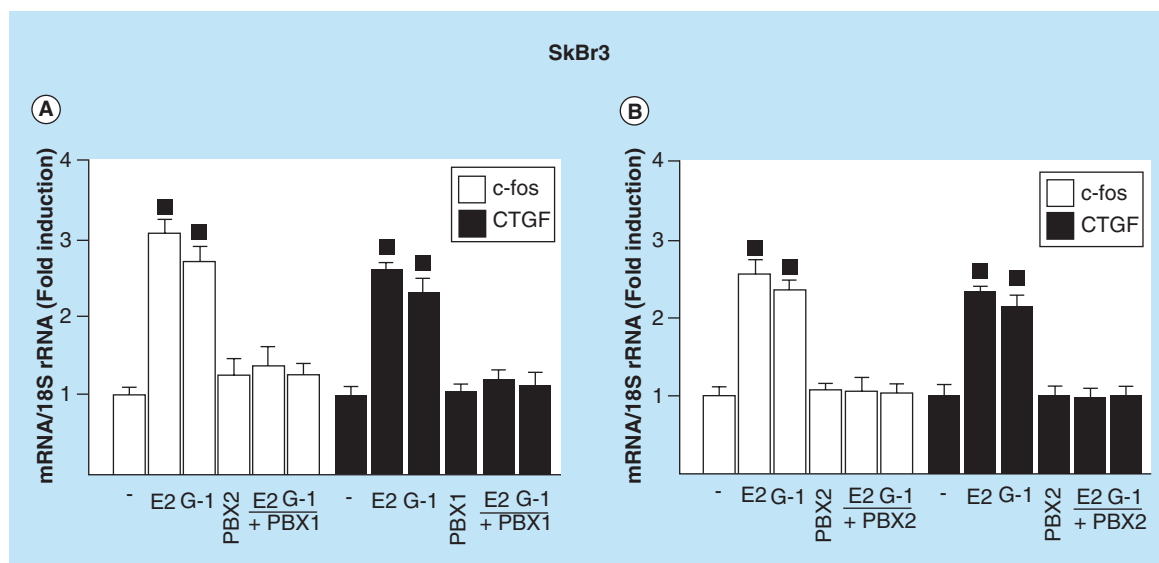
Figure 8. PBX1 and PBX2 inhibit GPER target genes induced by E2 and G-1. (A & B) The expression of *c-fos* and *CTGF* induced upon exposure for 1 h to 100 nM E2 and 1 μM G-1 is prevented in presence of 10 μM PBX1 or 10 μM PBX2 in SkBr3 cells, as evaluated by real-time PCR. Results obtained from experiments performed in triplicate were normalized for *18S* expression and results are shown as fold changes of mRNA expression compared with cells treated with vehicle (-). Each data point represents the mean ±SD of three independent experiments performed in triplicate. (•) indicates p < 0.05 for cells receiving vehicle (-) versus treatments.

4*H*-pyrrolo[2,1-*c*][1,4]benzoxazin-4-one   **3**   with 2-chloroquinoxaline or its acylation with 3,4,5-trimethoxybenzoyl chloride gave PBX1 and PBX2 in 91 and 89% yield, respectively.

Docking simulations

GPER binding pocket has already been described in our previous works as a deep cleft in the protein core surrounded by both hydrophobic and polar residues belonging to transmembrane helices TM III, TM V, TM VI and TM VII [12,20]. Using GPER molecular model as target [22], docking simulations were performed using the program GOLD which proved a good affinity between the protein and both the agonist G-1 and the antagonist MIBE (Figure 5A&B), as previously demonstrated both in silico and *in vitro* [5,12]. Using the same settings and parameters as for G-1 and MIBE, we performed docking simulations of the novel ligands PBX1 and PBX2. Both the newly designed moieties were positioned within the GPER binding site (Figure 5C&D), displaying a good affinity for GPER. Particularly, PBX1 binds to GPER by forming hydrogen bonds to residues Glu115 (belonging to helix TM II) and Ser134, and Gln138 (on helix TM III). Moreover, hydrophobic contacts with Leu119, Met133, Leu137, Phe206, Phe208 and Ile279 further stabilize the interaction. On the other side, PBX2 conserves the hydrogen bonding with Glu115, Ser134 and Gln138 and forms an additional hydrogen bond with Asn118 (TM II). The interaction of PBX2 with GPER is completed by hydrophobic contacts with residues

Leu119, Met133, Leu137, Phe206, Phe208, Ala209 and Ile279.

Binding experiments & MTT assays

On the basis of the results obtained in docking simulations, we next ascertained the ability of PBX1 and PBX2 to bind to GPER. To this end, we performed ligand binding assays using radiolabeled E2 in ER-negative and GPER-positive SkBr3 breast cancer cells [22]. PBX1 and PBX2 displaced the [3H]E2 in a dose-dependent manner, although in a lesser extent respect to E2 and the selective GPER ligand G-1 (Figure 6).

By MTT assays performed in SkBr3 cells, cell viability upon exposure for 48 h to increasing concentrations of PBX1 and PBX2 (from 1 to 200 μM) showed IC$_{50}$ values corresponding to 103.1 ±1.82 μM for PBX1 and 81.5 ±5.1 μM for PBX2, while 10 μM of both compounds did not displayed any cytotoxic effect (data not shown). Thus, we used this concentration in the next experimental assays.

Phosphorylation, gene regulation, growth & migration assays

Thereafter, we aimed to evaluate the potential of PBX1 and PBX2 to act as agonist or antagonist ligands of GPER. As the activation of GPER-mediated signaling triggers the phosphorylation of both EGFR and ERK1/2 in cancer cells [3,17], we evaluated these responses using PBX1 and PBX2. Interestingly, the phosphorylation of EGFR and ERK1/2 induced by E2 and G-1 was prevented in the presence of PBX1 and

PBX2 in SkBr3 cells and CAFs (Figure 7A–H), suggesting that both compounds act as GPER antagonists. On the contrary, the EGFR and ERK1/2 activation upon EGF exposure was not abrogated by PBX1 and PBX2 in SkBr3 cells (see Figure 1a in Supplementary Material).

By real-time PCR, we then determined that the increase of the GPER target genes *c-fos* and *CTGF* [2] induced by E2 and G-1 is prevented in the presence of PBX1 and PBX2 in SkBr3 cells (Figure 8).

Having established that PBX1 and PBX2 are inhibitors of GPER-mediated signaling, we wondered what might be the biological effects of the aforementioned results. To this end, we determined that the proliferation of SkBr3 cells and the migration of CAFs induced by E2 and G-1 are abolished in the presence of PBX1 or PBX2 (Figure 9), hence confirming that both compounds act as GPER antagonists.

Transfection assays

In order to verify whether PBX1 and PBX2 might be able to activate or inhibit the transcription mediated by the classical ER, we ascertained that only E2 trans-
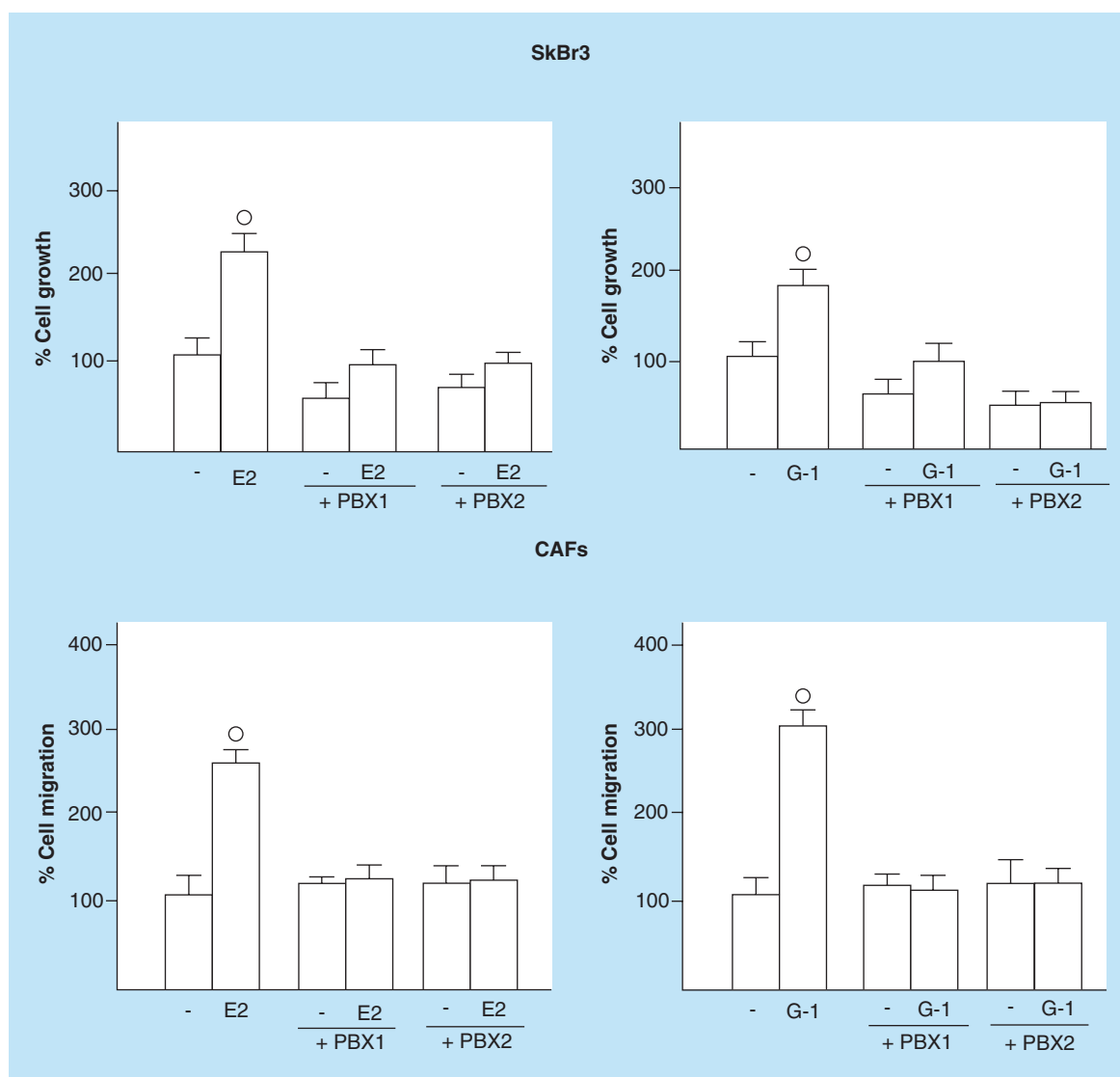

Figure 9. PBX1 and PBX2 inhibit cell proliferation and migration induced by E2 and G-1. The proliferation of SkBr3 cells induced by 100 nM E2 and 100 nM G-1 was inhibited in the presence of 10 µM PBX1 and 10 µM PBX2, as indicated. Cells were treated for 5 days and then the proliferation was evaluated by counting cells on day 6. The migration of CAFs induced by 100 nM E2 and 100 nM G-1 was inhibited in the presence of 10 µM PBX1 and 10 µM PBX2, as indicated. Each data point is the average ±SD of three independent experiments performed in triplicate. (○) indicates $p < 0.05$ for cells receiving vehicle (-) versus treatments.
CAF: Cancer-associated fibroblast.

activates the endogenous ERα in MCF7 breast cancer cells which were transiently transfected with an ER reporter gene (Figure 10A). Moreover, the ERα transactivation upon E2 treatment was abolished by using the ER antagonist ICI 182,780 (ICI) but not in the presence of PBX1 or PBX2 (Figure 10B). Similar results were obtained transfecting in Hek293 cells chimeric ERα and ERβ proteins consisting of the DNA binding domain of the yeast transcription factor Gal4 and the ligand binding domain of ERα and ERβ (Figure 10C–F). Taken to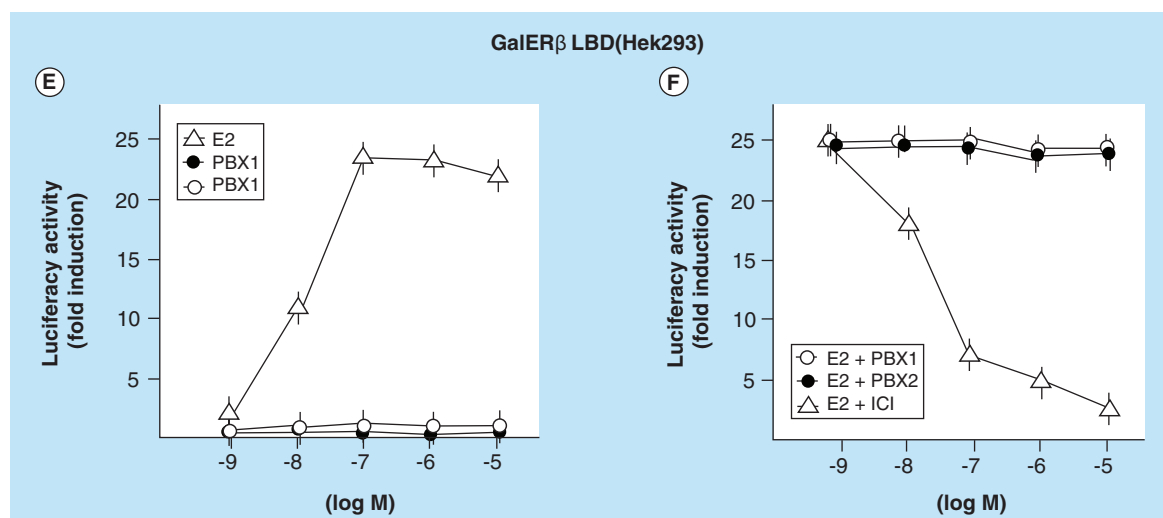gether, these findings demonstrate that the present compounds are selective GPER antagonists as they do not activate or inhibit ER-mediated responses.

Conclusion

It has been reported that GPER plays a role in diverse pathophysiological conditions including cancer, metabolic and immune disorders, osteoporosis, cognitive and behavioral alterations and neurodegenerative diseases [7–10]. Moreover, the potential involvement of GPER in the cardiovascular protection exerted by estrogens has been suggested [11]. Most of these func-
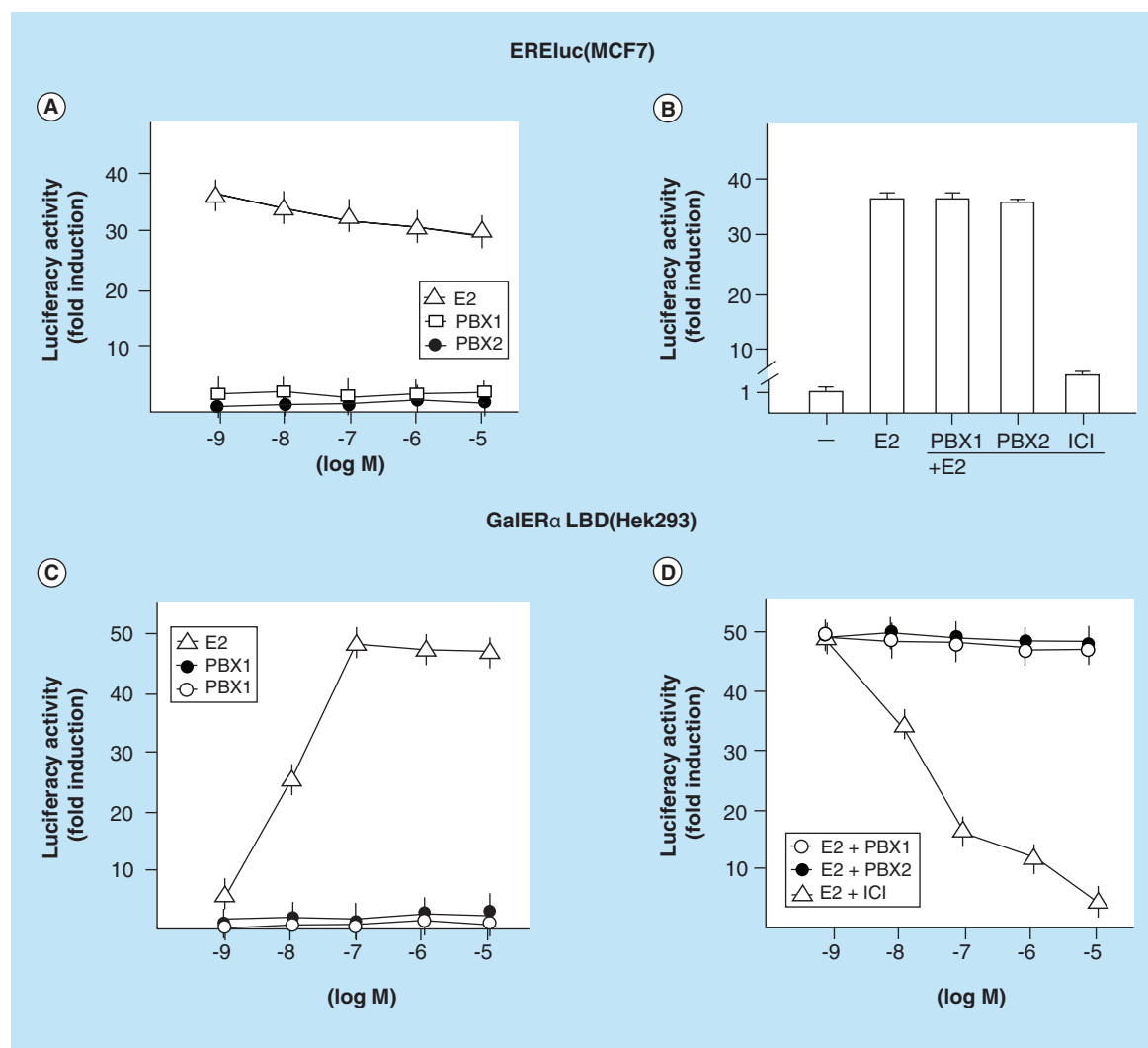
Figure 10. PBX1 and PBX2 do not activate or inhibit ER-mediated responses. (A) MCF-7 cells were transfected with the ER reporter plasmid (EREluc) along with the internal transfection control Renilla Luciferase and treated with increasing concentrations of E2, PXB1 and PXB2. **(B)** MCF-7 cells were transfected with EREluc and Renilla Luciferase and treated with 100 nM E2 in combination with 10 μM PXB1, PXB2 and ICI 182,780 (ICI), as indicated. Hek293 cells were transfected with Gal4 reporter gene GK1, the Gal4 fusion proteins encoding the Ligand Binding Domain (LBD) of ERα (GalERα) **(C)** or ERβ (GalERβ) **(E)** and Renilla Luciferase, then were treated with increasing concentrations of E2, PXB1 and PXB2. Hek293 cells were transfected with GK1, GalERα **(D)** or GalERβ **(F)** Renilla Luciferase and then treated with 100 nM **E2** in combination with increasing concentrations of PXB1, PXB2 and ICI, as indicated. The luciferase activities were normalized to the internal transfection control, the results of cells receiving vehicle (-) were set as 1 fold upon which the values of cells receiving treatments were calculated. Each data point represents the mean ±SD of three experiments performed in triplicate.

Figure 10. PBX1 and PBX2 do not activate or inhibit ER-mediated responses (cont.). (A) MCF-7 cells were transfected with the ER reporter plasmid (EREluc) along with the internal transfection control Renilla Luciferase and treated with increasing concentrations of E2, PXB1 and PXB2. **(B)** MCF-7 cells were transfected with EREluc and Renilla Luciferase and treated with 100 nM E2 in combination with 10 µM PXB1, PXB2 and ICI 182,780 (ICI), as indicated. Hek293 cells were transfected with Gal4 reporter gene GK1, the Gal4 fusion proteins encoding the Ligand Binding Domain (LBD) of ERα (GalERα) **(C)** or ERβ (GalERβ) **(E)** and Renilla Luciferase, then were treated with increasing concentrations of E2, PXB1 and PXB2. Hek293 cells were transfected with GK1, GalERα **(D)** or GalERβ **(F)** Renilla Luciferase and then treated with 100 nM **E2** in combination with increasing concentrations of PXB1, PXB2 and ICI, as indicated. The luciferase activities were normalized to the internal transfection control, the results of cells receiving vehicle (-) were set as 1 fold upon which the values of cells receiving treatments were calculated. Each data point represents the mean ±SD of three experiments performed in triplicate.

tions are unrelated to the activity exerted by the classical ER, hence chemical agents targeting selectively GPER might result useful in the treatment of a variety of pathologies [7]. For instance, the use of GPER antagonists has been hypothesized in the treatment of estrogen-sensitive malignancies like breast cancer. So far, only few compounds acting as antagonists of GPER have been identified and characterized [14,17,30].

The contribution of the stromal microenvironment to the tumor development has been highlighted by clinical evidence and the use of mouse models. Numerous studies have also suggested that CAFs, which are actively recruited within the tumor mass, play a main role toward tumor progression [31,32]. In addition, stromal fibroblasts may promote the local production of estrogens, which further stimulate the growth of breast carcinomas even through a cross-talk with important transduction pathways like those activated by growth factors [33].

In the present study, we described the design and the synthesis of two novel molecules namely PBX1 and PBX2 that exhibit peculiar chemical features. Both

compounds showed the ability to bind to GPER along with the property to prevent the activation of the GPER-mediated signaling, as the EGFR and ERK phosphorylation, the proliferation of SkBr3 cells and the migration of CAFs induced by E2 and G-1. Worthy, CAFs that were obtained from breast cancer patients, provided a unique experimental approach in evaluating the inhibitory actions triggered by PBX1 and PBX2 through GPER. Moreover, these compounds act in a selective manner through GPER, considering that both chemicals did not induce or abolish the transactivation of the classical ER, as demonstrated performing transfection assays in MCF7 and Hek293 cells. Based on these findings, we may consider PBX1 and PBX2 as leads for the development of a new class of selective antagonist ligands of GPER that may be useful in order to further dissect the biological function of this receptor. In addition, the GPER antagonism of the new compounds may be the starting point for the achievement of novel tools in the treatment of estrogen-sensitive tumors and other diseases that may benefit from the GPER inhibition.

Future perspective

The role exerted by GPER in estrogen-dependent tumors including breast cancer as well as in other pathophysiological conditions suggests that this receptor may be a promising therapeutic target in diverse diseases. Thus, the development of selective GPER

Key term

Transfection: Powerful tool used to study gene expression by introducing nucleic acids into cells. For instance, cloned genes can be transfected into cells in order to produce specific proteins and to evaluate their biochemical and biological features.

---

antagonists could allow additional therapeutic benefit respect to the current available drugs. In this regard, it should be mentioned that the discovery of novel active agents represents a major goal for medicinal chemists. The identification of new, more effective and selective GPER ligands starting from the leads described is worth for next investigation in order to address this receptor as a target in a variety of disorders.

Supplementary data

To view the supplementary data that accompany this paper please visit the journal website at: www.future-science.com/doi/full/10.4155/FMC.15.3

Executive summary

GPER inhibition
- Inhibition of GPER represents a valuable therapeutic approach in the treatment of estrogen-sensitive tumors like breast cancer.

Leads identification & synthesis
- Two new selective GPER antagonists, identified through molecular docking and ligand-based approach, could be useful for a rational design of safe and effective anticancer agents.

***In vitro* & *ex vivo* studies**
- Assays using cancer cells and cancer-associated fibroblasts obtained from breast cancer patients were used in order to validate the efficacy of the identified compounds as potential anticancer agents.

References

Papers of special note have been highlighted as:
- of interest; •• of considerable interest

1   Deroo BJ, Korach KS. Estrogen receptors and human disease. *J. Clin. Invest.* 116, 561–570 (2006).

2   Maggiolini M, Picard D. The unfolding stories of GPR30, a new membrane bound estrogen receptor. *J. Endocrinol.* 204, 105–114 (2010).

•• **Summarizes the involvement of GPER in diverse pathophysiological conditions.**

3   Filardo EJ, Quinn JA, Bland KI, Frackelton Jr AR. Estrogen-induced activation Erk-1 and Erk-2 requires the G protein-coupled receptor homolog, GPR30, and occurs *via* trans-activation of the epidermal growth factor receptor throughout release of HB-EGF. *Mol. Endocrinol.* 14, 1649–1660 (2000).

4   Prossnitz ER, Maggiolini M. Mechanisms of estrogen signaling and gene expression via GPR30. *Mol. Cell. Endocrinol.* 308, 32–38 (2009).

5   Bologa CG, Revankar CM, Young SM *et al.* Virtual and biomolecular screening converge on a selective agonist for GPR30. *Nat. Chem. Biol.* 2, 207–212 (2006).

6   Prossnitz ER, Oprea TI, Sklar LA, Arterburn JB. The ins and outs of GPR30: a transmembrane estrogen receptor. *J. Steroid Biochem. Mol. Biol.* 109, 350–353 (2008).

7   Prossnitz ER, Barton M. The G-protein-coupled estrogen receptor GPER in health and disease. *Nat. Rev. Endocrinol.* 7, 715–726 (2011).

• **Clarifies the role of GPER in different pathological conditions.**

8   Hammond R, Mauk R, Ninaci D, Nelson D, Gibbs RB. Chronic treatment with estrogen receptor agonists restores acquisition of a spatial learning task in young ovariectomized rats. *Horm. Behav.* 56, 309–314 (2009).

9   Blasko E, Haskell CA, Leung S *et al.* Beneficial role of the GPR30 agonist G-1 in an animal model of multiple sclerosis. *J. Neuroimmunol.* 214, 67–77 (2009).

10   Arterburn JB, Oprea TI, Prossnitz ER, Edwards BS, Sklar LA. Discovery of selective probes and antagonists for G protein-coupled receptors for FPR/FPRL1 and GPR30. *Curr. Top. Med. Chem.* 9, 1227–1236 (2009).

11   Lindsey SH, Cohen JA, Brosnihan KB, Gallagher PE, Chappell MC. Chronic treatment with the G protein-coupled receptor 30 agonist G-1 decreases blood pressure in ovariectomized mRen2. Lewis rats. *Endocrinology* 150, 3753–3758 (2009).

12   Lappano R, Rosano C, Santolla MF *et al.* Two novel GPER agonists induce gene expression changes and growth effects in cancer cells. *Curr. Cancer Drug Targ.* 12, 531–542 (2012).

• **Outlines the key role of GPER in cancer emergence and progression.**

13   Santolla MF, De Francesco EM, Lappano R, Rosano C, Abonante S, Maggiolini, M. Niacin activates the G protein-coupled estrogen receptor (GPER)-mediated signaling. *Cell. Signal.* 26(7), 1466–1475 (2014).

14   Dennis MK, Field AS, Burai R *et al.* Identification of GPER/GPR30 antagonist with improved estrogen receptor counterselectivity. *J. Steroid Biochem. Mol. Biol.* 127, 358–366 (2011).

• **Defines structural diverse features between GPER agonists and antagonists.**

---

15 Huryn DM, Resnick LO, Wipf P. Contributions of academic laboratories to the discovery and development of chemical biology tools. *J. Med. Chem.* 56, 7161–7176 (2013).

16 Burai R, Ramesh C, Nayak TK *et al.* Synthesis and characterization of tricarbonyl-Re/Tc(I) chelate probes targeting the G protein-coupled estrogen receptor GPER/GPR30. *PLoS ONE* 7, e46861 (2012).

•   **Adds more insights to define chemical features for the design of new GPER antagonists.**

17 Lappano R, Santolla MF, Pupo M *et al.* MIBE acts as antagonist ligand of both estrogen receptor α and GPER in breast cancer cells. *Breast Cancer Res.* 14, R12 (2012).

•   **Describes the effects of GPER activation/inhibition in breast cancer.**

18 Lorusso G, Rüegg C. The tumor microenvironment and its contribution to tumor evolution toward metastasis. *Histochem. Cell Biol.* 130, 1091–1103 (2008).

19 Sali A, Blundell TL. Comparative protein modelling by satisfaction of spatial restraints. *J. Mol. Biol.* 234, 779–815 (1993).

20 Rosano C, Lappano R, Santolla MF, Ponassi M, Donadini A, Maggiolin M. Recent advances in the rationale design of GPER ligands. *Curr. Med. Chem.* 19, 6199–6206 (2012).

•• **Describes the importance of rational design of selective GPER ligands, in order to dissect the functions mediated by this receptor.**

21 Murshudov GN, Skubák P, Lebedev AA *et al.* REFMAC5 for the refinement of macromolecular crystal structures. *Acta Crystallogr. D* 67, 355–367 (2011).

22 Lappano R, Rosano C, De Marco P, De Francesco EM, Pezzi V, Maggiolini M. Estriol acts as a GPR30 antagonist in estrogen receptor-negative breast cancer cells. *Mol. Cell Endocrinol.* 204, 105–114 (2010).

23 Chimento A, Casaburi I, Bartucci M *et al.* Selective GPER activation decreases proliferation and activates apoptosis in tumor Leydig cells. *Cell Death Dis.* 4, e747 (2013).

24 Amaro AA, Esposito AI, Mirisola V *et al.* Endocrine disruptor agent nonyl phenol exerts an estrogen-like transcriptional activity on estrogen receptor positive breast cancer cells. *Curr. Med. Chem.* 21, 630–640 (2014).

25 Pettersen EF, Goddard TD, Huang CC *et al.* UCSF Chimera - a visualization system for exploratory research and analysis. *J. Comput. Chem.* 25, 1605–1612 (2004).

26 Lappano R, Recchia AG, De Francesco EM *et al.* The cholesterol metabolite 25-hydroxycholesterol activates estrogen receptor α-mediated signaling in cancer cells and in cardiomyocytes. *PLoS ONE* 6, e16631 (2011).

27 Jirkovsky I, Humber LG, Baudy R. 4-Substituted-4H-pyrrolo[2,1-c][1,4]benzoxazines. *J. Heterocyclic Chem.* 13, 311–316 (1976).

28 Lancelot J-C, Rault S, Laduree D, Robba M. Pyrido[3,2-e]pyrrolo[1,2-a]pyrazines. *Chem. Pharm. Bull.* 33, 2798–2802 (1985).

29 Ren P-D, Pan S-F, Dong T-W, Wu S-H. The novel reduction systems: $NaBH_4$-$SbCl_3$ or $NaBH_4$-$BiCl_3$ for conversion of nitroarenes to primary amines. *Synthetic Commun.* 25, 3799–3803 (1995).

30 Dennis MK, Burai R, Ramesh C *et al. In vivo* effects of a GPR30 antagonist. *Nat. Chem. Biol.* 5, 421–427 (2009).

•• **Identifies a GPER antagonist counteracting biological responses induced by estrogens.**

31 Bhowmick NA, Moses HL. Tumor-stroma interactions. *Curr. Opin. Genet. Dev.* 15, 97–101 (2005).

32 Bhowmick NA, Neilson EG, Moses HL. Stromal fibroblasts in cancer initiation and progression. *Nature* 432, 332–337 (2004).

33 Yamaguchi Y, Hayashi S. Estrogen-related cancer microenvironment of breast carcinoma. *Endocr. J.* 56, 1–7 (2009).

Dottorato di ricerca in Medicina Traslazionale (XXIX Ciclo)
Giudizio del Supervisore sull'attività della dottoranda Silvia Avino

La dott.ssa Silvia Avino ha iniziato il corso di dottorato in Medicina Traslazionale 02-11-2013 con un progetto di ricerca avente come scopo principale la valutazione di nuovi meccanismi molecolari coinvolti nello sviluppo e nella progressione del mesotelioma, tumore aggressivo che coinvolge principalmente la superficie mesoteliale della pleura e delle cavità peritoneali.
In particolare, lo studio ha dimostrato che IGF-I è in grado di indurre l'up-regolazione dei livelli proteici di GPER e dei geni target CTGF ed EGR1 attraverso il coinvolgimento del pathway trasduzionale IGF-IR/ERK/p-38 nelle cellule di mesotelioma IST-MES1 e di tumore polmonare A549. Inoltre, è stato osservato che il trattamento con IGF-I induce in tali cellule l'up-regolazione di Collagen Type I Alpha 1 (COL1A1) e di alcuni geni target di DDR1 quali MATN-2, FBN-1, NOTCH 1 e HES-1. Inoltre, il coinvolgimento di GPER ed IGF-IR nell'attivazione dei geni target di DDR1 in seguito al trattamento con IGF-I è stato dimostrato silenziando l'espressione di entrambi i recettori con uno specifico short hairpin (shGPER e shIGF-IR). E' stata infine valutata la capacità di IGF-I di indurre risposte biologiche complesse coinvolte nella progressione tumorale. In particolar modo, è stato dimostrato che il silenziamento dell'espressione di GPER e di IGF-IR in cellule IST-MES1 e A549 inibisce la capacità di IGF-I di stimolare la chemiotassi e la migrazione cellulare. Gli esperimenti sono stati realizzati autonomamente dalla dott.ssa Avino mediante saggi di biologia molecolare.

La dott.ssa Avino ha svolto uno stage di un anno (Luglio 2014-Luglio 2015) presso il Laboratorio diretto dal Prof. J. Silvio Gutkind – National Institutes of Health, Bethesda, Maryland, USA.

L'attività di ricerca ha consentito la pubblicazione dei seguenti lavori su riviste internazionali peer-reviewed:

1.**Avino S**, De Marco P, Cirillo F, Santolla MF, De Francesco EM, Perri MG, Rigiracciolo D, Dolce V, Belfiore A, Maggiolini M, Lappano R and Vivacqua A. Stimulatory actions of IGF-I are mediated by IGF-IR cross-talk with GPER and DDR1 in mesothelioma and lung cancer cells. Oncotarget. doi: 10.18632/oncotarget.10348. [Epub ahead of print] 2016.

2.De Francesco EM, Rocca C, Scavello F, Amelio D, Rigiracciolo D, Pasqua T, Scarpelli A, **Avino S**, Cirillo F, Amodio N, Cerra MC, Maggiolini M, Angelone T. GPER activation decreases cardiotoxicity induced by doxorubicin in male rats. Journal of Cellular Physiology, J Cell Physiol. 2017 Jul;232(7):1640-1649.

3.De Marco P, Lappano R, Francesco EM, Cirillo F, Pupo M, **Avino S**, Vivacqua A, Abonante S, Picard D, Maggiolini M. GPER signalling in both cancer-associated fibroblasts and breast cancer cells mediates a feedforward IL1β/IL1R1 response. Sci Rep. 6:24354; 2016.

4.Lappano R, Rigiracciolo D, De Marco P, **Avino S**, Cappello AR, Rosano C, Maggiolini M, De Francesco EM. Recent Advances on the Role of G Protein-Coupled Receptors in Hypoxia-Mediated Signaling. AAPS J. 18(2):305-10; 2016.

5.Rigiracciolo DC, Scarpelli A, Lappano R, Pisano A, Santolla MF, **Avino S**, De Marco P, Bussolati B, Maggiolini M, De Francesco EM. GPER is involved in the stimulatory effects of aldosterone in breast cancer cells and breast tumor-derived endothelial cells. Oncotarget. 7(1):94-111. 2016.

6.O'Hayre M, Inoue A, Kufareva I, Wang Z, Mikelis CM, Drummond RA, **Avino S**, Finkel K, Kalim KW, Di Pasquale G, Guo F, Aoki J, Zheng Y, Lionakis MS, Molinolo AA, Gutkind JS. Inactivating mutations in GNA13 and RHOA in Burkitt's lymphoma and diffuse large B-cell lymphoma: a tumor suppressor function for the Gα13/RhoA axis in B cells. Oncogene. doi: 10.1038/onc.2015.442. [Epub ahead of print].2015.

7.Santolla MF, **Avino S**, Pellegrino M, De Francesco EM, De Marco P, Lappano R, Vivacqua A, Cirillo F, Rigiracciolo DC, Scarpelli A, Abonante S, Maggiolini M. SIRT1 is involved in oncogenic signaling mediated by GPER in breast cancer. Cell Death Dis. 6:e1834. 2015.

8.Maggiolini M, Santolla MF, **Avino S**, Aiello F, Rosano C, Garofalo A, Grande F. Identification of two benzopyrroloxazines acting as selective GPER antagonists in breast cancer cells and cancer-associated fibroblasts. Future Med Chem. 7(4):437-48. 2015.

Il giudizio complessivo sull'attività di ricerca svolta dalla Dott.ssa Silvia Avino è, pertanto, ampiamente positivo.

Rende 26/04/2017

Il supervisore
Prof. Marcello Maggiolini